

## PROJECT ADMINISTRATION DATA SHEET



ORIGINAL



REVISION NO. \_\_\_\_\_

Project No. A-3449

GTRION

DATE 1/18/83Project Director: V. K. Tripp~~SMOCC~~ Lab ECSL/EEDSponsor: Scientific-Atlanta, Inc.Type Agreement: Purchase Order No. 580173Award Period: From 1/1/83 To 4/30/83 (Performance) 6/15/83 (Reports)Sponsor Amount: Total Estimated: \$ 43,882 7/29/83 Funded: \$ 43,882

Cost Sharing Amount: \$ \_\_\_\_\_ Cost Sharing No: \_\_\_\_\_

Title: Dual Reflector Surface Tolerance AnalysisADMINISTRATIVE DATAOCA Contact Faith G. Costello

## 1) Sponsor Technical Contact:

Jim CookScientific-AtlantaElectro-Products Division3845 Pleasantdale RoadAtlanta, GA 30340

## 2) Sponsor Admin/Contractual Matters:

Lindsey H. Strudwick, Manager of  
PurchasingScientific-Atlanta, Inc.Electro-Products Division3845 Pleasantdale RoadAtlanta, GA 30340

Defense Priority Rating: \_\_\_\_\_

Military Security Classification: \_\_\_\_\_  
(or) Company/Industrial Proprietary: \_\_\_\_\_RESTRICTIONS

See Attached \_\_\_\_\_ Supplemental Information Sheet for Additional Requirements.

Travel: Foreign travel must have prior approval – Contact OCA in each case. Domestic travel requires sponsor approval where total will exceed greater of \$500 or 125% of approved proposal budget category.

Equipment: Title vests with Sponsor; however, none proposed.COMMENTS:COPIES TO:Research Administrative Network  
Research Property Management  
Accounting  
Procurement/EES Supply ServicesResearch Security Services  
~~Reports Coordinator (OCA)~~  
GTRI  
LibraryResearch Communications (2)  
Project File  
Other \_\_\_\_\_  
Other \_\_\_\_\_

SPONSORED PROJECT TERMINATION SHEETDate August 16, 1983

Project Title: "Dual Reflector Surface Tolerance Analysis"

Project No: A-3449

Project Director: V. K. Tripp

Sponsor: Scientific-Atlanta, Inc.

Effective Termination Date: 7/29/83Clearance of Accounting Charges: --

Grant/Contract Closeout Actions Remaining:

- ☒ Final Invoice ~~and Closing Documents~~
- ☐ Final Fiscal Report
- ☐ Final Report of Inventions
- ☐ Govt. Property Inventory & Related Certificate
- ☐ Classified Material Certificate
- ☐ Other \_\_\_\_\_

Assigned to: ECSL (School/Laboratory)COPIES TO:

Administrative Coordinator  
Research Property Management  
Accounting  
Procurement/EES Supply Services

Research Security Services  
Reports Coordinator (OCA) ✓  
Legal Services (OCA)  
Library

EES Public Relations (2)  
Computer Input  
Project File  
Other \_\_\_\_\_



ENGINEERING EXPERIMENT STATION  
Georgia Institute of Technology  
A Unit of the University System of Georgia  
Atlanta, Georgia 30332

14 January 1983

Scientific Atlanta, Inc.  
Electro Products Division  
3845 Pleasantdale Road  
Atlanta, Georgia 30340

Attention: Mr. Jim Cook

Reference: Purchase Order No. 580173  
"Dual Reflector Surface Tolerance Analysis"  
(Georgia Tech Ref. No. A-3449)

Subject: Work Plan

Gentlemen:

A detailed plan of work to accomplish the objectives of the referenced research project is presented herewith. The objective of this project is to determine what antenna construction tolerances must be maintained in order to meet the specified radiation performance. Two types of electrically large axially symmetric reflector antennas and four types of surface errors are to be analyzed. The work is divided into three main technical tasks besides the reporting task as outlined in the proposal. The third task depends on the completion of the first two tasks, and since the schedule is very tight, the first two tasks will be performed concurrently. The schedule is presented in Figure 1, and the tasks and subtasks are described below.

I. Model Antennas

Though very large, the antennas under consideration are theoretically uncomplicated; and therefore, the primary effort of this task is not mathematical modeling, but implementation of the model in a computer language. The plan is to code a physical optics technique that takes advantage of rotational symmetry. The program will have an option of using complete circular symmetry for fast calculation of perfectly symmetrical antennas. But the design of the program will need to take into account the error types to be used with it. Some errors are repeated with each azimuthal sector of the reflector. Thus, the program will need to have another option to perform azimuthal integration over one sector, but not over the complete 360 degrees.

The program will be coded in FORTRAN IV with small routines and adequate internal documentation. The coding must be done with the fact in mind that error modeling routines will be added later for various error types.

Validation of the code is basically debugging, making sure that the code represents the mathematical models. Verification is the actual test of the models themselves. This is done by calculating cases for which the answers are known.

## II. Model Errors

The primary effort of this task is mathematical modeling. First, the new error theory mentioned in the proposal will be expressed in polar coordinates. Then each random error type will be investigated to determine whether it can be properly described in the format of this new theory. It is strongly anticipated that the first two error types can be readily handled by this theory (the segment dye defect and the deformation due to support structure). The error models resulting from this analysis will then be coded into routines that will interface with the program of Task 1.

The subreflector surface errors will be investigated in the same way. However, they are not so likely to be amenable to treatment by the new theory. This depends on the precise nature of the error, which is yet to be determined. There is a back-up analysis based on annular rings that is sure to work, but it is not the preferred approach because it does not correspond well to the rest of the modeling approach of this project. That is, a completely separate computer program might be required to analyze this error type, in that event.

The irregularities of welds and gaps near the joints are not random and therefore will not require the same kind or level of modeling effort. These errors will simply be imposed on the reflector before integration.

## III. Calculations

The new random error theory referred to above assumes many randomly positioned defects. The defects are arbitrary except for the fact that they are all identical. Therefore, the application of the theory involves two parts. The first is to define the scattering from one defect, and the second is to determine the statistics of the scattering from many such defects in random positions. All the subtasks except for the field error analysis are structured in this way, even for the deterministic errors. The present plan is to determine the scattering from each type of single defect by analysis, but measurements can be used if necessary. Scattering from solitary defects of the first three types can probably be determined

Purchase Order No. 580173  
Work Plan  
14 January 1983  
Page 3

by integrating over a reflector containing one defect and subtracting the pattern from the pattern of a perfect reflector. (This plan is not yet very firm with the subreflector errors.) For these types, the second part of the calculation is simply to execute the computer programs coded in the first two tasks.

The modeling of single joint defects will be somewhat different. This task is simply to determine the surface contours of these defects, rather than to calculate scattering. Then the analysis of multiple defects is accomplished by executing the physical optics program coded in Task 1.

Field statistics are an entirely different problem from pattern statistics. Therefore, this task is handled separately and may not even be dependent on Tasks 1 and 2. Pattern statistics are generally made difficult by the fact that they are not linearly related to the aperture errors. Since this subtask involves a "linear" problem, it is anticipated that the analysis will be comparatively straightforward.

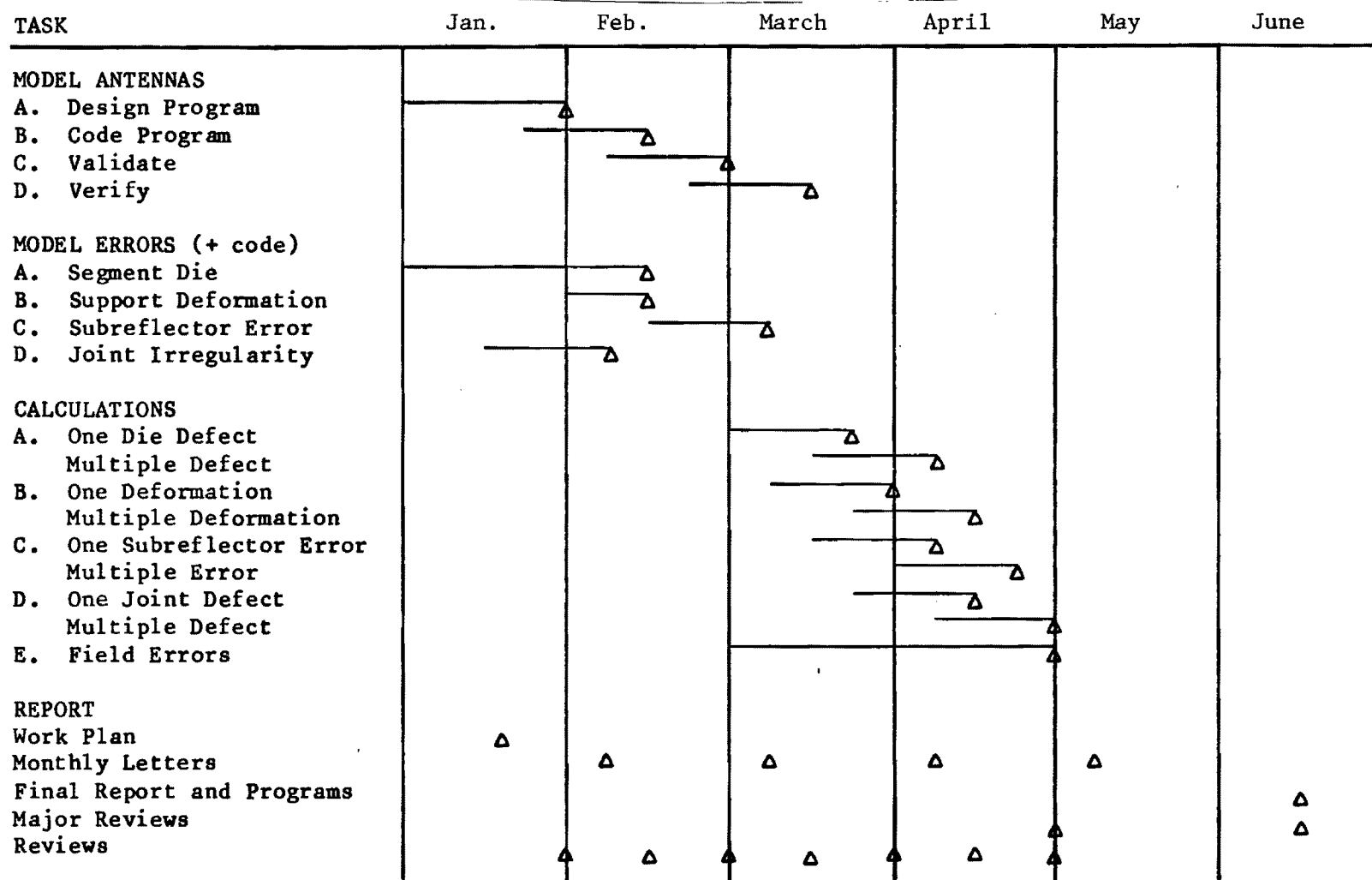
Respectfully submitted,

Victor K. Tripp     //  
Project Director

Approved:

Charles E. Ryan, Jr.  
Chief,  
EM Effectiveness Division

Figure 1. Schedule for detailed work plan.



A-3447

ENGINEERING EXPERIMENT STATION  
**Georgia Institute of Technology**  
A Unit of the University System of Georgia  
Atlanta, Georgia 30332

1 February 1983

Scientific Atlanta, Inc.  
Electro Products Division  
3845 Pleasantdale Road  
Atlanta, Georgia 30340

Attention: Mr. Jim Cook

Reference: Purchase Order No. 580173  
"Dual Reflector Surface Tolerance Analysis"  
(Georgia Tech Ref. No. A-3449)

Subject: Monthly Progress Letter No. 1  
Covering the month ending 31 January 1983

Gentlemen:

A summary of activity and progress on the referenced project for the period 1 January 1983 through 31 January 1983 is herewith presented. The objective of this project is to determine what tolerances must be maintained in the construction of high-gain reflector antennas in order to meet specifications of radiation performance. So far, the work has been performed as planned.

I. TECHNICAL ACTIVITY

There are three major technical tasks in this project.

- Task 1. Modeling of Antennas
- Task 2. Modeling of Errors
- Task 3. Calculations

Progress was made in the first two tasks last month.

Task 1

The purpose of this task is to develop the primary tool with which the effects of most of the antenna error types can be evaluated. This tool will be a Fortran computer program capable of evaluating the radiation patterns in the presence of deterministic and random reflector errors. At present, it is expected that one program with several interchangeable subroutines will most efficiently handle all errors, except possibly for subreflector errors.

In January, the planning of the program was done. This program was primarily intended to handle deterministic errors, but random errors were modeled in January and found to be compatible with the main features of the deterministic model. Thus, one program has been planned to handle both. This approach has the advantage that it may be possible to analyze antennas with both error types together.

All error types (including subreflectors) appear to be repeated with each reflector sector. This feature is fortunate because integration can be limited to one sector only. In some cases, integration will not be required in the azimuthal dimension at all. This is true for all non-error cases and for subreflector error. In any case, the complete aperture can then be composed of a circular array of sectors. It happens that the circular array approach was also successful in modeling random errors, which is why the two error analyses are compatible.

The program will be structured in a modular way to provide ease of understanding, to facilitate the debugging, and to allow for future modifications. The main program calls subroutines in which most tasks are performed. The subroutines can be verified or modified separately or in small groups without changing and recompiling the whole program. Likewise, different models can be introduced without disrupting the whole program. For instance, the defect model can be completely changed simply by replacing the subroutine GPRT.

A description of the significant sub-programs follows. All are constructed as subroutines unless otherwise indicated.

- |       |  |
|-------|--|
| PACAA | is the main program which reads the data from file INPUT and performs most of the unrepeatd calculations. ( <u>P</u> robabilistic <u>A</u> nalysis of a <u>C</u> ircular <u>A</u> rray of <u>A</u> pertures).  |
| POL1  | calculates the coefficients of the mean power components to obtain the radiation in a given polarization.  |
| POL2  | is an entry point in POL1. It returns the orthogonal polarization.   |
| GPRT  | calculates the transform of the perturbation dyadic due to one defect. Versions which have been implemented are (a) isotropic point sources, (b) Gaussian bumps, (c) Gaussian phase bumps, (d) square hat box phase bumps, and (e) circular hat box phase bumps. |
| PDF   | is a function that calculates the probability density function for a defect position in the aperture. The uniform case and projectile shower case have been implemented.   |



CINTIG	calculates the aperture integrals for the dyadic in the mean power formula.
APER	calculates the complex incident electric field for the unperturbed case. Two versions have been implemented (a) a scalar reflector, and (b) an approximate vector reflector.
ILLUM	calculates the complex incident electric fields with deterministic errors.
BEAM	calculates pattern performance parameters near the main beam.
OUTDAT	converts fields to amplitude and phase and plots the desired patterns.
FT	performs a "Fourier Transform" by integrating over one reflector sector.

## Task 2

The purpose of this task is to develop effective mathematical ways of handling each error type. To be effective, a mathematical model must be amenable to implementation in a computer program that can evaluate the expressions of the model within reasonable time and memory limits.

In recent years, Georgia Tech has developed a new approach to the treatment of random aperture errors. It was first published as a scalar theory<sup>1</sup>, and recently, it has been submitted for publication in vector form<sup>2</sup>. As demonstrated in those two documents, this approach has significant advantages over earlier approaches. Therefore, the primary approach to modeling the present errors was to apply this new aperture error approach.

At the center of the new theory is the fact that certain statistical integrals take the form of convolutions. This feature is made possible by the fact that scattering from one defect is independent of the position of

1. V. K. Tripp, "A New Approach to Random Aperture Errors," IEEE/AP-S International Symposium, Los Angeles, CA, pp. 140-143, June 16-19, 1981.
2. V. K. Tripp, "A New Approach to the Analysis of Random Errors in Aperture Antennas," submitted for publication in IEEE Trans. AP.

the defect and that all defects are the same. This requirement is expressed as follows.

$$g(x,y,x_1,y_1) = g(x-x_1,y-y_1)$$

The first attempt to model sector die errors began with a modification of this requirement to the following form.

$$g(\rho,\phi,\rho_1,\phi_1) = g(\rho-\rho_1,\phi-\phi_1)$$

where  $g$  is the electric field scattering function,  
 $x,y$  are rectangular aperture coordinates of observation,  
 $\rho,\phi$  are polar aperture coordinates, and  
 $x_1,y_1,\rho_1,\phi_1$  are similar coordinates of the defect position.

This approach did not work. The integrals were convolutions in polar coordinates, but no "convolution theorem" is available for Fourier Transforming such integrals.

The next approach was to use the original error model, but confine it to one sector and consider an array of sectors. This approach worked and is documented in the attached technical memorandum of 27 January. This subtask was completed ahead of schedule in order to better design the program of Task 1.

## II. REPORTING (TRIPS/VISITS)

No trips or visits took place in January.

## III. PLANNED ACTIVITY

Next month the computer program will be coded and validated. This is a tight schedule, but several subroutines are already in existence. Also next month, the remaining details will be obtained for the other error types so they can be properly modeled. Segment deformation and joint irregularities will be modeled next month.

## IV. PROBLEMS

No significant problems were encountered in January.

Monthly Progress Letter No. 1  
1 February 1983  
Page 5

V. SCHEDULE

The project is considered to be on schedule. Computer program coding is slightly behind schedule, but segment die modeling was completed ahead of schedule.

VI. FINANCES

Official accounting data has not yet been compiled, but estimated expenditures are about \$3,500, all in personal services and overhead.

Respectfully submitted,

Victor K. Tripp  
Project Director

Approved:

Charles E. Ryan, Jr.  
Chief,  
EM Effectiveness Division

ENGINEERING EXPERIMENT STATION  
Georgia Institute of Technology  
A Unit of the University System of Georgia  
Atlanta, Georgia 30332

27 January 1983

TECHNICAL MEMORANDUM

TO: Project File, A-3449

FROM: V. K. Tripp

REFERENCE: "A New Approach to the Analysis of Random Errors  
in Aperture Antennas", by V. K. Tripp, submitted  
for publication in IEEE, Trans. A.P.

SUBJECT: A model of reflector defects caused by die errors

Introduction

Some circularly symmetrical antenna reflectors are constructed by attaching a number of identical azimuthal sectors along their radial edges. Each sector is fabricated with the use of a die built for that purpose; the same die is used for all sectors of a given reflector. One kind of surface error to which such a reflector is susceptible is caused by randomly positioned defects in the sector die. Clearly, such errors are repeated periodically with azimuth angle in the reflector, though in one given sector they are random. Within one sector, the defect positions are probably all independent of each other.

Error Model for One Sector

The characteristics of the errors of a given sector, as described above, closely resemble those of the error model in the reference paper. That model is essentially defined by Equations (8) through (11), which are repeated below.

$$\underline{E}(\underline{r}) = \sum_{n=1}^N \underline{g}(\underline{r}, \underline{r}_n) \underline{E}_0(\underline{r}_n) \quad (1)$$

$$\underline{g}(\underline{r}, \underline{r}_n) = \underline{g}(\underline{r} - \underline{r}_n) \quad (2)$$

$$P_J(\underline{r}_1, \underline{r}_2, \dots, \underline{r}_N) = p(\underline{r}_1) p(\underline{r}_2) \dots p(\underline{r}_N) \quad (3)$$

where  $\underline{r} = x\hat{x} + y\hat{y}$  is a position in the aperture,  
 $\underline{r}_n$  is a defect position in the aperture,  
 $N$  is the number of defects (in one sector, here),  
 $\underline{E}_0$  is the aperture electric field with no errors,  
 $\underline{E}$  is the additive aperture field error,  
 $\underline{g}$  is a dyadic scattering function for one defect,  
 $P_J$  is the joint probability density function  
(pdf) of defect positions (completely specifies  
randomness), and  
 $p$  is the pdf for one defect.

This is a very general error model, for which the power-pattern average has been derived in closed form, as presented in the paper. Therefore, it is prudent to assess the applicability of this model to the present problem of die errors. Equation (1) should be a very good approximation unless the functions  $\underline{g}$  are so extensive that the incident field  $\underline{E}_0$  cannot be adequately represented by its value at one point ( $\underline{r}_n$ ). This is not believed to be the case; specifically,

Assumption 1.  $\underline{E}_0$  does not vary much over the extent of one defect.

The accuracy of Equation (2) depends on the precise nature of the defects, but it appears to be reasonable as applied to one sector. It states:

Assumption 2. The scattering pattern is the same for all defects (in a given sector), independent of position.

Even if this assumption is not strictly true it will be an especially good approximation for simple (circularly symmetrical) defects, and for cases of only one defect. It is expected to be quite applicable to dent type defects that cause phase error.

The accuracy of Equation (3) also depends on the cause of the defects. In words, it says:

Assumption 3. All defect positions are independent and have the same statistics.

This is expected to be a good approximation for a single sector, and of course, it is exactly true for the case of only one defect. However, it is certainly not applicable to defects in different sectors, since their positions are precisely repeated in every sector. They have the same statistics, but they are completely dependent on each other. This is precisely why the theory must be modified.

### A Circular Array of Sectors

With the error model of the reference paper, we can calculate the mean power pattern of one sector of a reflector containing die defects. The next task is to consider a whole reflector, which will be simply a circular array of such sectors. We place the origin at the center of the circle (the vertex of every sector) so that each element of the array is only a rotation from the reference sector.

Consider the aperture field and its transform for one sector.

$$\underline{E}_a(\underline{r}) = \underline{E}_o(\underline{r}) + \underline{E}(\underline{r}) \quad (4)$$

$$\underline{f}(\theta, \phi) = \widetilde{\underline{E}_a(\rho, \psi)} \quad (5)$$

where  $\underline{E}_a$  is the total aperture field,  
 $\underline{f}$  is its Fourier transform (equal to the far field for our purposes),  
 $\theta, \phi$  are standard spherical far-field coordinates,  
 $\rho, \psi$  are polar aperture coordinates, and  
 $\sim$  represents the Fourier Transform (FT) performed in rectangular coordinates.

Later we will find it useful to know that rotation of coordinates propagates through the FT:

$$\underline{f}(\theta, \phi - \phi_o) = \widetilde{\underline{E}_a(\rho, \psi - \phi_o)}, \quad (6)$$

where  $\phi_o$  is an arbitrary constant.

Statistics of  $\underline{f}$  are not generally very useful; we need to know those of  $\underline{f} \underline{f}^\dagger$  ( $+$  represents transpose-conjugate). Specifically, the statistic  $\langle \underline{f} \underline{f}^\dagger \rangle$  will be investigated since it contains the information needed to get the mean power pattern in any polarization (as explained in the reference). Now Reference Equation (3) can be written,

$$\langle \underline{f} \underline{f}^\dagger \rangle = \langle \widetilde{\underline{E}_a \underline{E}_a^\dagger} \rangle \quad (7)$$

for any one sector. For the total aperture (array),

$$\underline{f}_t(\theta, \phi) = \sum_m^M \underline{f}(\theta, \phi - \phi_m), \quad (8)$$

where  $\underline{f}_t$  is the total far field,  
 $M$  is the number of equal sectors in the reflector, and  
 $\phi_m = \frac{2\pi m}{M}$  is the rotation to the  $m$ -th sector.

Then for the array, the desired statistic is

$$\langle \underline{f}_t \underline{f}_t^\dagger \rangle = \sum_{\ell}^M \sum_m^M \langle \underline{E}_a(\rho', \psi' - \phi_{\ell}) \underline{E}_a^\dagger(\rho, \psi - \phi_m) \rangle, \quad (9)$$

since the mean operation can always be exchanged with summation. For the same reason, Reference Equations (5) through (7) are still valid, but now  $\underline{r}'$  and  $\underline{r}$  may be in different sectors. Thus, we have for Reference Equation (7),

$$\langle \underline{f}_t \underline{f}_t^\dagger \rangle = \sum_{\ell}^M \sum_m^M \left[ \langle \underline{E}_{a\ell} \rangle \langle \underline{E}_{am}^\dagger \rangle + \underline{V}_{E\ell m} \right], \quad (10)$$

where  $\underline{V}_{E\ell m}$  is the error field correlation, and  
 $\underline{E}_{a\ell} = \underline{E}_a(\rho, \psi - \phi_{\ell})$ , etc.

In Equation (10) the double transform term is the only one presenting a problem. The others can be rotated to the coordinate system of the reference sector, then Fourier Transformed, and then rotated back. In the scalar case,  $E_o(\rho, \psi) = E_o(\rho, \psi - \phi_m)$ ; then all  $2m$  single transforms are identical except for rotation. In any case, they are similar and straightforward.

If we parallel the analysis of the reference paper, we hope to find the following in lieu of its Equations (26) and (27).

$$\underline{C} = \int_{\text{Sector}} \underline{E}_{o\ell} \underline{E}_{om}^\dagger p \, d\underline{r}, \quad (11)$$

$$\underline{V}_{E\ell m} = N \underline{g}_{\ell} (\underline{C} - \underline{E}_{c\ell P} \underline{E}_{omP}^\dagger) \underline{g}_m \quad (12)$$

These expressions say that  $V_{E\ell m}$  are all equal if  $\underline{E}_0$  and  $\underline{g}$  are rotationally symmetrical. This is intuitively satisfying because we know that the defect positions (and hence  $p$ ) have rotational symmetry.  $V_{E\ell m}$  is a measure of the "sameness" between  $\underline{E}(\rho', \psi' - \phi_\ell)$  and  $\underline{E}(\rho, \psi - \phi_m)$  caused by defect scattering. One would expect this function to depend mainly on  $(\rho', \psi')$  and  $(\rho, \psi)$  and be relatively independent of  $\ell$  and  $m$ .

### Detailed Analysis

Unfortunately, it is not quite so easy. Whenever  $\ell \neq m$ , we are dealing with defects that are not independent. Thus, Reference Equation (13) doesn't hold, but rather we have the mean defined as follows.

$$A = \int_{-\infty}^{\infty} \int_{-\infty}^{\infty} A(\underline{r}_\ell, \underline{r}_m) p_2(\underline{r}_\ell, \underline{r}_m) d\underline{r}_\ell d\underline{r}_m, \quad (13)$$

where  $A$  is a nominal function of two random defect positions,  
 $\underline{r}_\ell = (\rho'_n, \psi'_n - \phi_\ell)$  is the position of defect  $n$  in sector  $\ell$ ,  
 $\underline{r}_m = (\rho_n, \psi_n - \phi_m)$  is the position of defect  $n$  in sector  $m$ , and  
 $p_2$  is their joint pdf.

To reduce this integral, we observe that the conditioned pdf, the pdf of  $\underline{r}_m$  given the value of  $\underline{r}_\ell$ , is

$$p_c(\underline{r}_m | \underline{r}_\ell = \text{constant}) = \delta(\rho'_n \cos \psi'_n - \rho_n \cos \psi_n, \rho'_n \sin \psi'_n - \rho_n \sin \psi_n). \quad (14)$$

That is, given the defect position in sector  $\ell$ , the defect position in sector  $m$  is an exact rotation from  $\ell$  to  $m$ .

Then using the theorem\*

$$\langle A(\underline{r}_\ell, \underline{r}_m) \rangle = \langle \langle A(\underline{r}_\ell, \underline{r}_m) | \underline{r}_\ell = \underline{r}_{0\ell} \rangle \rangle, \quad (15)$$

we do the integration over  $\underline{r}_m$  first, and the delta function leaves

$$\langle A \rangle = \int_{-\infty}^{\infty} A(\underline{r}_{0\ell}, \underline{r}_{0m}) p(\underline{r}_0) d\underline{r}_0, \quad (16)$$

just as in the reference paper. Here  $\underline{r}_{0\ell} = (\rho_0, \psi_0 - \phi_\ell)$ , etc.

\*A. Papoulis, "Probability, Random Variables, and Stochastic Processes," McGraw Hill, 1965, Equation (7-59).



More explicitly,

$$\begin{aligned} \langle A(\rho'_1, \psi'_1 - \phi'_\ell, \rho'_m, \psi'_m - \phi'_m, \rho'_1, \psi'_1 - \phi'_\ell, \rho'_1, \psi'_1 - \phi'_m) \rangle = \\ \int A(\rho'_1, \psi'_1 - \phi'_\ell, \rho'_m, \psi'_m - \phi'_m, \rho'_1, \psi'_1 - \phi'_\ell, \rho'_1, \psi'_1 - \phi'_m) p(\rho_1, \psi_1) \rho_1 d\rho_1 d\psi_1. \end{aligned} \quad (17)$$

Then the equivalent of Reference Equation (38) is written,

$$\langle \underline{G}'_\ell \underline{G}_m^\dagger \rangle = \int \underline{g}(\underline{r}'_\ell - \underline{r}_{1\ell}) \underline{E}_0(\underline{r}_{1\ell}) \underline{E}_0^\dagger(\underline{r}_{1m}) \underline{g}^\dagger(\underline{r}_m - \underline{r}_{1m}) p(\underline{r}_1) d\underline{r}_1. \quad (18)$$

Now we observe that

$$\begin{aligned} p(\underline{r}_1) &= p(\underline{r}_{1m}), \text{ and} \\ d\underline{r}_1 &= d\underline{r}_{1m}, \text{ and we let} \\ \underline{r}_1 &= \underline{r}_{1m} - \underline{r}_{m\ell}. \end{aligned} \quad (19)$$

Then the  $\underline{g}^\dagger$  function is seen to be convolved with the remaining integrand.

$$\langle \underline{G}'_\ell \underline{G}_m^\dagger \rangle = \left[ \underline{g}(\underline{r}'_\ell - (\underline{r}_m - \underline{r}_{m\ell})) \underline{E}_0(\underline{r}_m - \underline{r}_{m\ell}) \underline{E}_0^\dagger(\underline{r}_m) p(\underline{r}_m) \right] * \underline{g}^\dagger(\underline{r}_m). \quad (20)$$

Next we observe that  $\underline{r}_m - \underline{r}_{m\ell} = \underline{r}_\ell$  and follow the approach of Reference Equation (39). (This  $\underline{r}_\ell$  is an unprimed variable, but rotated from the  $m$  sector to the  $\ell$  sector where the primes are.)

$$\underline{g}(\underline{r}'_\ell - \underline{r}_\ell) = \int \underline{g}(\underline{r}'_\ell - \underline{r}_1) \delta(\underline{r}_\ell - \underline{r}_1) d\underline{r}_1. \quad (21)$$

That is,

$$\underline{g}(\underline{r}'_\ell - \underline{r}_\ell) = \underline{g}(\underline{r}'_\ell) * \delta(\underline{r}_\ell - \underline{r}'_\ell) \quad (22)$$

Thus, we have achieved a form similar to Reference Equation (41), as follows.

$$\langle \underline{G}'_\ell \underline{G}_m^\dagger \rangle = \underline{g}(\underline{r}'_\ell) * \left[ \delta(\underline{r}_\ell - \underline{r}'_\ell) \underline{E}_0(\underline{r}'_\ell) \underline{E}_0^\dagger(\underline{r}_m) p(\underline{r}_m) \right] * \underline{g}^\dagger(\underline{r}_m) \quad (23)$$

Now with the double FT, we have a formula similar to Reference Equation (25). The only remaining task is to determine the double FT of the center term  $\underline{H}_{\ell m}$  of Reference Equation (22).

$$\underline{H}_{\ell m} = \iint \delta(\underline{r}_\ell - \underline{r}_\ell) \underline{E}_0(\underline{r}'_\ell) \underline{E}_0^+(\underline{r}_m) p(\underline{r}_m) \exp(j\mathbf{k} \cdot (\underline{r}'_\ell - \underline{r}_m)) \frac{d\underline{r}'_\ell}{(24)} d\underline{r}_m$$

Letting  $\underline{r}_\ell = \underline{r}_m + \underline{r}_{\ell m}$  again, the  $\delta$  function reduces this expression to a single integral

$$\underline{H}_{\ell m} = \int \underline{E}_0(\underline{r}_m + \underline{r}_{\ell m}) \underline{E}_0^+(\underline{r}_m) p(\underline{r}_m) \exp(-j\mathbf{k} \cdot \underline{r}_{\ell m}) d\underline{r}_m \quad (25)$$

where  $\underline{r}_{\ell m} = (\rho_m, \psi_m + \phi_\ell - \phi_m)$  is the vector from  $\underline{r}_m$  to the corresponding point in the  $\ell$  sector.

Finally, the formula for the mean power pattern components can be written:

$$\begin{aligned} \langle \underline{f} \underline{f}^+ \rangle = & \sum_{\ell}^M \sum_{m}^M \left[ \underline{E}_{o\ell} + N \underline{g}_{\ell} \underline{E}_{o\ell}^p \right] \left[ \underline{E}_{om} + N \underline{g}_m \underline{E}_{om}^p \right]^+ \\ & + N \sum_{\ell}^M \sum_{m}^M \underline{g}_{\ell} \left[ \underline{H}_{\ell m} - \underline{E}_{o\ell}^p \underline{E}_{om}^p \right] \underline{g}_m^+, \end{aligned} \quad (26)$$

where  $\ell, m$  are indices on sectors indicating rotation by  $\frac{2\pi\ell}{M}$  or  $\frac{2\pi m}{M}$ , and

$\underline{H}_{\ell m}$  is a single transform dyadic defined in Equation (25).

### Conclusion

A closed form solution has been derived for the effects of segment die defects on the radiated vector power pattern. It is closely related to a theory developed, tested, and published by Georgia Tech. This relation reduces the risk and requirements for verification. In the programming of this solution, transforms should be done in polar coordinates to facilitate the rotation operation. Since a polar integration routine must be written for other error types, it might be used here also.

VKT:bg

A - 3449



ENGINEERING EXPERIMENT STATION  
**Georgia Institute of Technology**  
A Unit of the University System of Georgia  
Atlanta, Georgia 30332

4 March 1983

Scientific Atlanta, Inc.  
Electro Products Division  
3845 Pleasantdale Road  
Atlanta, Georgia 30340

Attention: Mr. Jim Cook

Reference: Purchase Order No. 580173  
"Dual Reflector Surface Tolerance Analysis"  
(Georgia Tech Ref. No. A-3449)

Subject: Monthly Progress Letter No. 2  
Covering the month ending 28 February 1983

Gentlemen:

A summary of activity and progress on the referenced project for the period 1 February 1983 through 28 February 1983 is herewith presented. The objective of this project is to determine relationships between construction errors and radiation performance of high-gain reflector antennas.

I. TECHNICAL ACTIVITY

There are three major technical tasks in this project.

- Task 1. Modeling of Antennas
- Task 2. Modeling of Errors
- Task 3. Calculations

Progress was made in the first two tasks last month.

Task 1

The purpose of this task is to develop the primary tool with which the effects of most of the antenna error types can be evaluated. This tool will be a Fortran computer program capable of evaluating the radiation patterns in the presence of deterministic and random reflector errors. At present, it is expected that one program with several interchangeable subroutines will most efficiently handle all errors, except possibly for subreflector errors.

In February, the detailed design of the computer program was completed, and most of the coding was done. The main program is designed according to the diagram in Figure 1. It is designed specifically for randomly positioned errors and deterministic errors. For deterministic errors, the innermost loop will be bypassed, and the value of  $V_F$  will be zero. For random errors,  $E_d$  will be zero. This algorithm is intended to treat both types of errors together.

For the present, it is assumed that all errors are periodic with reflector sectors. It may be advisable to perform some measurements to determine how accurate this assumption is. The present program also contains no diffraction calculations. It is believed that the primary performance problem encountered by Scientific Atlanta can be investigated with the present program. If it is later determined that wide-angle radiation must also be investigated, the best approach probably is to use another program. Alternatively, the addition of diffraction calculations to this program will be considered at that time.

The integration will be performed over the reflector surface except for the evaluation of  $\hat{A}_{\ell n}$ , which is related to random error correlation. It will be integrated over an aperture. The integration technique will be to divide a sector into patches that are large compared to a wavelength, but small compared to surface curvature and illumination gradients. The summation will be done for one patch and then repeated with more sample points, for which the phase is calculated. The number of sample points will be incremented until the sum converges. Then the next patch will be similarly summed. Radial integration will be performed before azimuthal integration.

#### Task 2.

The purpose of this task is to develop effective mathematical ways of handling each error type. The first step in this task is to obtain information regarding each error type sufficient to model it. Progress was made on this step in February, as such information was obtained in the briefing discussed in the next section.

#### II. REPORTING (TRIPS/VISITS)

On 23 February, Jim Cook of Scientific Atlanta met with Vic Tripp at Georgia Tech. There was discussion of the work progress, of antenna performance problems, of construction and surface measurement techniques, and of possible sources of error. The following points were made and are recorded here for reference.

1. A reflector is divided into as many as 32 sectors.
2. The feed pattern is very circularly symmetrical, and it is accurately described by  $\cos^n \theta$ .
3. Polarization can be approximated by the Huygens pattern.
4. Far-field pattern statistics are required, not incident or near-field statistics, except as a possible intermediate step.
5. The U.S. standard sidelobe specification is

<u>Level (dBi)</u>	<u>Region (deg. from boresight)</u>
29-25 log $\theta$	1 - 7
8	7 - 9.2
32-25 log $\theta$	9.2 - 48
-10	$\geq 48$

6. The primary performance problem is a sidelobe 3 to 5 dB above specification in the region between 2 and 6 degrees.
7. The secondary problem is general difficulty with the -10 dB specification beyond 48°.
8. SA's surface measurement technique is mechanical rather than optical. It produces sample points in cylindrical coordinates, for which processing software has been developed.
9. The number of surface sample points is usually not a multiple of the number of sectors in the reflector.

### III. PLANNED ACTIVITY

Next month, the computer program will be completed, including coding, validation, and verification. A trip will be made to Scientific Atlanta to obtain information and insight regarding error mechanisms and possible modeling techniques. Finally, all mathematical models will be completed. That is, Tasks 1 and 2 will be completed. Task 3 will be started as a part of the program verification.

### IV. PROBLEMS

No technical problems were encountered in February.

### V. SCHEDULE

The program is now behind schedule as shown in Figure 1. However, nothing has slipped that cannot be caught up. The slippage will not effect the deadline dates.

Monthly Progress Letter No. 2  
4 March 1983  
Page 4

VI. FINANCES

The total charges in February are \$205.33.

Respectfully submitted,

Victor K. Tripp  
Project Director

Approved:

Charles E. Ryan, Jr.  
Chief,  
EM Effectiveness Division

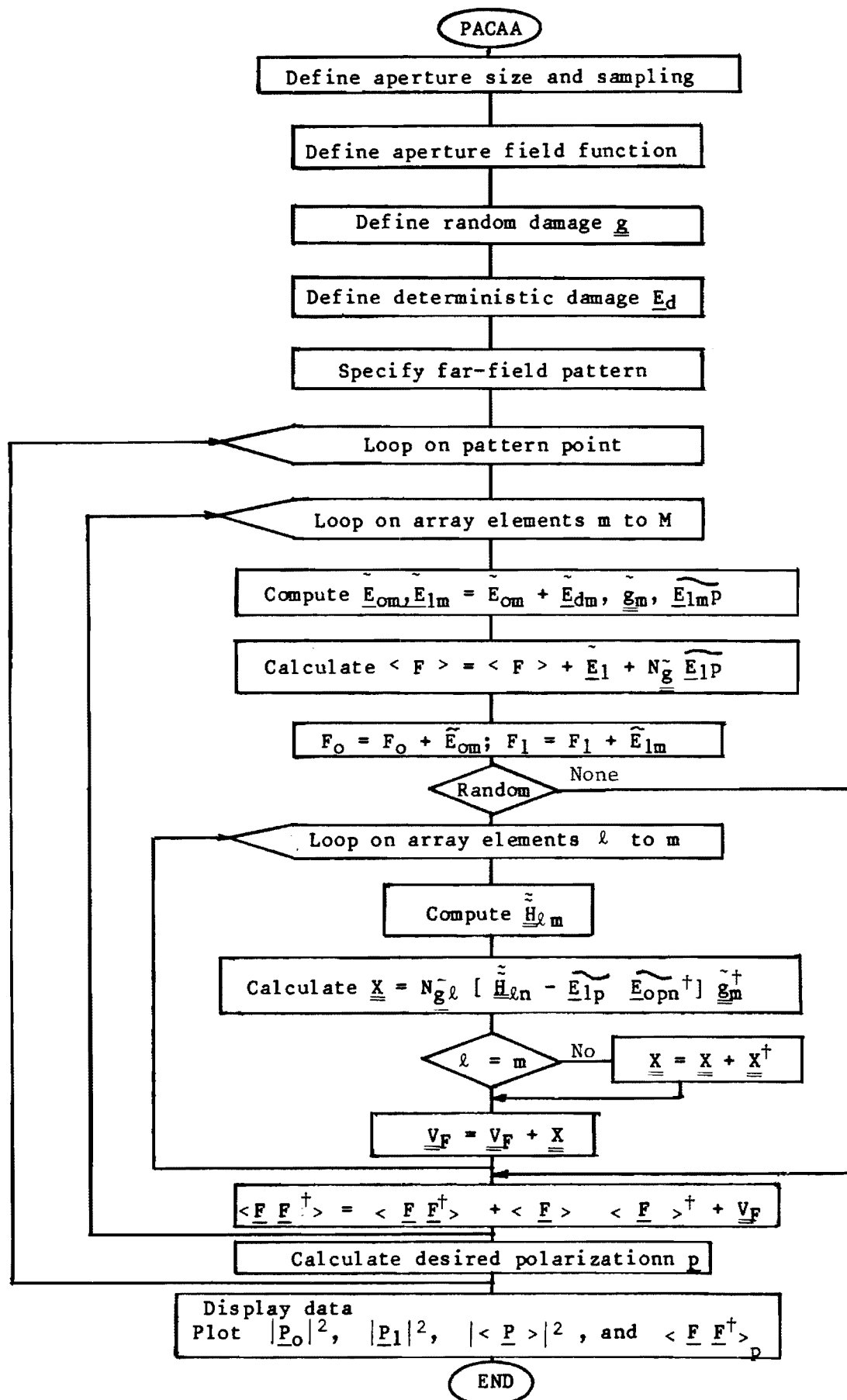
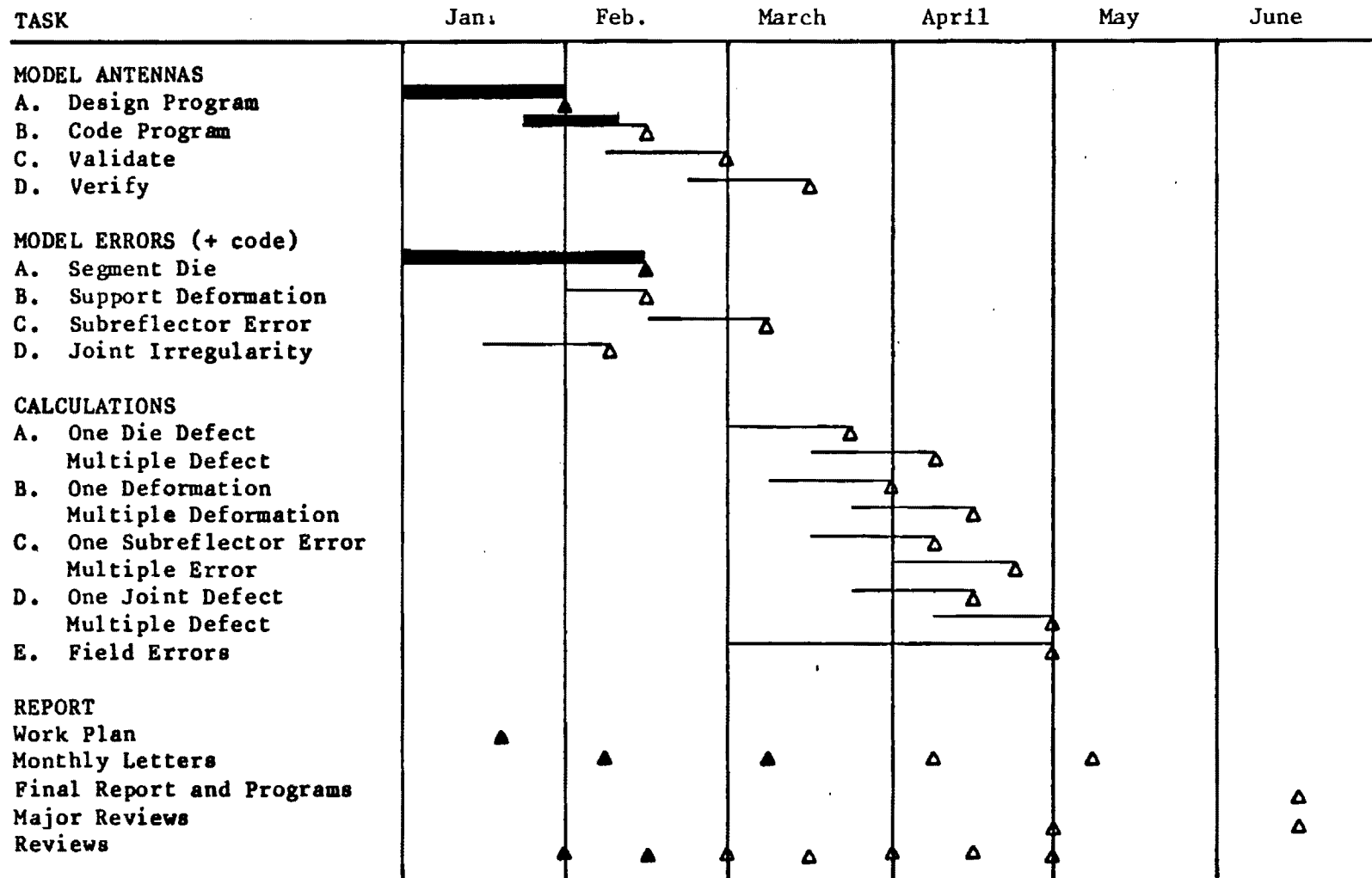


Figure 1. Design of main error analysis program.

Figure 2. Schedule for detailed work plan.







ENGINEERING EXPERIMENT STATION  
**Georgia Institute of Technology**  
A Unit of the University System of Georgia  
Atlanta, Georgia 30332

14 April 1983

Scientific Atlanta, Inc.  
Electro Products Division  
3845 Pleasantdale Road  
Atlanta, Georgia 30340

Attention: Mr. Jim Cook

Reference: Purchase Order No. 580173  
"Dual Reflector Surface Tolerance Analysis"  
(Georgia Tech Ref. No. A-3449)

Subject: Monthly Progress Letter No. 3  
Covering the month ending 31 March 1983

Gentlemen:

A summary of activity and progress on the referenced project for the period 1 March 1983 through 31 March 1983 is herewith presented. The objective of this project is to determine relationships between construction errors and radiation performance of high-gain dual reflector antennas.

#### I. TECHNICAL ACTIVITY

There are three major technical tasks in this project.

- Task 1. Modeling of Antennas
- Task 2. Modeling of Errors
- Task 3. Calculations

Progress was made in all three tasks last month.

#### Task 1

The purpose of this task is to develop the primary tool with which the effects of most of the antenna error types can be evaluated. This tool is a FORTRAN computer program capable of evaluating the radiation patterns in the presence of deterministic and random reflector errors. It is believed that this program with its interchangeable subroutines will most efficiently handle all errors, except possibly for subreflector errors.

In this period, the FORTRAN coding of the computer program was completed and validation was essentially completed. The design was changed somewhat to allow deterministic errors that are not repeated per sector. At present, only the two integration routines remain to be validated against known results. Also, the plotting routines will require minor modification before the program is finalized, but they are presently adequate for program validation.

#### Task 2.

The purpose of this task is to develop effective mathematical ways of handling each error type. The first step in this task is to obtain information regarding each error type sufficient to model it. Much progress was made in March on this task. Information regarding error sources was obtained during a trip to Scientific-Atlanta, which is reported below. Also, many error types were modeled and coded. Table I shows a summary of the kinds of errors that seem to be possible and the status of the investigation of each. In this table, "M" means that a mathematical description of the error has been devised that is amenable to analysis. "C" means that the descriptions have been implemented in computer routines. "Q" means that information has been obtained to assign numerical values to the descriptive parameters of the models.

Modeling of the Regular Joint Errors is in progress, but modeling of the subreflector errors has been postponed. This model and code would be essentially unrelated to that of the other error types, and the error is not expected to be significant. Thus, the benefit-to-cost ratio of the analysis of this type appears to be the lowest of that of the four types. Aside from this error type, this task is nearly complete.

#### Task 3.

The purpose of this task is to obtain the quantitative information for each error type and to analyze the effects of hardware errors on pattern performance. Progress was made on this task in March by obtaining quantitative information on several error types. Those for which such information was obtained are marked with a "Q" in Table I. Analysis will start as soon as the computer program is verified.

## II. REPORTING (TRIPS/VISITS)

On 11 March, Vic Tripp visited Jim Cook of Scientific Atlanta at the SA plant on Pleasantdale Road. The primary purpose of the trip was to observe construction techniques and reflector surface measurements, in order to gain insight into surface error problems. Such insight will help in determining which error types should be analyzed and in defining the approach to the analysis.

### Surface Construction

All reflectors that were encountered were composed of multiple interchangeable sectors, but there were several methods of constructing a sector. One way was to weld several singly curved plates onto a frame. For 10 and 11 M reflectors there were typically two rings of plates with 2 and 4 plates per sector, respectively, beginning with the inner ring. With 24 sectors, that makes 144 plates.

With this construction, there is inherent "chordal" error due to faceting, which has been well analyzed. There is also some curvature introduced in the azimuth direction by welding, which has been generally found to reduce the chordal error. This effect is somewhat dependent on the constructing personnel.

Another common method of section fabrication is to stamp them on a large die. The stamped shape includes a flange around the edges that is used for connecting the sections. The flange is also necessary to preserve the parabolic curvature, since the metal contains stresses that tend to flatten it. This construction also depends on the press set-up for each stamping run.

The third method is to stretch the sheet metal beyond yield over the die. This technique eliminates internal stresses and therefore the need for a flange. It is also more repeatable from one run to the next than is the stamping method. However, this approach is not favored because it is more expensive.

### Support Structure

The most accurate and repeatable construction technique for supporting the surface sections is an array of trusses. They extend radially from the hub to the reflector edge, one for each surface sector. The hub contact points are machined and the truss points are all machined together where contact is made to the hub or to the reflector surface. To assemble, a somewhat flexible surface section is drawn down against the truss contact points along one edge. The adjacent edge of the next section is made to match the edge resting on the truss. This method is accurate, and the best fit focal length is very repeatable. This approach can yield surface error as low as .025" RMS, but it is expensive.

The second major method of supporting the surface sections is to connect them at the edges and basically let the paraboloidal shape maintain itself. In this case, heavier surface sheet metal is used, typically 1/8" as opposed to 1/16" for the truss method. In addition to attaching the paraboloid to the center hub, there are radial struts extending from the rear of the hub to points near the reflector edge. This method has been shown to be highly sensitive to errors in section width. Such errors distort the whole shape.

A third construction technique is closely related to the second, but is intended to alleviate the distortion problem. This has been accomplished by attaching the edges in a manner that does not pull them tightly together. Instead, both flanges are held in a curved radial channel.

#### Surface Errors

- (1) Die defects are a source of error that has already been addressed in this investigation. All three surface construction techniques would appear to be susceptible to this type of error, since it results from an error in the tool that defines the surface. However, the shape of the defect would be different for each type of construction. This type of error will be precisely repeated in each sector. Standard SA measurements may not reveal this kind of error.
- (2) Deformations produced by the support structure should depend on the construction techniques, both the surface section and support structure. The most prevalent error of this category would appear to be strain in the surface adjacent to the edges of the section as shown in Figure 1. This kind of error may be essentially absent from the faceted sections because they are backed with braces that the small panels are welded to. Also, they may be worse in the stamped sections than in the stretch-formed ones because internal stress may cause such strain even before assembly of the antenna. They would definitely be expected with the second support technique discussed above. This type of error was not obvious in the antennas inspected at SA, however, except for several antennas being displayed that were not made by SA. Again, this kind of error should be closely repeated by each section. SA measurements would indicate this type of error by plots that turn up at both ends.

A second error type of this category would be large scale distortions extending across a section. The surface distortion caused by width tolerances in the second support would be included in this error type. Also included, would be deformations caused by gravity and wind loading. Such deformations caused by construction would be expected to be quite repeatable, but not those from other causes. Another unrepeatable cause of this error would be poor assembly. One assembled antenna was observed in which the surface was not resting on a strut contact point. Measurement plots having significant first or second order components, either radially or azimuthally, would indicate the errors of this kind that were repeated with the sections.

- (3) Joint problems are another kind of error that is also shown in Figure 1. A gap between sections will produce a line of interrupted current depending on the polarization. More accurately, it will introduce lumped reactances in the surface. This is also true at those points

where the sections make contact, but there the reactance will be different. The joints can be crudely viewed as waveguides with open or shorted ends. This type of error might be expected to repeat with each joint, but it probably does not. This is because the lumped reactances are very sensitive to the length and width of the gap.

Also, because of this sensitivity, the effects of joint errors are probably irregular with respect to the radial distance. At least they will depend on the contact points, and they may be randomly irregular also.

Another kind of joint problem would be assembly error. The assembler may not properly match the surface levels of adjacent sections.

- (4) Finally, subreflector errors are a possible source of significant error. There seems to be little data available on them, and it is not known whether they are significant. Only surface milling will be considered because positioning errors would not produce the kind of pattern errors being addressed. The subreflectors observed at SA contained only one kind of discernable error, circumferential grooves. They were very smooth and shallow and had about a  $\frac{1}{4}$  inch period. They looked like they were on the order of  $10^{-3}$  inches in depth, and they were very periodic.

### III. PLANNED ACTIVITY

Next month, the computer program will be verified, the modeled errors will be quantified, and finally they will be analyzed. Also, the joint errors will be modeled to some extent.

### IV. PROBLEMS

No technical problems were encountered in March.

### V. SCHEDULE

The program is still behind schedule as shown in Figure 2. It was not caught up in March as had been hoped. Now there is significant risk that the results will not all be obtained by the end of April. The error analyses are therefore prioritized as follows:

- Support structure errors
- Irregular joint errors
- Die defects
- Regular joint errors
- Subreflector errors

Monthly Progress Letter No. 3  
14 April 1983  
Page 6

VI. FINANCES

The total charges as of the end of March are \$2048.

Respectfully submitted,

Victor K. Tripp  
Project Director

Approved:

Charles E. Ryan, Jr.  
Chief,  
EM Effectiveness Division

**TABLE 1**  
**ERROR MODELING**

<u>Classification</u>	<u>Status</u>
<u>A. Die Defects (R)</u>	
1. Flats	M, C
2. Other defects from profile data	M, C
<u>B. Support Structure</u>	
1. Global (function of $\rho$ )	
a. Sector width errors (R)	M, C, Q
b. Intentional shaping (R)	
2. Global to sector	M, C
a. Spring back (R)	
b. Gravity sag and wind strain	
c. Assembly (registration on truss)	
3. Local	M, C, Q
a. Chordal (R)	
b. Rise near joints (R)	
<u>C. Joints</u>	
1. Regular	
a. Grooves and gaps (R?)	
b. Conducting T-gasget (R)	
2. Irregular	
a. Flange bend radius (R?)	M, C, Q
b. Height mismatch (assembly)	M, C, Q
c. Weld effects	M, C,
<u>D. Subreflector (R)</u>	Q
<p>"R" Repeated per sector</p> <p>"M" Error is mathematically modeled</p> <p>"C" Model is implemented in computer code</p> <p>"Q" Quantitative information has been obtained</p>	

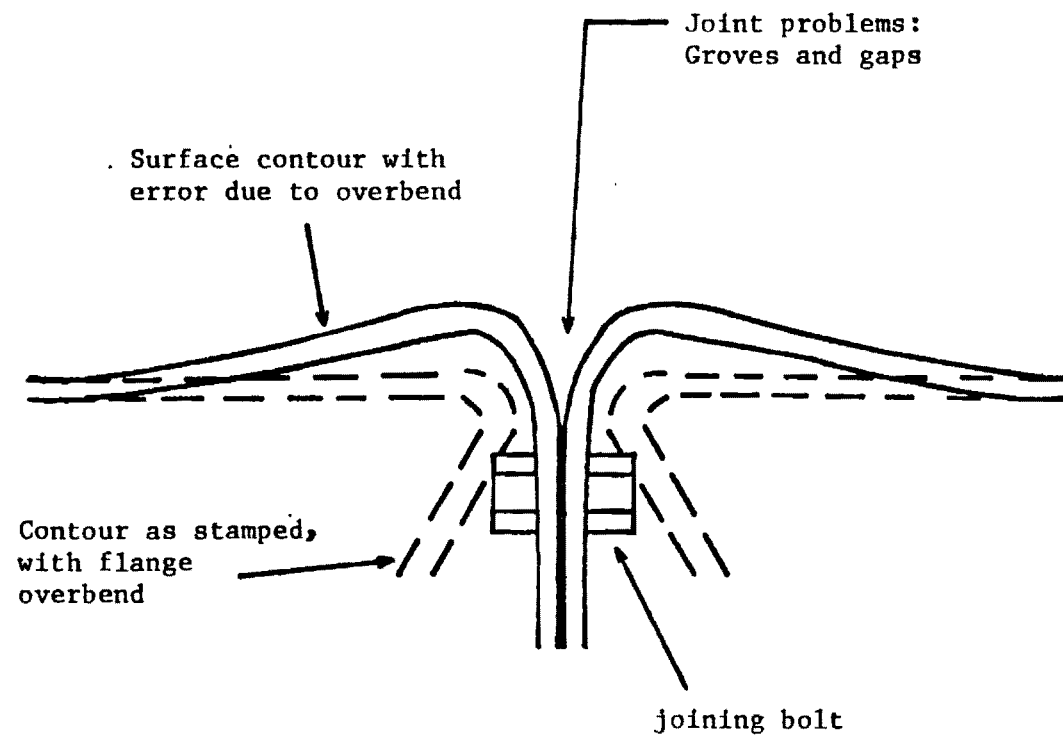
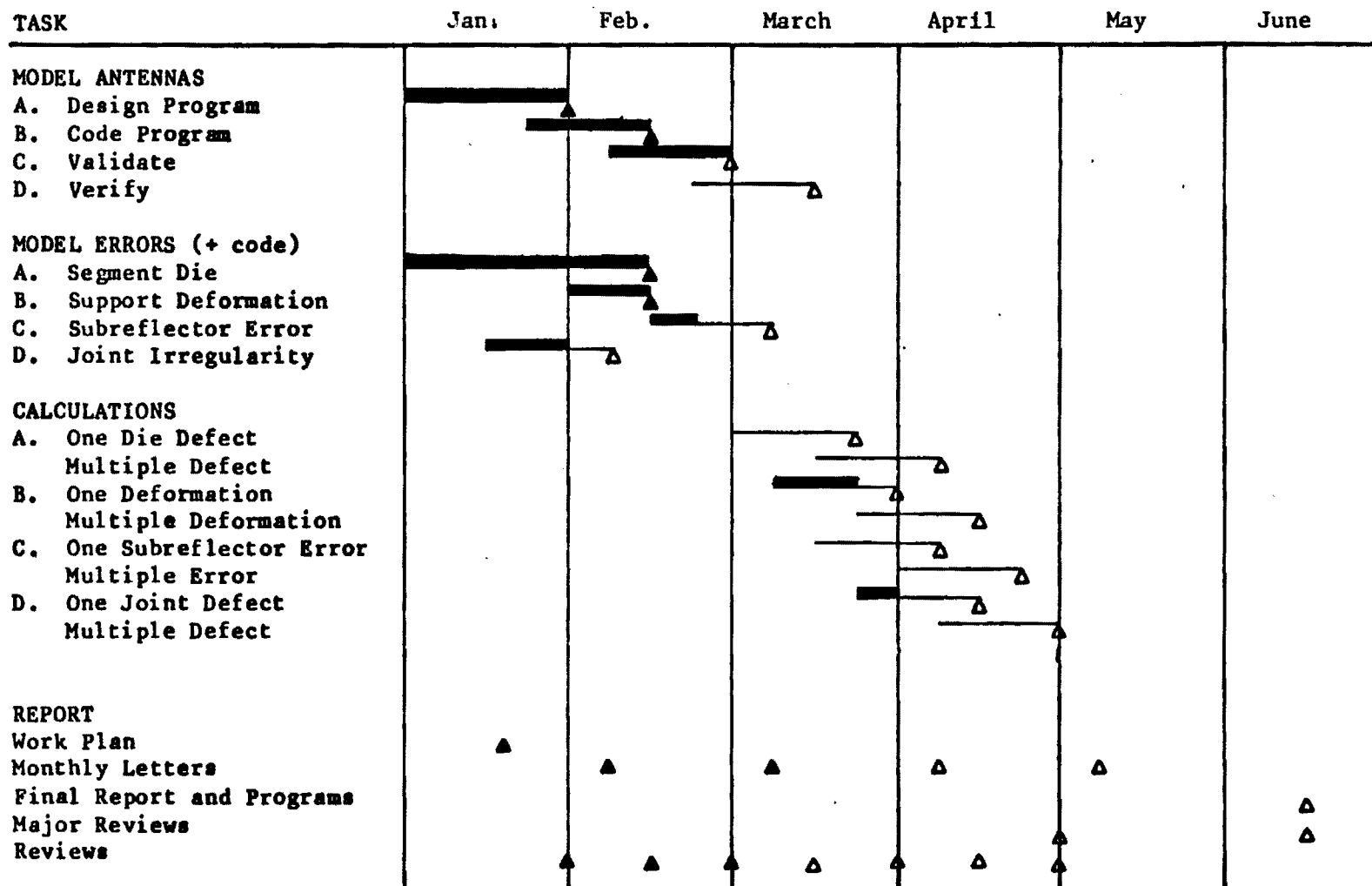


Figure 1. Surface deformations and joint problems in reflectors.



Figure 2. Schedule for detailed work plan.





ENGINEERING EXPERIMENT STATION  
Georgia Institute of Technology  
A Unit of the University System of Georgia  
Atlanta, Georgia 30332

12 May 1983

Scientific Atlanta, Inc.  
Electro Products Division  
3845 Pleasantdale Road  
Atlanta, Georgia 30340

Attention: Mr. Jim Cook

Reference: Purchase Order No. 580173  
"Dual Reflector Surface Tolerance Analysis"  
(Georgia Tech Ref. No. A-3449)

Subject: Monthly Progress Letter No. 4  
Covering the month ending 30 April 1983

Gentlemen:

A summary of activity and progress on the referenced project for the period 1 April 1983 through 30 April 1983 is herewith presented. The objective of this project is to determine relationships between construction errors and radiation performance of high-gain dual reflector antennas.

I. TECHNICAL ACTIVITY

There are three major technical tasks in this project.

- Task 1. Modeling of Antennas
- Task 2. Modeling of Errors
- Task 3. Calculations

Progress was made in all three tasks last month.

Task 1.

The purpose of this task is to develop the primary tool with which the effects of most of the antenna error types can be evaluated. This tool is a FORTRAN computer program capable of evaluating the radiation patterns in the presence of deterministic and random reflector errors.

In April, the validation and verification of the computer program were completed, making this task complete. Validation is used here to mean the determination that the FORTRAN code correctly represents the mathematical models. Verification is the assessment of the accuracy of the models by numerical evaluation of known cases. Besides the testing of individual routines, the whole program was validated for the following characteristics:

1. Symmetry was established for rotation by one sector and for arbitrary rotation for the case of no errors. This was accomplished by appropriately positioning pattern points and, by observing the symmetry of  $H_{\ell n}$  with respect to  $\ell$  and  $n$  (sector indices). Results generally agreed to  $\sim 10^{-4}$ , but were slightly variant when the integrating routine happened to select a different number of subdivisions in a given cell on the reflector.
2. Independence of the number of sectors was established in circularly symmetric cases. Here, again, many points were within  $\sim 10^{-4}$ , but some varied as much as  $\frac{1}{2}$  dB at  $\sim 20$  dB below the peak, probably for the reasons mentioned above.
3. The values on axis were compared to hand-calculated values, and the correct trends were observed as the pattern points moved off axis.
4. Independence of the sample point spacing was established. Very good agreement down to  $-30$  dB showed that the automatic subdividing of the sample cell was working properly.

Verification was performed by the following calculations:

1. The pattern for a uniform aperture was compared to the known Fourier Transform,  $\frac{J_1(x)}{x}$ . The calculations of beamwidth and first sidelobe level and position were in very good agreement.
2. Gain reduction on axis due to randomly distributed point sources was 1.17 dB compared to 1.29 dB calculated with a different program.
3. The pattern for an aperture with a 12.4 dB edge taper was compared to those computed with two other reflector programs, and was found to lie in the narrow region between them.

#### Task 2.

The purpose of this task is to develop effective mathematical ways of handling each error type and to implement them in the computer program. The investigation of joint irregularities was completed last month, by considering grooves. This investigation is reported in the attached Technical Memorandum. The two main conclusions to be drawn from it are: (1) the problem is amenable to analysis, and (2) the effort would be beyond the schedule and budget limits of this project. An effort of several man-months should be allowed to adequately address this problem.

#### Task 3.

The purpose of this task is to obtain the quantitative information for each error type and to analyze the effects of hardware errors on pattern performance. Progress was made on this task in April by obtaining further information on various types of error and by investigating the modeling of one die defect. Fred Fonda of Scientific Atlanta sent several examples of surface measurement data and provided various other quantitative information on all four types of error.

The die defect to be modeled is a flat patch on the reflector surface. The way in which it must be modeled to interface with this computer program is to express it as an additive perturbation of the error-free aperture field and to obtain its Fourier Transform. The desired model of a flat patch would be a parabolic phase bump on the otherwise flat aperture phase front. However, such a form is not readily transformed in closed form. A circularly symmetric gable function would closely approximate such a bump and is believed to be transformable in closed form. This is the form most likely to be used.

### II. REPORTING (TRIPS/VISITS)

No trips or visits occurred in April.

### III. PLANNED ACTIVITY

Next month, the remaining quantification of errors will be completed and the computer program will be used to analyze them.

### IV. PROBLEMS

No technical problems were encountered in April except that joint groove errors were found to be beyond the scope of the project.

Monthly Progress Letter No. 4  
12 May 1983  
Page 4

V. SCHEDULE

Some catching up was done in April, though the schedule is still slipped, as shown in Figure 1.

VI. FINANCES

The total charges expended or encumbered against this project at the end of April were \$13,705.

Respectfully submitted,

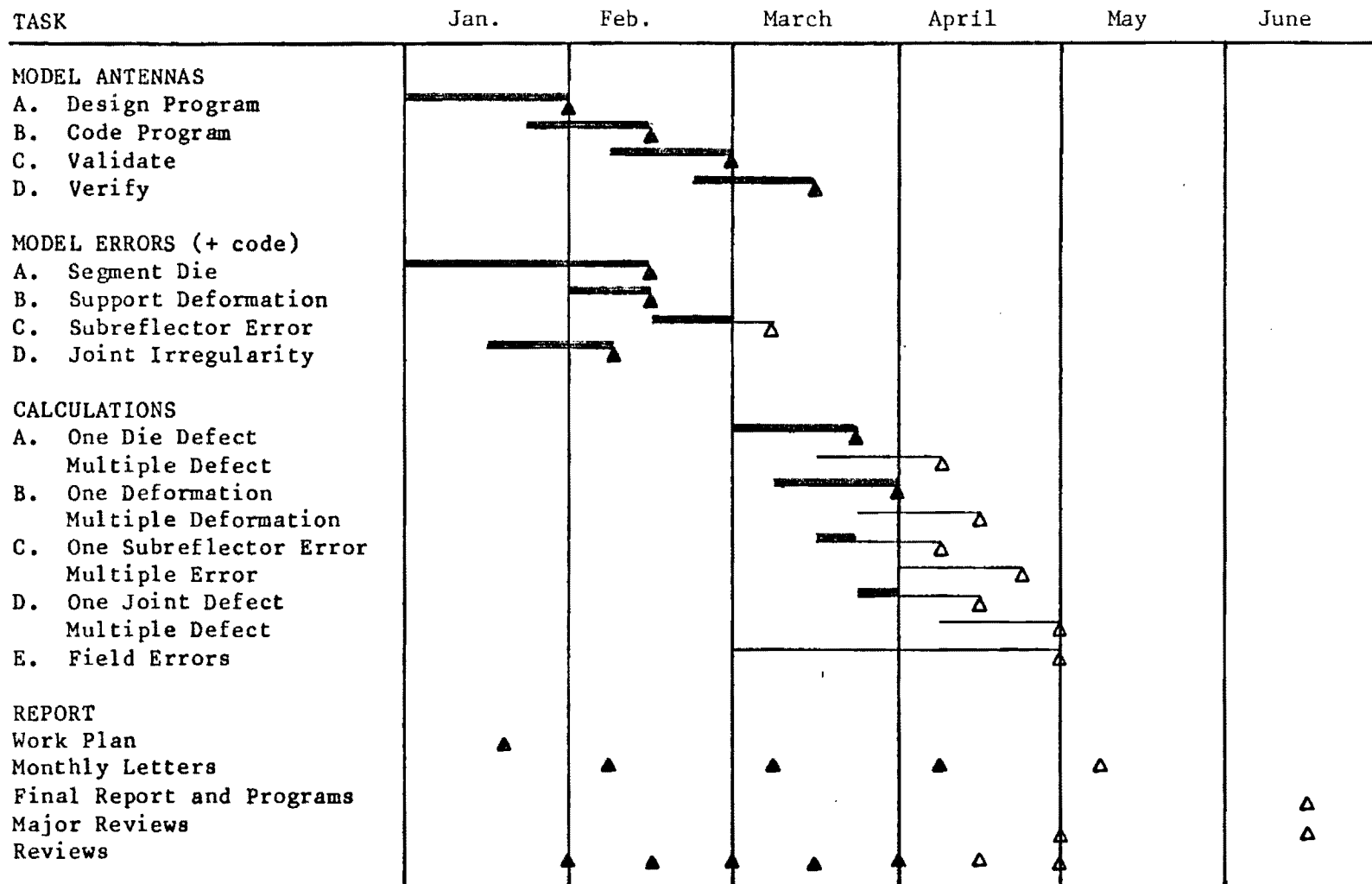
Victor K. Tripp  
Project Director

Approved:

Charles E. Ryan, Jr.  
Chief,  
EM Effectiveness Division

Attachment

Figure 1. Schedule for detailed work plan.





ENGINEERING EXPERIMENT STATION  
Georgia Institute of Technology  
A Unit of the University System of Georgia  
Atlanta, Georgia 30332

17 April 1983

TECHNICAL MEMORANDUM

TO: A-3449 Project File

FROM: J. Wang

SUBJECT:

A computational approach for an umbrella-shaped reflector antenna with slitted joints between gores.

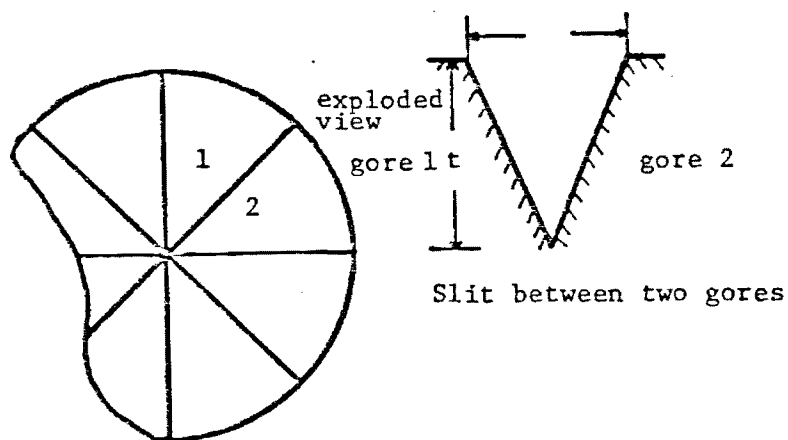
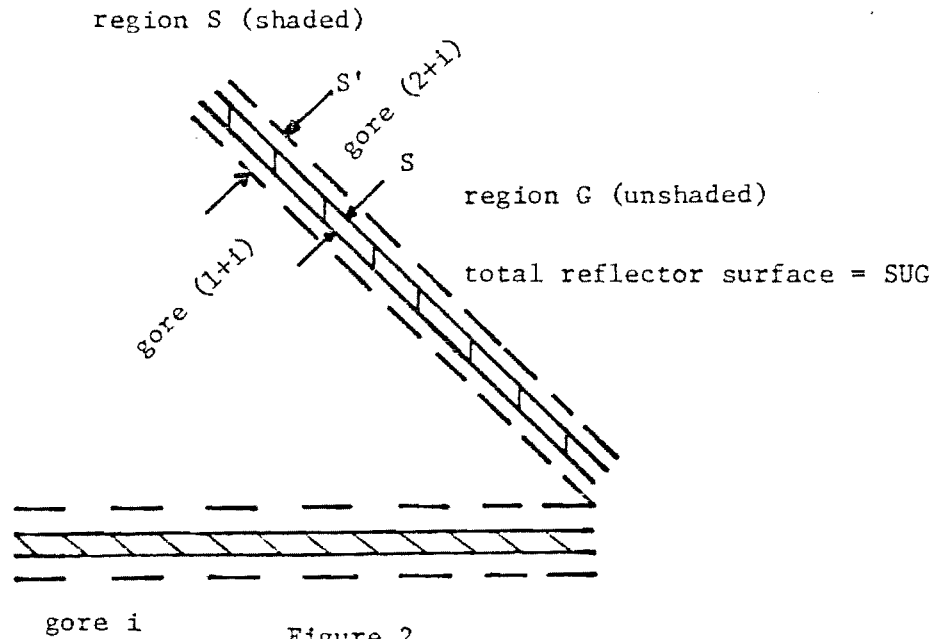


Figure 1.

The reflector antenna is shown with an exploded view at the joint between gores in Figure 1. An appropriate analysis is to divide the reflector surface into two regions: (1) a region covering and extended beyond the slit area, (2) the rest of the reflector surface. This is shown in Figure 2. The total reflected field  $\underline{E}^t$  can be considered to be

$$\underline{E}^t = \underline{E}^s + \underline{E}^R \quad (1)$$

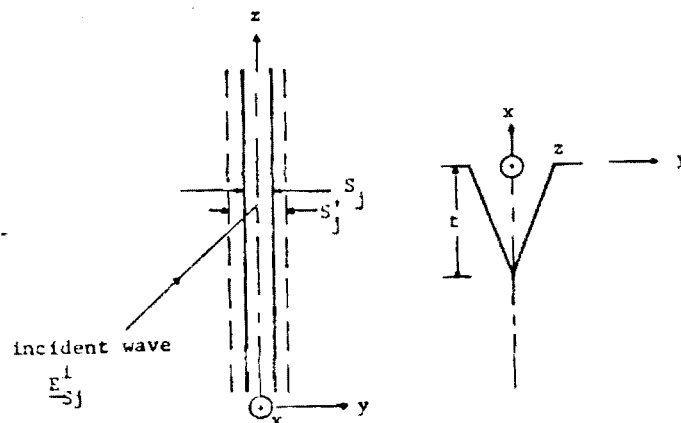


where  $\underline{E}^R$  = the reflected field in the absence of the slits  
 (perfect reflector)

and  $\underline{E}^S$  is defined by Equation (1).

$\underline{E}^S$  can be considered to be originated from the shaded region S in Figure 2. We expect S' to be perhaps  $\lambda/2$  wider than S. We also observe that for polarizations parallel to the slit, the slit poses no discontinuity problem, and it has the retrodirective property of a dihedral corner reflector. Thus, for a narrow S, the electric field component polarized parallel to the slit yields negligible  $\underline{E}^S$ . In general, the incident field has a component that is perpendicular to the slit under consideration, and the appropriate  $\underline{E}^S$  for this component must be evaluated.

The problem is now reduced to one shown in Figure 3. The incident wave is first decomposed into two components, one perpendicular to the





slit and the other parallel to it, namely

$$\underline{E}_{Sj}^i = E_{Sj}^i \hat{\theta} + E_{Sj}^i \hat{\phi} \quad (2)$$

where  $E_{Sj}^i$  is the only component need to be considered in the analysis.  $S_j$  refers to the  $j$ th joint.

We are now in a position to draw a large body of knowledge in the literature that can be applied to the scattering problem depicted in Figure 3. We will mention a few techniques in the following.

- (1) A field  $\underline{H}_{Sj}$  can be assumed over  $S'_j$ . This field should, in combination with the H-field due to  $\underline{E}^R$ , satisfy the boundary condition over  $S'_j$ . Note that the surface current does not have to vanish at the edge of the slit, but can flow into the tapered (wedged) parallel-plate waveguide formed by the slit.  $\underline{H}_{Sj}$  consists of two components, one propagates into the waveguide, and one reflected out of the waveguide. They have to be properly chosen to satisfy the boundary conditions on the surfaces (walls) of the waveguide.
- (2) The edges of the slit are, in reality, rounded, and the model in Figure 3 may have to be modified accordingly. In this case, the effect of the slit can be modeled by conventional error analysis if  $t$  is small, say, less than  $\lambda/4$ . The primary effects are depolarization and phase errors, which can be easily dealt with by conventional error analysis techniques.
- (3) It appears that the first order effect of the slits can be traced to the phase change over  $S'$  relative to the outside region. A simple model, which computes the phase change as a function of  $S$  and  $t$ , can be realistically established. This phase change is expected to differ from the  $180^\circ$  phase change over a perfectly conducting surface. There are, most likely, data and equations in the literature that can be readily used to derive the phase of the reflected wave from the slit. If not, numerical methods can be established to compute the needed phase data for specific slit configurations.

JJW:bg

ENGINEERING EXPERIMENT STATION  
**Georgia Institute of Technology**  
A Unit of the University System of Georgia  
Atlanta, Georgia 30332

7 June 1983

Scientific Atlanta, Inc.  
Electro Products Division  
3845 Pleasantdale Road  
Atlanta, Georgia 30340

Attention: Mr. Jim Cook

Reference: Purchase Order No. 580173  
"Dual Reflector Surface Tolerance Analysis"  
(Georgia Tech Ref. No. A-3449)

Subject: Monthly Progress Letter No. 5  
Covering the month ending 31 May 1983

Gentlemen:

A summary of activity and progress on the referenced project for the period 1 May 1983 through 31 May 1983 is herewith presented. The objective of this project is to determine relationships between construction errors and radiation performance of high-gain dual reflector antennas.

I. TECHNICAL ACTIVITY

There are three major technical tasks in this project.

- Task 1. Modeling of Antennas
- Task 2. Modeling of Errors
- Task 3. Calculations

Task 1.

This task is complete. Revised flow charts of the whole program and the main routine are shown in Figures 1 and 2, respectively.

Task 2.

The purpose of this task is to develop effective mathematical methods of handling each error type and to implement them in the computer program.

This task was completed in May. The Work Plan indicated that four kinds of errors would be modeled as shown in Figure 3. Three of these error types have been addressed, but the subreflector error has been abandoned in lieu of measurement errors. That is, subroutines were written to allow the Scientific Atlanta surface measurement data to be used by the computer program. Due to the unplanned effort involved and the results of early calculations, the analysis of subreflector errors was abandoned. Calculations thus far have indicated that most of the performance error can be accounted for by primary-reflector errors alone.

The model for random die defect errors has been found to be too slow as implemented. Therefore, efforts have been directed at modifying the mathematical model to allow more numerically efficient implementation. In particular, the integral that represents correlation between sectors has been cast in the form of Fourier Transforms. One such modification is recorded in the attached Technical Memorandum from C. Papanicolopoulos. Another modification has not yet been documented. Subsequent to this effort, it has been shown by other calculations that this kind of error is probably insignificant. Thus, further effort is not appropriate in this area.

### Task 3.

The purpose of this task is to obtain the quantitative information for each error type and to analyze the effects of hardware errors on pattern performance. Most of the effort in May was directed toward this task.

It was reported last month that a circularly symmetric gable would probably be used to model "die defects." However, such a function in the exponential form that represents phase did not show much promise of being Fourier Transformable in closed form. A little more effort was spent on this task before other calculations showed that die defects should be insignificant. For the record, a parabolic function with a rectangular parameter shows the most promise. Its transform should be the product of two rapidly converging series.

Many calculations were performed in May on various antenna and error configurations. The primary configurations are summarized in the attached Technical Memorandum of 19 May. Again, measurement errors are considered in lieu of subreflector errors. The most interesting result was that the "cusp error" exhibited a performance characteristic similar to problems that have been observed, but not yet explained, by Scientific Atlanta. This characteristic is an increased level of the third or fourth sidelobe and beyond. Most of these calculations were made for theta cuts with theta between  $0^\circ$  and  $10^\circ$ . Generally, two cuts were made to test circular symmetry. The results have been plotted and will be included in the final report.

## II. REPORTING (TRIPS/VISITS)

Jim Cook of Scientific Atlanta visited Vic Tripp of Georgia Tech on 9 May and 17 May. Mr. Cook was accompanied by Young Kwan on the first visit. The purpose of the visits was to review progress and to give Georgia Tech information regarding the configurations of most interest to Scientific Atlanta.

## III. PLANNED ACTIVITY

Next month, the calculations will be completed, the report will be written and the program will be documented.

## IV. PROBLEMS

No significant problems were encountered in May.

## V. SCHEDULE

The work is nearly complete as shown in Figure 3. The program termination will be extended to the end of June to accommodate the schedule of the Major Review. Calculation of "Field Errors" has been removed from the schedule because it was originally included as the result of a misunderstanding.

## VI. FINANCES

The total charges expended or encumbered against this project as of the end of May were \$28,864.

Respectfully submitted,

Victor K. Tripp  
Project Director

Approved:

Charles E. Ryan, Jr.  
Chief,  
EM Effectiveness Division

Attachment

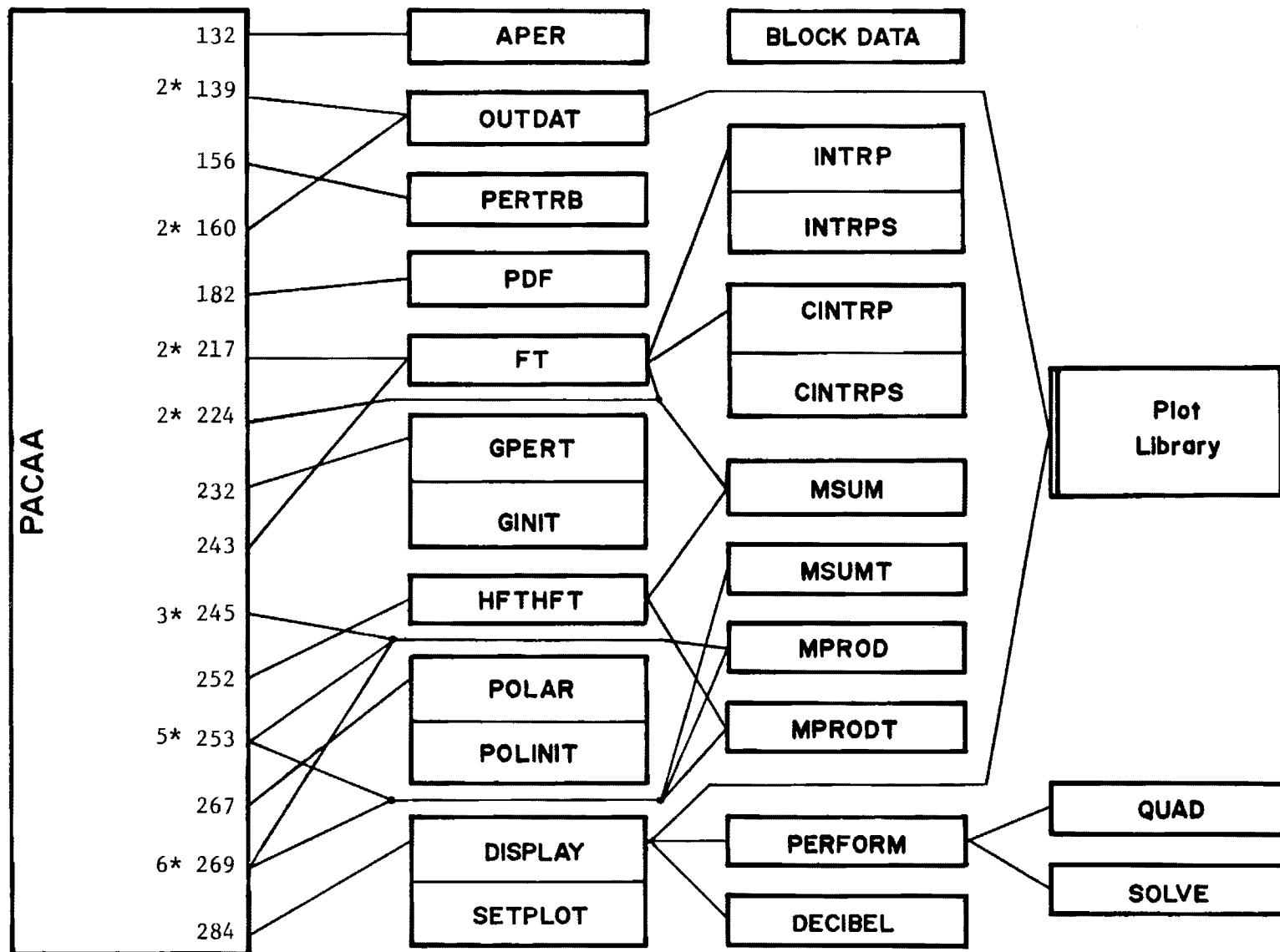


Figure 1. Block diagram of entire program.

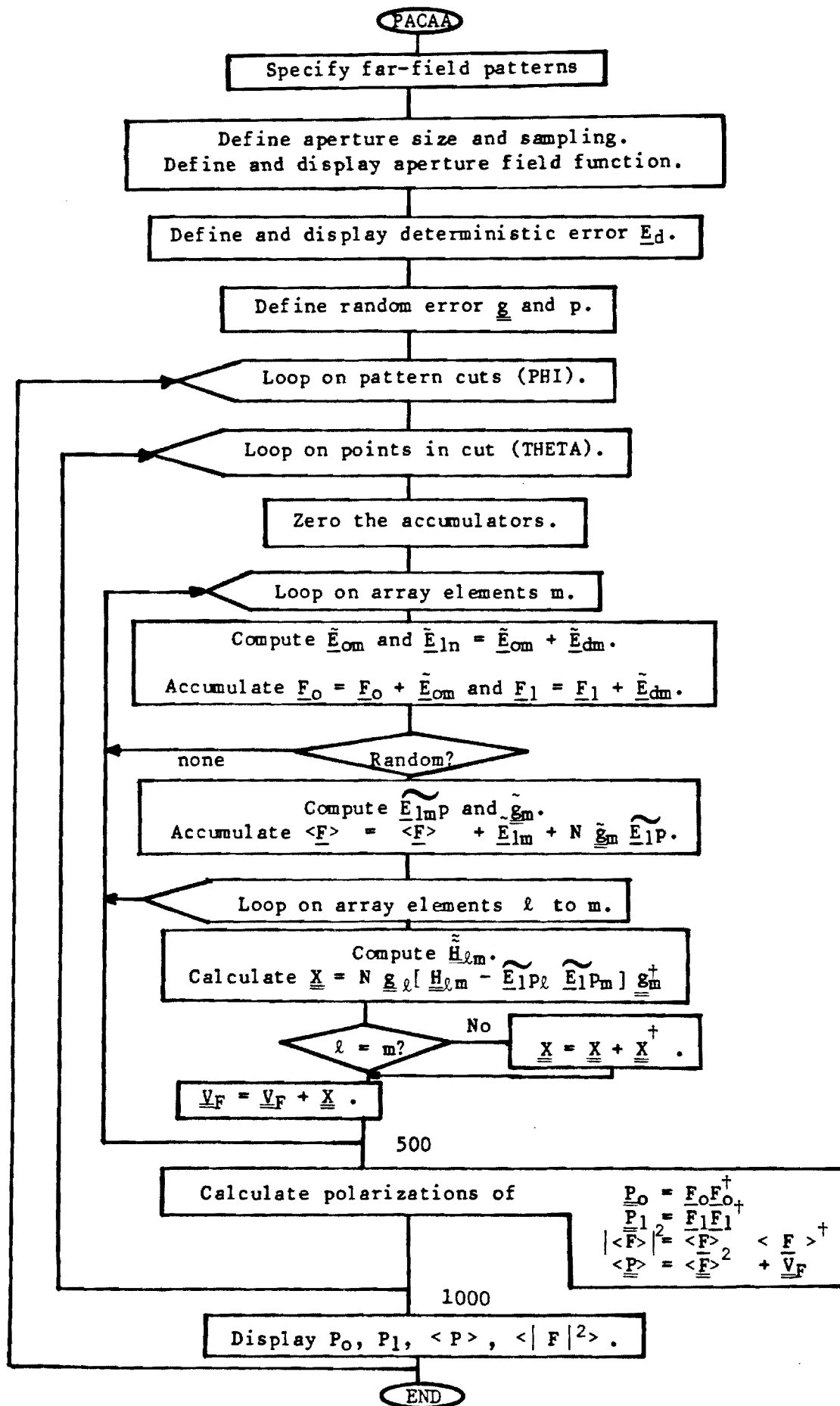


Figure 2. Flow chart of main routine.

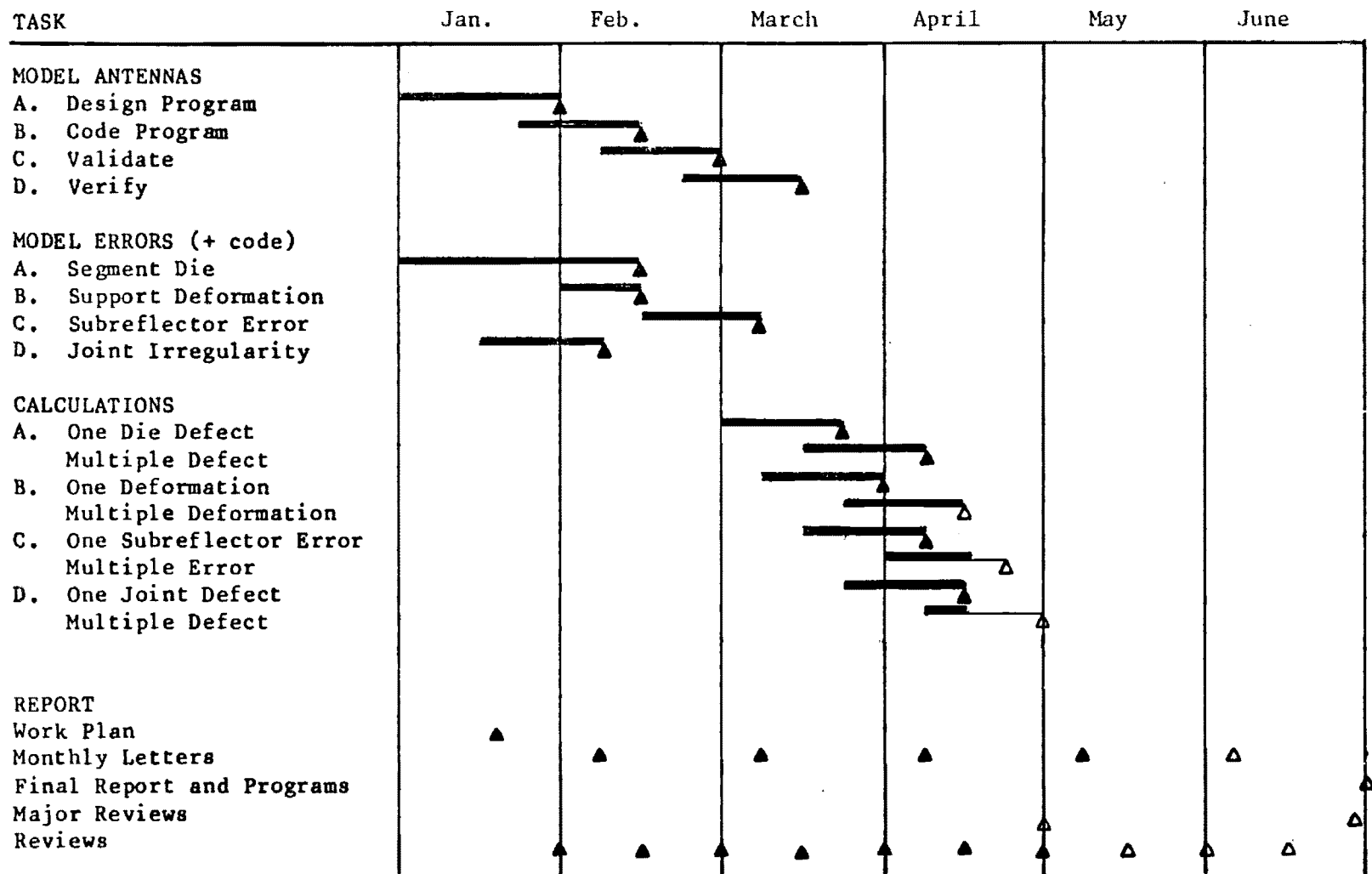


Figure 3. Schedule for detailed work plan.



ENGINEERING EXPERIMENT STATION  
Georgia Institute of Technology  
A Unit of the University System of Georgia  
Atlanta, Georgia 30332

19 May 1983

TECHNICAL MEMORANDUM

TO: Project File A-3449-000 . . .  
FROM: V. K. Tripp  
SUBJECT: Antenna and Error Configurations Analyzed in May

A. ANTENNAS

1. 50λ Diameter  $f = 20 \lambda$   
 $e = 2$   
 $d_s = 6 \lambda$  (Used, but may not be accurate)

Feed =  $\cos^{16} \theta$ ,  $\theta_{\max} \approx 23$   
Edge taper = -12.44 dB. (Includes space loss)  
8 sectors

2. 100λ Diameter  $d_s = 12 \lambda$   
 $f_p = 35$   $f_c = 21 \lambda$   
 $e = 1.552$   
 $\theta_p = 71.075^\circ$   $\theta_s = 17.575^\circ$

$$\text{Feed} = \frac{\exp[-(A\theta)^2] + b}{1 + b} \quad b = -50 \text{ dB} = .0031623$$
$$A = \frac{1.179}{\theta_s} = 3.8436$$

Edge taper = -12.18 dB  
8 sectors

3. 216λ Diameter
- |                          |                           |              |
|--------------------------|---------------------------|--------------|
| $f_p = 68''$             | $d_s = 23''$              |              |
| $f/D = .316$             | $f_c = 40''$              | $e = 1.4683$ |
| $\theta_p = 76.91^\circ$ | $\theta_s = 17.127^\circ$ |              |

Freq.	b	Taper	A	A/θ <sub>s</sub>
11.95 GHz	-50 dB	-10 dB	1.076	3.5996
14.5 GHz	-50 dB	-16 dB	1.3635	4.5614



## B. ERRORS

### General

Measurements used in these calculations were made of normal surface error on a 5.5 M antenna on 14 March 1980. Total surface error was .023". The first five error problems were assigned 9 May. All were performed on the 100 $\lambda$  reflector and some were repeated on the 50  $\lambda$  reflector.

#### 1. Profile Errors

The following profile errors were used after scaling the radii to correspond to a 50 $\lambda$  maximum. Error values were entered at every 2 $\lambda$  which were obtained by rough interpolation of these data.

Given % radius	Radius Used	Error
.31	16	-.015
.45	22	+.005
.53	26	-.013
.64	32	+.008
.75	38	+.010
.84	42	+.006
.95	48	-.009

#### 2. Die Defects

These errors were gable functions separable in theta and phi and located at 40 $\lambda$ , 17.5°. They were .063" deep x 4 $\lambda$ , 5° in size and were repeated in each of 8 sectors.

#### 3. Assembly Error

Measurements of error on the first radius were used to define the leading edge of every sector. The numbers entered every 2 $\lambda$  were obtained by linear interpolation between scaled measurement radii. The rest of the sector was made to taper linearly to zero at the other edge. The measured values are:

Measurement Radius	Scaled Radius	Error
-	0	-.051*
31.312	14.46	.003
45.018	20.79	.035
57.839	26.71	-.033
70.037	32.34	.014
81.689	37.73	.013
90.579	41.83	.021
101.449	46.85	.017

\*This number was estimated because extrapolated value was too extreme.

#### 4. Measured Error

In this case, the aperture sample points were made to fall at the same  $\phi$  angles as the measurement data, and the whole reflector was considered to be one sector. At each angle there were not enough sample points so a linear interpolation was used. Furthermore, the program uses a bilinear interpolation in each aperture cell to perform its integration. An error was rather arbitrarily assigned at a radius of zero because extrapolation to the minimum radius would have yielded unreasonably high errors.

#### 5. Cusp Error

This joint error is approximated by errors that are independent of radius. Each edge of each sector was made .025" high with a taper to zero at  $2.3^\circ$  each way from the joint. The angle was chosen to make the cusps extend  $\pm 2$ " at the reflector edge.

#### 6. Larger Cusp Error (17 May)

This case was similar to the above. The same antenna was used except this one was divided into 16 sectors. Each edge was raised  $.125 \lambda$  and tapered to zero error at  $\pm 4^\circ$ . At the reflector edge  $4^\circ$  is 3.5".

#### 7. Measured Error on Larger Reflector (17 May)

This case was similar to number 4 except that Antenna 3 was used with errors measured on 4 March 1980. In this case, the error at zero was set at  $-.066$ ". The method used to set the origin error in Case 4 would have yielded  $.079$ ". This was deemed too large, and a number was chosen that would yield the same average slope in this region of the reflector.

VKT:bg

ENGINEERING EXPERIMENT STATION  
Georgia Institute of Technology  
A Unit of the University System of Georgia  
Atlanta, Georgia 30332

8 June 1983

MEMORANDUM

TO: Project File A-3449

FROM: Chris D. Papanicolopoulos

REFERENCE: Tech Memo to Project File A-3449, 27 January 1983

SUBJECT: Determination of the Double Fourier Transform  
of the Center Term  $\underline{H}_{\ell m}$  of Reference Equation (22)

Problem

The task in hand is defined as follows:

Reference Equation (25) is given by,

$$\underline{H}_{\ell m} \approx \int \underline{E}_O(\underline{r}_m + \underline{r}_{\ell m}) \underline{E}_O^*(\underline{r}_m) P(\underline{r}_m) \exp(-j\mathbf{k} \cdot \underline{r}_{\ell m}) d\underline{r}_m . \quad (1)$$

We seek to obtain a reduced form for the integrand function in Equation (1) such that the integration can be performed in closed form in terms of Fourier Transforms.

This can be accomplished by means of coordinate transformations. Simplifying the notation, let

$$\underline{d} \equiv \underline{r}_{\ell m} = \underline{r}_m - \underline{r}'_{\ell} . \quad (2)$$

The relation between  $\underline{r}_m$  and  $\underline{r}'_{\ell}$  can be expressed by means of an orthogonal transformation equation:

$$\underline{R} \underline{r}_m = \underline{r}'_{\ell} , \quad (3)$$

where  $\underline{R}$  is the orthogonal transformation operator corresponding to a rotation of a two-dimensional Cartesian system (x,y) by an angle  $\theta$  around the z axis.

Thus, more explicitly Equation (3) in matrix notation becomes ,

$$\begin{bmatrix} \cos\theta & \sin\theta \\ -\sin\theta & \cos\theta \end{bmatrix} \begin{bmatrix} x \\ y \end{bmatrix} = \begin{bmatrix} x' \\ y' \end{bmatrix} \quad (4)$$

where  $\underline{r}_m = x\hat{i} + y\hat{j}$ ,  $\underline{r}'_m = x'\hat{i}' + y'\hat{j}'$  and  $\hat{i}$ ,  $\hat{j}$  are the unit vectors in the (x,y) and (x',y') system correspondingly.

#### Analysis

Using Equation (4)  $\underline{d}$  becomes ,

$$\underline{d} = \underline{I}\underline{r}_m - \underline{R}\underline{r}_m \quad , \quad (5)$$

$$\text{or } \underline{d} = [\underline{I} - \underline{R}] \underline{r}_m \quad . \quad (6)$$

Where  $\hat{I}$  is the identity operator in a two-dimensional orthogonal basis. Thus, we obtain  $\underline{d}$  explicitly in matrix notation:

$$\underline{d} = \begin{bmatrix} 1-\cos\theta & -\sin\theta \\ +\sin\theta & 1-\cos\theta \end{bmatrix} \begin{bmatrix} x \\ y \end{bmatrix} \quad (7)$$

As a consequence of Equation (6) we can express the integrand function  $\underline{E}_0(\underline{r}_m + \underline{r}_{\ell m}) \underline{E}_0^+(\underline{r}_m) p(\underline{r}_m)$  as a function of  $\underline{r}_m$  only, thus:

$$\underline{F}(\underline{r}_m) = \underline{E}_0(\underline{r}_m + \underline{r}_{\ell m}) \underline{E}_0^+(\underline{r}_m) p(\underline{r}_m) \quad , \quad (8)$$

$$\text{or } \underline{F}(x,y) = \underline{E}_0(\underline{R} \underline{r}_m) \underline{E}_0^+(\underline{r}_m) p(\underline{r}_m) \quad . \quad (9)$$

From Equation (9) and letting  $d\mathbf{r}_m = dx dy$ , Equation (1) reduces to,

$$\underline{\tilde{H}} = \int \underline{F}(x,y) e^{-j\mathbf{k} \cdot \underline{d}} dx dy. \quad (10)$$

Furthermore, expressing the vector  $\underline{k}$  in terms of its Cartesian components,

$$\underline{k} = k_x \hat{i} + k_y \hat{j}, \quad (11)$$

we can express the dot product  $\underline{k} \cdot \underline{d}$ , making use of Equation (7), as,

$$\underline{k} \cdot \underline{d} = \{ k_x x (1 - \cos \theta) - k_x y \sin \theta + k_y x \sin \theta + k_y y (1 - \cos \theta) \}. \quad (12)$$

After factorization of the coefficients of the  $x$  &  $y$  we obtain,

$$\underline{k} \cdot \underline{d} = x \{ k_x (1 - \cos \theta) + k_y \sin \theta \} + y \{ k_y (1 - \cos \theta) - k_x \sin \theta \}. \quad (13)$$

At this point let

$$k_x (1 - \cos \theta) + k_y \sin \theta = k'_x, \text{ and} \quad (14)$$

$$k_y (1 - \cos \theta) - k_x \sin \theta = k'_y. \quad (15)$$

Then we observe that the relation between  $k'_x, k'_y$  and  $k_x, k_y$  is a simple orthogonal transformation relation which can be given by ,

$$\begin{bmatrix} 1 - \cos \theta & \sin \theta \\ -\sin \theta & 1 - \cos \theta \end{bmatrix} \begin{bmatrix} k_x \\ k_y \end{bmatrix} = \begin{bmatrix} k'_x \\ k'_y \end{bmatrix}, \quad (16)$$

or in condensed form, by

$$\underline{\underline{A}} \underline{k} = \underline{k}' ,$$

where A is the operator of the orthogonal transformation,

$$\text{and } \underline{\underline{A}} = \{ \underline{\underline{I}} - \underline{\underline{R}} \}^{-1} . \quad (17)$$

thus utilizing Equations (13), (14), and (15), the exponential term in Equation (10)  $e^{-j\underline{k} \cdot \underline{d}}$  becomes,

$$e^{-j\underline{k} \cdot \underline{d}} = e^{-j(k'_x x + k'_y y)} , \quad (18)$$

which implies that Equation (10) can be reduced to the following Fourier Transform:

$$\underline{\underline{H}} = \int \underline{\underline{F}}(x,y) e^{-j(k'_x x + k'_y y)} dx dy . \quad (19)$$

### Conclusions

$\theta$  and therefore R depend only on  $\ell-m$ . Therefore, there are M different transformations A. If E is rotationally symmetrical (p always is), then there are M Fourier Transforms. Otherwise, there are  $M^2/2$  FT's. But since the integrals are expressed as FT's, they are done once, and all pattern points are interpolated. (Since we want polar patterns, all must be interpolated even if k is not linearly transformed.) There is still the problem that a sector (region bounded by polar coordinate constants) is not convenient to Fourier Transform in this way.

CP:bg



ENGINEERING EXPERIMENT STATION  
**Georgia Institute of Technology**  
A Unit of the University System of Georgia  
Atlanta, Georgia 30332

18 August 1983

Scientific Atlanta, Inc.  
Electro Products Division  
3845 Pleasantdale Road  
Atlanta, Georgia 30340

Attention: Mr. Jim Cook

Reference: Purchase Order No. 580173  
"Dual Reflector Surface Tolerance Analysis"  
(Georgia Tech Ref. No. A-3449)

Subject: Monthly Progress Letter No. 6  
Covering the month ending 30 June 1983

Gentlemen:

A summary of activity and progress on the referenced project for the period 1 June 1983 through 30 June 1983 is herewith presented. The objective of this project is to determine relationships between construction errors and radiation performance of high-gain dual reflector antennas.

I. TECHNICAL ACTIVITY

There are three major technical tasks in this project.

- Task 1. Modeling of Antennas
- Task 2. Modeling of Errors
- Task 3. Calculations

The first two tasks were completed last month, and Task 3 was completed in June. The effort of Task 3 involved further calculations with the surface error program, primarily for a 96-inch reflector at 20 and 30 GHz. Results from measured surface errors indicated that higher error levels may be allowable than those indicated by conventional rules. The details are contained in the final report.

## II. REPORTING (TRIPS/VISITS)

A major program review was held at NASA-Lewis in Cleveland, OH, on 28-29 June. Victor Tripp of Georgia Tech accompanied Jim Cook, Bob Sullins and others of Scientific-Atlanta and participated in the briefing on 28 June. Most of the calculations contained in the final report were reviewed, and the observation that "cusp" errors are a primary problem was presented.

During June, the computer program was finalized and prepared for delivery, and much of the documentation was written.

Also in June, the final report was prepared.

## III. PLANNED ACTIVITY

Next month, the final report and computer-program documentation will be printed. Also, another calculation will be performed that will not be included in the final report, as agreed by Scientific-Atlanta.

## IV. PROBLEMS

None.

## V. SCHEDULE

The program is being extended to the end of July to allow Georgia Tech to calculate a special surface-error configuration.

## VI. FINANCES

The total charges expended or encumbered against this project as of the end of June were \$35,782.59.

Respectfully submitted,

VICTOR A. TRIPP  
Project Director

Approved:

Charles E. Ryan, Jr.  
Chief,  
EM Effectiveness Division



**FINAL TECHNICAL REPORT  
GIT/EES PROJECT A-3449**

## **SURFACE TOLERANCE ANALYSIS OF SYMETRICAL DUAL-REFLECTOR ANTENNAS**

**By  
V. K. Tripp**

**June 1983**

**Prepared for  
SCIENTIFIC-ATLANTA, INC.  
ELECTRO PRODUCTS DIVISION  
ATLANTA, GEORGIA 30340**

**Under  
Purchase Order No. 580173**

### **GEORGIA INSTITUTE OF TECHNOLOGY**

**A Unit of the University System of Georgia  
Engineering Experiment Station  
Atlanta, Georgia 30332**



1983



FINAL TECHNICAL REPORT  
GIT/EES PROJECT A-3449

**SURFACE TOLERANCE ANALYSIS OF SYMMETRICAL  
DUAL-REFLECTOR ANTENNAS**

By

V. K. Tripp

June 1983

Prepared for

Scientific-Atlanta, Inc.  
Electro Products Division  
Atlanta, Georgia 30340

Under

Purchase Order No. 580173

By

Electromagnetic Effectiveness Division  
Electronics and Computer Systems Laboratory  
Engineering Experiment Station  
Georgia Institute of Technology  
Atlanta, Georgia 30332

THIS PAGE INTENTIONALLY LEFT BLANK

## PREFACE

The research reported in this document was performed at the Engineering Experiment Station (EES) of the Georgia Institute of Technology for the Electro Products Division of Scientific-Atlanta, Inc. in fulfillment of Purchase Order No. 580173. Technical direction was exercised through Mr. Jim Cook of Scientific-Atlanta, and Mr. Victor Tripp was the Project Director at Georgia Tech. The work was performed by the personnel of the Electronics and Computer Systems Laboratory of EES. The work was primarily performed by personnel of the Electromagnetic Effectiveness Division (EED), but a contribution was made by personnel of the Electromagnetic Compatibility Division. The work reported herein was performed between 1 January 1983 and 30 June 1983.

The author would like to acknowledge the extensive support provided by Mr. Jim Cook of Scientific-Atlanta. Mr. Fred Fonda also provided helpful information. Appreciation is also expressed to the participants at Georgia Tech, especially Barry Cown, Chris Papanicolopoulos, and Darrell Acree. Thanks are also extended to Dr. Charles E. Ryan, Jr. for administrative support and Miss Beatriz Gonzalez for typing this report.

Respectfully submitted,

Victor K. Tripp  
Project Director

Approved:

Charles E. Ryan, Jr.  
Chief,  
EM Effectiveness Division

THIS PAGE INTENTIONALLY LEFT BLANK

## TABLE OF CONTENTS

<u>Section</u>	<u>Page</u>
I. INTRODUCTION . . . . .	1
II. ANTENNA MODELING . . . . .	3
A. General Features . . . . .	3
B. Specific Models . . . . .	5
1. Illumination Function . . . . .	5
2. Reflector Integration . . . . .	9
III. ERROR MODELING . . . . .	13
A. Die Defects . . . . .	13
B. Support Structure . . . . .	14
1. Global Errors . . . . .	14
2. Errors that are Global per Sector . . . . .	15
3. Local Errors . . . . .	16
C. Joint Errors . . . . .	18
D. Measured Errors . . . . .	18
IV. RESULTS . . . . .	21
A. Die Defects . . . . .	21
B. Profile Error . . . . .	23
C. Assembly Error . . . . .	24
D. Cusp Error . . . . .	24
E. Measured Error . . . . .	28
V. CONCLUSIONS . . . . .	33
 <u>Appendices</u>	
A. A NEW APPROACH TO THE ANALYSIS OF RANDOM ERRORS IN APERTURE ANTENNAS . . . . .	37
B. A MODEL OF REFLECTOR ERRORS CAUSED BY DIE DEFECTS . .	64
C. CALCULATED PATTERNS . . . . .	71

THIS PAGE INTENTIONALLY LEFT BLANK

## LIST OF FIGURES

<u>Figure</u>	<u>Page</u>
1. Coordinate system for antenna model. . . . .	4
2. Geometry of a dual-reflector antenna . . . . .	6
3. Reflector perturbation and ray path-length error . .	7
4. Errors at joints of reflector sector panels. . . . .	17
5. Measured errors of 14 March 1980 for a 5.5 M reflector, as used with Antenna II. . . . .	25
6. Measured errors of 4 March 1980 for a 5.5M reflector, as used with Antenna III . . . . .	29
7. Data of Figure 6 scaled by .75,as used with Antenna IV . . . . .	31



THIS PAGE INTENTIONALLY LEFT BLANK

## LIST OF TABLES

<u>Table</u>		<u>Page</u>
1.	ANTENNAS ANALYZED. . . . .	22
2.	PROFILE ERROR INPUT. . . . .	23
3.	RADIAL ASSEMBLY ERROR INPUT FOR ANTENNA II . . . . .	26
4.	RADIAL ASSEMBLY ERRORS FOR ANTENNA I . . . . .	26
5.	NORMALIZED AZIMUTHAL ASSEMBLY ERRORS FOR ANTENNAS I AND II . . . . .	27
6.	CUSP ERRORS. . . . .	27
7.	PERFORMANCE WITH MEASURED ERROR. . . . .	32

THIS PAGE INTENTIONALLY LEFT BLANK

## SECTION I

### INTRODUCTION

High-gain, dual-reflector antennas are finding much application as earth-station antennas for satellite communication. Surface tolerance in high-gain reflector antennas is always important because the gain is reduced by surface errors. However, satellite communications antennas also have rigid specifications on the sidelobe levels that limit surface tolerances even further. In addition, as operating frequencies are increased the surface errors must be reduced in proportion to the wavelength decrease. Thus, the surface tolerance requirements can readily become the primary cost factor in the production of satellite antennas. This is especially true since the relationship between cost and surface accuracy is not linear; the cost accelerates greatly as different manufacturing techniques are required to meet lower tolerance specifications.

Because of this cost acceleration at low tolerance levels, it is important to know the relationship between performance and surface accuracy. Rules of thumb for this relationship have long been used since accuracy cost has not been such a critical factor. With the tighter specifications and higher frequencies of the future, it will be important to have a much better understanding of the relationship between surface errors and performance. The relationship of error type and performance is also important since some types of error are much more costly to eliminate than others are.

This study was, therefore, initiated with the objectives of (1) identifying the sources of error that most degrade performance, and (2) determining the relationship between these errors and the antenna performance. The purpose is to obtain information that will allow the manufacture of antennas that meet performance specifications with minimum cost. The performance requirements considered in this investigation concerned primarily sidelobe levels, but antenna gain was also involved. Scientific-Atlanta has observed specific angular regions in which specified sidelobe levels are characteristically exceeded. Therefore, one objective of this investigation was to determine if this observed performance degradation was caused by a particular type of error. If the dominant

error type can be identified, it may be feasible to correct the source of that particular error type. This approach may be more cost-effective than reducing the tolerance on all the possible manufacturing errors.

The approach to this investigation centers around the development of a computer program to evaluate patterns of a large dual-reflector antenna, including manufacturing error effects. The computer program is limited to circularly symmetric antennas and provides for polarization calculations. Possible sources of error were then identified, and those kinds of error deemed most significant were mathematically modeled. The error models were implemented in computer code for use with the reflector-antenna program. Finally, the antenna and error models were evaluated for the antennas and characteristic error types of interest to Scientific-Atlanta. The error configurations that resulted in significant performance degradation were further investigated. As a result of these investigations, the dominant error types were identified and the performance of the antenna as a function of error magnitude was assessed.

## SECTION II

### ANTENNA MODELING

There are many computer programs available that evaluate the radiation patterns of reflector antennas. Indeed, the author of this report has written and documented three such programs of varying degrees of speed and generality. However, it was decided that a computer program specific to this investigation would be worth the development effort. The more general existing programs would be too costly to execute for the very large reflectors being considered here. On the other hand, the faster of the existing programs are somewhat more specialized and would not be readily adaptable or very accurate.

This section discusses the general characteristics of the models programmed and the reasons for choosing them. For more detail, the reader is referred to the computer program documentation [1] .

#### A. General Features

All of the antennas to be considered in this investigation are rotationally symmetric. Indeed, they would be circularly symmetric except for errors that are associated with the construction sector panels. (Strictly speaking, polarization calculations will not possess this symmetry.) Because of the symmetry, these surface errors are much easier to describe in cylindrical coordinates than in rectangular coordinates. For this reason, the cylindrical coordinate system shown in Figure 1 was used for the antenna models. This choice allows calculation reduction by use of symmetry for some cases. In addition, the random-error integration must be done by sector, and this task is much more convenient in a polar coordinate system.

The physical-optics method of calculation was chosen for closely related reasons. First, it is much more accurate than aperture techniques. Second, although the primary advantage of an aperture technique is that it allows the use of the Fast Fourier Transform (FFT) algorithm, in this case

---

[1] V. K. Tripp, "Physical Optics Program for the Analysis of Error in Circularly Symmetrical Reflector Antennas," Georgia Institute of Technology, Project A-3449, Computer Program Documentation, for Scientific-Atlanta, June 1983.

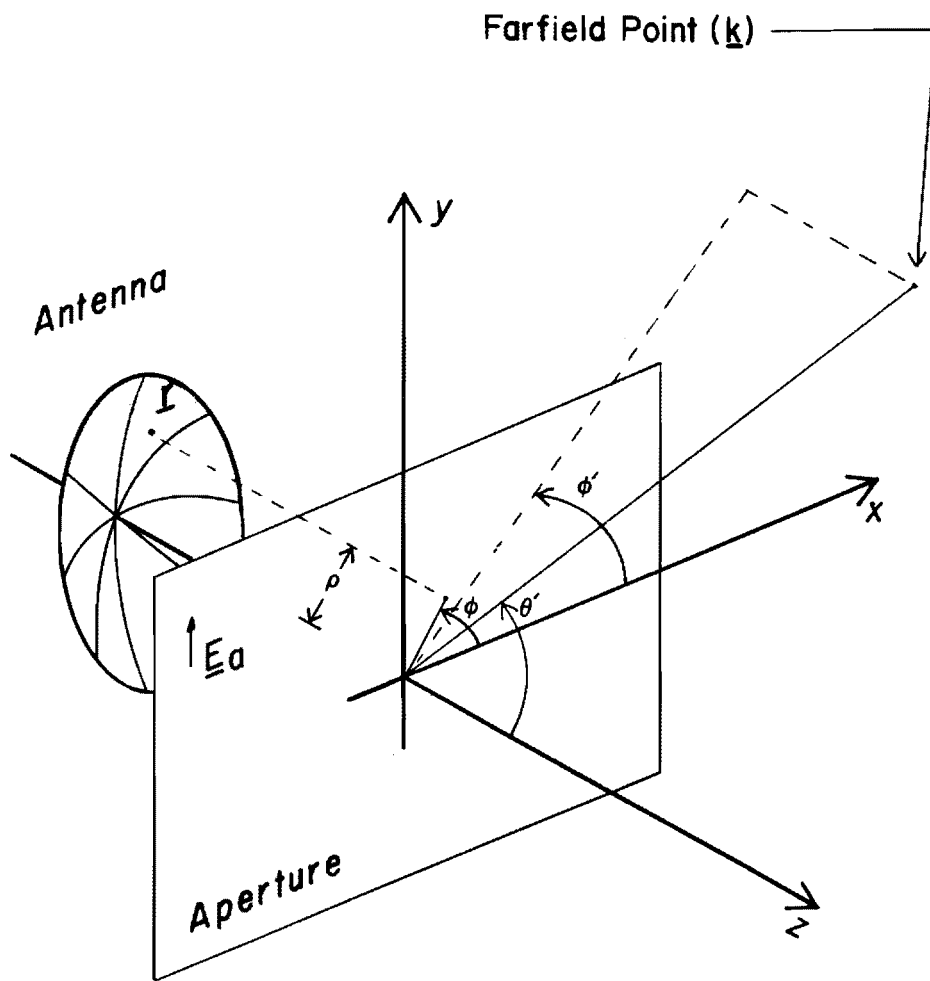


Figure 1. Coordinate system for antenna model.

the FFT algorithm cannot be used because of the choice of cylindrical coordinates. Since integration over the reflector is only slightly more expensive than the alternative of integrating over the aperture, it was selected as the approach.

Diffraction was not included in this model because it is not very significant near the main beam for such large reflectors. It has been found in retrospect that the results were adequate without including diffraction. That is, error sources were identified and adequately related to performance characteristics using only the physical optics contribution. On the other hand, a diffraction calculation could only improve the accuracy of the model, and consideration should be given to adding it in the future.

Electric field polarization was included in the model. For the investigation performed, it was not found to be very useful, but the extra development effort it entailed was also not very large. It may be found useful for other applications of this computer program.

No attempt is made by this program to evaluate antenna directivity or gain. Thus, the output patterns are not absolute values, but they are normalized to a peak of 0 dB. The statistical patterns are normalized by the same number as the unperturbed pattern so that the difference between patterns is correct. It would probably never be practical to include a directivity calculation based on pattern integration; however, one could calculate the absolute values of the radiated pattern in terms of the input power and calculate a reasonable directivity number by that method.

## **B. Specific Models**

### **1. Illumination Function**

To calculate the currents on the reflector, the program begins with an assumed primary feed pattern defined by a few pattern parameters. It then determines an aperture field by ray tracing from the feed to a hyperbolic subreflector, from the subreflector to a parabolic main reflector, and finally to the aperture. Figures 2 and 3 illustrate the antenna and a typical ray. The aperture field is the main quantity that is stored, displayed, and used in the program. The reflector currents are calculated at the time they are used in the integration procedure. This approach appears to involve backtracking, but it happens that the



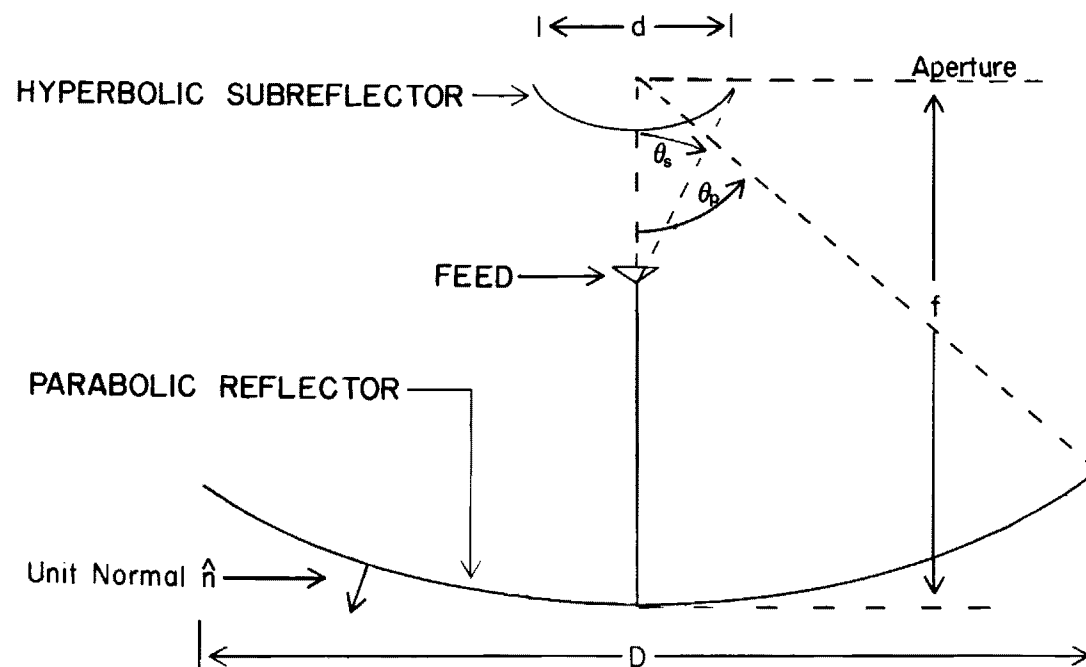


Figure 2. Geometry of a dual-reflector antenna.

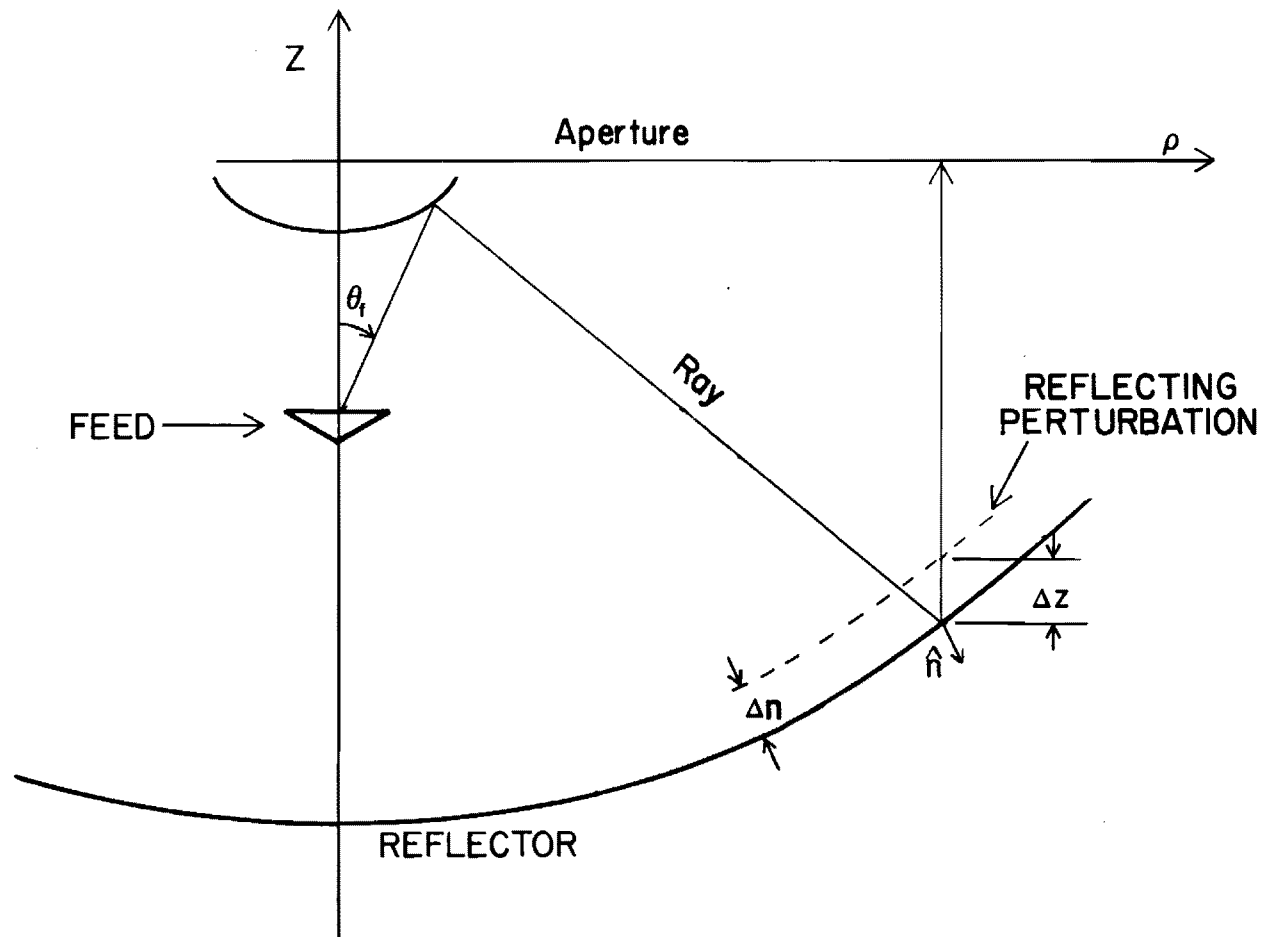


Figure 3. Reflector perturbation and ray path-length error.

mathematics is not at all more complicated, and the aperture field is much easier to understand and work with than the reflector current. As discussed in the next section, this approach does not limit the analysis to parabolic reflectors, but it does limit the extent to which reflectors can deviate from the countour assumed by the feed routines.

Two models of feed patterns have been implemented in the program: a one parameter pattern and a two parameter pattern. The first model is simply,

$$F = (\cos\theta_f)^n , \quad (1)$$

where  $F$  is the radiated field and  $n$  is the input parameter. The second model is the Gaussian function on a pedestal. That is,

$$F = \frac{10^{-a(\frac{\theta_f}{\theta_s})^2} + b}{1 + b} , \quad (2)$$

where  $\theta_s$  is half the subtended subreflector angle and  $a$  and  $b$  are input parameters. Notice that both of these patterns are circularly symmetric.

Ray tracing from the feed to the aperture is rather straightforward. The relationship between the radiation angle from the feed  $\theta_f$  and the aperture radius  $\rho$  is given by,

$$\tan \frac{\theta_f}{2} = \frac{\rho}{2f} \frac{e-1}{e+1} , \quad (3)$$

where  $f$  is the parabola focal length and  $e$  is the hyperbola eccentricity. Letting the right-hand side of Equation (3) be  $B$ , it is easy to show that

$$(\cos\theta_f)^n = \left[ \frac{1-B^2}{1+B^2} \right]^n . \quad (4)$$

This is the aperture field for the first feed model, not counting ray divergence or "space loss". For the second model, the angle,

$$\theta_f = 2 \tan^{-1} B ,$$

is simply substituted into Equation (2).

For these dual reflector antennas, the ray divergence has a small effect on the aperture fields. Nevertheless, it is easy to compute so there is little reason to neglect it. The ray divergence is computed by calculating the derivative of  $\theta_f$  with respect to  $\rho$ . When this quantity is normalized to the value at 0, we obtain the following divergence expression:

$$E(\rho) = \frac{F(\rho)}{1 + B^2}, \quad (6)$$

where  $E$  is the aperture field and  $F$  is the ray value traced from the feed. The quantity  $E$  is exactly what the program computes for the aperture field.

## 2. Reflector Integration

The aperture field is defined on a polar grid that can be divided into any number of equal sectors. The grid points all lie on lines of constant radius and lines of constant azimuthal angle. The grid is the same for each sector, but within a sector the spacing between rows of sample points is arbitrary. This allows the user to specify perturbations that cover a small region without using a tight spacing for the whole reflector.

Deterministic errors are introduced into the antenna system by perturbing the aperture field. For instance, a bump in the reflector would be represented by a phase bump of appropriate size in the aperture. The only restriction on such reflector bumps is that they not be so large that they perturb significantly the amplitude and polarization of the reflected fields. That is, the reflector normal must not change significantly because this program assumes the normal to be that of a paraboloid.

Shaping of the main reflector can also be readily taken into account since it involves a very minor perturbation from the paraboloid. This would be done in the same way that errors are introduced, by applying a phase perturbation to the aperture field. In this case, the perturbation would be a function only of radius.

The errors are input to the program in terms of reflector perturbation normal to the reflector surface. The reflector surface errors introduce path-length errors, and hence phase errors, into the reflected rays as illustrated in Figure 3. For an axial reflector error  $\Delta z$ , the phase error  $\Delta\psi$  is given by,

$$\Delta\psi = 2 k_0 \Delta z \quad . \quad (7)$$

For reflector errors measured normal to the surface,  $\Delta n$ , the phase is given by,

$$\Delta\psi = 2k_0 \Delta n \sqrt{\left(\frac{\rho}{2f}\right)^2 + 1} \quad . \quad (8)$$

The computer program indicates the definition of reflector perturbation that is used for each calculation.

The integration is performed, as mentioned earlier, over the reflector current rather than over the aperture field. In the physical optics method, the radiated field is defined by the integral,

$$\underline{F}(\underline{k}) = 2 \int_{\text{Refl.}} - \hat{n} \times \underline{H} \exp(j\underline{k} \cdot \underline{r}) d\underline{r} \quad (9)$$

where  $\hat{n}$  is the unit downward normal to the reflector,  
 $\underline{H} = \underline{\ell} \times \underline{E}$  is the field incident on the reflector  
in direction  $\underline{\ell}$ , and  
 $\underline{r}$  is the reflector surface position variable.

The expression for  $\hat{n}$  is

$$\hat{n} = \frac{\frac{\partial z}{\partial x} \hat{x} + \frac{\partial z}{\partial y} \hat{y} - \hat{z}}{\left(\frac{\partial z}{\partial x}\right)^2 + \left(\frac{\partial z}{\partial y}\right)^2 + 1} \equiv \frac{\underline{n}}{|\underline{n}|} \quad (10)$$

In order to integrate over two variables only, we need the integration element,

$$\rho \, d\rho \, d\phi = \hat{n} \cdot \hat{z} \, |d\mathbf{r}| = \frac{-1}{|\underline{n}|} \, |d\mathbf{r}| \quad (11)$$

With this substitution the integral becomes,

$$\underline{F}(\underline{k}) = 2 \int_D \underline{n} \times \underline{H} \exp(j\underline{k} \cdot \underline{r}) \rho \, d\rho \, d\phi, \quad (12)$$

where D is the projection of the reflector surface onto the x-y plane.

It can now be shown that,

$$\underline{n} \times \underline{H}_r = [E_{ax}\hat{x} + E_{ay}\hat{y} + \frac{\hat{z}}{2f} (x E_{ax} + y E_{ay})] \exp(-jk_0 z), \quad (13)$$

where:  $r$  subscript means evaluation at  $(\rho, \phi, z)$ ,  
 $a$  subscript means evaluation at  $(\rho, \phi, 0)$  (aperture), and  
 $f$  is the reflector focal length.

The  $z$  component was not included in the integration routine of this program because it is dependent on the other components and can be recovered in the far field. Even if it were not recovered, it's effect on patterns near boresight would be negligible.

The exponent in the integrand can be expressed as,

$$\begin{aligned} \underline{k} \cdot \underline{r} &= \rho k_0 \sin\theta' \cos(\phi - \phi') + k_0 \cos\theta' z' , \\ &= \rho k_\rho \cos(\phi - \phi') + \left(\frac{\rho^2}{4f} - f\right) k_z . \end{aligned} \quad (14)$$

Thus, the integral as finally implemented is,

$$\underline{F}(\theta', \phi') = \int_D 2 \underline{E}_a \exp \left[ (j\rho k_0 \sin\theta' \cos(\phi - \phi') + jk_0(\cos\theta' - 1) \left(\frac{\rho^2}{4f} - f\right)) \right] \rho \, d\rho \, d\phi \quad (15)$$

The integration algorithm begins with cells as defined by the aperture sampling. Each cell is then divided into enough subcells that the variation of the exponent is less than one radian in either direction across one subcell. Then the exponent and the function  $E_a$  are obtained from a four-point bivariate interpolation. Finally, each subcell is summed with an appropriate area increment factor.

It should be mentioned here that the integral over one cell with the interpolated surface can be done analytically in terms of sine and cosine integrals. Thus, it is not necessary to divide the cell into subcells. However, the expressions are quite involved, and it is unknown whether the analytical approach would be any faster than the numerical approach. This question would be worth investigating if this computer program finds heavy use.

### SECTION III

#### ERROR MODELING

Error models can generally be divided into two types, random and deterministic. Deterministic errors are completely defined and can be modeled in the same way that any other antenna characteristic is modeled. Random errors are not completely defined, but occur in unpredictable ways. Their definition takes the form of characteristics that apply on average to a large number of errors. These characteristics are called statistics. The analysis of random error consists of determining the statistics of the antenna performance from the statistics of the errors.

There are furthermore two fundamental methods of treating random errors, probabilistic and Monte Carlo. In the Monte Carlo approach, an ensemble of random error configurations is evaluated one by one, and statistics are calculated from the appropriate performance parameters of each evaluation. The formula used to calculate a statistic is simply the definition of that statistic. In the probabilistic approach, the statistics of the performance parameters are derived analytically from the statistics of the errors. Thus, the desired results are obtained from the derived formula, rather than from the aggregate of repeated evaluations. The probabilistic approach is generally much less costly to apply and is usually more accurate, but only certain statistics can be derived in this way.

Nearly all the work done on this program consisted of deterministic analysis. However, a probabilistic model was developed for die defects, and some results were calculated with a probabilistic model intended to represent measured errors.

#### A. Die Defects

The antennas under consideration are all large and circularly symmetrical. Therefore, the common construction technique is to fabricate the reflector surface in identical sectors. The number of sectors varies between 8 and 32, depending on the antenna's size and other features. Since all of these sectors are stamped or stretch-formed on the same die, an error in the die would be repeated in each sector. These errors typically are something like flat spots on the order of one-half foot across, and about one to four may develop on the die in random positions.



A probabilistic approach was initially applied to the analysis of die defect errors. A new probabilistic theory has been recently developed at Georgia Tech to handle defects that are randomly positioned in aperture antennas. This theory is presented in Appendix A. It was modified in the current effort to handle a circular array of apertures, each having such random errors precisely corresponding to those of its neighbors. The derivation for this modification is presented in Appendix B.

This model was implemented in the computer program, but it is too expensive to run for large reflectors with several segments. However, for single piece reflectors, it can be used to analyze globally random errors along with various kinds of deterministic error. Also, for small reflectors, it can be used to analyze sector defects along with other errors.

Little effort was spent trying to streamline the random error calculations because deterministic calculations showed that die defects are not significant. Die defects were deterministically modeled by four pyramids spread over each sector in an eight sector antenna. The peak of the pyramid was set at a level somewhat higher than the maximum deviation that would occur in a flat spot, and the pyramids at large radii were proportionately wider and higher.

## **B. Support Structure Errors**

The errors discussed in this section are considered to be closely related to the structure supporting the surface panels; however, it will be seen that for some errors, the support structure effects cannot be separated from panel fabrication effects.

### **1. Global Errors**

These are errors which are not confined to one panel or repeated with each panel, but rather extend throughout the reflector. All those considered are functions of radius only. Subreflector errors are of this type since they consist of concentric rings in the milled surface. Such errors are known to be additive with main reflector errors, but they are much easier to control since subreflectors are much smaller. For instance, they are often small enough to be milled from a single piece of metal. These errors were considered, but they were not modeled since they were so small that they would very likely be negligible. The depth of the

concentric grooves was on the order of .001" to .002", and the grooves were irregularly spaced with an average of one-quarter wavelength spacing. Based on reasonable engineering judgement, these errors are too small to be significant.

Another example of this kind of error is that arising from the variation in panel width in those construction techniques in which the panels are bolted directly together. When all the panels are bolted together, the height of the surface at any given radius must be sensitive to the total circumference of the structure at the radii of the nearest bolts. Though the modeling was available to evaluate these kinds of errors, it was not done since these construction techniques are not strong candidates for the production of high-precision antennas. Parenthetically, the intentional shaping of a reflector can be readily introduced into this computer program in the same way that this kind of error was modeled. That is, the shaping, which is a function of radius only, is applied to the aperture fields in the same way that an error perturbation would be applied.

Profile errors are the only errors of this type that were analyzed. These are errors extracted from surface measurement data by averaging along arcs of constant radius. Profile errors are a deterministic component of the measured errors, and a specific case of these errors was evaluated to determine their effect.

## **2. Errors that are Global per Sector**

These are errors that extend over a complete sector, but not beyond. They may or may not be repeated from one sector to the next. Spring back errors are a good example of an error of this kind that is repeated from sector to sector. It arises from the fact that stamped panels are under a stress that tends to return them to their original flat position. Gravity sag and wind strain are examples of this type of error that would not repeat from one sector to the next. They would not repeat because the reflector is not flat, and some parts of it will intercept wind or gravitational forces at different angles than other parts. None of these three kinds of error were evaluated because they have been well analyzed by mechanical engineers and are relatively easy to detect and correct.

One of the construction techniques for large high-precision reflectors involves the use of rigid radial trusses. These trusses have periodic milled surfaces upon which the surface panel must register in the assembly procedure. If the assembler fails to register one edge of a panel, a surface error consisting of a slope from one panel edge to the other results. Errors of this type were modeled using the same assembly error on each panel. One edge was positioned correctly while the other edge was perturbed by an error that varied with radius. Thus, the error at any given radius was a sawtooth function of the azimuthal angle. The error for the perturbed edge was taken from measured surface error along one radius.

Assembly errors would clearly be better represented by random errors than deterministic errors; however, these errors, being periodic, are considered quite severe. And since the evaluation of these errors showed little effect, further modeling was not deemed appropriate.

### **3. Local Errors**

These errors extend only over a small portion of each sector. They are related to die errors in this respect and in that they are repeated per sector; however, they are not random. One example of such errors is the chordal type that accompany the faceted construction. These were modeled, but not evaluated because they had been previously analyzed by Scientific-Atlanta. Since this kind of error is sensitive to welding techniques, there may be occasion to use this model to evaluate problems arising in the future from welding anomalies.

Cusp errors consist of a rise in the surface as the joint is approached from either direction. These errors are associated with the joints, but they are not considered joint errors since they extend back into the panel several inches. They are caused by strain due to assembly of panels with overbent flanges as illustrated in Figure 4. There may be other causes for these errors since they are very common in reflector antennas and very pronounced in some of the reflectors on the market. One would expect these errors to be fairly constant as a function of radius, but in this modeling effort they were scaled linearly with the radius. That is, the width of the cusps were constant in terms of the azimuthal angle. Evaluations were performed for this kind of error on 8 sector and 16 sector antennas. The errors in the latter case were made unrealistically

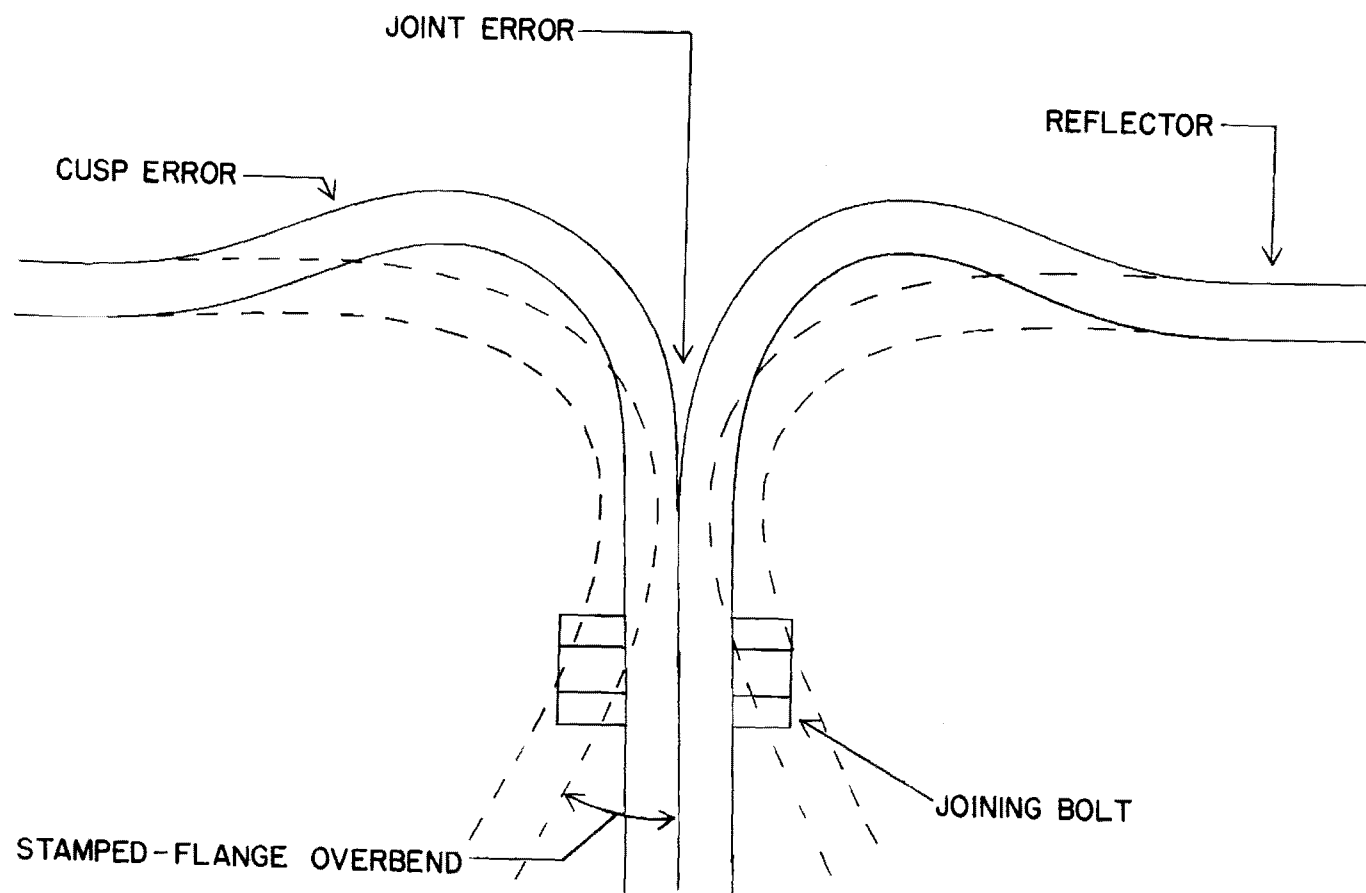


Figure 4. Errors at joints of reflector sector panels.

large in order to clearly exhibit performance characteristics. Cusp errors were found to produce pattern characteristics similar to those measured by Scientific-Atlanta.

### **C. Joint Errors**

Joint problems are another type of error shown in Figure 4. Primarily these are gaps or grooves between the flanges of adjacent panels. The gap between panels will produce a line of interrupted current, depending on the polarization. More accurately, it will introduce "lumped" reactances in the surface. This is also true at those points where the sections make contact, but there the reactance will be different. The joints can be crudely viewed as waveguides with open or shorted ends. This type of error might be expected to repeat with each joint, but it probably does not because the reactance will be very sensitive to the length and the width of the gap. Also, because of this sensitivity, the effects of joint errors are probably irregular with respect to the radial distance. At least they will depend on the contact points, and they may be randomly irregular also.

Variations in flange bend radius are another source of joint error. These errors occur because of deformations of the dies with use. Any ten or twenty panels should be very similar, but samples 100 panels apart, for instance, will show variations of the inside bend radius between  $\frac{1}{4}$  inch and  $\frac{1}{2}$  inch. The correlation distance of the bend radius along the groove is generally between one and forty inches.

Such joint errors were considered, and they are believed to be amenable to analysis. However, this analysis must start with a literature search and must become rather involved. Therefore, the modeling of these errors was considered to be beyond the scope of the this project and was not further pursued. Fortunately, these errors are not expected to be highly significant.

### **D. Measured Errors**

Subroutines were written for the program that allow input of actual surface errors as measured by Scientific-Atlanta. This feature has been found to be valuable because errors that are known to be realistic or even typical can be applied to various reflector configurations and evaluated at chosen frequencies. For these calculations, an unsector antenna is used;

that is, the number of sectors is specified as one by the user. The errors are read as printed by the Scientific-Atlanta reports. First, the radial sample points are read, and then the set of reflector errors at each of these points is read for an azimuth angle of  $0^{\circ}$ , followed by subsequent azimuth angles. The program interpolates in radius, but not in azimuth; therefore, the reflector azimuthal sample points must coincide with the angles at which measurement data is available. Two sets of measurement data were evaluated for various antenna configurations as discussed in the next section.

THIS PAGE IS INTENTIONALLY LEFT BLANK

## SECTION IV

### RESULTS

Many different antenna and error combinations were analyzed in this effort. Each configuration used one of the four antenna models that are specified in Table 1. Antennas I and II were used with a frequency specification that would make the input dimensions to be specified in wavelengths. Antennas III and IV are specified in inches because more than one frequency was used in each case. Antenna III was used with frequencies of 11.95 and 14.5 GHz, and Antenna IV was used with frequencies of 20 and 30 GHz.

The pattern plots discussed in this section are located in Appendix C for convenience and are of three general types. Two are phase plots of the aperture field, and one contains far-field power patterns. The far field plots show two curves: the solid line is the normalized power pattern for an antenna with no error, and the hashed line is the power pattern with error present.

All calculations but one are made for errors that are defined by reflector deviation in the z-direction. That is, the reflector displacements given below are in inches parallel to the antenna axis. The preferred method is generally to define error as displacement normal to the reflector surface at each point, especially since that is the way the measured data are defined. The former definition of error was used in these calculations due to an oversight; but the worst case error was recalculated with the latter definition, and the difference in the radiation patterns was found to be very small near the pattern peak.

#### A. Die Defects

Antenna II was used for this calculation with four defects per sector. They are modeled by pyramids that are four inches by five degrees at the base. They occur at the four intersection points of the two radial lines at  $17.5^\circ$  and  $37.5^\circ$  and the two arcs at 18 inches and 40 inches radius. The defects at 18 inches are 17 mils high and those at 40 inches are 34 mils high. The first type of aperture phase pattern for this configuration is shown in Figure C-1. This pattern is a radial cut through the aperture with the phase plotted in degrees. (Azimuthal cuts of the same type will be



**TABLE 1**  
**ANTENNAS ANALYZED**

Parameter	Value for Antenna No.			
	I	II	III	IV
<b>REFLECTORS</b>				
Diameter (main)	50	100	216"	96"
Focal Length	20	35	60"	30.22"
Subreflector Width	6	12	23"	10.2"
Eccentricity	2.000	1.552	1.468	1.468
Sectors	8	8,16,1	1	1
Edge angle, $\theta_s$	23.54°	17.58°	17.13°	17.13°
Edge angle, $\theta_p$	64.01°	71.08°	76.91°	76.91°
<b>FEED</b>				
Type	Cos <sup>n</sup>	Gaus.	Gaus.	Gaus.
Pedestal	None	-50 dB	-50 dB	-50 dB
Parameter (a)	n=16	1.39	1.158 <sup>(1)</sup> 1.859 <sup>(2)</sup>	1.859
Edge taper (main)	-12.4 dB	-12.2 dB	-10.2 dB <sup>(1)</sup> -16.2 <sup>(2)</sup>	-16.2 dB

(1) For frequency of 11.95 GHz

(2) For frequency of 14.50 GHz

shown for other configurations.) The second type of aperture pattern includes the whole aperture and is shown in Figure C-2. This pattern should be circular because the dependent variables are lines of constant  $\rho$  and  $\phi$ , that is, radius and azimuth, but the figure is "unrolled" by the plotting routines. Thus, the far end of the plot ( $2\pi$  radians) is the same radial line as the near end (0 radians). The three-dimensional plots are intended for the purpose of gaining insight into the overall effect of errors, but it is difficult to obtain the quantitative phase information from them.

The far-field patterns are presented in Figure C-3. Clearly, the effect of die defects of this type on pattern performance is negligible. Indeed, it is so insignificant that further calculations on this type of error were not performed.

#### **B. Profile Error**

Profile error is a global type of error, as discussed in the last section, because it extends throughout the reflector and is a function only of radius. These errors were obtained by an approximate scaling of the profile errors listed in the Scientific-Atlanta measurement report of 14 March 1980 for a 5.5 meter antenna. (The total surface error for this antenna was .023 inches RMS.) Calculations were made on Antenna II, using the error data shown in Table 2 as input to the computer program.

**Table 2**  
**PROFILE ERROR INPUT**

<u>Aperture Radius</u>	<u>Surface Error</u>
16	-.015
22	+.005
26	-.013
32	+.008
38	+.010
42	+.006
48	-.009

Figures C-4 and C-5 show the aperture error as interpolated from the above input data. Figure C-6 shows that the effects of profile error on performance are small, though not as insignificant as those of die defects. In this case, the gain was reduced by .05 dB and the first sidelobe increased .02 dB. The greatest effect occurred around the fifth sidelobe which increased by about a  $1\frac{1}{2}$  dB.

### **C. Assembly Error**

Assembly errors for Antennas I and II were modeled as discussed in the last section. The first radius of the measurement data shown in Figure 5 was used for input, but in the case of Antenna I it was reversed for variety. The errors for both antennas were completely defined by Tables 3 through 5.

Figures C-7 and C-8 show the aperture error for Antenna II. One may observe that the azimuthal variable in Figure C-8 is not linear. The data are stored in the computer in sectors, each of whose last azimuthal angle coincides with the first angle of the next sector. These angles that are repeated appear in this three-dimensional plot with a separation. Usually this anomaly is not noticeable, but in case of doubt, one can refer to the two-dimensional phase plot. The two-dimensional plot, which will always be correct, should be used for quantitative information.

The performance at  $0^\circ$  azimuth is shown in Figure C-9. Another pattern was calculated at  $22\frac{1}{2}^\circ$ , which is centered between two sector edges, and it was found to vary insignificantly from that shown at  $0^\circ$ . Figures C-10 through C-12 show similar data for Antenna I. The error has very little effect on pattern in either case. For Antenna I, the gain is reduced by .05 dB, and that for Antenna II, by .06 dB. Again, the first sidelobe changes very little, and most of the effect is seen in the third through fifth sidelobes.

### **D. Cusp Error**

Cusp errors were analyzed for Antenna I and two configurations of Antenna II. The errors are defined for all three cases in Table 6. The results for Antenna I are shown in Figures C-13 through C-16. These errors are unrealistically large, but the results still serve to demonstrate the interesting feature that the sidelobes are much more degraded in the far field cuts along the joint angles than between them. In particular, Figure

THE RADII AT WHICH ERROR IS DEFINED ARE:

0.000 14.460 20.790 26.710 32.340 37.730 41.830 46.850

THE ERRORS (INCHES NORMAL TO THE REFLECTOR) ARE:

1	-.051	.003	.035	-.033	.014	.013	.021	.017
2	-.051	.007	.043	-.026	.012	.015	.025	.011
3	-.051	-.004	.031	-.041	.013	.010	.015	-.003
4	-.051	-.021	.038	-.031	-.016	-.007	.017	-.001
5	-.051	-.025	.038	-.024	0.000	-.014	-.003	-.016
6	-.051	-.010	.051	-.024	-.001	.002	.022	-.003
7	-.051	-.015	.043	-.035	-.003	-.014	-.003	-.003
8	-.051	-.011	.031	-.046	-.024	-.021	-.002	-.017
9	-.051	-.013	.027	-.048	-.008	-.016	-.012	-.031
10	-.051	-.013	.039	-.046	-.033	-.027	-.004	-.008
11	-.051	-.016	.035	-.042	-.012	-.019	-.005	-.021
12	-.051	-.013	.028	-.023	-.002	-.009	.010	.013
13	-.051	-.001	.035	-.020	-.004	-.018	-.002	-.004
14	-.051	-.008	.038	-.022	-.002	-.001	.018	.007
15	-.051	-.001	.056	-.007	.024	.026	.041	.024
16	-.051	-.001	.056	-.016	.012	.027	.037	.023
17	-.051	.002	.057	-.022	.010	.010	.025	.003
18	-.051	0.000	.057	-.026	-.008	.002	.017	.015
19	-.051	-.002	.057	-.024	-.006	.010	.029	.017
20	-.051	-.027	.021	-.046	-.012	.005	.006	-.018
21	-.051	-.004	.045	-.027	-.002	.013	.028	-.006
22	-.051	-.020	.028	-.030	.001	.016	.001	-.019
23	-.051	-.012	.030	-.020	.012	.008	.019	-.013
24	-.051	-.034	.009	-.054	-.027	-.001	-.003	-.016
25	-.051	-.009	.032	-.037	-.005	-.007	-.021	-.017
26	-.051	-.020	.023	-.049	-.022	-.009	-.005	-.024
27	-.051	-.006	.042	-.027	-.005	-.008	.021	-.008
28	-.051	-.020	.020	-.049	-.004	-.013	-.013	-.025
29	-.051	0.000	.043	-.031	-.001	-.007	.019	-.019
30	-.051	-.010	.026	-.052	-.020	-.009	.002	-.016
31	-.051	-.009	.042	-.031	-.001	.012	.031	-.010
32	-.051	-.026	.018	-.037	-.006	-.007	-.013	-.028
33	-.051	-.001	.039	-.024	.004	.007	-.022	-.024
34	-.051	-.034	.006	-.048	.008	.003	-.017	-.026
35	-.051	-.008	.041	-.015	.024	.027	.037	-.014
36	-.051	-.029	.018	-.051	-.007	.008	-.012	-.020
37	-.051	-.010	.052	-.021	0.000	.011	.030	-.001
38	-.051	-.007	.046	-.035	.018	.035	.026	0.000
39	-.051	-.003	.045	-.013	.023	.049	.064	-.020
40	-.051	-.001	.037	-.052	-.002	.012	.004	-.011
41	-.051	-.008	.042	-.030	.003	.018	.029	-.011
42	-.051	-.012	.032	-.037	.015	.023	.023	-.003
43	-.051	-.013	.036	-.034	-.006	.006	.024	-.009
44	-.051	-.023	.015	-.058	-.011	.001	.009	-.023
45	-.051	-.008	.024	-.044	-.012	-.004	.019	-.001
46	-.051	-.001	.025	-.049	-.016	-.015	.002	-.021
47	-.051	-.003	.036	-.041	-.014	-.007	.007	-.024
48	-.051	-.004	.035	-.034	.005	.010	.024	-.019
49	-.051	-.003	.033	-.043	-.012	-.001	.021	-.013

Figure 5. Measured errors of 14 March 1980, for a 5.5M reflector, as used with Antenna II.

**TABLE 3**  
**RADIAL ASSEMBLY ERROR INPUT FOR ANTENNA II**

Measurement Radius (in.)	Scaled Radius (in.)	Surface Error (in.)
-	0	-.051*
31.312	14.46	.003
45.018	20.79	.035
57.839	26.71	-.033
70.037	32.34	.014
81.689	37.73	.013
90.579	41.83	.021
101.449	46.85	.017

\*This number was estimated because extrapolated value was too extreme.

**TABLE 4**  
**RADIAL ASSEMBLY ERRORS FOR ANTENNA I**

Point	Radius (in.)	Displacement (in.)
1	3.000	.0110
2	5.000	.0130
3	7.000	.0150
4	9.000	.0170
5	11.000	.0170
6	13.000	.0130
7	15.000	.0120
8	17.000	0.0000
9	19.000	-.0260
10	21.000	.0300
11	23.000	.0080
12	25.000	-.0150

**TABLE 5**  
**NORMALIZED AZIMUTHAL ASSEMBLY ERRORS FOR ANTENNAS I AND II**

Point	Angle (deg.)	Displacement (in.)
1	0	.9900
2	5	.8800
3	10	.7700
4	15	.6600
5	20	.5500
6	25	.4400
7	30	.3300
8	35	.2200
9	40	.1100
10	45	0.0000

**TABLE 6**  
**CUSP ERRORS**

	Ant. I	Ant. II-A	Ant. II-B
Height	.25"	.025"	.125"
Width	$\pm 2.5^\circ$	$\pm 2.3^\circ$	$\pm 4.0^\circ$
Width at Edge	$\pm 1.1"$	$\pm 2.0"$	$\pm 3.5"$
Number	8	8	16

C-15, taken above the first joint, shows severe degradation, whereas Figure C-16, taken between the first and second joints, shows very little sidelobe-level increase.

Configuration II-A is illustrated in Figures C-17 through C-20. Though this error may be unrealistically small, it also demonstrates the same phenomenon, as can be seen in Figures C-19 and C-20. Again, Configuration II-B involves rather severe errors, and the same far field phenomenon is observed. Here the difference between the patterns at the joint angles and inter-joint angles is not so great. This is probably because the angles are closer together due to the increased number of sectors (16 instead of 8).

The pattern performance characteristics produced by cusp error are particularly significant because they correspond well to characteristics measured by Scientific-Atlanta. These characteristics are: (1) good sidelobe levels through about the third sidelobe with increased levels thereafter, (2) higher sidelobe levels on the joint angles than between them. It is very interesting that the level of the first and second sidelobes showed essentially no change relative to the peak, even though the peak was reduced by 1 dB for Antenna I and 1.5 dB for Antenna II-B.

#### **E. Measured Error**

Actual reflector errors measured by Scientific-Atlanta were analyzed with Antennas II, III, and IV. The measured errors were scaled in radius and used with Antenna II. An error value of  $-.051$  was added at the origin in order to prevent the program from obtaining extreme values by extrapolation near the center of the dish. The errors as input to and printed by the program are shown in Figure 5. The results shown in Figures C-25 through C-29 exhibit some of the characteristics of the performance as measured, but not in such a clear way as the cusp errors did. However, the cusp errors may not be well represented in this data because the separation between measurement points in azimuth is  $7.35^\circ$ . Thus, if cusp errors are the major source of error and they are not included in this data, the calculated patterns will necessarily differ from the measured patterns.

Another set of measured data shown in Figure 6 was also extended to zero and scaled in radius for use with Antenna III. The phase sign for this data was changed to make calculations correspond to sign conventions;

THE RADII AT WHICH ERROR IS DEFINED ARE:

0.000 31.571 45.141 57.888 70.025 81.830 90.430 101.529

THE ERRORS (INCHES NORMAL TO THE REFLECTOR) ARE:

1	-.0666	-.0223	.0002	-.0223	.0200	.0311	.0122	-.0003
2	-.0666	-.0222	.0224	-.0112	.0110	.0225	.0344	-.0006
3	-.0666	-.0332	.0113	-.0311	.0116	.0226	.0002	-.0113
4	-.0666	-.0007	.0411	-.0001	.0223	.0336	.0500	-.0001
5	-.0666	-.0330	.0211	-.0311	.0220	.0330	.0112	-.0002
6	-.0666	-.0007	.0330	-.0007	.0227	.0443	.0544	.0012
7	-.0666	-.0114	.0115	-.0311	.0117	.0225	.0116	.0111
8	-.0666	-.0112	.0227	.0004	.0333	.0440	.0466	.0007
9	-.0666	-.0114	.0115	-.0119	.0228	.0118	.0002	-.0025
10	-.0666	-.0311	.0007	-.0223	.0112	.0111	.0112	-.0027
11	-.0666	-.0335	-.0003	-.0334	.0113	-.0110	-.0227	-.0053
12	-.0666	-.0442	-.0002	-.0229	-.0005	-.0008	-.0004	-.0041
13	-.0666	-.0335	-.0001	-.0226	.0114	.0003	-.0002	-.0034
14	-.0666	-.0226	.0112	-.0117	.0112	.0118	.0116	-.0026
15	-.0666	-.0332	.0001	-.0336	.0006	0.0000	-.0003	-.0012
16	-.0666	-.0334	.0001	-.0223	.0110	-.0003	-.0221	-.0035
17	-.0666	-.0227	.0003	-.0221	.0225	.0005	-.0009	-.0038
18	-.0666	-.0223	.0119	-.0009	.0226	.0220	.0116	-.0010
19	-.0666	-.0220	.0116	-.0111	.0334	.0226	.0116	-.0020
20	-.0666	-.0220	.0118	-.0117	.0113	.0114	.0115	-.0021
21	-.0666	-.0225	.0114	-.0222	.0222	.0119	.0111	-.0024
22	-.0666	-.0336	.0007	-.0225	.0111	-.0001	-.0009	-.0026
23	-.0666	-.0338	.0004	-.0330	.0117	-.0112	-.0004	-.0035
24	-.0666	-.0611	-.0115	-.0443	-.0007	-.0007	-.0116	-.0033
25	-.0666	-.0330	.0116	-.0220	.0119	.0119	.0117	-.0113
26	-.0666	-.0227	.0220	-.0111	.0220	.0228	.0223	-.0010
27	-.0666	-.0112	.0440	.0001	.0337	.0441	.0444	.0011
28	-.0666	-.0330	.0110	-.0226	.0110	.0116	.0008	-.0018
29	-.0666	-.0112	.0333	-.0001	.0335	.0446	.0448	.0013
30	-.0666	-.0223	.0008	-.0221	.0224	.0339	.0226	.0005
31	-.0666	-.0111	.0224	-.0113	.0229	.0339	.0335	-.0009
32	-.0666	-.0337	-.0008	-.0443	.0004	.0110	-.0220	-.0031
33	-.0666	-.0112	.0119	-.0119	.0226	.0336	.0228	-.0022
34	-.0666	-.0221	.0003	-.0332	.0110	.0118	.0001	-.0012
35	-.0666	-.0115	.0114	-.0227	.0008	.0119	.0223	-.0015
36	-.0666	-.0555	-.0117	-.0335	.0003	-.0003	-.0227	-.0031
37	-.0666	-.0332	-.0001	-.0113	.0119	.0111	.0116	-.0016
38	-.0666	-.0554	-.0330	-.0557	.0114	.0114	-.0008	-.0017
39	-.0666	-.0117	.0112	-.0225	.0116	.0226	.0227	-.0015
40	-.0666	-.0442	-.0114	-.0444	.0118	.0222	-.0008	-.0016
41	-.0666	-.0113	.0116	-.0223	.0112	.0225	-.0227	-.0018
42	-.0666	-.0440	-.0003	-.0663	-.0003	.0222	-.0007	-.0027
43	-.0666	-.0117	.0008	-.0336	.0005	.0117	.0114	-.0030
44	-.0666	-.0337	.0002	-.0446	.0114	.0226	-.0006	-.0017
45	-.0666	-.0332	.0111	-.0118	.0220	.0223	.0114	-.0025
46	-.0666	-.0445	0.0000	-.0337	.0220	.0116	-.0110	-.0053
47	-.0666	-.0229	.0005	-.0338	.0004	.0116	.0111	-.0025
48	-.0666	-.0338	-.0114	-.0558	.0114	.0331	.0112	-.0023
49	-.0666	-.0004	.0114	-.0337	.0003	.0223	.0220	-.0014

Figure 6. Measured errors of 4 March 1980 for a 5.5M reflector as used with Antenna III.



however, the only effect on amplitude patterns is to rotate the cut angle  $\phi$  by  $180^\circ$ . That is, earlier patterns can be considered to be those of, say,  $180^\circ$  and  $202\frac{1}{2}^\circ$  instead of  $0^\circ$  and  $22\frac{1}{2}^\circ$ , respectively.

This configuration was analyzed for frequencies of 11.95 and 14.5 GHz. The patterns are shown in Figures C-30 through C-36. Only the aperture phase plots for the high frequency are shown since the other frequency is the same except for a scale factor.

The same data set was scaled in radius for Antenna IV. Then, the error values themselves were scaled by one-half and by three-fourths, and each of these two error sets was analyzed at the frequencies of 20 and 30 GHz. The RMS values of the data sets were then .012 and .018 inches, respectively. The latter case is shown in Figure 7. The far field patterns for these four configurations are shown in Figures C-37 through C-44. These error levels are very high for these frequencies, two to three times higher than allowed by conventional reckoning. It appears that errors of this level may affect the first sidelobes more than the present error levels do. However, the first sidelobe can generally be brought down nearly to its original level by empirical focusing of the feed.

At this point in the investigation, it was discovered that all errors had been defined axially rather than normal to the reflector. To determine whether any configurations needed to be re-analyzed with the more severe "normal" error definition, the case having the most severe errors was reevaluated with the error definition properly modified. The results are shown in Figures C-45 through C-48. Though increased performance degradation can be observed, it is clearly not sufficient to warrant the repetition of all the analyses.

The summary of these measured error configurations is presented in Table 7 with a few of the performance parameters. This is a very brief indication of performance that is intended primarily to specify the configurations calculated. The case with error defined normal to the reflector was not included because it is not really comparable to these cases.

THE RADII AT WHICH ERROR IS DEFINED ARE:

0.000 14.032 20.063 25.728 31.122 36.369 40.191 45.124

THE ERRORS (INCHES NORMAL TO THE REFLECTOR) ARE:

1	-.050	-.017	.002	-.017	.015	.023	.009	-.002
2	-.050	-.017	.018	-.009	.008	.019	.026	-.005
3	-.050	-.024	.010	-.023	.012	.020	.002	-.010
4	-.050	-.005	.031	-.001	.017	.027	.038	-.001
5	-.050	-.023	.016	-.023	.015	.023	.009	-.002
6	-.050	-.005	.023	-.005	.020	.032	.041	.009
7	-.050	-.011	.011	-.023	.013	.019	.012	.008
8	-.050	-.009	.020	-.003	.025	.030	.035	.005
9	-.050	-.011	.011	-.014	.021	.014	.002	-.019
10	-.050	-.023	.005	-.017	.009	.008	.009	-.020
11	-.050	-.025	-.002	-.026	.010	-.008	-.020	-.040
12	-.050	-.032	-.002	-.022	-.004	-.006	-.003	-.031
13	-.050	-.026	-.001	-.020	.011	.002	-.002	-.026
14	-.050	-.020	.009	-.013	.009	.014	.012	-.020
15	-.050	-.024	.001	-.027	.005	0.000	-.002	-.009
16	-.050	-.026	.001	-.017	.008	-.002	.016	.026
17	-.050	-.020	.002	-.016	.019	.004	-.007	-.029
18	-.050	-.017	.014	-.007	.020	.015	.012	-.008
19	-.050	-.015	.012	-.008	.026	.020	.012	-.015
20	-.050	-.015	.014	-.013	.010	.011	.011	-.016
21	-.050	-.019	.011	-.017	.017	.014	.008	-.018
22	-.050	-.027	.005	-.019	.008	-.001	-.007	-.020
23	-.050	-.029	.003	-.023	.013	-.009	.003	-.026
24	-.050	-.046	-.011	-.032	-.005	-.005	-.012	-.025
25	-.050	-.023	.012	-.015	.014	.014	.013	-.010
26	-.050	-.020	.015	-.008	.015	.021	.017	.008
27	-.050	-.009	.030	-.001	.028	.031	.033	.008
28	-.050	-.023	.008	-.020	.008	.012	.006	-.014
29	-.050	-.009	.025	-.001	.026	.035	.036	.010
30	-.050	-.017	.006	-.016	.018	.029	.020	.004
31	-.050	-.008	.018	-.010	.022	.029	.026	-.007
32	-.050	-.028	-.006	-.032	.003	.008	-.015	-.023
33	-.050	-.009	.014	-.014	.020	.027	.021	-.017
34	-.050	-.016	.002	-.024	.008	.014	.001	-.009
35	-.050	-.011	.011	-.020	.006	.014	.017	-.011
36	-.050	-.041	-.013	-.026	.002	-.002	-.020	-.023
37	-.050	-.024	-.001	-.010	.014	.008	.012	-.012
38	-.050	-.041	-.023	-.043	.011	.011	-.006	-.013
39	-.050	-.013	-.009	-.019	.012	.020	-.020	-.011
40	-.050	-.032	-.011	-.033	.014	.017	-.006	-.012
41	-.050	-.010	.012	-.017	.009	.019	.020	-.014
42	-.050	-.030	-.002	-.047	-.002	.017	-.003	-.020
43	-.050	-.013	.006	-.027	.004	.013	-.011	-.023
44	-.050	-.028	.002	-.035	.011	.020	-.005	-.013
45	-.050	-.024	.008	-.014	.015	.017	-.011	-.019
46	-.050	-.034	0.000	-.028	.015	.012	-.008	-.040
47	-.050	-.022	-.004	-.029	.003	.012	.008	-.019
48	-.050	-.029	-.011	-.044	.011	.023	.009	-.017
49	-.050	-.003	.011	-.028	.002	.017	.015	-.011

Figure 7. Data of Figure 6 scaled by .75, as used with Antenna IV.

**TABLE 7**  
**PERFORMANCE WITH MEASURED ERROR**

Antenna	II	III	III	IV	IV	IV	IV
Frequency (GHz)	11.8	11.95	14.5	20	30	20	30
Error Case (date)	14	4	4	4	4	4	4
Error RMS (in.)	.023	.024	.024	.012	.012	.018	.018
RMS (wavelengths)	.023	.024	.030	.020	.030	.029	.043
Gain Loss (dB)	-.3	-.4	-.6	-.3	-.6	-.6	-1.43
Sidelobe Change*							
(dB) at 0°	2.3	4.3	9.0	7.2	10	10	12
90°	-2.3	3.6	7.7	5.4	7.5	8.0	10.7

\*Shoulders are considered as sidelobes.

## SECTION V

### CONCLUSION

The first conclusion to be drawn from this investigation is that the computer program developed in it has been shown to be a viable tool for analyzing various kinds of reflector surface errors, especially deterministic error. The program will also analyze random error, but since it is restricted to a small reflector of few sections, it has not yet been shown to be useful in treating satellite antennas. On the other hand, it has not yet been shown that the errors occurring in reflector antennas have a significant random component.

Probably the most important conclusion to be drawn from this work is that cusp errors are the most likely source of present performance limitations. They can significantly raise the third or fourth sidelobe and, to a lesser extent, many sidelobes thereafter. If one type of error is to be selected to eliminate, it is probably cusp error.

Finally, this investigation has shown that errors of the kind that actually occur can be tolerated at higher levels than would be indicated by conventional reckoning. Conventional rules relating the sidelobe levels to surface error are usually based on random error of a particular kind. For instance, Gaussian shaped correlation regions of an assumed radius are most often used. Since the actual error appears to be composed primarily of deterministic components, it is not reasonable to expect that it should closely conform to such rules. It would appear that if particular error sources that cause particular performance problems can be isolated, as the cusp error was, that remaining errors may be tolerated at much higher levels. This observation and the isolation of the dominant cusp-error effects have fulfilled the objectives of this investigation.

THIS PAGE INTENTIONALLY LEFT BLANK

## **APPENDICES**

- A. A NEW APPROACH TO THE ANALYSIS OF RANDOM ERRORS INN APERTURE ANTENNAS**
- B. A MODEL OF REFLECTOR ERRORS CAUSED BY DIE DEFECTS**
- C. CALCULATED PATTERNS**

THIS PAGE IS INTENTIONALLY LEFT BLANK

A New Approach to the Analysis of Random  
Errors in Aperture Antennas\*

Victor K. Tripp, Member, IEEE

Engineering Experiment Station  
Georgia Institute of Technology  
Atlanta, Georgia 30332

ABSTRACT -- A closed form vector expression has been derived for the mean power pattern radiated from an aperture with random perturbations. The expression is in terms of the Fourier Transforms of three unrestricted functions: (1) the vector electric field of the unperturbed aperture, (2) the scattering dyadic of one of N defects, and (3) the probability density function of the position of a defect. The derivation was made possible by the fact that the aperture mean and correlation functions take the form of convolution integrals.

---

\*This work was supported by the Naval Surface Weapons Center, Dahlgren, VA under Contract No. N60921-80-C-A113. It has been submitted for publication in the IEEE Transactions of the Antennas and Propagation Society.



## I. INTRODUCTION

Random errors in aperture antennas are important in the analysis of antenna performance and in the specification of antenna construction tolerances. Past work has generally concentrated on aperture phase errors caused by inaccuracies in the fabrication of reflectors, lenses, or radomes. Ruze [1] treated this problem with a useful model of error statistics that was amenable to analytical solution. His model calculated the scalar average power pattern due to a uniform distribution of small phase errors in an aperture field.

Ruze's work has been extended by several authors. Scheffler [2] obtained an asymptotic expression for large phase errors. Schanda [3,4] extended the model to treat amplitude errors having the same restrictions and form of statistics as phase errors. Phase and amplitude errors were restricted to be uncorrelated with each other. Whereas phase errors readily approximate reflector tolerances, it is not clear what physical phenomenon this type of amplitude error represents. Allen [5] applied this basic approach to arrays and obtained some further results, such as beam skew and pattern variance, but his approach is not readily applicable to continuous apertures since all element errors are assumed independent. Vu [6,7] generalized the basic model to incorporate non-uniform error statistics and taper functions, but only for one-dimensional apertures. Finally, the vectorial problem of error analysis has been addressed [8] in a treatment not closely related to Ruze's work, but bound by similar restrictions.

In this paper, a fundamentally different approach to the problem of random errors in aperture antennas is presented. The common approach is to introduce random error directly into the aperture field and to assume the statistics of the field variable. This new approach introduces the error as the field scattered from defects, which are randomly positioned. In this case, the assumed error statistics are for the physical variables defining defect positions, rather than for electric field variables on the aperture. With only minor restrictions, a closed form vector expression is derived for the mean radiated power pattern in terms of the unperturbed aperture field, the scattering pattern of a defect, and the probability density function of a defect position. This expression is an extension of a scalar expression previously published by the author [9].

The assumptions required to accomplish the derivation are minimal, and thus, many of the restrictions inherent in previous error models are not present in this model. A few of the important features of this model are that errors are not assumed to be small, the error distribution over the aperture is not restricted, probability density functions of fields need not be normal, and the correlation function is not assumed to be Gaussian or "hatbox". Thus, the approach presented in this paper is believed to be applicable to a very wide class of problems. The restricting assumptions that remain are pointed out in the analysis of the next section, and the accuracy and ease of implementation are demonstrated in Section III.

## II. ANALYSIS

The analysis begins with the well-known double Fourier Transform integral that expresses the radiated power in terms of the aperture fields. The mean power is then written in terms of two aperture field statistics, the mean and the covariance. Next, the random error component of the aperture field is defined in terms of scattering patterns from randomly positioned defects. Subsequently, the aperture statistics are expressed as convolution integrals, allowing reduction of the double Fourier Transform to an expression involving only single transforms and integrals.

### A. Formulation of the Problem

Consider a complex electric field  $\underline{E}_a$  defined on an aperture  $S$  in an infinite plane, and equal to zero outside  $S$  (Figure 1). The radiated electric field  $\underline{F}$  at position  $(r, \theta, \phi)$  is given by,<sup>10</sup>

$$\underline{F}(r, \theta, \phi) = jk_0 \frac{e^{-jk_0 r}}{2\pi r} \left[ \underline{f} - \hat{z} \frac{\sin \theta}{\cos \theta} \left[ f_x \cos \phi + f_y \sin \phi \right] \right] \quad (1)$$

where  $\underline{f} = \hat{x} f_x + \hat{y} f_y$  is the Fourier Transform of  $\underline{E}$ , and  $k_0$  is the free space propagation constant.

The power received by an antenna at this position will depend on the polarization of the receive antenna. For a given polarization  $\gamma$ ,  $F_\gamma$  can be expressed as a linear combination of  $f_x$  and  $f_y$ . Then the power received is a quadratic combination of  $f_x$  and  $f_y$ . Dropping the dependence on  $r$ , the power patterns for  $\theta$  and  $\phi$  polarization, for instance, are proportional to,

$$P_\theta = |f_x|^2 \cos^2 \phi + |f_y|^2 \sin^2 \phi + 2 \operatorname{Re} \{ f_x^* f_y \} \cos \phi \sin \phi, \text{ and}$$

$$P_\phi = \cos^2 \theta \left[ |f_x|^2 \sin^2 \phi + |f_y|^2 \cos^2 \phi - 2 \operatorname{Re} \{ f_x^* f_y \} \cos \phi \sin \phi \right]. \quad (2)$$

Therefore, the essence of the task of calculating the mean power pattern for an arbitrary polarization is to calculate the four quantities,

$$\langle f_i^* f_j \rangle = \int_S \int_S \langle E_{ai}^*(\underline{r}) E_{aj}(\underline{r}') \rangle \exp(j\mathbf{k} \cdot (\underline{r}' - \underline{r})) d\underline{r} d\underline{r}', \quad (3)$$

where  $\underline{r} = (\hat{x}x + \hat{y}y + \hat{z}0)$  is the aperture position vector,  
 $\underline{r}'$  is a similar vector,  
 $\underline{k} = (\hat{x}k_x + \hat{y}k_y + \hat{z}k_z)$  is the propagation vector with  $|\underline{k}| = k_0$ , and  
 $i, j$  are either the  $x$  or the  $y$  aperture coordinate.

Conventional approaches [1-4] to the problem of random aperture errors introduce a random error factor into the aperture field  $\underline{E}_a$  in Equation (3). The factor is a function of  $\underline{r}$  and  $\underline{r}'$  and is intended to approximate the effects of physical defects. However, the form of the function must be restricted in order to make the integrals reducible from double to single (two-dimensional) Fourier Transforms. This restriction is so severe that only a few error functions have been found to be usable. Typically, only the pill-box and the Gaussian bump functions are used as correlation functions for field errors. Thus, attempts must be made to approximate all physical damage types by these two elementary functions. Furthermore, errors are usually required to be uncorrelated between amplitude and phase.

One way in which the present approach differs from conventional approaches is that the aperture error function is represented as an additive perturbation, such that,

$$\underline{E}_a(\underline{r}) = \underline{E}_0(\underline{r}) + \underline{E}(\underline{r}), \quad (4)$$

where  $\underline{E}_0$  is the unperturbed aperture field, and  
 $\underline{E}$  is the error field (perturbation).

Next, the bracketed part of the integrand in Equation (3) is rewritten in terms of the statistics of the error field  $\underline{E}$ . To simplify the expressions, matrix notation will be used. Vectors will be one-dimensional column matrices with two components. Dyadics will be represented by 2x2 matrices. Denoting  $\underline{E}(\underline{r}')$  by  $\underline{E}'$ , etc., we obtain from Equation (4) the expression,

$$\begin{aligned} \langle \underline{E}'_a \underline{E}_a^\dagger \rangle &= \underline{E}'_0 \underline{E}_0^\dagger + \langle \underline{E}'_0 \underline{E}^\dagger \rangle + \langle \underline{E}' \underline{E}_0^\dagger \rangle + \langle \underline{E}' \underline{E}^\dagger \rangle \\ &= (\underline{E}'_0 + \langle \underline{E}' \rangle) (\underline{E}_0^\dagger + \langle \underline{E}^\dagger \rangle) + \underline{V}_E \\ &= \langle \underline{E}'_a \rangle \langle \underline{E}_a^\dagger \rangle + \underline{V}_E, \end{aligned} \quad (5)$$

where

$$\underline{v}_E = \langle \underline{E}' \underline{E}'^\tau \rangle - \langle \underline{E}' \rangle \langle \underline{E}'^\tau \rangle. \quad (6)$$

Here  $\underline{v}_E(\underline{r}', \underline{r})$  is the covariance dyadic of the error field  $\underline{E}$ , and  $\tau$  denotes the transpose conjugate.

In this analysis, it will be convenient to represent Fourier Transformation by the symbol  $\sim$ . It should be remembered that the conjugate transform is used for functions of the unprimed variable  $\underline{r}$ . With this notation, Equation (3) can be rewritten with the help of Equation (5) as,

$$\langle \underline{f} \underline{f}^\tau \rangle = \langle \widetilde{\underline{E}}_a \rangle \langle \widetilde{\underline{E}}_a^\tau \rangle + \underline{v}_E. \quad (7)$$

Now the transform of the average of  $\underline{E}$  and the double transform of its covariance are needed in order to evaluate Equation (7).

#### B. Error Model

The primary question at this point is what restrictions must be placed on the error fields in order to evaluate Equation (7). The answer introduces the primary difference between the conventional and present approaches. In this model, the randomness is not introduced directly into the aperture field, but rather into the positions of scattering centers on the aperture. The scattering centers represent physical defects such as holes or dents in the antenna or radome. The defect positions are the true source of randomness for many applications, such as hail damage to reflectors or radomes. The error field is assumed to be composed of contributions from  $N$  such defects and is given as,

$$\underline{E}(\underline{r}) = \sum_{n=1}^N \underline{g}(\underline{r}, \underline{r}_n) \underline{E}_0(\underline{r}_n), \quad (8)$$

where  $\underline{g}$  is the dyadic scattering function, and  $\underline{r}_n$  is the random position of the  $n$ th defect.

Notice that the incident field on the scatterer is simply the unperturbed aperture field, and the dyadic  $\underline{g}$  describes the effects of one defect. The component  $g_{ij}$  is the field in polarization  $i$  at aperture position  $\underline{r}$ ,

scattered from a defect at position  $\underline{r}_n$  with a unit incident field of polarization  $j$ .

The second assumption is that all defects produce the same scattered pattern independent of their position; that is,

$$\underline{g}(\underline{r}, \underline{r}_n) = \underline{g}(\underline{r} - \underline{r}_n) . \quad (9)$$

Figures 2 and 3 illustrate the way in which this approach would model a one dimensional reflector with three defects. Figure 2 illustrates the positioning and superpositioning of scattered fields for a uniform aperture field. Figure 3 shows superposition of the error with a realistic aperture field.

The final assumption is that the joint probability density  $p_J$  of the  $N$  random variables  $\underline{r}_n$  can be written as,

$$P_J (\underline{r}_1, \underline{r}_2, \dots, \underline{r}_N) = p(\underline{r}_1)p(\underline{r}_2)\dots p(\underline{r}_N) , \quad (10)$$

where  $p$  is the probability density function of the position of one defect. Equation (10) means that all defect positions are independent and have the same statistics. This assumption is not significantly restrictive since it describes the real world in most cases. Furthermore, the function  $p$  remains arbitrary.

The three assumptions represented by Equations (8-10) are all that is required to evaluate Equation (3) in closed form. They form a very general error model that is applicable to many types of antenna defects.

### C. Derivation of the Error-Field Mean and Covariance

To evaluate Equation (3), the mean and covariance of the error field  $E$  must be expressed in terms of known quantities. In addition, these expressions must be transformable. Equation (7) (equivalent to (3)) shows that only these two quantities are needed because  $\langle \underline{E}_a \rangle$  is simply  $\underline{E}_0$  plus the mean error  $\langle \underline{E} \rangle$ .

In order to derive  $\langle \underline{E} \rangle$  in terms of the known quantities  $p$ ,  $\underline{E}_0$  and  $\underline{g}$ , it is useful to define a vector  $\underline{G}$  to represent the scattered field from

one defect. Specifically, for the  $n$ th defect, we have ,

$$\underline{G}_n(\underline{r}) = \underline{g}(\underline{r} - \underline{r}_n) \underline{E}_0(\underline{r}_n) . \quad (11)$$

Then it can be shown, as in Appendix A, that

$$\langle \underline{E} \rangle = N \langle \underline{G}_n \rangle \quad \text{for any } n. \quad (12)$$

The bracket or "mean" operator is written explicitly for easy reference as ,

$$\langle A(\underline{r}) \rangle \equiv \int_{-\infty}^{\infty} A(\underline{r}, \underline{r}_n) p(\underline{r}_n) d\underline{r}_n . \quad (13)$$

Equation (6) shows that if one can express the correlation  $\langle \underline{E}' \underline{E}^\dagger \rangle$  in terms of the known quantities, then  $\underline{V}_E$  follows immediately. From Equations (8) and (11), we have

$$\begin{aligned} \langle \underline{E}' \underline{E}^\dagger \rangle &= \left\langle \sum_{m=1}^N \underline{G}_m' \sum_{n=1}^N \underline{G}_n^\dagger \right\rangle \\ &= \sum_n \langle \underline{G}_n' \underline{G}_n^\dagger \rangle + \sum_{m \neq n} \langle \underline{G}_m' \underline{G}_n^\dagger \rangle . \end{aligned} \quad (14)$$

Observe that the random variables  $\underline{r}_m$  and  $\underline{r}_n$  are independent when  $m \neq n$ , and therefore,  $\underline{G}_m$  and  $\underline{G}_n$  are independent. That is,

$$\langle \underline{G}_m' \underline{G}_n^\dagger \rangle = \langle \underline{G}_m' \rangle \langle \underline{G}_n^\dagger \rangle . \quad (15)$$

Next, the same derivation used in Appendix A can be employed to show that

$$\sum_n \langle \underline{G}_n' \underline{G}_n^\dagger \rangle = N \langle \underline{G}_n' \underline{G}_n^\dagger \rangle \quad \text{for any } n. \quad (16)$$

A similar relation holds for the double summation of Equation (14), but it has  $N(N-1)$  terms. Then, dropping the subscripts of  $\underline{G}$ , Equation (14) can be written as,

$$\langle \underline{E}' \underline{E}^\dagger \rangle = N \langle \underline{G}' \underline{G}^\dagger \rangle + N(N-1) \langle \underline{G}' \rangle \langle \underline{G}^\dagger \rangle . \quad (17)$$

Finally, using Equation (6) and Equation (12), the covariance can be written as,

$$\begin{aligned} \underline{v}_E &= N ( \langle \underline{G}' \underline{G}^\dagger \rangle - \langle \underline{G}' \rangle \langle \underline{G}^\dagger \rangle ) \\ &\equiv N \underline{v}_G . \end{aligned} \quad (18)$$

Using the definition of  $\underline{G}$ , its covariance  $\underline{v}_G$  can in turn be written as,

$$\begin{aligned} \langle \underline{G}' \underline{G}^\dagger \rangle &= \langle (\underline{g}' \underline{E}_0) (\underline{g} \underline{E}_0)^\dagger \rangle \\ &= \langle \underline{g}' \underline{E}_0 \underline{E}_0^\top \underline{g}^\dagger \rangle . \end{aligned} \quad (19)$$

#### D. Reduction of the Fourier Transforms

This step in the analysis determines whether the present analysis will be useful. The double, two-dimensional Fourier Transform of Equations (3) and (7) is not practical to evaluate for many problems of interest. However, it will be shown that the double Fourier Transform can be reduced to a single (still two-dimensional) transform that is readily evaluated on a modern computer.

Equation (12) is written explicitly as,

$$\langle \underline{E} \rangle = N \int_{\infty} \underline{g} (\underline{r} - \underline{r}_1) \underline{E}_0(\underline{r}_1) p(\underline{r}_1) d\underline{r}_1, \quad (20)$$

where  $n$  has been set to 1 since the expression applies to any defect. Now we make the observation that this is a convolution integral. Introducing the function,

$$\underline{h} \equiv \underline{E}_0 p, \quad (21)$$

one can write ,

$$\langle \underline{E} \rangle = N \underline{g} * \underline{h}, \quad (22)$$



where \* represents the convolution of matrix elements in the format of Cayley multiplication. Then according to the convolution theorem,

$$\langle \tilde{\underline{E}} \rangle = N \tilde{\underline{g}} \tilde{\underline{h}} . \quad (23)$$

In a similar manner, Appendix B shows that Equation (19) can be written in terms of convolutions. Then Equation (18) can be written as ,

$$\underline{V_E} = N \underline{g'} * \underline{H} * \underline{g}^T - N (\underline{g'} * \underline{h'}) (\underline{g} * \underline{h})^T , \quad (24)$$

where  $\underline{H} = \underline{E_0}(\underline{r}) \underline{E_0}(\underline{r})^T p(\underline{r}) \delta(\underline{r}' - \underline{r})$  .

Then it follows that,

$$\tilde{\underline{V_E}} = N \tilde{\underline{g}} \tilde{\underline{H}} \tilde{\underline{g}}^{\dagger} - N \tilde{\underline{g}} \tilde{\underline{h}} \tilde{\underline{h}}^{\dagger} \tilde{\underline{g}}^{\dagger} . \quad (25)$$

The last remaining double transform is easily reduced due to the  $\delta$  function. It becomes,

$$\tilde{\underline{H}} = \int_S \underline{E_0} \underline{E_0}^{\dagger} p \, d\underline{r} \equiv \underline{C} . \quad (26)$$

Thus, the double transform of  $\underline{H}$  is a constant dyadic  $\underline{C}$ , and it represents a measure of the mean incident power on the defects.

Gathering terms, Equation (25) can be written as,

$$\tilde{\underline{V_E}} = N \tilde{\underline{g}} (\underline{C} - \tilde{\underline{h}} \tilde{\underline{h}}^{\dagger}) \tilde{\underline{g}}^{\dagger} . \quad (27)$$

Finally, in terms of the transforms of the three known functions, Equation (7) can be written as,

$$\langle \underline{f} \underline{f}^{\dagger} \rangle = [\tilde{\underline{E_0}} + N \tilde{\underline{g}} \tilde{\underline{h}}] [\underline{E_0} + N \underline{g} \underline{h}]^{\dagger} + N \tilde{\underline{g}} [\underline{C} - \tilde{\underline{h}} \tilde{\underline{h}}^{\dagger}] \tilde{\underline{g}}^{\dagger} , \quad (28)$$

where  $\underline{g}$  is the scattering coefficient dyadic,  
 $\underline{E}_0$  is the unperturbed aperture field,  
 $\underline{h} = \underline{E}_0 \underline{p}$ ,  
 $\underline{p}$  is the probability density function of one defect  
 position, and  
 $\underline{C}$  is a constant dyadic.

### III. NUMERICAL EVALUATION

A theory of statistical antenna damage is difficult to validate experimentally, because it requires a statistical ensemble of damaged antennas. For a significant ensemble, the expense in measurement time and hardware could easily become prohibitive. In this case, results of the present method were compared with numerically simulated data. A Monte Carlo computer program was written to generate the needed ensemble of damaged antennas, analyze the performance of each, and calculate the desired performance statistics.

One scalar configuration used to validate the theory consisted of a focus-fed paraboloid of about 18 wavelengths diameter, with an edge taper of about 12 dB. Eight defects were randomly distributed with uniform density over the surface. These defects were isotropic point sources. Figure 4 shows the average power patterns calculated with the new model, according to Equation (28), and with the Monte Carlo program. A twenty element ensemble was used for the latter calculation. The results are clearly in excellent agreement.

Although the model approximates the illumination of each defect with a constant, a configuration was evaluated that included a defect about five wavelengths in diameter. In this case, a single defect was randomly positioned with a uniform density, and ten elements were used for the Monte Carlo ensemble. The Monte Carlo program modeled the defect as a Gaussian reflector bump. The z coordinate of the reflector was perturbed by

$$Z_p(\underline{r}, \underline{r}_n) = \frac{1}{2k_o} \psi(\underline{r} - \underline{r}_n), \quad (29)$$

where  $\underline{r}_n$  is the defect position,  
 $k_o$  is the propagation constant, and

$$\psi = \exp \frac{-|\underline{r} - \underline{r}_n|^2}{(2.38)^2} \quad (30)$$

In the probabilistic model, the scalar scattering function was the following Gaussian phase bump,

$$g(\underline{r} - \underline{r}_n) = \exp(j\psi) - 1. \quad (31)$$

Even for this large defect of the "construction tolerance" type, the results shown in Figures 5 and 6 are in good agreement.

The present Monte Carlo computer program was limited to scalar analysis, but the vector capabilities of the analytical model were examined by comparing results with limited published experimental data [8]. In the experimental case, a reflector of about four wavelengths in diameter was focus fed by a linearly polarized horn. The errors were introduced by randomly changing the height of eight regions of the reflector. For the calculated case, an unperturbed field was assumed as follows,

$$\underline{E}_0(\underline{r}) = \hat{x} \cos(.456 |\underline{r}|) + \hat{y} \sin \left( \pi \frac{|\underline{r}|}{R} \right) \sin \phi \cos \phi, \quad (32)$$

where  $R$  is the reflector radius, and  
 $\phi = \tan^{-1}(y/x)$ .

The error was modeled as eight square phase patches in random positions. Good agreement was obtained as shown in Figure 7, indicating that the new model will be useful for vector calculations. This is to be expected since the vector derivation involves exactly the same assumptions as the scalar case.

Since the Fourier Transform is a well known and widely used technique, the implementation of this new approach was not difficult. Furthermore, with the efficiency of the Fast Fourier Transform (FFT) algorithm, the computations were inexpensive. The hemispherical patterns from which Figures 5 and 6 were taken required seven times as much calculation time with the Monte Carlo program as they did with the program of Equation (28). In the most general vector case, Equation (28) requires eight Fourier Transforms and four real aperture integrals. Therefore, it can be expected to take a little more than four times as long to compute the mean vector pattern as it does to compute the unperturbed vector pattern.

An advantage of this model is that, due to its generality, it interfaces naturally with measurement data. The complex far fields of  $\underline{E}_0$  and  $\underline{g}$  can be measured, and the results can be inserted directly into the formula, without any curve fitting, filtering, or other manipulation. Alternatively, these quantities can be measured on an aperture with a near

field range, and the data can then be transformed for use in Equation (28). This near-field technique has been well exercised for various undamaged aperture antennas, but recently it has been applied by the author to scattering from defects as well. The undamaged antenna is measured, as well as the antenna with a defect. Then the fields are subtracted and normalized numerically to obtain the complex scattering function  $\underline{g}$ . Thus, the model is directly suitable for practical application to measurements of antenna and defect patterns.

#### IV. CONCLUSIONS

A vector formula for the mean radiated power pattern has been derived with a new model of an aperture antenna having randomly positioned defects. This antenna error model and the pattern formula are applicable to a large class of problems. The generality of the model is indicated by the fact that only three basic assumptions (Equations (8-10)) were required in the derivation. Generality is also shown by the accurate numerical evaluation of diverse damage cases, including multiple small defects and a solitary large deformation. The assumptions are so minimal that many of the restrictions inherent in conventional error models are not present here. The following features are inherent in this model:

1. Errors need not be small.
2. The error distribution over the aperture is not restricted.
3. Probability density functions of fields need not be normal.
4. Amplitude and phase errors need not be independent.
5. The correlation function is not assumed to be Gaussian or "hatbox".
6. No fields are assumed to be scalar.

Numerical evaluation has demonstrated several other features. First, the model was found to be easy to implement in FORTRAN and efficient to execute on a modern mainframe computer. Also, the accuracy of the model was demonstrated for defects as large as several wavelengths. This feature could not be determined from the derivation alone. In addition, the model can be directly applied to measurement data without the need of smoothing it or "fitting" it to analytical expressions.

A final conclusion can be drawn from the experience of using the model; it is a physically realistic model. In modeling a random error problem, assigning statistics or probability density functions to the random variables often involves engineering judgement and approximation. This is especially true when statistics are assumed for dependent variables, such as aperture fields, rather than for independent variables, such as reflector deformations. In this model, much estimation is often eliminated because the statistics are assumed for a primary physical parameter (the defect position) rather than for a function of a primary

random parameter. The position statistics were often found to be much simpler and much more readily determined than those of the aperture field perturbations that depend on them.

## V. REFERENCES

1. J. Ruze, "Antenna Tolerance Theory - A Review," Proceedings IEEE, Vol. 54, pp. 633-640, April 1966.
2. H. Scheffler, "Über die Genauigkeitsforderungen bei der Herstellung optischer Flächen für astronomische Teleskope," Z. Astrophys. (Germany), Vol. 55, pp. 1-20, 1962.
3. E. Schanda, "The Effects of Random Amplitude and Phase Errors of Continuous Apertures," IEEE Trans. Antennas Propagat., Vol. AP-15, pp. 471-473, May 1967.
4. E. Schanda, "Das Deugungsbild elektromagnetischer Wellen von Aperturen mit statistischen Amplitudenfehlern," Helv. Phys. Acta, Vol. 39, p. 568, 1966.
5. J. L. Allen, et al., "Phased Array Radar Studies, 1 July 1960 to 1 July 1961," Lincoln Laboratory, M.I.T. Technical Report No. 236, Part 3, Chapter III, DDC 271724, November 1961.
6. The Bao Vu, "The Effect of Aperture Errors on the Antenna Radiation Pattern," Proceedings IEE (London), Vol. 116, pp. 195-202, 1969.
7. The Bao Vu, "Nonconstant Correlation Interval in Antenna Tolerance Theory," IEEE Trans. Antennas Propagat., pp. 118-119, January 1970.
8. S. I. Ghobrial, "Axial Cross Polarization in Reflector Antennas with Surface Imperfections," IEEE Trans. Antennas and Propagat., Vol. AP-28, No. 5, September 1980, p. 610.
9. V. K. Tripp, "A New Approach to Random Aperture Errors," IEEE/AP-S International Symposium, Los Angeles, California, pp. 140-143, June 16-19, 1981.
10. R. E. Collin and F. J. Zucker, "Antenna Theory, Part 1", McGraw-Hill, 1969, Equation 3.14.



APPENDIX A  
DERIVATION OF THE ERROR-FIELD MEAN

For clarity, Equation (12) is derived without the use of matrix conventions. Using Equations (8 and 9) we have,

$$\langle E_i \rangle = \int_{-\infty}^{\infty} \sum_{n=1}^N \sum_j g_{ij}(\underline{r}-\underline{r}_n) E_{oj}(\underline{r}_n) p_J(\underline{r}_1, \underline{r}_2, \dots, \underline{r}_N) d\underline{r}_1, d\underline{r}_2 \dots d\underline{r}_N, \quad (33)$$

where the  $i$  and  $j$  indices vary over the two aperture dimensions  $x$  and  $y$ .

Each of the  $N$  terms can be integrated separately and Equation (10) can be used to obtain,

$$\langle E_i \rangle = \sum_{n=1}^N \int \sum_j g_{ij}(\underline{r}-\underline{r}_n) E_{oj}(\underline{r}_n) p(\underline{r}_1) p(\underline{r}_2) \dots p(\underline{r}_N) d\underline{r}_1 d\underline{r}_2 \dots d\underline{r}_N. \quad (34)$$

Then the integral can be separated by variables;

$$\langle E_i \rangle = \sum_{n=1}^N \int \sum_j g_{ij}(\underline{r}-\underline{r}_n) E_{oj}(\underline{r}_n) d\underline{r}_n \int p(\underline{r}_1) d\underline{r}_1 \dots \int p(\underline{r}_N) d\underline{r}_N \quad (35)$$

(subscript  $\neq n$ ).

Now we use the definition of the mean and the normalization property of the probability density function (the defect must occur somewhere) to obtain,

$$\langle E_i \rangle = \sum_{n=1}^N \langle G_i(\underline{r}, \underline{r}_n) \rangle [1]^{N-1}, \quad (36)$$

where  $G_i(\underline{r}, \underline{r}_n) = \sum_j g_{ij}(\underline{r}-\underline{r}_n) E_{oj}(\underline{r}_n)$ .

Finally, the observation that all  $N$  terms are identical yields,

$$\langle E_i \rangle = N \langle G_i \rangle. \quad (37)$$

APPENDIX B  
REDUCTION OF THE CORRELATION OF G

In order to evaluate the (double) Fourier Transform of  $\underline{V}_E$ , we express Equation (19) in the form of a convolution integral. Dropping matrix conventions for clarity, Equation (19) can be written as follows,

$$\begin{aligned} \langle G_i^* G_j^* \rangle &= \sum_k \sum_\ell \int g_{ik}(\underline{r}' - \underline{r}_1) E_{ok}(\underline{r}_1) E_{o\ell}^*(\underline{r}_1) g_{\ell j}^*(\underline{r} - \underline{r}_1) p(\underline{r}_1) d\underline{r}_1 \\ &= \sum_k \sum_\ell \left[ g_{ik}(\underline{r}' - \underline{r}) E_{ok}(\underline{r}) E_{o\ell}^*(\underline{r}) p(\underline{r}) \right] * g_{\ell j}^*(\underline{r}). \end{aligned}$$

Now the quantity in brackets can be handled as a convolution by introducing a delta function  $\delta(\underline{r}_1 - \underline{r})$  and integrating over  $\underline{r}_1$ . That is,

$$g_{ik}(\underline{r}' - \underline{r}) = \int \delta(\underline{r}_1 - \underline{r}) g_{ik}(\underline{r}' - \underline{r}_1) d\underline{r}_1,$$

by the properties of the  $\delta$  function; and thus,

$$g_{ik}(\underline{r}' - \underline{r}) = \delta(\underline{r}' - \underline{r}) * g_{ik}(\underline{r}'),$$

by the definition of convolution. Then,

$$\langle G_i^* G_j^* \rangle = \sum_k \sum_\ell g_{ik}(\underline{r}') * H_{k\ell}(\underline{r}, \underline{r}') * g_{\ell j}^*(\underline{r}),$$

where  $H_{k\ell} = E_{ok}(\underline{r}) E_{o\ell}^*(\underline{r}) p(\underline{r}) \delta(\underline{r}' - \underline{r})$ .

Since the mean  $\langle G_i \rangle$  has already been expressed as a convolution, the covariance  $\underline{V}_G$ , and hence  $\underline{V}_E$ , can be expressed in terms of convolutions. The result is Equation (24).

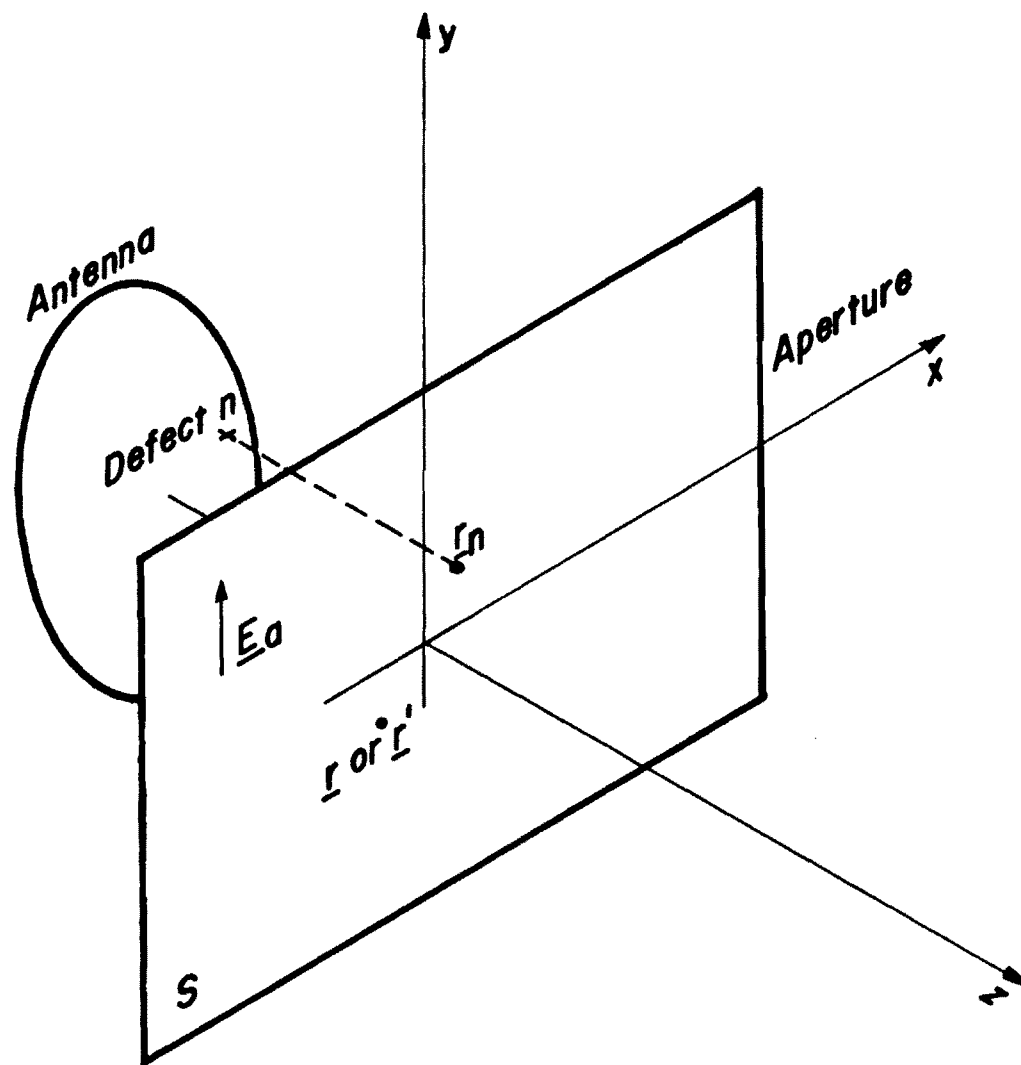
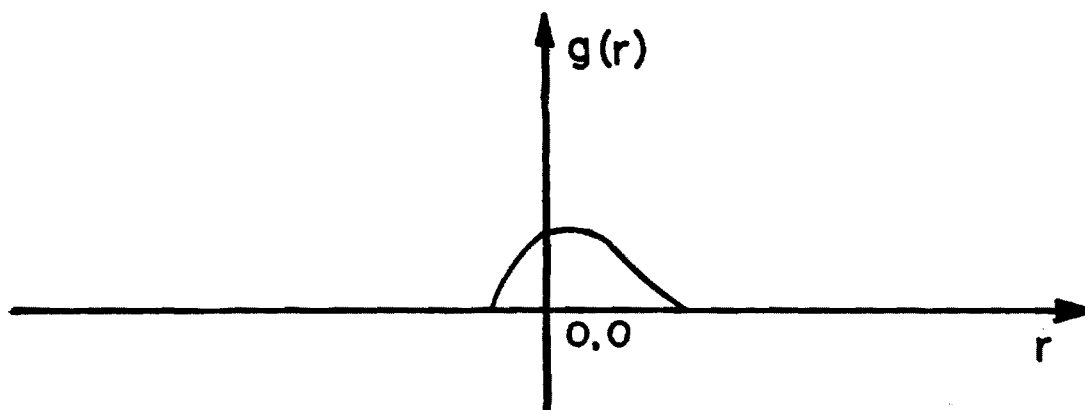
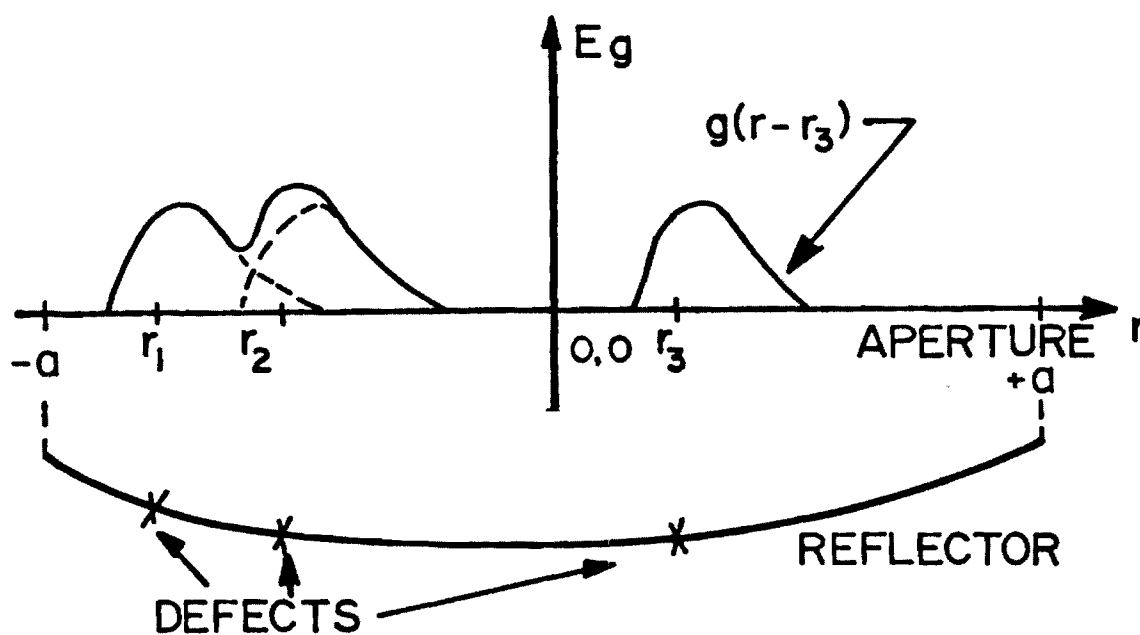


Figure 1. Coordinate system for aperture analysis.

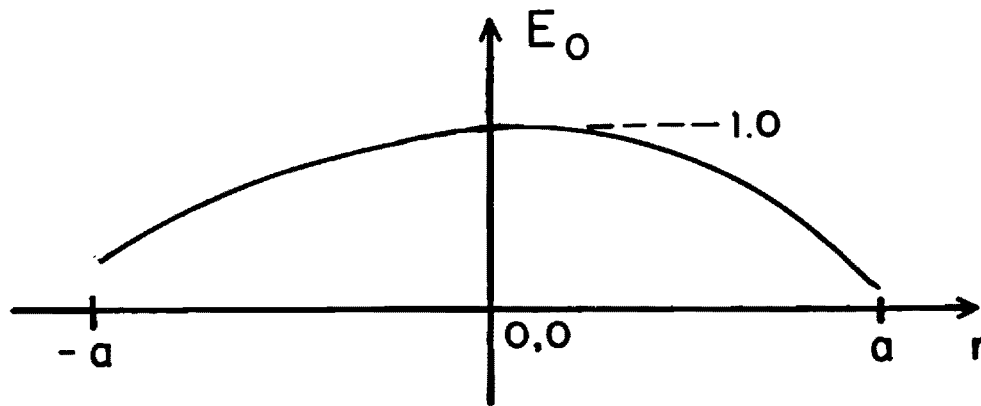


a) Scattering function

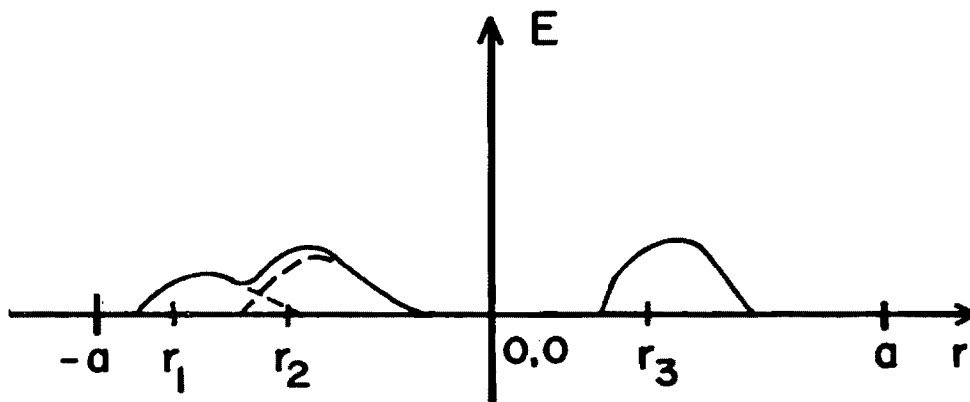


b) Sum of scattering functions  $E_g = \sum_n^3 g(r-r_n)$

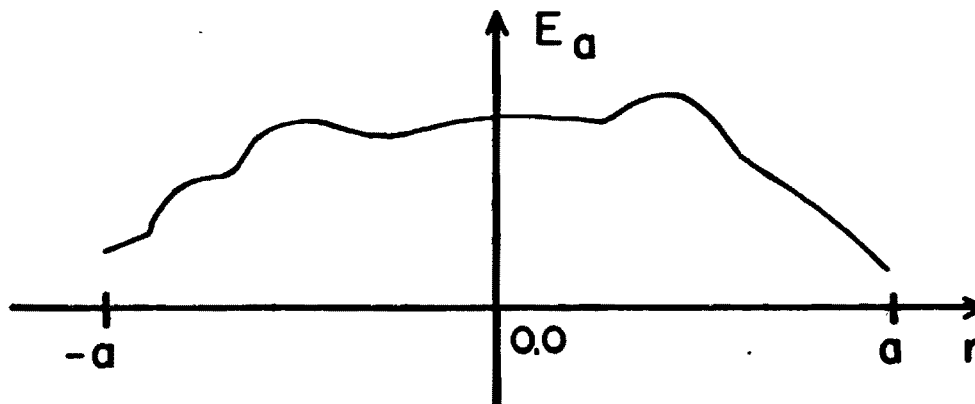
Figure 2. Example of the function  $g(r)$  and functions  $g(r-r_n)$  describing the field scattered from defects at  $r_n$ . (In general  $g$  is a complex dyadic, and  $r$  and  $r_n$  are two dimensional.)



a) Unperturbed aperture



b) Perturbation  $\sum_n^3 E_0(r_n)g(r-r_n)$



c) Total field  $E_a = E_0 + E$

Figure 3 . Example of an aperture field with and without perturbations.

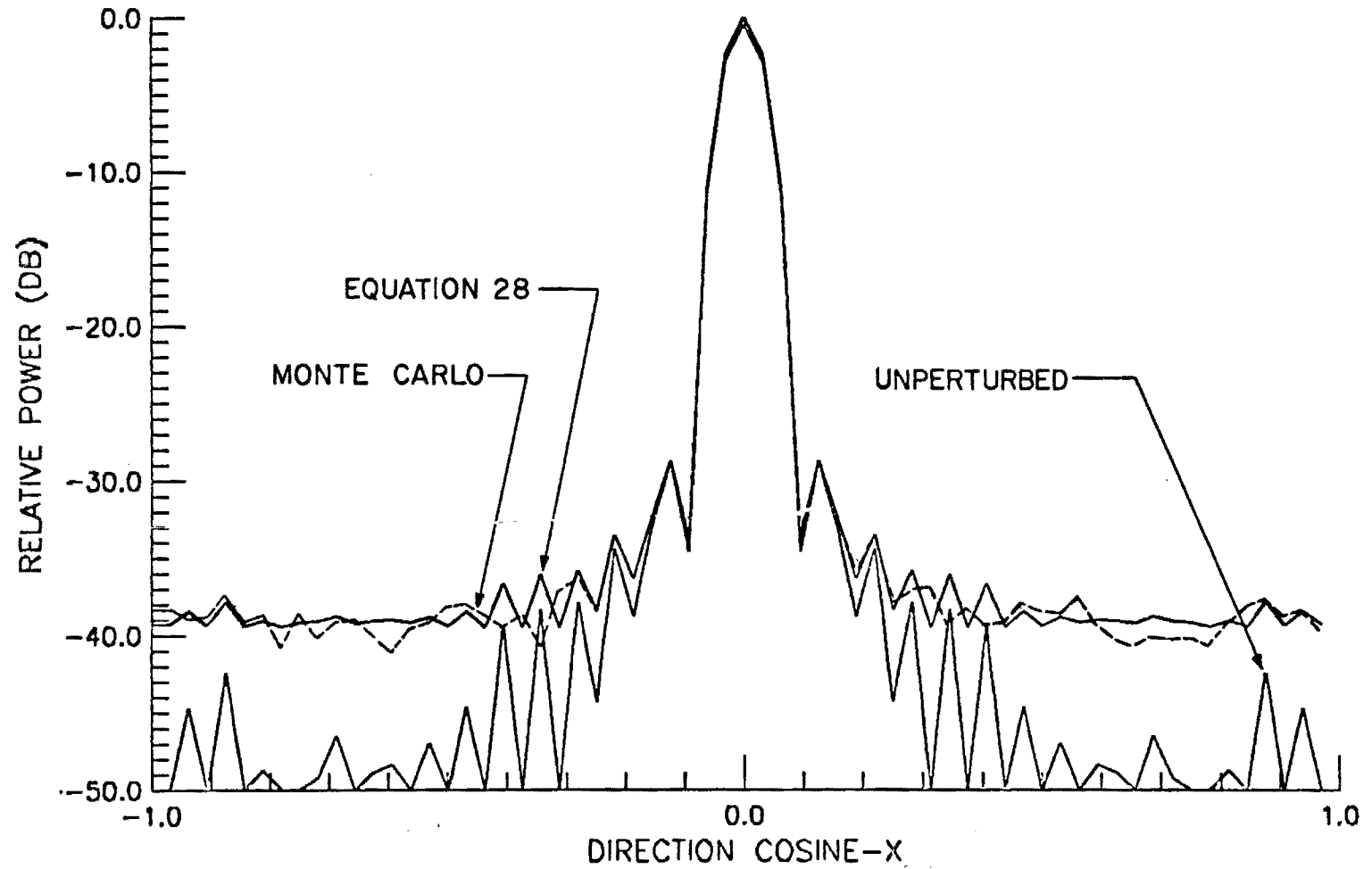


Figure 4. Mean principal-plane pattern of a reflector antenna having eight randomly positioned, point scatterers.

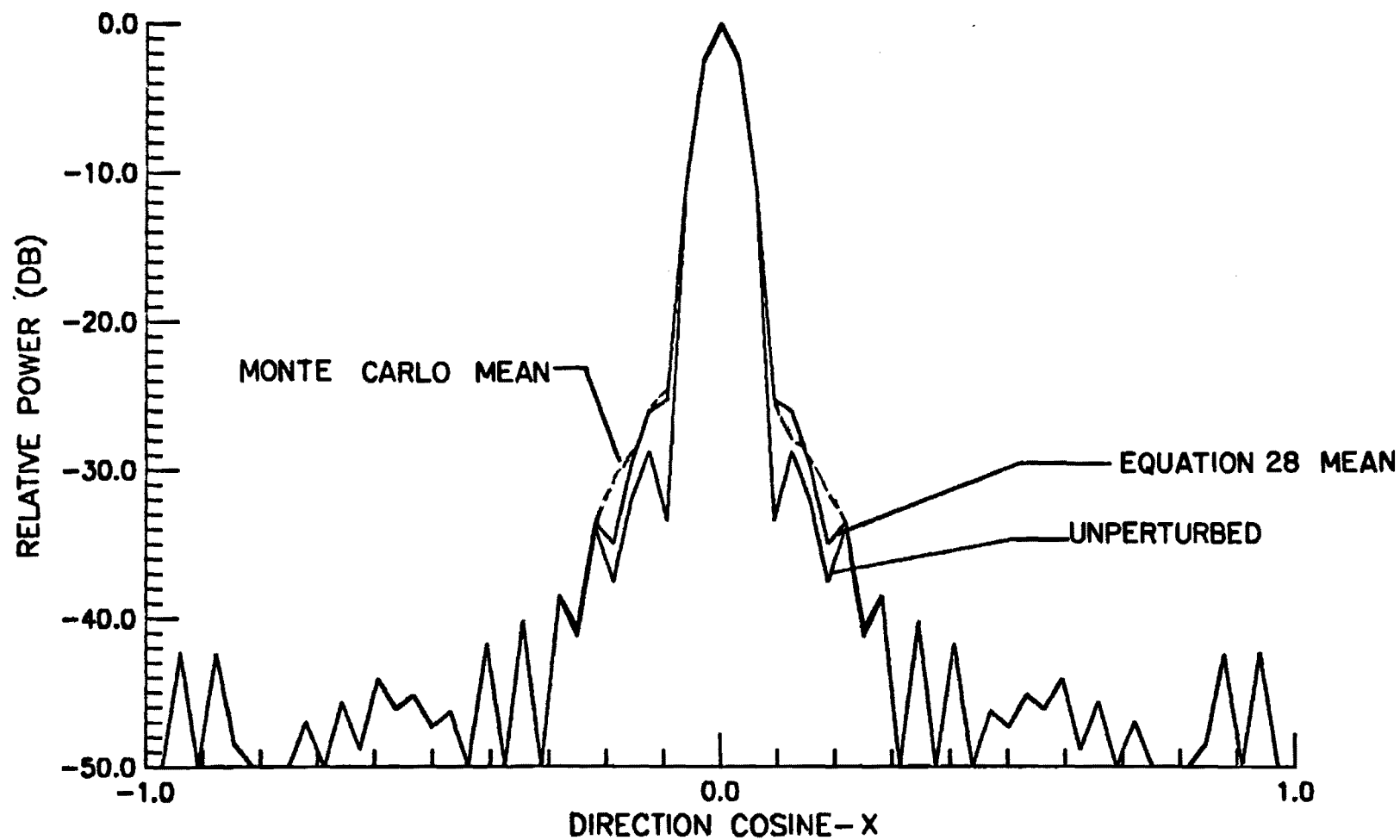


Figure 5. Mean horizontal power pattern of a reflector antenna having one randomly positioned, Gaussian phase bump about  $5\lambda$  in diameter.



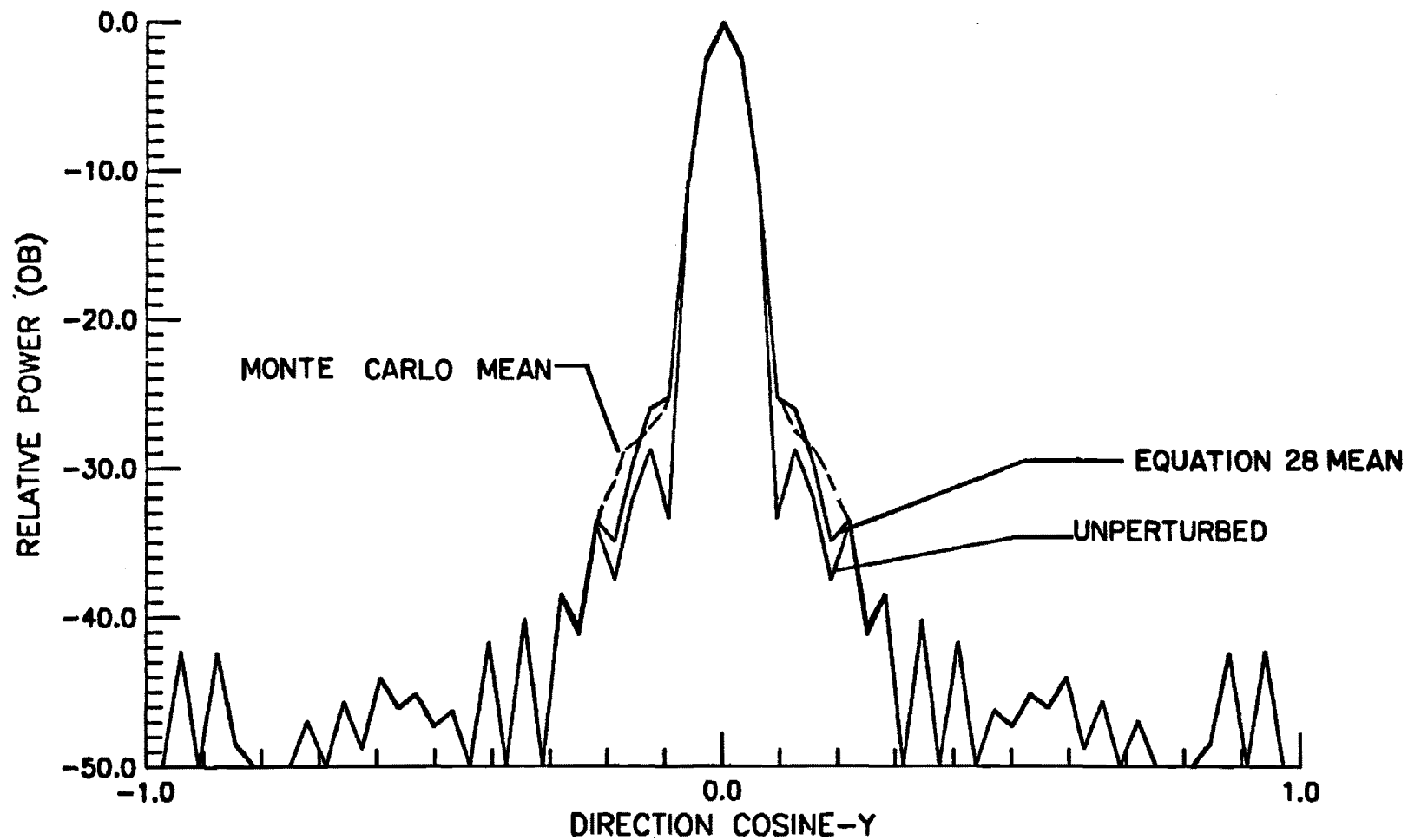


Figure 6. Mean vertical power pattern of a reflector antenna having one randomly positioned, Gaussian phase bump about  $5\lambda$  in diameter.

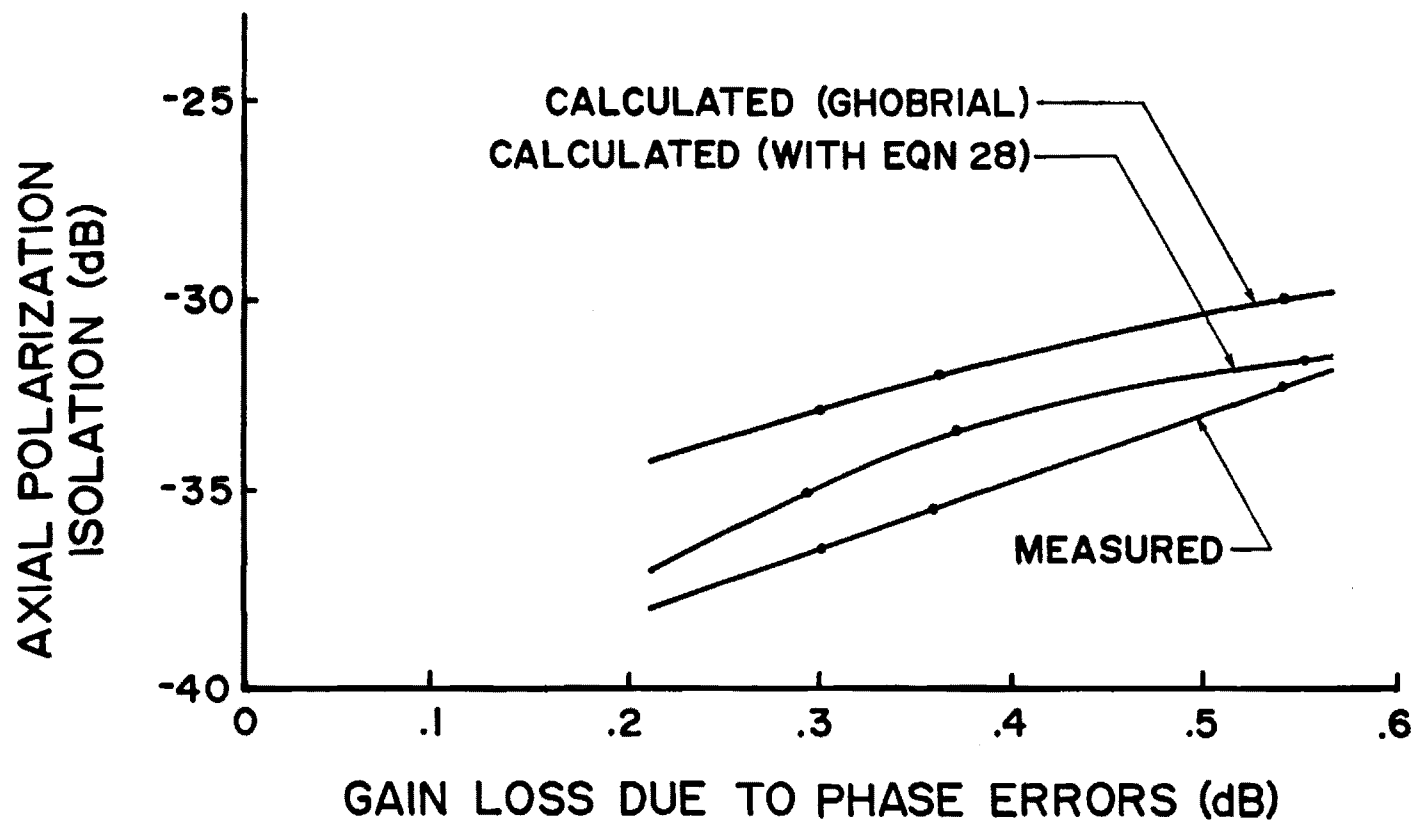


Figure 7. Comparison of mean axial polarization data obtained by two probabilistic models and a measurement.

## APPENDIX B

### A Model of Reflector Errors Caused by Die Defects

#### Introduction

Some circularly symmetrical antenna reflectors are constructed by attaching a number of identical azimuthal sectors along their radial edges. Each sector is fabricated with the use of a die built for that purpose; the same die is used for all sectors of a given reflector. One kind of surface error to which such a reflector is susceptible is caused by randomly positioned defects in the sector die. Clearly, such errors are repeated periodically with azimuth angle in the reflector, though in one given sector they are random. Within one sector, the defect positions are probably all independent of each other.

#### Error Model for One Sector

The characteristics of the errors of a given sector, as described above, closely resemble those of the error model in the reference paper. That model is essentially defined by Equations (8) through (11), which are repeated below.

$$\underline{E}(\underline{r}) = \sum_{n=1}^N \underline{g}(\underline{r}, \underline{r}_n) \underline{E}_0(\underline{r}_n) \quad (1)$$

$$\underline{g}(\underline{r}, \underline{r}_n) = \underline{g}(\underline{r} - \underline{r}_n) \quad (2)$$

$$P_J(\underline{r}_1, \underline{r}_2, \dots, \underline{r}_N) = P(\underline{r}_1) P(\underline{r}_2) \dots P(\underline{r}_N) \quad (3)$$

where  $\underline{r} = x\hat{x} + y\hat{y}$  is a position in the aperture,  
 $\underline{r}_n$  is a defect position in the aperture,  
 $N$  is the number of defects (in one sector, here),  
 $\underline{E}_0$  is the aperture electric field with no errors,  
 $\underline{E}$  is the additive aperture field error,  
 $\underline{g}$  is a dyadic scattering function for one defect,  
 $p_J$  is the joint probability density function  
 (pdf) of defect positions (completely specifies  
 randomness), and  
 $p$  is the pdf for one defect.

This is a very general error model, for which the power-pattern average has been derived in closed form, as presented in the paper. Therefore, it is prudent to assess the applicability of this model to the present problem of die errors. Equation (1) should be a very good approximation unless the functions  $\underline{g}$  are so extensive that the incident field  $\underline{E}_0$  cannot be adequately represented by its value at one point ( $\underline{r}_n$ ). This is not believed to be the case; specifically,

Assumption 1.  $\underline{E}_0$  does not vary much over the extent of one defect.

The accuracy of Equation (2) depends on the precise nature of the defects, but it appears to be reasonable as applied to one sector. It states:

Assumption 2. The scattering pattern is the same for all defects (in a given sector), independent of position.

Even if this assumption is not strictly true it will be an especially good approximation for simple (circularly symmetrical) defects, and for cases of only one defect. It is expected to be quite applicable to dent type defects that cause phase error.

The accuracy of Equation (3) also depends on the cause of the defects. In words, it says:

Assumption 3. All defect positions are independent and have the same statistics.

This is expected to be a good approximation for a single sector, and of course, it is exactly true for the case of only one defect. However, it is certainly not applicable to defects in different sectors, since their positions are precisely repeated in every sector. They have the same statistics, but they are completely dependent on each other. This is precisely why the theory must be modified.

### A Circular Array of Sectors

With the error model of the reference paper, we can calculate the mean power pattern of one sector of a reflector containing die defects. The next task is to consider a whole reflector, which will be simply a circular array of such sectors. We place the origin at the center of the circle (the vertex of every sector) so that each element of the array is only a rotation from the reference sector.

Consider the aperture field and its transform for one sector.

$$\underline{E}_a(\underline{r}) = \underline{E}_0(\underline{r}) + \underline{E}(\underline{r}) \quad (4)$$

$$\underline{f}(\theta, \phi) = \widetilde{\underline{E}_a(\rho, \psi)} \quad (5)$$

where  $\underline{E}_a$  is the total aperture field,  
 $\underline{f}$  is its Fourier transform (equal to the far field for our purposes),  
 $\theta, \phi$  are standard spherical far-field coordinates,  
 $\rho, \psi$  are polar aperture coordinates, and  
 $\widetilde{\phantom{x}}$  represents the Fourier Transform (FT) performed in rectangular coordinates.

Later we will find it useful to know that rotation of coordinates propagates through the FT:

$$\underline{f}(\theta, \phi - \phi_0) = \widetilde{\underline{E}_a(\rho, \psi - \phi_0)}, \quad (6)$$

where  $\phi_0$  is an arbitrary constant.

Statistics of  $\underline{f}$  are not generally very useful; we need to know those of  $\underline{f} \underline{f}^\dagger$  ( $\dagger$  represents transpose-conjugate). Specifically, the statistic  $\langle \underline{f} \underline{f}^\dagger \rangle$  will be investigated since it contains the information needed to get the mean power pattern in any polarization (as explained in the reference). Now Reference Equation (3) can be written,

$$\langle \underline{f} \underline{f}^\dagger \rangle = \langle \widetilde{\underline{E}_a \underline{E}_a^\dagger} \rangle \quad (7)$$

for any one sector. For the total aperture (array),

$$\underline{f}_t(\theta, \phi) = \sum_m^M \underline{f}(\theta, \phi - \phi_m), \quad (8)$$

where  $\underline{f}_t$  is the total far field,  
 $M$  is the number of equal sectors in the reflector, and  
 $\phi_m = \frac{2\pi m}{M}$  is the rotation to the  $m$ -th sector.

Then for the array, the desired statistic is

$$\langle \underline{f}_t \underline{f}_t^\dagger \rangle = \sum_{\ell}^M \sum_m^M \langle \underline{E}_a(\rho', \psi' - \phi_{\ell}) \underline{E}_a^\dagger(\rho, \psi - \phi_m) \rangle, \quad (9)$$

since the mean operation can always be exchanged with summation. For the same reason, Reference Equations (5) through (7) are still valid, but now  $\underline{r}'$  and  $\underline{r}$  may be in different sectors. Thus, we have for Reference Equation (7),

$$\langle \underline{f}_t \underline{f}_t^\dagger \rangle = \sum_{\ell}^M \sum_m^M \left[ \langle \widetilde{\underline{E}_{a\ell}} \rangle \langle \widetilde{\underline{E}_{am}}^\dagger \rangle + \underline{\underline{V}}_{E\ell m} \right], \quad (10)$$

where  $\underline{\underline{V}}_{E\ell m}$  is the error field correlation, and  
 $\underline{E}_{a\ell} = \underline{E}_a(\rho, \psi - \phi_{\ell})$ , etc.

In Equation (10) the double transform term is the only one presenting a problem. The others can be rotated to the coordinate system of the reference sector, then Fourier Transformed, and then rotated back. In the scalar case,  $E_o(\rho, \psi) = E_o(\rho, \psi - \phi_m)$ ; then all  $2m$  single transforms are identical except for rotation. In any case, they are similar and straightforward.

If we parallel the analysis of the reference paper, we hope to find the following in lieu of its Equations (26) and (27).

$$\underline{\underline{C}} = \int_{\text{Sector}} \underline{E}_{o\ell} \underline{E}_{om}^\dagger \underline{p} \, d\underline{r}, \quad (11)$$

$$\underline{\underline{V}}_{E\ell m} = N \underline{\underline{g}}_{\ell} (\underline{\underline{C}} - \widetilde{\underline{E}_{o\ell} \underline{p}} \widetilde{\underline{E}_{om} \underline{p}}^\dagger) \underline{\underline{g}}_m \quad (12)$$

These expressions say that  $V_{E\ell m}$  are all equal if  $E_0$  and  $\underline{g}$  are rotationally symmetrical. This is intuitively satisfying because we know that the defect positions (and hence  $p$ ) have rotational symmetry.  $V_{E\ell m}$  is a measure of the "sameness" between  $E(\rho', \psi' - \phi_\ell)$  and  $E(\rho, \psi - \phi_m)$  caused by defect scattering. One would expect this function to depend mainly on  $(\rho', \psi')$  and  $(\rho, \psi)$  and be relatively independent of  $\ell$  and  $m$ .

### Detailed Analysis

Unfortunately, detailed analysis is not easy. Whenever  $\ell \neq m$ , we are dealing with defects that are not independent. Thus, Reference Equation (13) doesn't hold, but rather we have the mean defined as follows.

$$A = \int_{-\infty}^{\infty} \int_{-\infty}^{\infty} A(\underline{r}_\ell, \underline{r}_m) p_2(\underline{r}_\ell, \underline{r}_m) d\underline{r}_\ell d\underline{r}_m, \quad (13)$$

where  $A$  is a nominal function of two random defect positions,  
 $\underline{r}_\ell = (\rho'_n, \psi'_n - \phi_\ell)$  is the position of defect  $n$  in sector  $\ell$ ,  
 $\underline{r}_m = (\rho_n, \psi_n - \phi_m)$  is the position of defect  $n$  in sector  $m$ , and  
 $p_2$  is their joint pdf.

To reduce this integral, we observe that the conditioned pdf, the pdf of  $\underline{r}_m$  given the value of  $\underline{r}_\ell$ , is

$$p_c(\underline{r}_m | \underline{r}_\ell = \text{constant}) = \delta(\rho'_n \cos \psi'_n - \rho_n \cos \psi_n, \rho'_n \sin \psi'_n - \rho_n \sin \psi_n). \quad (14)$$

That is, given the defect position in sector  $\ell$ , the defect position in sector  $m$  is an exact rotation from  $\ell$  to  $m$ .

Then using the theorem<sup>\*</sup>

$$\langle A(\underline{r}_\ell, \underline{r}_m) \rangle = \langle \langle A(\underline{r}_\ell, \underline{r}_m) | \underline{r}_\ell = \underline{r}_{0\ell} \rangle \rangle, \quad (15)$$

we do the integration over  $\underline{r}_m$  first, and the delta function leaves

$$\langle A \rangle = \int_{-\infty}^{\infty} A(\underline{r}_{0\ell}, \underline{r}_{0m}) p(\underline{r}_0) d\underline{r}_0, \quad (16)$$

just as in the reference paper. Here  $\underline{r}_{0\ell} = (\rho_0, \psi_0 - \phi_\ell)$ , etc.

<sup>\*</sup>A. Papoulis, "Probability, Random Variables, and Stochastic Processes," McGraw Hill, 1965, Equation (7-59).

More explicitly,

$$\begin{aligned} \langle A(\rho'_1, \psi'_1 - \phi_\ell, \rho_1, \psi_1 - \phi_m, \rho'_1, \psi'_1 - \phi_\ell, \rho_1, \psi_1 - \phi_m) \rangle = \\ \int A(\rho'_1, \psi'_1 - \phi_\ell, \rho_1, \psi_1 - \phi_m, \rho'_1, \psi'_1 - \phi_\ell, \rho_1, \psi_1 - \phi_m) p(\rho_1, \psi_1) \rho_1 d\rho_1 d\psi_1. \end{aligned} \quad (17)$$

Then the equivalent of Reference Equation (38) is written,

$$\langle \underline{G}'_\ell \underline{G}_m^\dagger \rangle = \int \underline{g}(\underline{r}'_\ell - \underline{r}_{1\ell}) \underline{E}_0(\underline{r}_{1\ell}) \underline{E}_0^\dagger(\underline{r}_{1m}) \underline{g}^\dagger(\underline{r}_m - \underline{r}_{1m}) p(\underline{r}_1) d\underline{r}_1. \quad (18)$$

Now we observe that

$$\begin{aligned} p(\underline{r}_1) &= p(\underline{r}_{1m}), \text{ and} \\ d\underline{r}_1 &= d\underline{r}_{1m}, \text{ and we let} \\ \underline{r}_1 &= \underline{r}_{1m} - \underline{r}_{m\ell}. \end{aligned} \quad (19)$$

Then the  $\underline{g}^\dagger$  function is seen to be convolved with the remaining integrand.

$$\langle \underline{G}'_\ell \underline{G}_m^\dagger \rangle = \left[ \underline{g}(\underline{r}'_\ell - (\underline{r}_m - \underline{r}_{m\ell})) \underline{E}_0(\underline{r}_m - \underline{r}_{m\ell}) \underline{E}_0^\dagger(\underline{r}_m) p(\underline{r}_m) \right] * \underline{g}^\dagger(\underline{r}_m). \quad (20)$$

Next we observe that  $\underline{r}_m - \underline{r}_{m\ell} = \underline{r}_\ell$  and follow the approach of Reference Equation (39). (This  $\underline{r}_\ell$  is an unprimed variable, but rotated from the  $m$  sector to the  $\ell$  sector where the primes are.)

$$\underline{g}(\underline{r}'_\ell - \underline{r}_\ell) = \int \underline{g}(\underline{r}'_\ell - \underline{r}_1) \delta(\underline{r}_\ell - \underline{r}_1) d\underline{r}_1. \quad (21)$$

That is,

$$\underline{g}(\underline{r}'_\ell - \underline{r}_\ell) = \underline{g}(\underline{r}'_\ell) * \delta(\underline{r}_\ell - \underline{r}'_\ell) \quad (22)$$

Thus, we have achieved a form similar to Reference Equation (41), as follows.

$$\langle \underline{G}'_\ell \underline{G}_m^\dagger \rangle = \underline{g}(\underline{r}'_\ell) * \left[ \delta(\underline{r}_\ell - \underline{r}'_\ell) \underline{E}_0(\underline{r}'_\ell) \underline{E}_0^\dagger(\underline{r}_m) p(\underline{r}_m) \right] * \underline{g}^\dagger(\underline{r}_m) \quad (23)$$



Now with the double FT, we have a formula similar to Reference Equation (25). The only remaining task is to determine the double FT of the center term  $\underline{H}_{\ell m}$  of Reference Equation (22).

$$\underline{\tilde{H}}_{\ell m} = \iint \delta(\underline{r}_{\ell} - \underline{r}_{\ell}') \underline{E}_0(\underline{r}_{\ell}') \underline{E}_0^{\dagger}(\underline{r}_m) p(\underline{r}_m) \exp(j\mathbf{k} \cdot (\underline{r}_{\ell}' - \underline{r}_m)) d\underline{r}_{\ell}' d\underline{r}_m \quad (24)$$

Letting  $\underline{r}_{\ell} = \underline{r}_m + \underline{r}_{\ell m}$  again, the  $\delta$  function reduces this expression to a single integral

$$\underline{\tilde{H}}_{\ell m} = \int \underline{E}_0(\underline{r}_m + \underline{r}_{\ell m}) \underline{E}_0^{\dagger}(\underline{r}_m) p(\underline{r}_m) \exp(-j\mathbf{k} \cdot \underline{r}_{\ell m}) d\underline{r}_m \quad (25)$$

where  $\underline{r}_{\ell m} = (\rho_m, \psi_m + \phi_{\ell} - \phi_m)$  is the vector from  $\underline{r}_m$  to the corresponding point in the  $\ell$  sector.

Finally, the formula for the mean power pattern components can be written:

$$\begin{aligned} \langle \underline{ff}^{\dagger} \rangle = & \sum_{\ell}^M \sum_m^M \left[ \underline{\tilde{E}}_{o\ell} + N \underline{\tilde{g}}_{\ell} \underline{\widetilde{E}}_{o\ell}^p \right] \left[ \underline{\tilde{E}}_{om} + N \underline{\tilde{g}}_m \underline{\widetilde{E}}_{om}^p \right]^{\dagger} \\ & + N \sum_{\ell}^M \sum_m^M \underline{\tilde{g}}_{\ell} \left[ \underline{\tilde{H}}_{\ell m} - \underline{\widetilde{E}}_{o\ell}^p \underline{\widetilde{E}}_{om}^{p\dagger} \right] \underline{\tilde{g}}_m^{\dagger}, \end{aligned} \quad (26)$$

where  $\ell, m$  are indices on sectors indicating rotation by  $\frac{2\pi\ell}{M}$  or  $\frac{2\pi m}{M}$ , and

$\underline{\tilde{H}}_{\ell m}$  is a single transform dyadic defined in Equation (25).

### Conclusion

A closed form solution has been derived for the effects of segment die defects on the radiated vector power pattern. It is closely related to a theory developed, tested, and published by Georgia Tech. This relation reduces the risk and requirements for verification. In the programming of this solution, transforms should be done in polar coordinates to facilitate the rotation operation. Since a polar integration routine must be written for other error types, it might be used here also.

VKT:bg

**APPENDIX C**  
**CALCULATED PATTERNS**

**List of Figures**

<b>Figure C-</b>	<b>Page</b>
1. Radial aperture phase for die-defect errors in Antenna II. . . . .	75
2. Total-aperture phase for die-defect errors in Antenna II. . . . .	76
3. Radiation pattern for die-defect errors in Antenna II. . . . .	77
4. Radial aperture phase for profile errors in Antenna II. . . . .	78
5. Total-aperture phase for profile errors in Antenna II. . . . .	79
6. Radiation pattern for profile errors in Antenna II. . . . .	80
7. Aperture phase on first radius for assembly errors in Antenna II . . . . .	81
8. Total-aperture phase for assembly error in Antenna in Antenna II . . . . .	82
9. Radiation pattern for assembly errors in Antenna II. . . . .	83
10. Aperture phase on first radius for assembly errors in Antenna I. . . . .	84
11. Total-aperture phase for assembly errors in Antenna I . . . . .	85
12. Radiation pattern for assembly errors in Antenna I. . . . .	86
13. Azimuthal aperture phase for cusp errors in Antenna I . . . . .	87
14. Total-aperture phase for cusp errors in Antenna I . . . . .	88
15. Radiation pattern above a reflector joint for cusp errors in Antenna I . . . . .	89

## List of Figures

<u>Figure C-</u>	<u>Page</u>
16. Radiation pattern between reflector joints for cusp errors in Antenna I . . . . .	90
17. Azimuthal aperture phase for cusp errors in Antenna II. . . . .	91
18. Total-aperture phase for cusp errors in Antenna II. . . . .	92
19. Radiation pattern above a reflector joint for cusp errors in Antenna II. . . . .	93
20. Radiation pattern between antenna joints for cusp errors in Antenna II. . . . .	94
21. Azimuthal aperture phase for severe cusp errors in Antenna II. . . . .	95
22. Total-aperture phase for severe cusp errors in Antenna II. . . . .	96
23. Radiation pattern above a reflector joint for severe cusp errors in Antenna II . . . . .	97
24. Radiation pattern between reflector joints for severe cusp errors in Antenna II . . . . .	98
25. Radial aperture phase for measured errors in Antenna II. . . . .	99
26. Azimuthal aperture phase for measured errors in Antenna II. . . . .	100
27. Total-aperture phase for measured errors in Antenna II. . . . .	101
28. Horizontal radiation pattern for measured errors in Antenna II. . . . .	102
29. Vertical radiation pattern for measured errors in Antenna II. . . . .	103
30. Radial aperture phase for measured errors in Antenna III at 14.5 GHz . . . . .	104
31. Azimuthal aperture phase for measured errors in Antenna III at 14.5 GHz . . . . .	105

## List of Figures

<u>Figure C-</u>	<u>Page</u>
32. Total-aperture phase for measured errors in Antenna III at 14.5 GHz . . . . .	106
33. Horizontal radiation pattern for measured errors in Antenna III at 11.95 GHz. . . . .	107
34. Vertical radiation patterns for measured errors in Antenna III at 11.95 GHz. . . . .	108
35. Horizontal radiation pattern for measured error in Antenna III at 14.5 GHz . . . . .	109
36. Vertical radiation pattern for measured error in Antenna III at 14.5 GHz . . . . .	110
37. Horizontal radiation pattern for .012 RMS measured error in Antenna IV at 20 GHz . . . . .	111
38. Vertical radiation pattern for .012 RMS measured error in Antenna IV at 20 GHz . . . . .	112
39. Horizontal radiation pattern for .012 RMS measured error in Antenna IV at 30 GHz . . . . .	113
40. Vertical radiation pattern for .012 RMS measured error in Antenna IV at 30 GHz . . . . .	114
41. Horizontal radiation pattern for .018 RMS measured error in Antenna IV at 20 GHz . . . . .	115
42. Vertical radiation pattern for .018 RMS measured error in Antenna IV at 20 GHz . . . . .	116
43. Horizontal radiation pattern for .018 RMS measured error in Antenna IV at 30 GHz . . . . .	117
44. Vertical radiation pattern for .018 RMS measured error in Antenna IV at 30 GHz . . . . .	118
45. Radial aperture phase for normal .018 RMS measured error in Antenna IV at 30 GHz . . . . .	119
46. Total-aperture phase for normal .018 RMS measured error in Antenna IV at 30 GHz . . . . .	120
47. Horizontal radiation pattern for normal .018 RMS measured error in Antenna IV at 30 GHz. . . . .	121

## List of Figures

<u>Figure C-</u>	<u>Page</u>
48. Vertical radiation pattern for normal .018 RMS measured error in Antenna IV at 30 GHz. . . . .	122

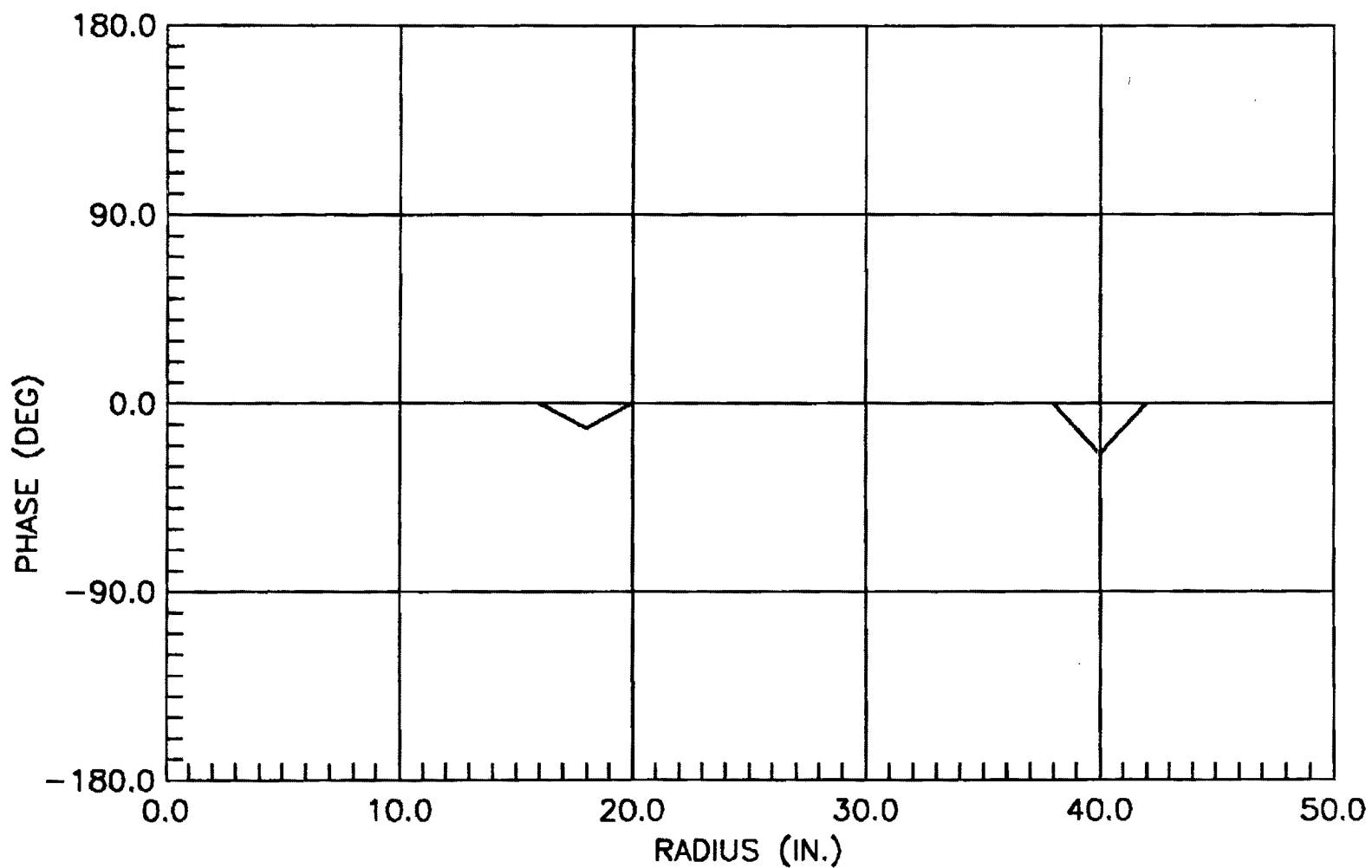


Figure C-1. Radial aperture phase for die-defect errors in Antenna II.

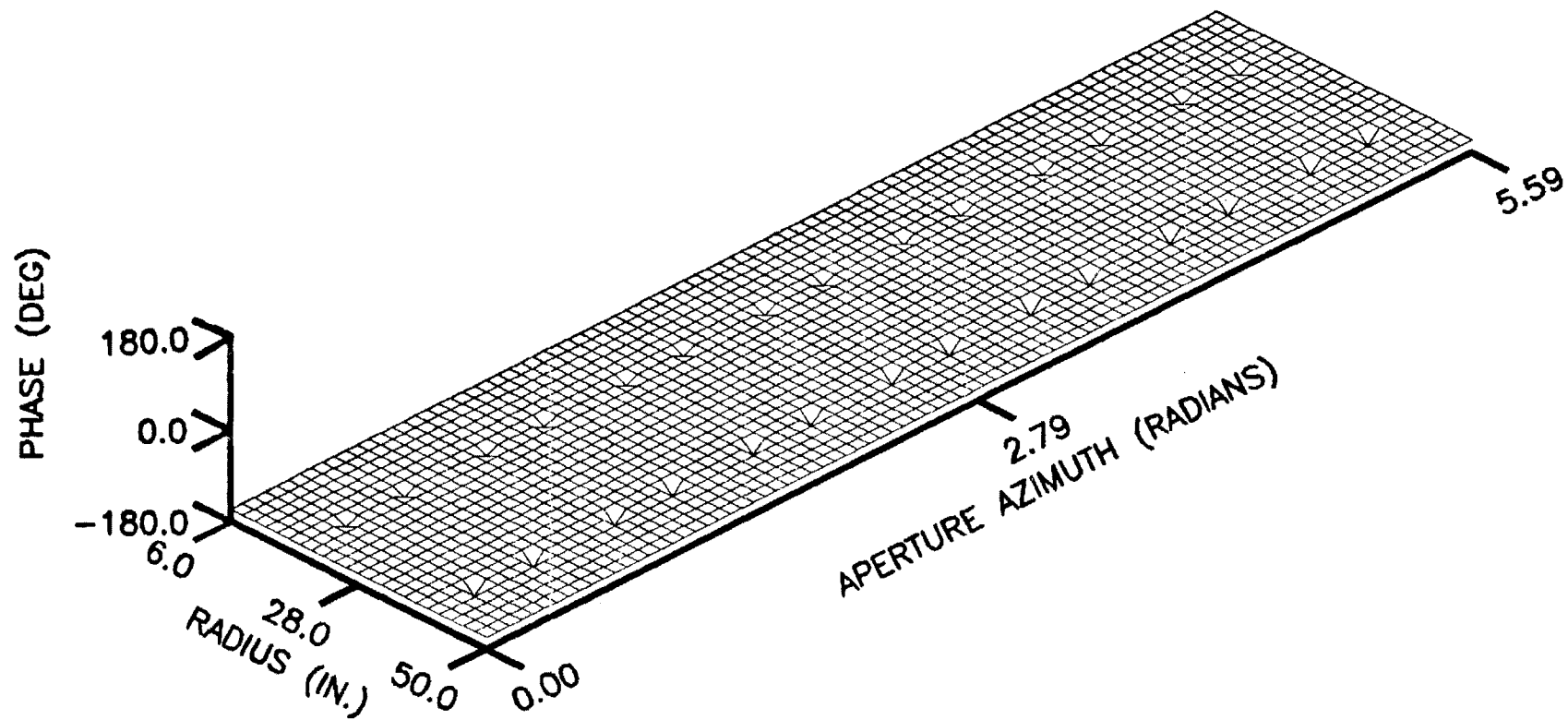


Figure C-2. Total-aperture phase for die-defect errors in Antenna II.

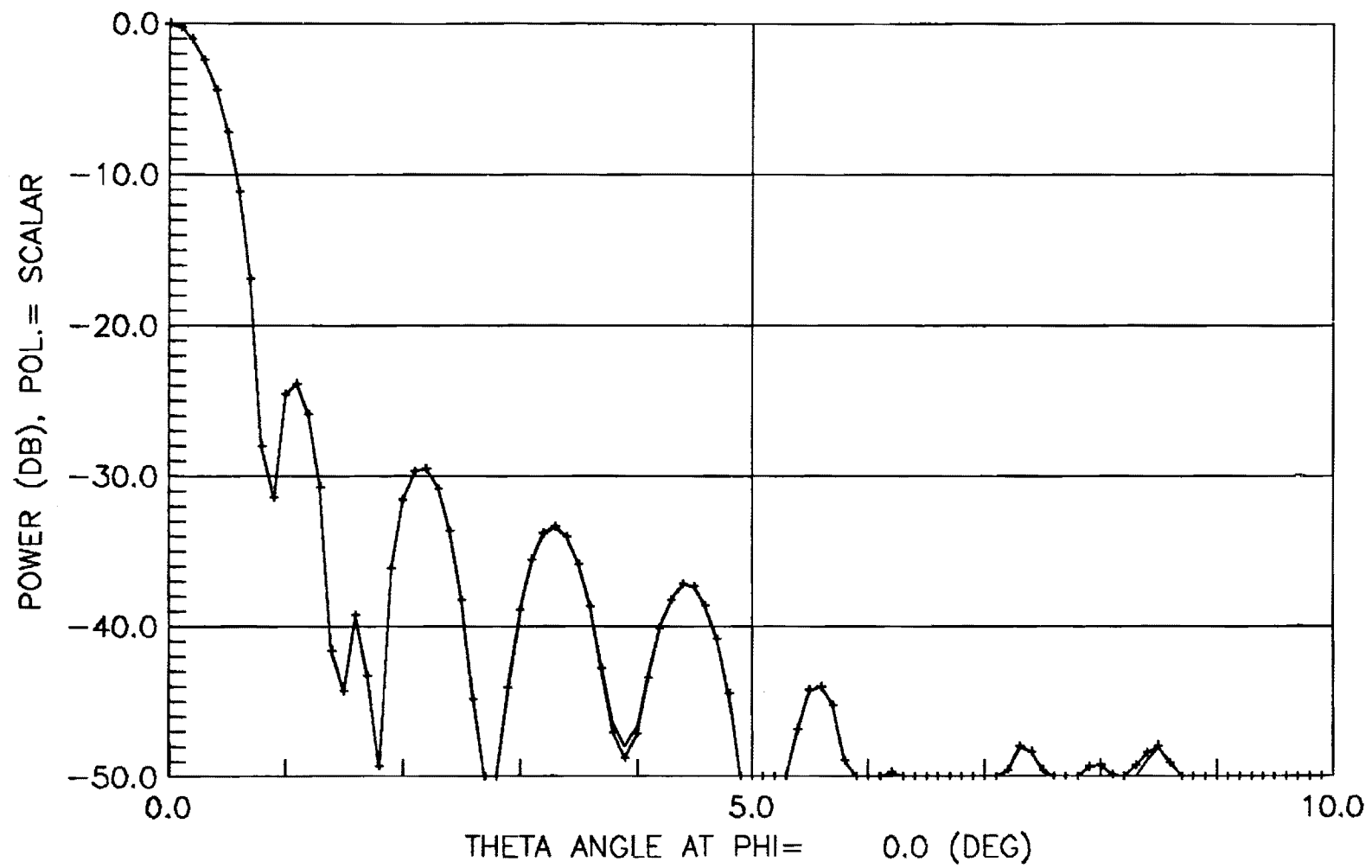


Figure C-3. Radiation pattern for die-defect errors in Antenna II.



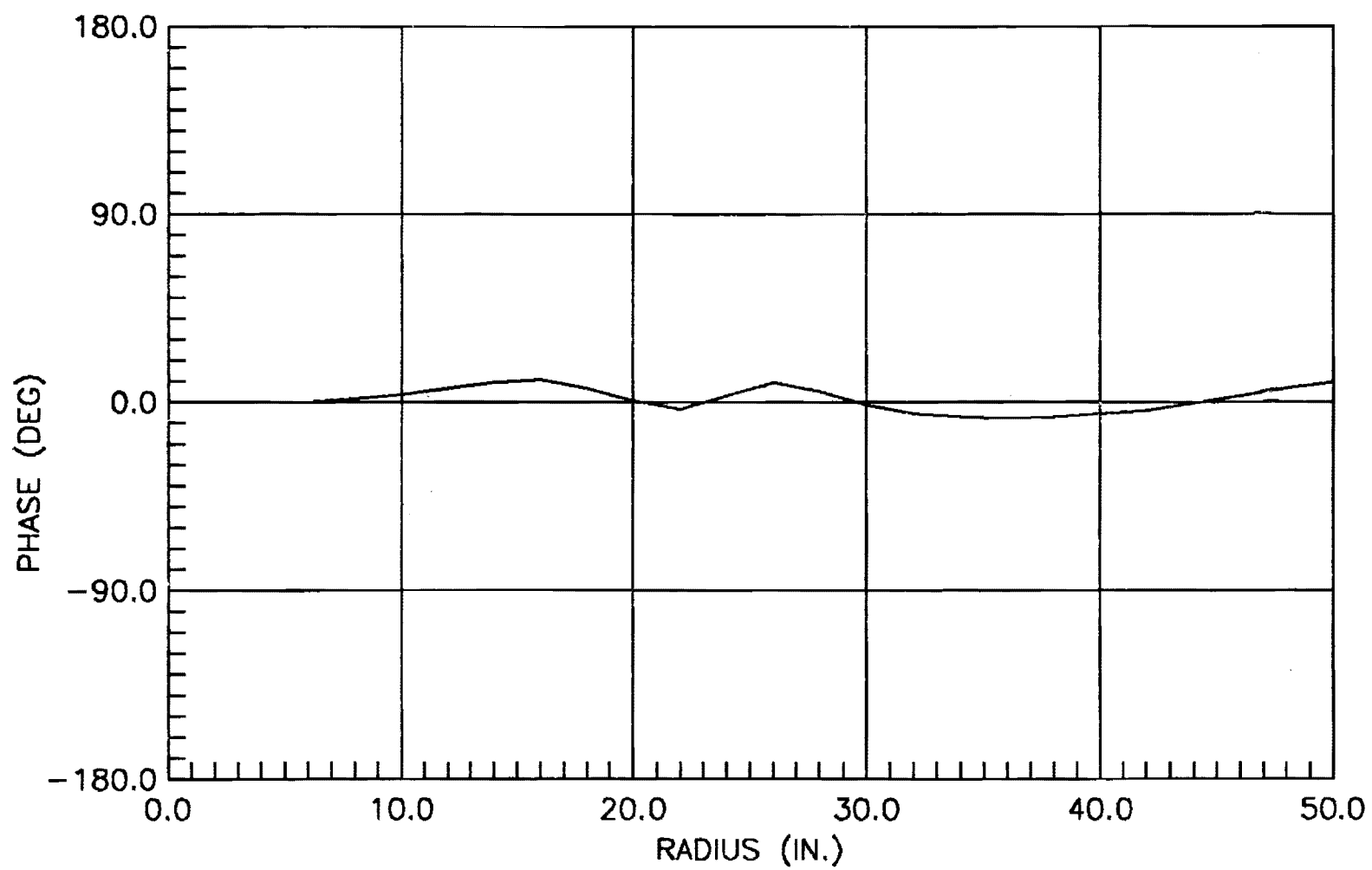


Figure C-4. Radial aperture phase for profile errors in Antenna II.

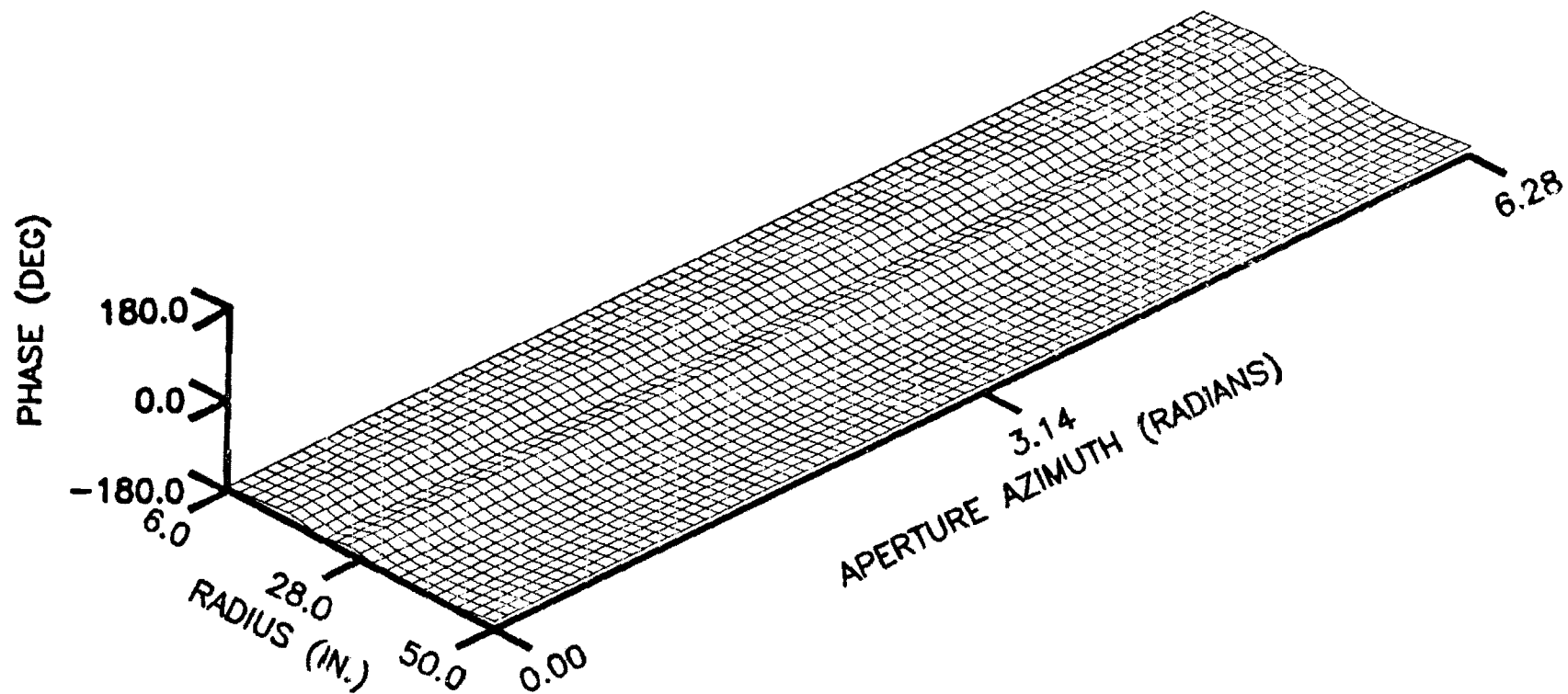


Figure C-5. Total-aperture phase for profile errors in Antenna II.

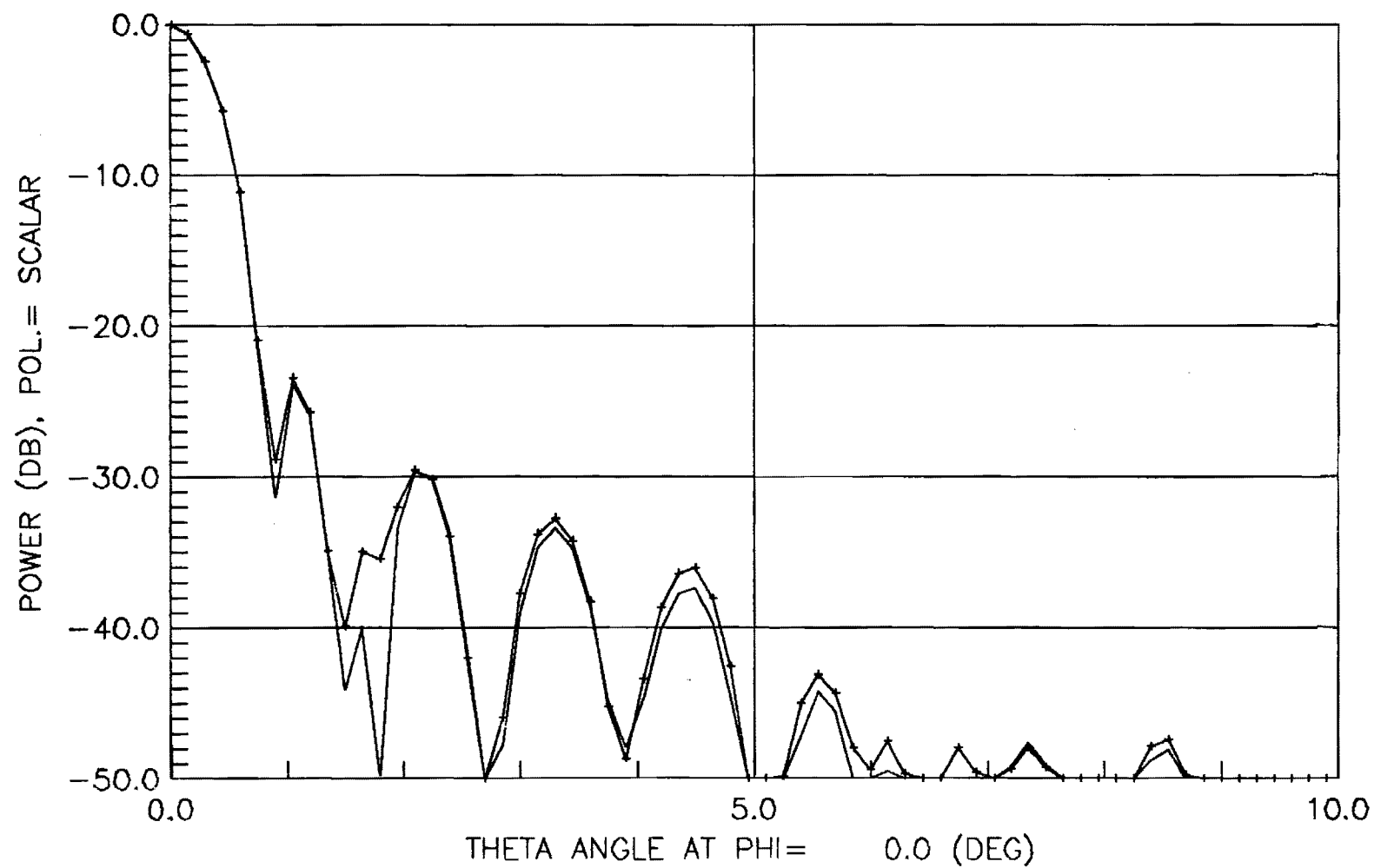


Figure C-6. Radiation pattern for profile errors in Antenna II.

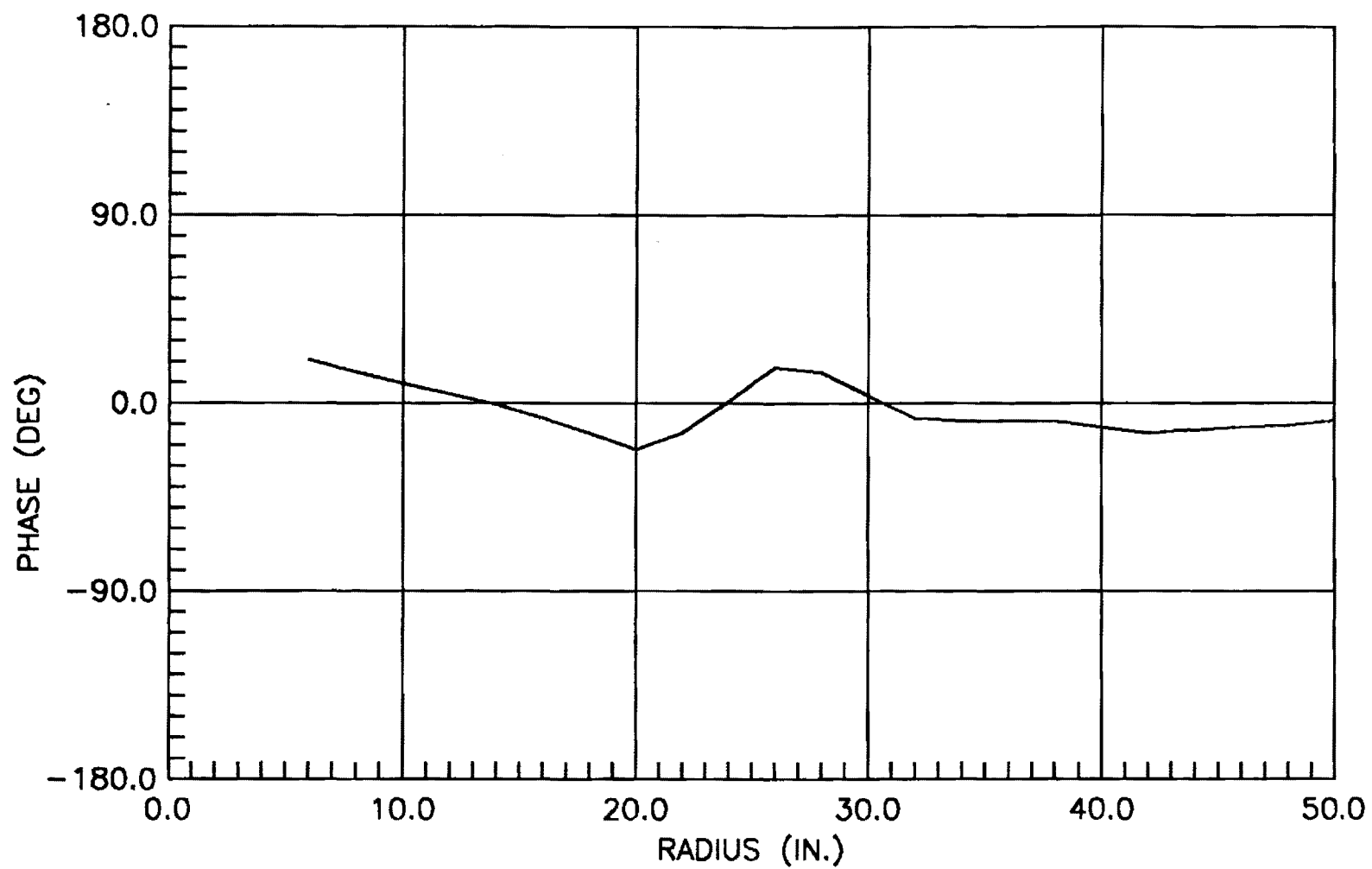


Figure C-7. Aperture phase on first radius for assembly errors in Antenna II.

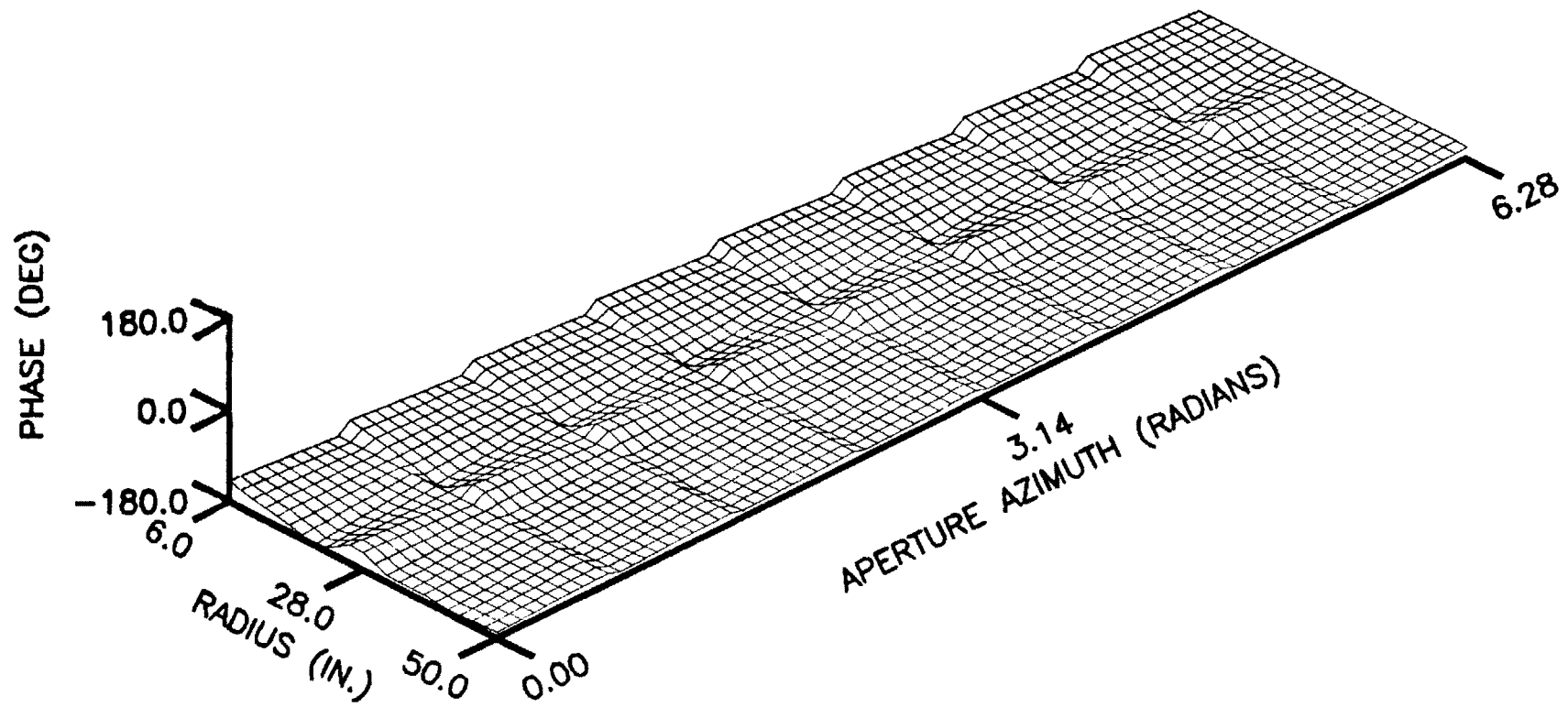


Figure C-8. Total-aperture phase for assembly error in Antenna II.

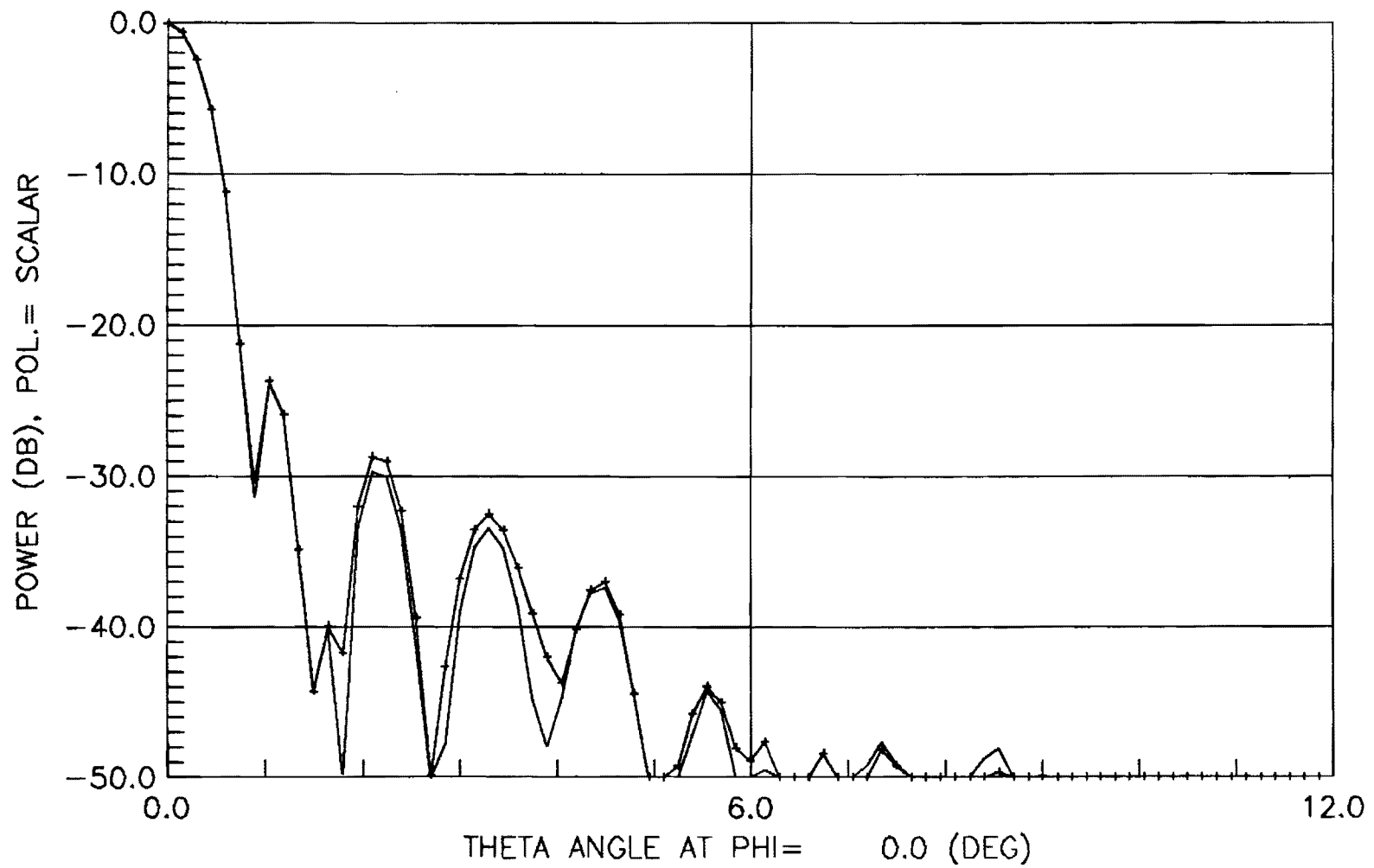


Figure C-9. Radiation pattern for assembly errors in Antenna II.

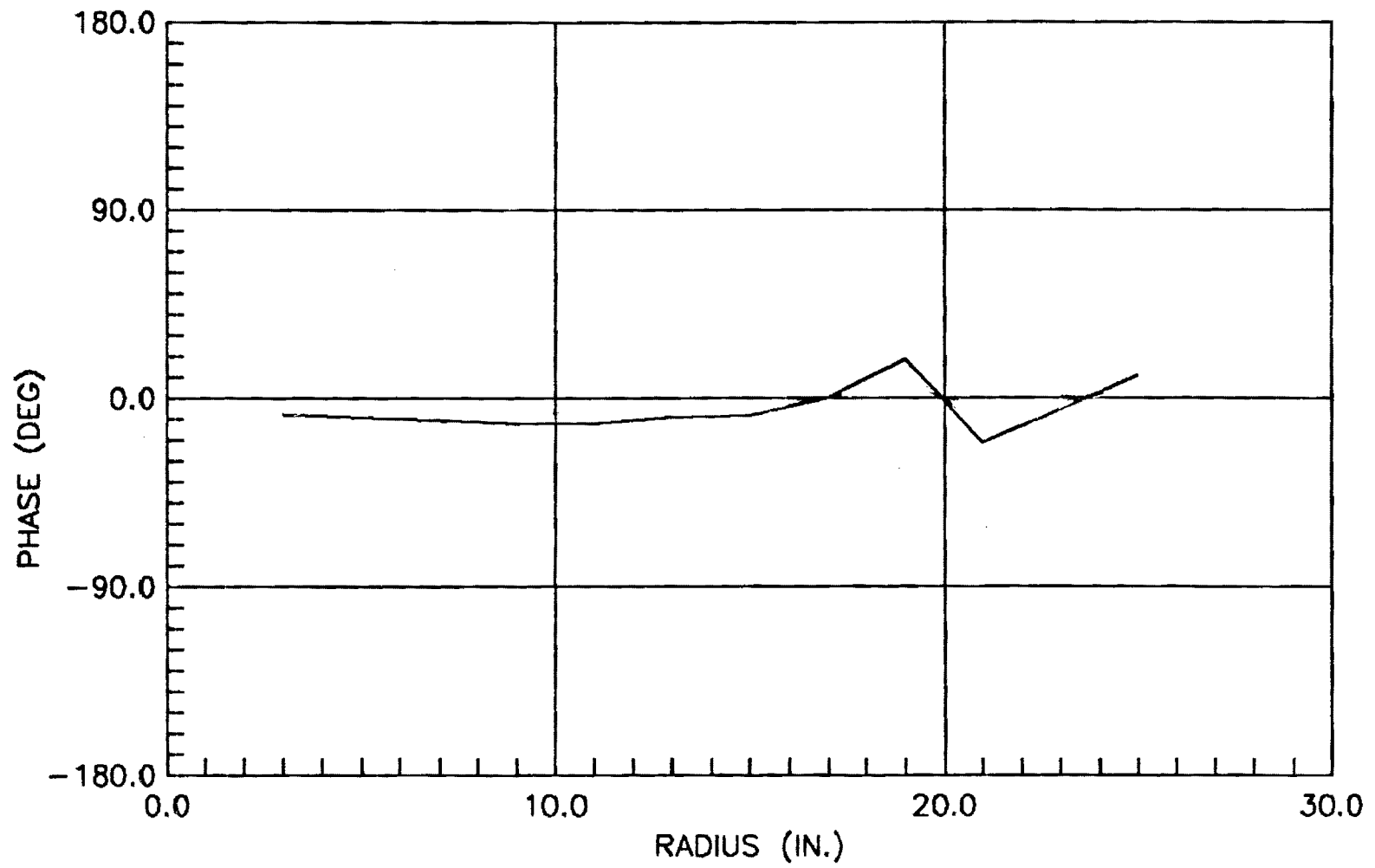


Figure C-10. Aperture phase on first radius for assembly errors in Antenna I.

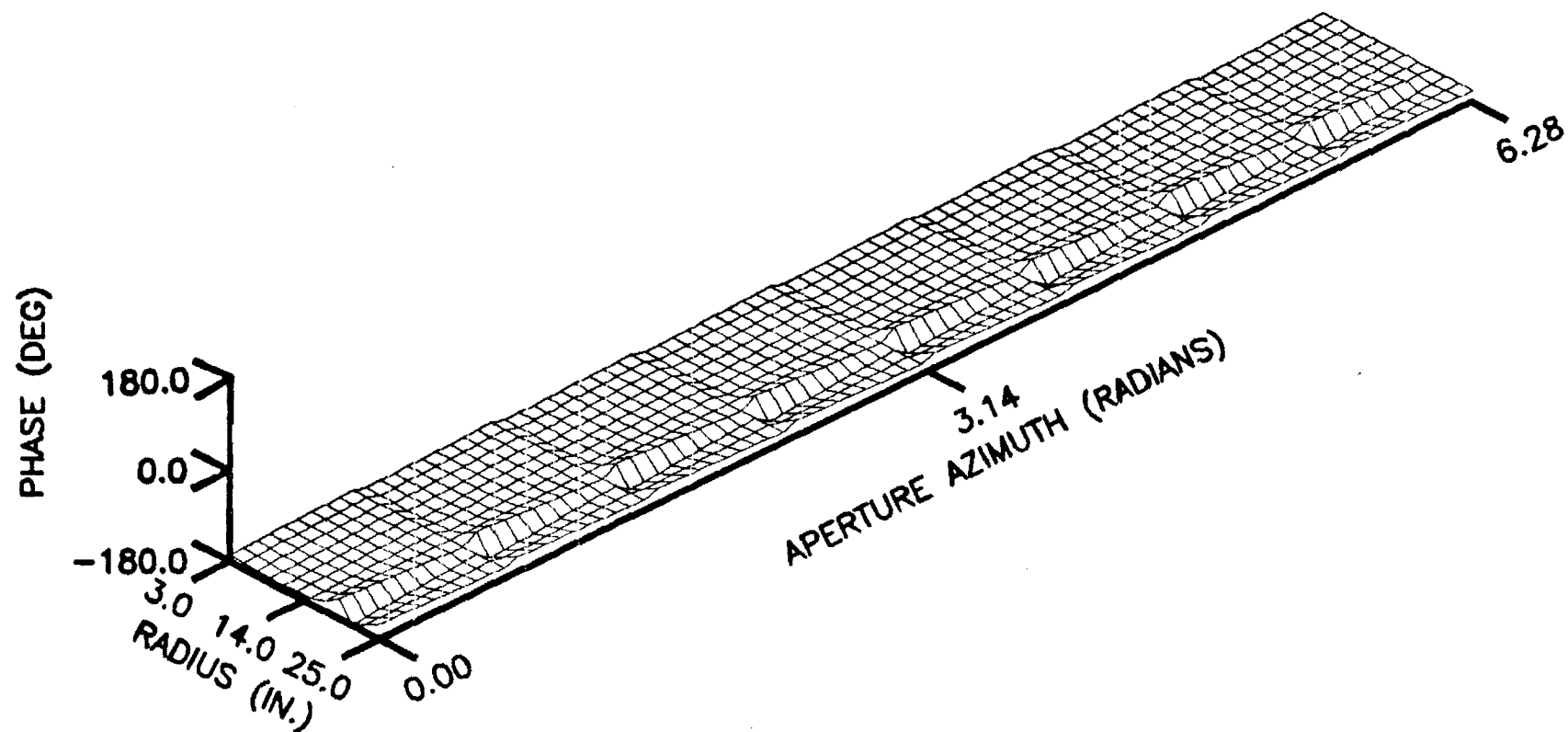


Figure C-11. Total-aperture phase for assembly errors in Antenna I.



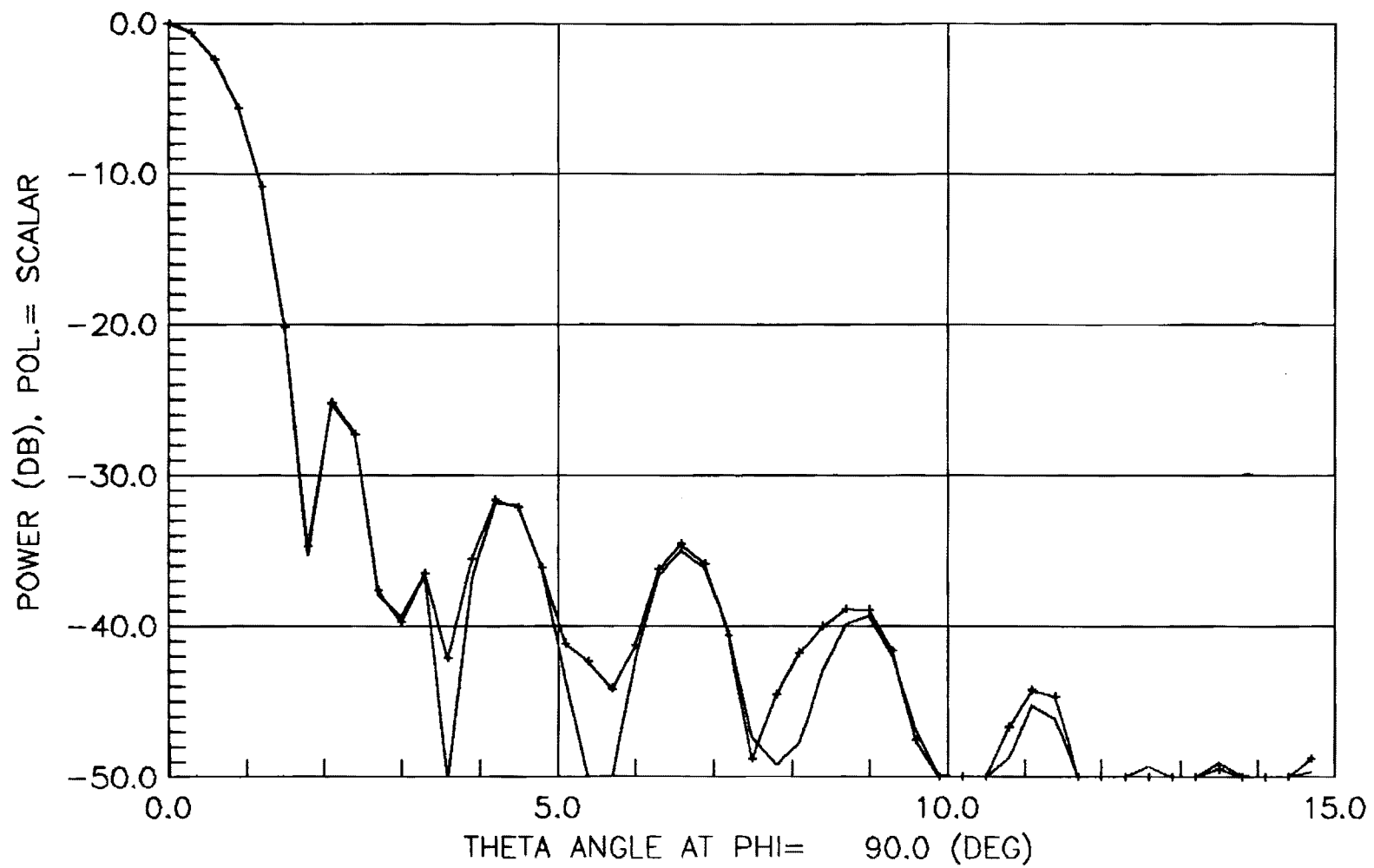


Figure C-12. Radiation pattern for assembly errors in Antenna I.

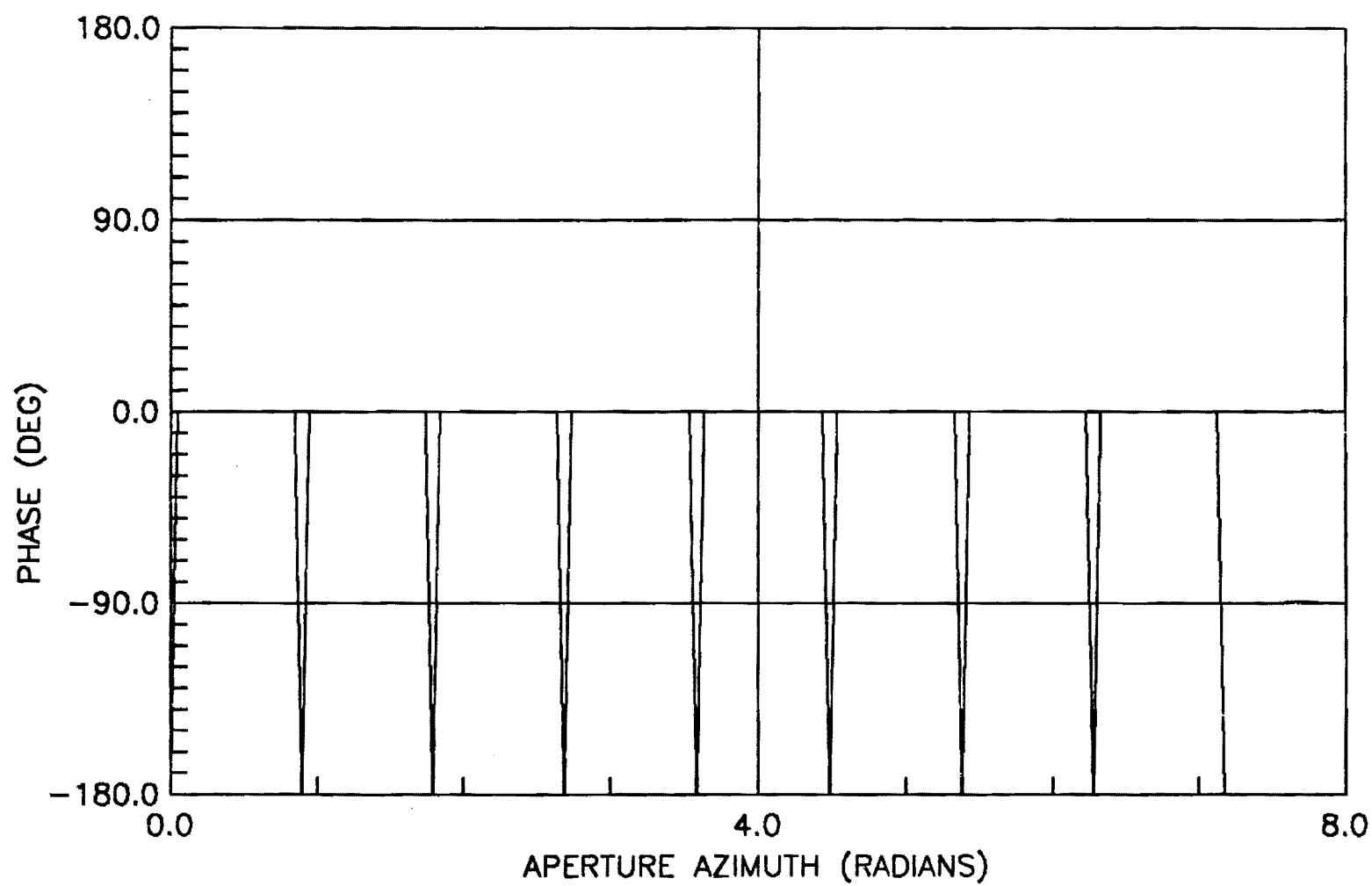


Figure C-13. Azimuthal aperture phase for cusp errors in Antenna I.

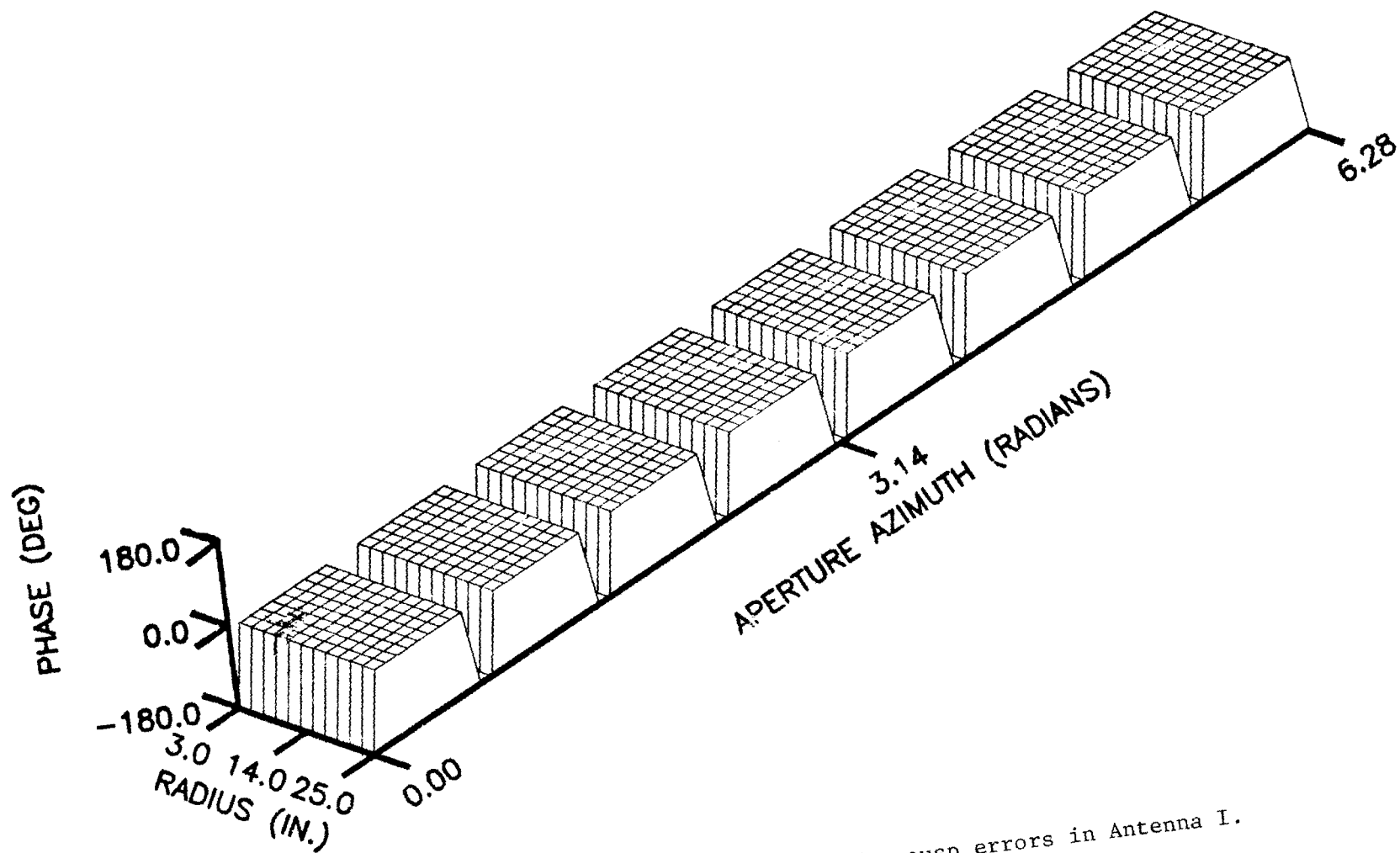


Figure C-14. Total-aperture phase for cusp errors in Antenna I.

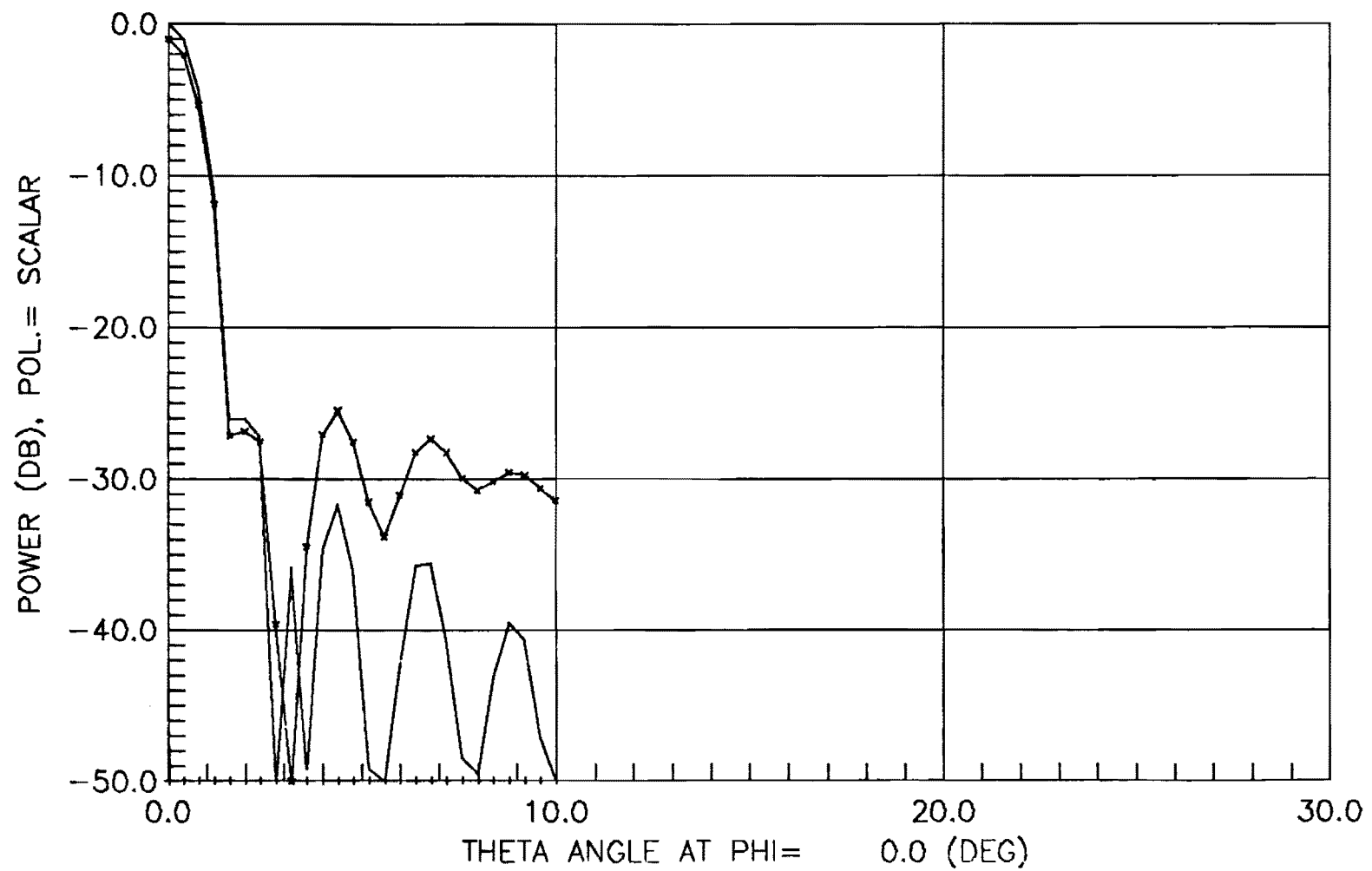


Figure C-15. Radiation pattern above a reflector joint for cusp errors in Antenna I.

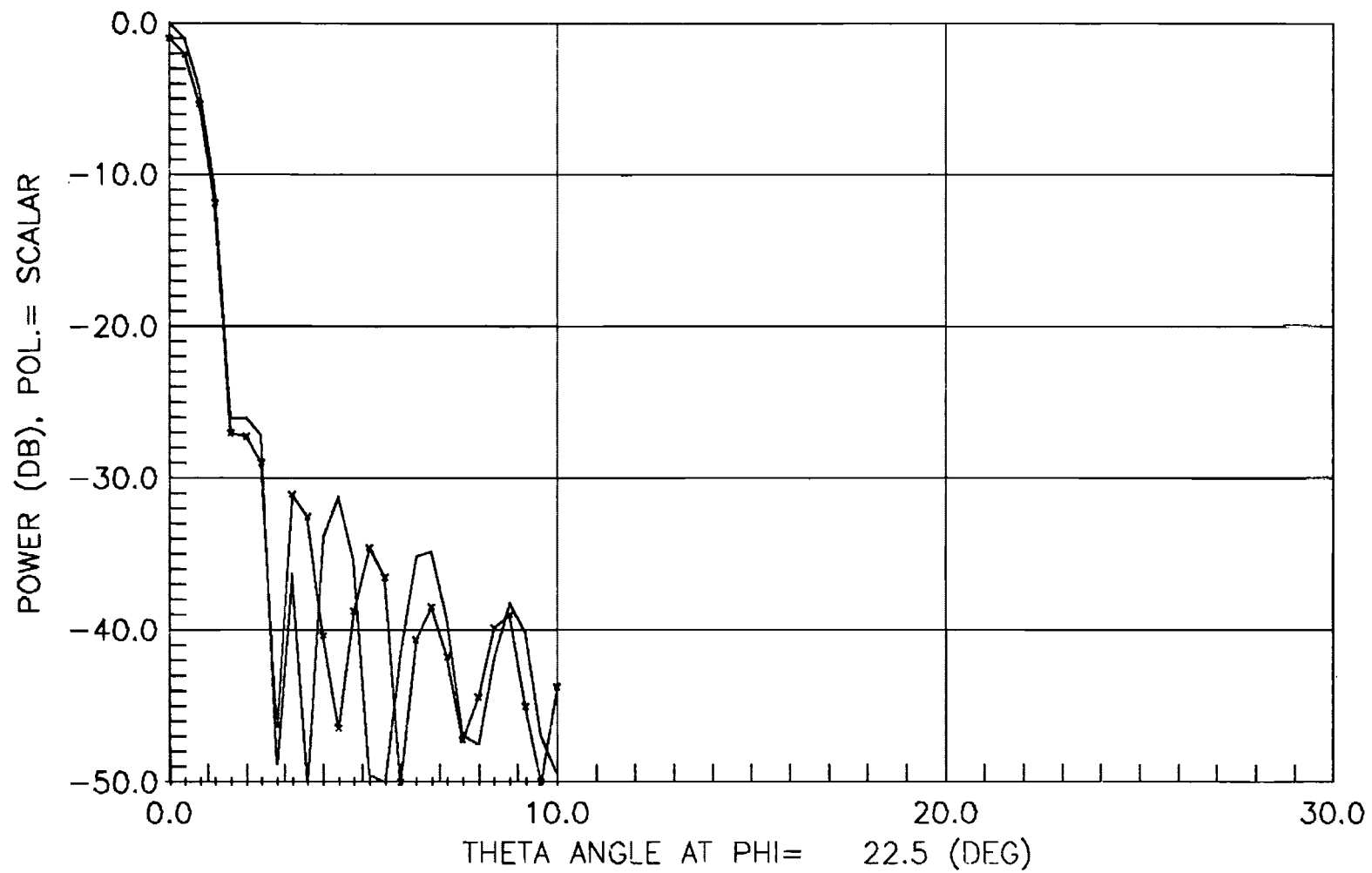


Figure C-16. Radiation pattern between reflector joints for cusp errors in Antenna I.

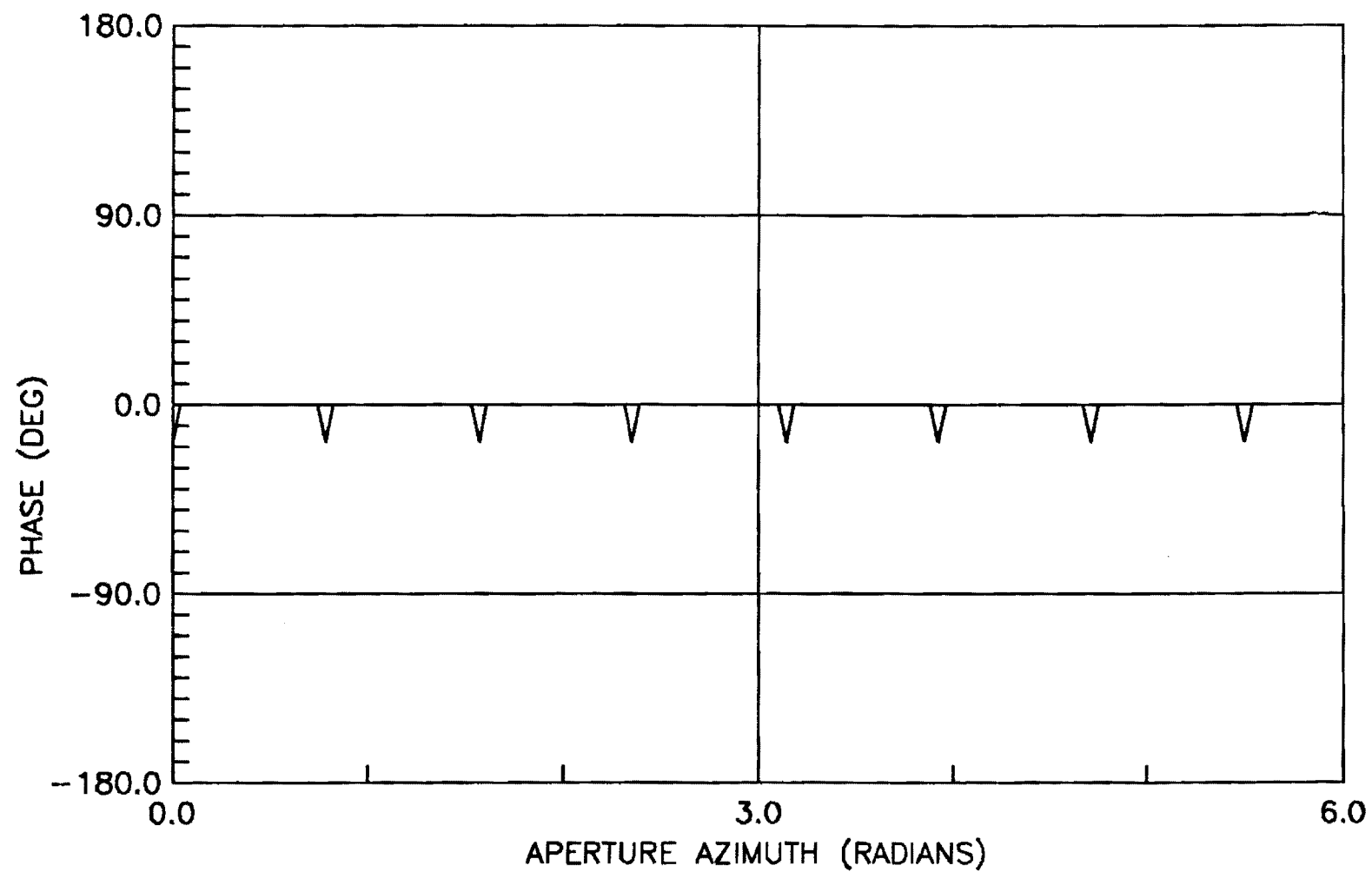


Figure C-17. Azimuthal aperture phase for cusp errors in Antenna II.

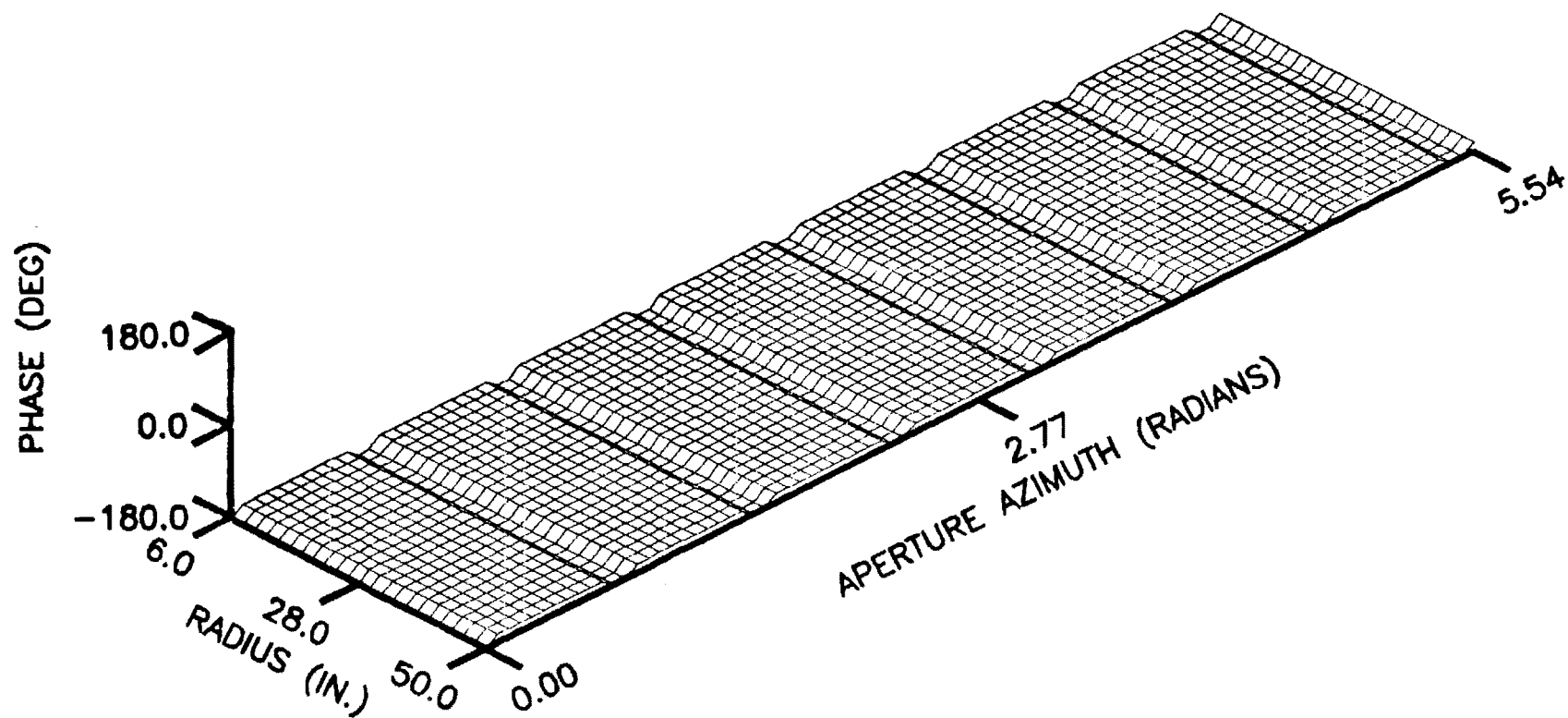


Figure C-18. Total-aperture phase for cusp errors in Antenna II.

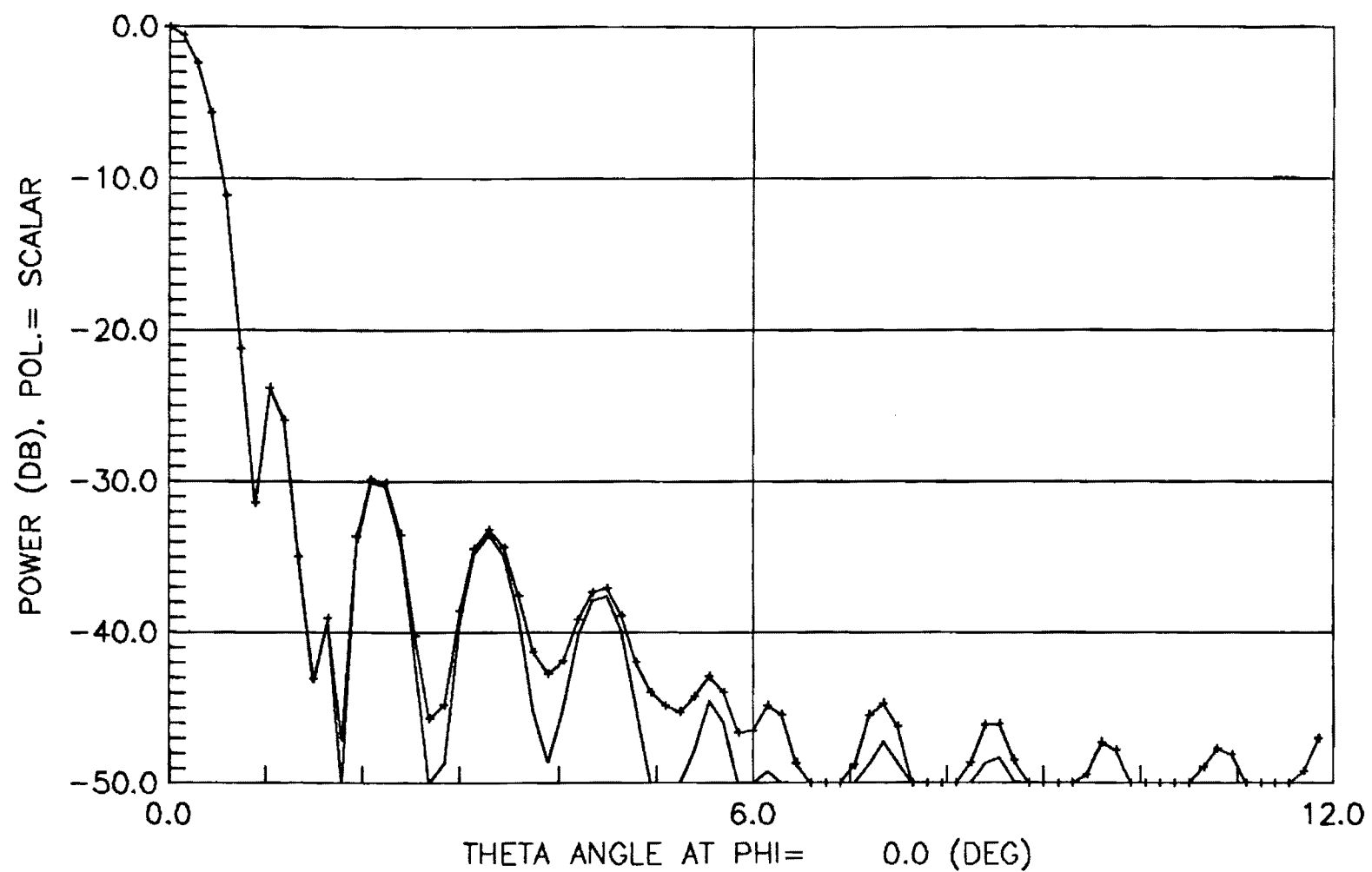


Figure C-19. Radiation pattern above a reflector joint for cusp errors in Antenna II.



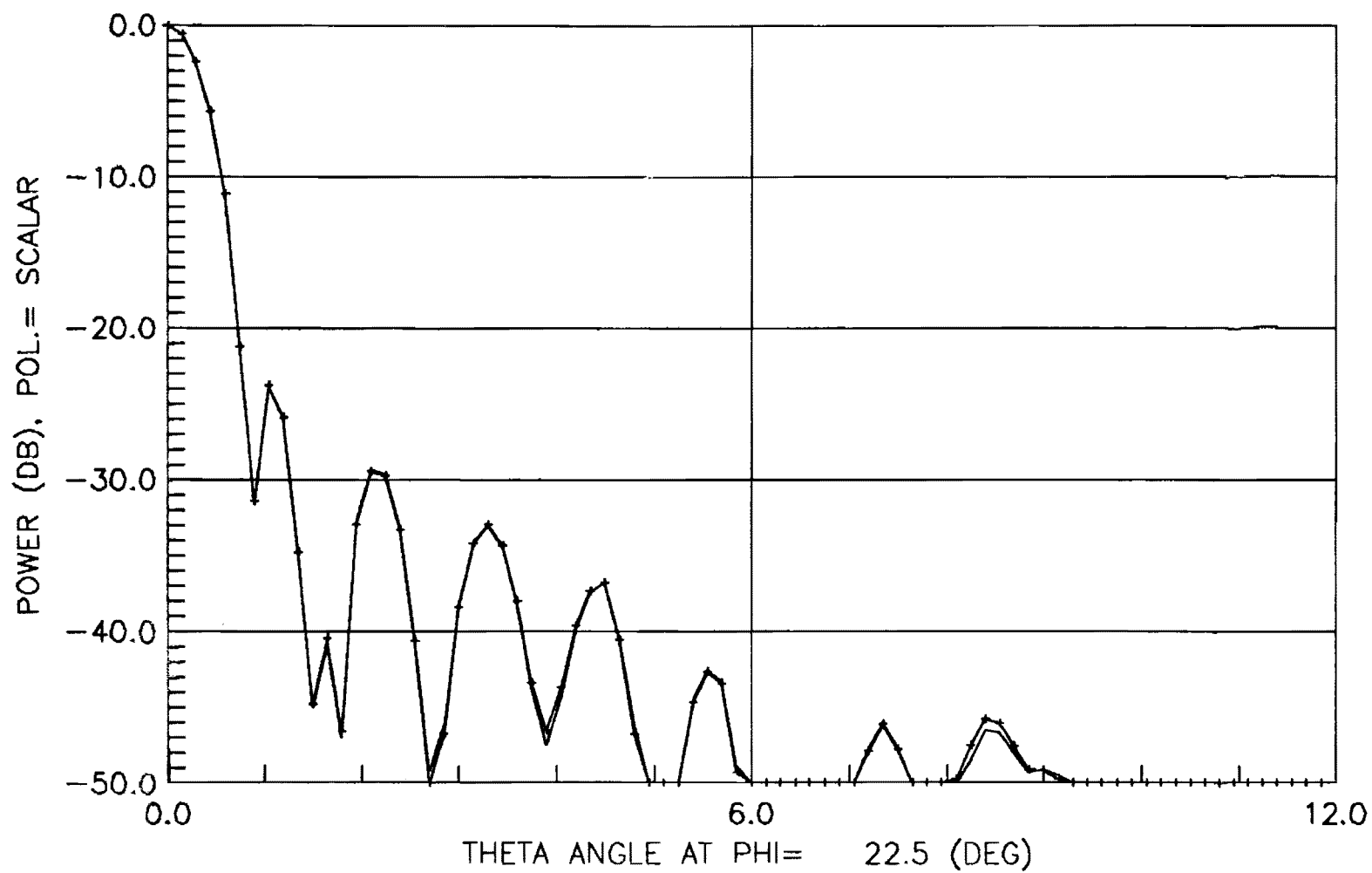


Figure C-20. Radiation pattern between antenna joints for cusp errors in Antenna II.

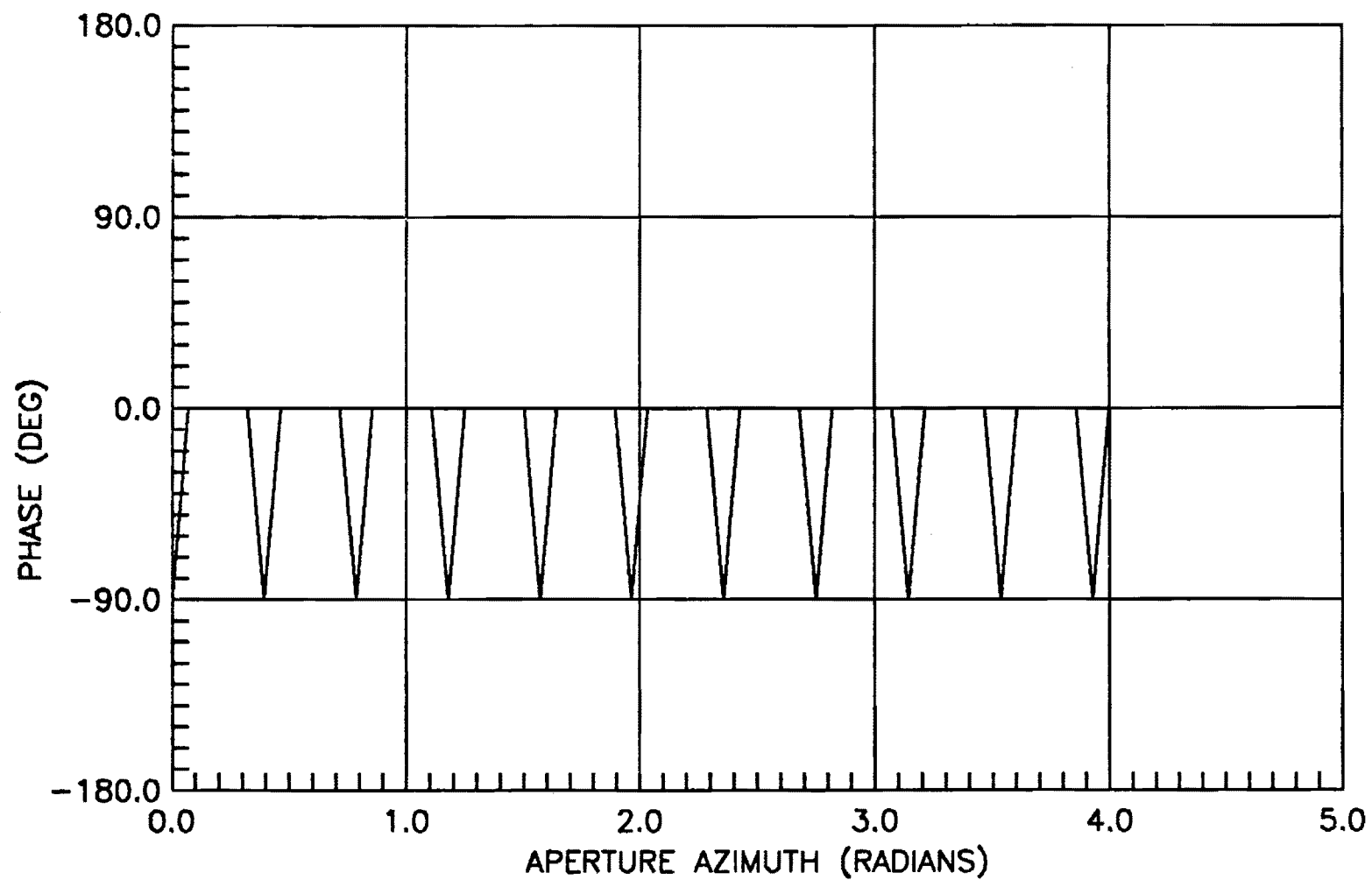


Figure C-21. Azimuthal aperture phase for severe cusp errors in Antenna II.

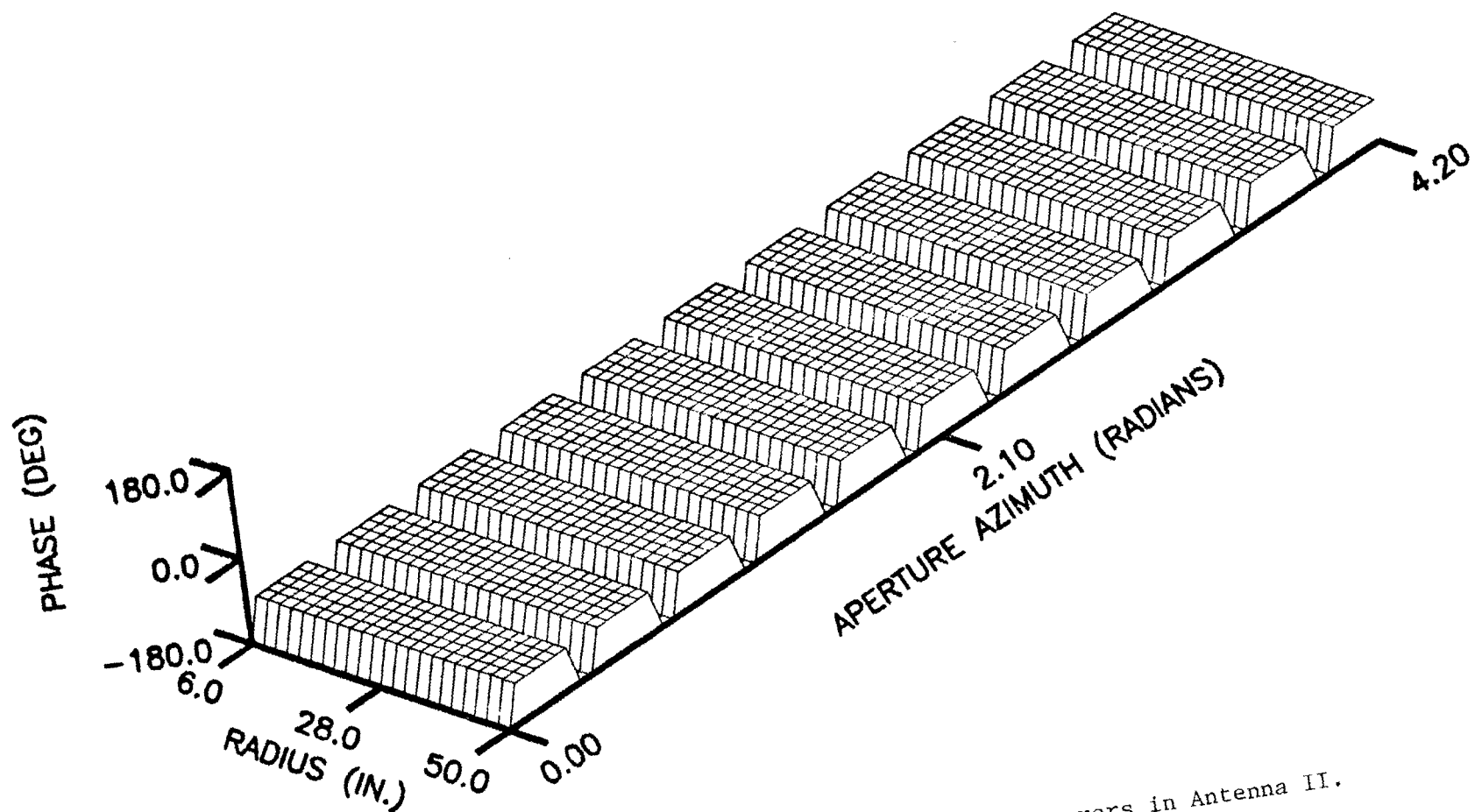


Figure C-22. Total-aperture phase for severe cusp errors in Antenna II.

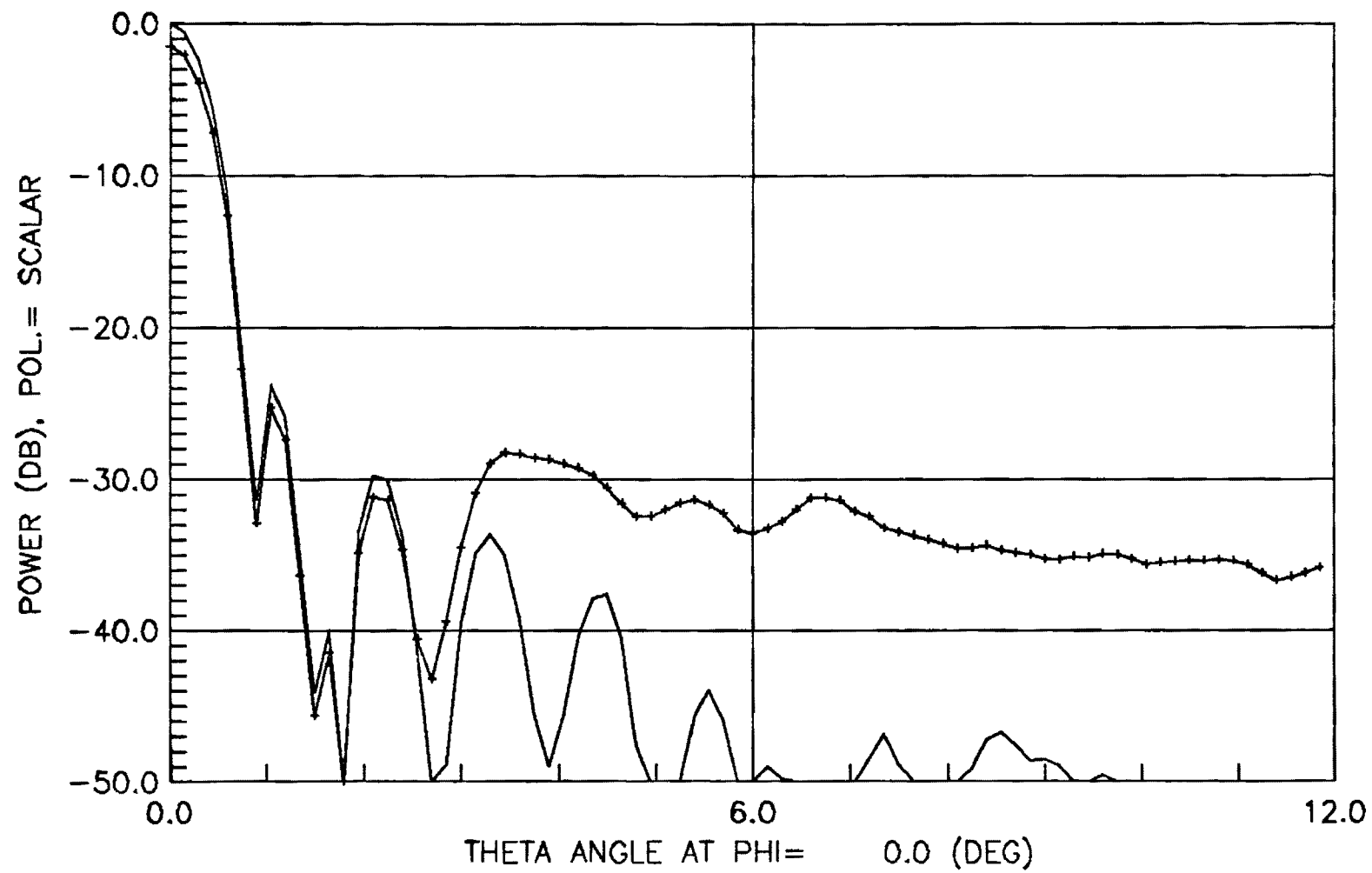


Figure C-23. Radiation pattern above a reflector joint for severe cusp errors in Antenna II.

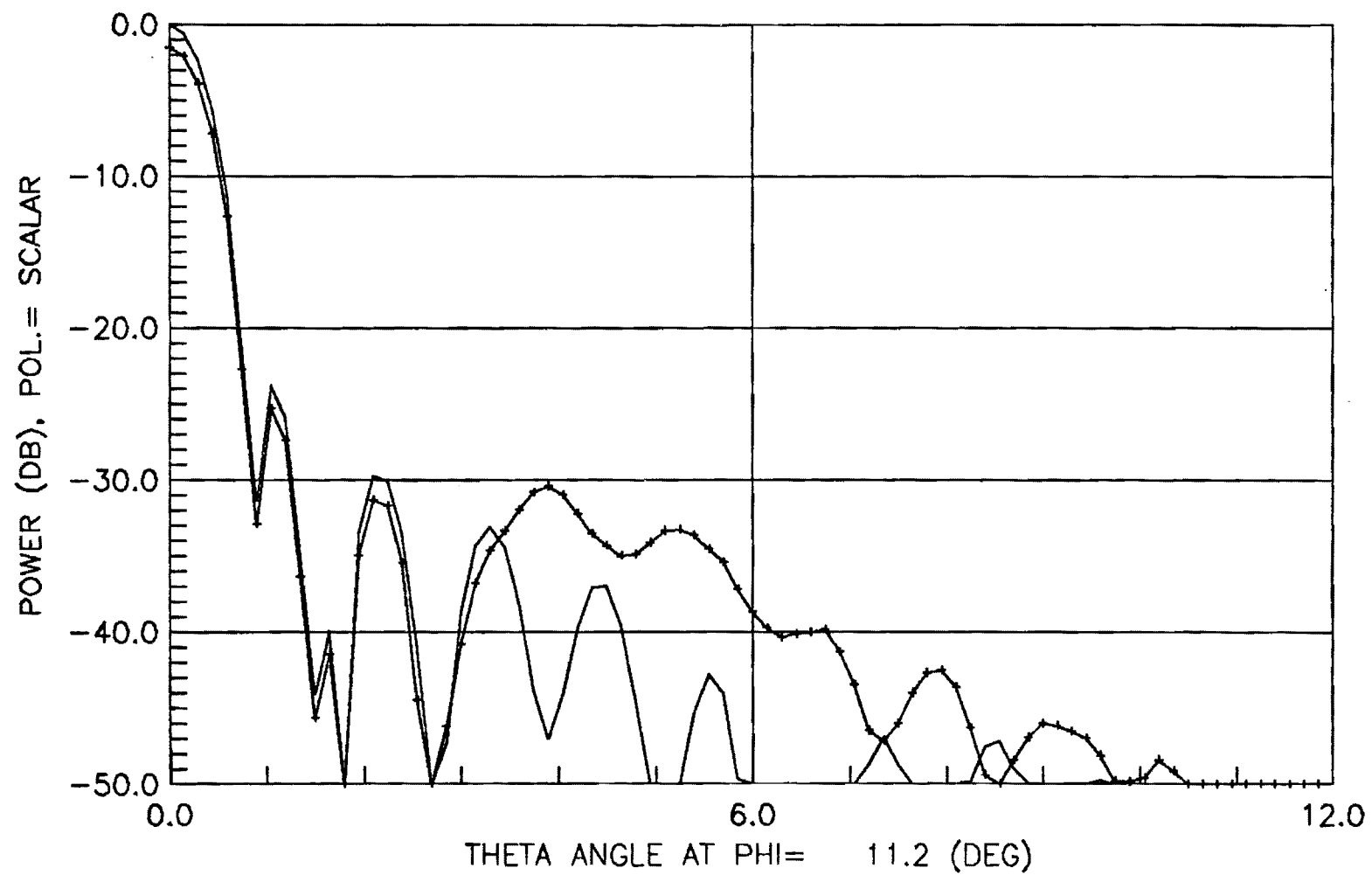


Figure C-24. Radiation pattern between reflector joints for severe cusp errors in Antenna II.

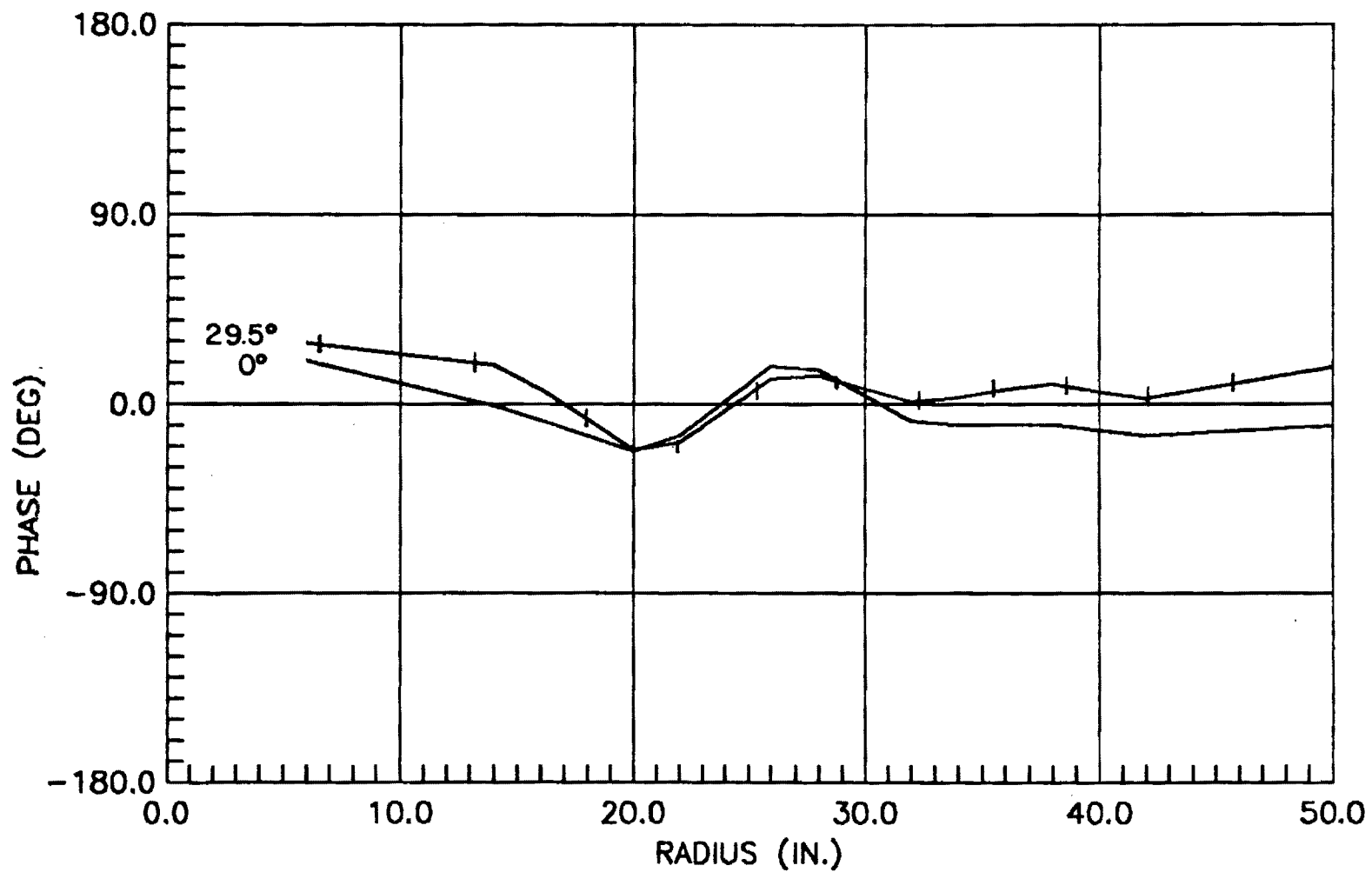


Figure C-25. Radial aperture phase for measured errors in Antenna II.

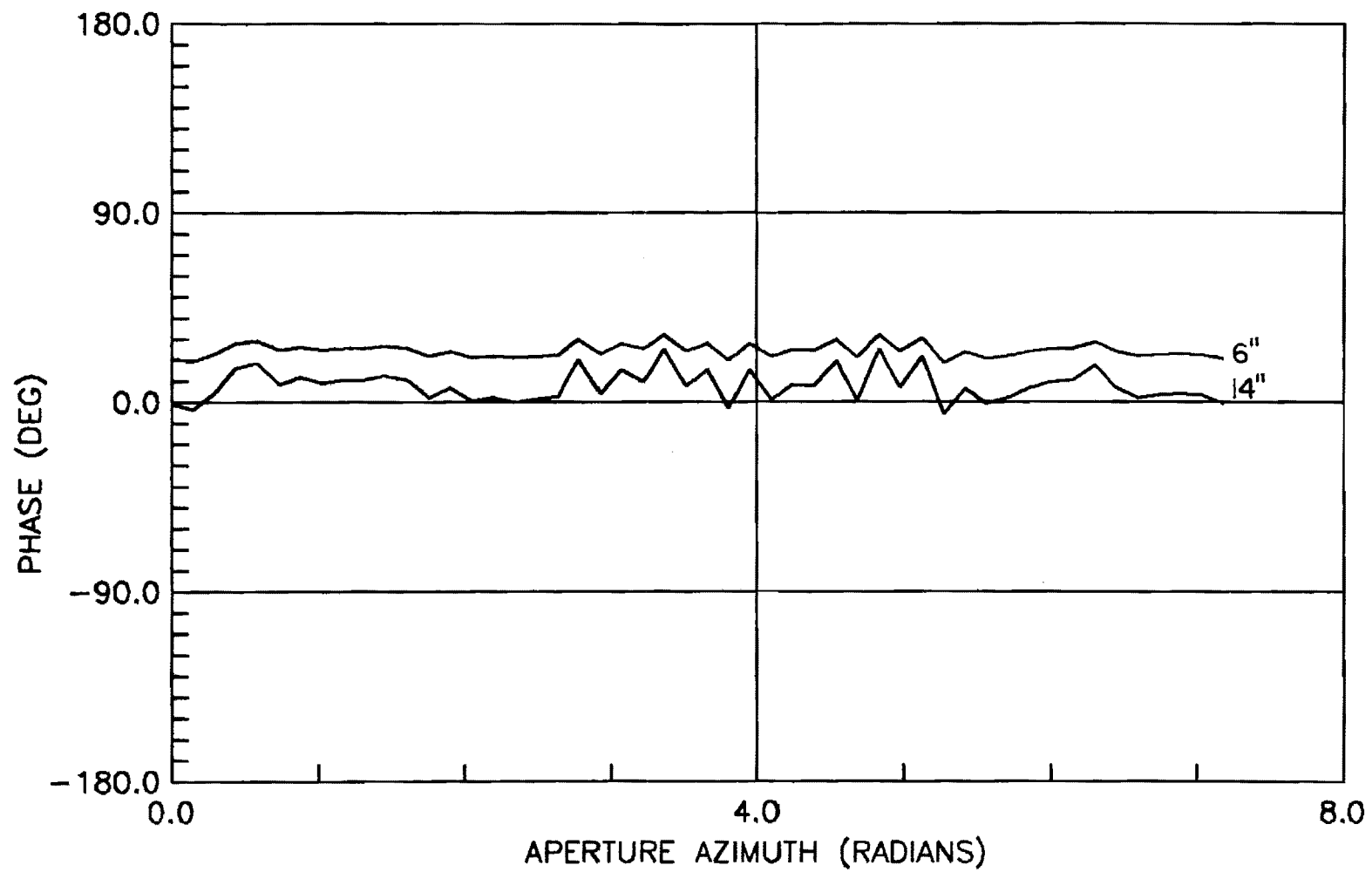


Figure C-26. Azimuthal aperture phase for measured errors in Antenna II.

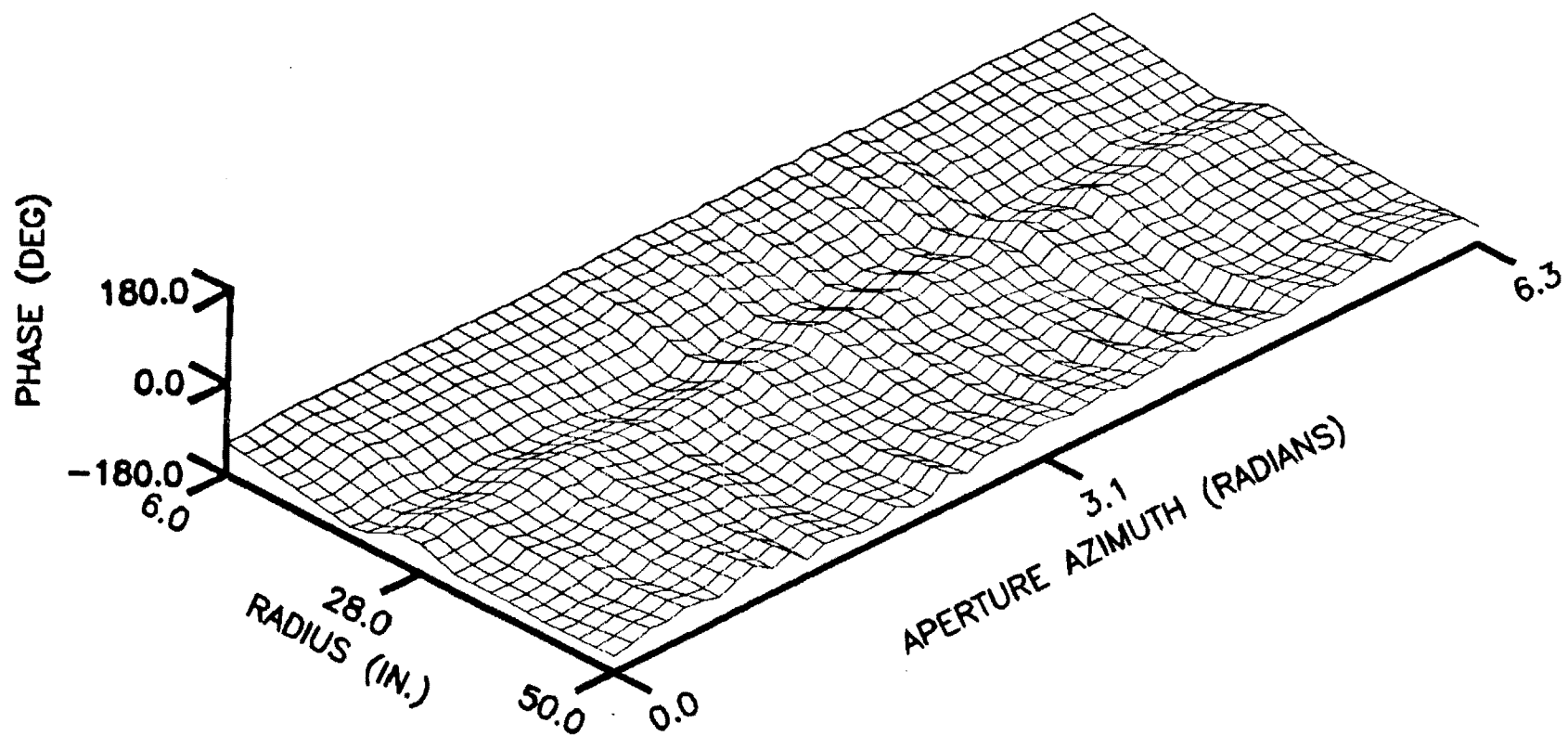


Figure C-27. Total-aperture phase for measured errors in Antenna II.



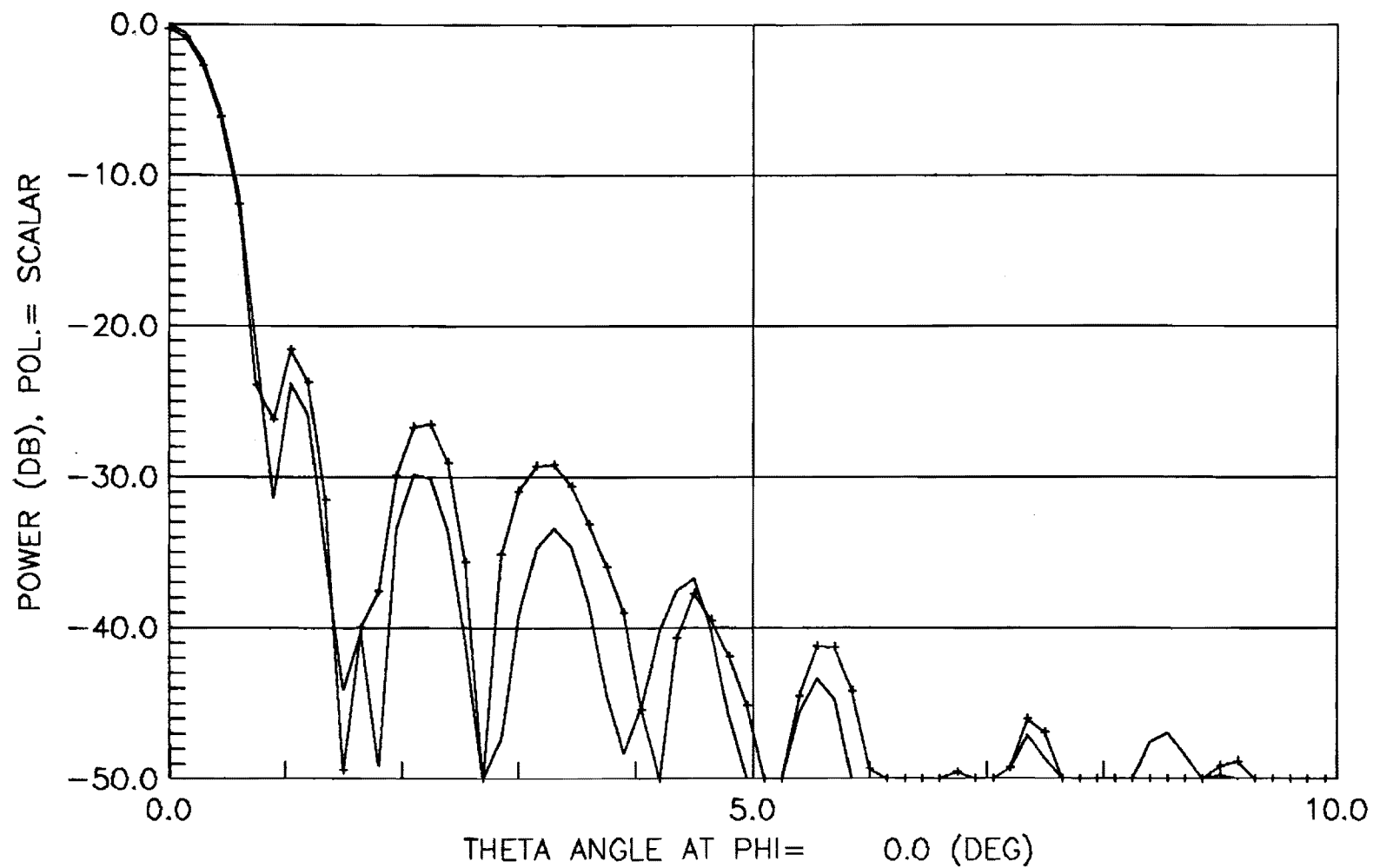


Figure C-28. Horizontal radiation pattern for measured errors in Antenna II.

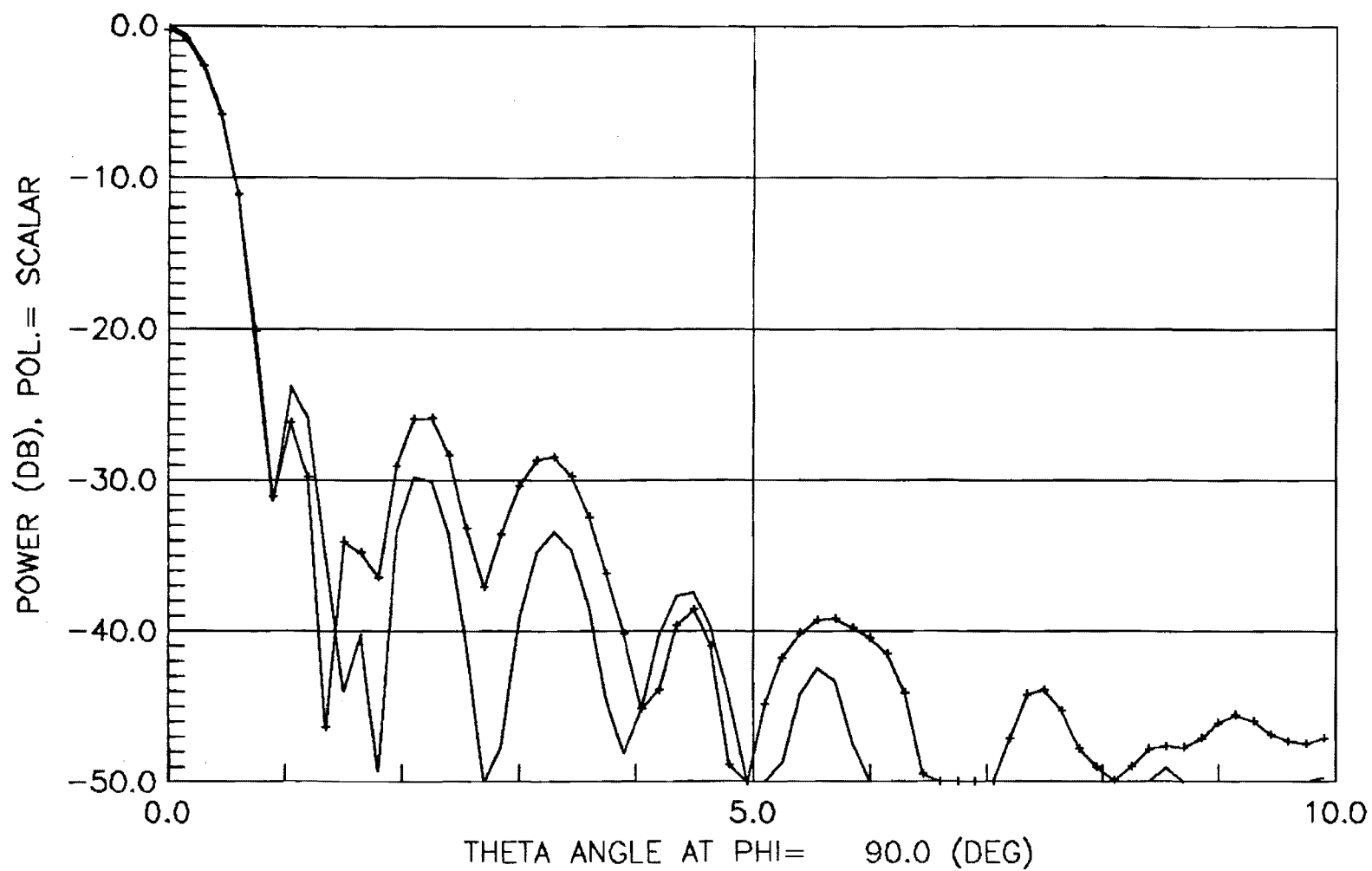


Figure C-29. Vertical radiation pattern for measured errors in Antenna II.

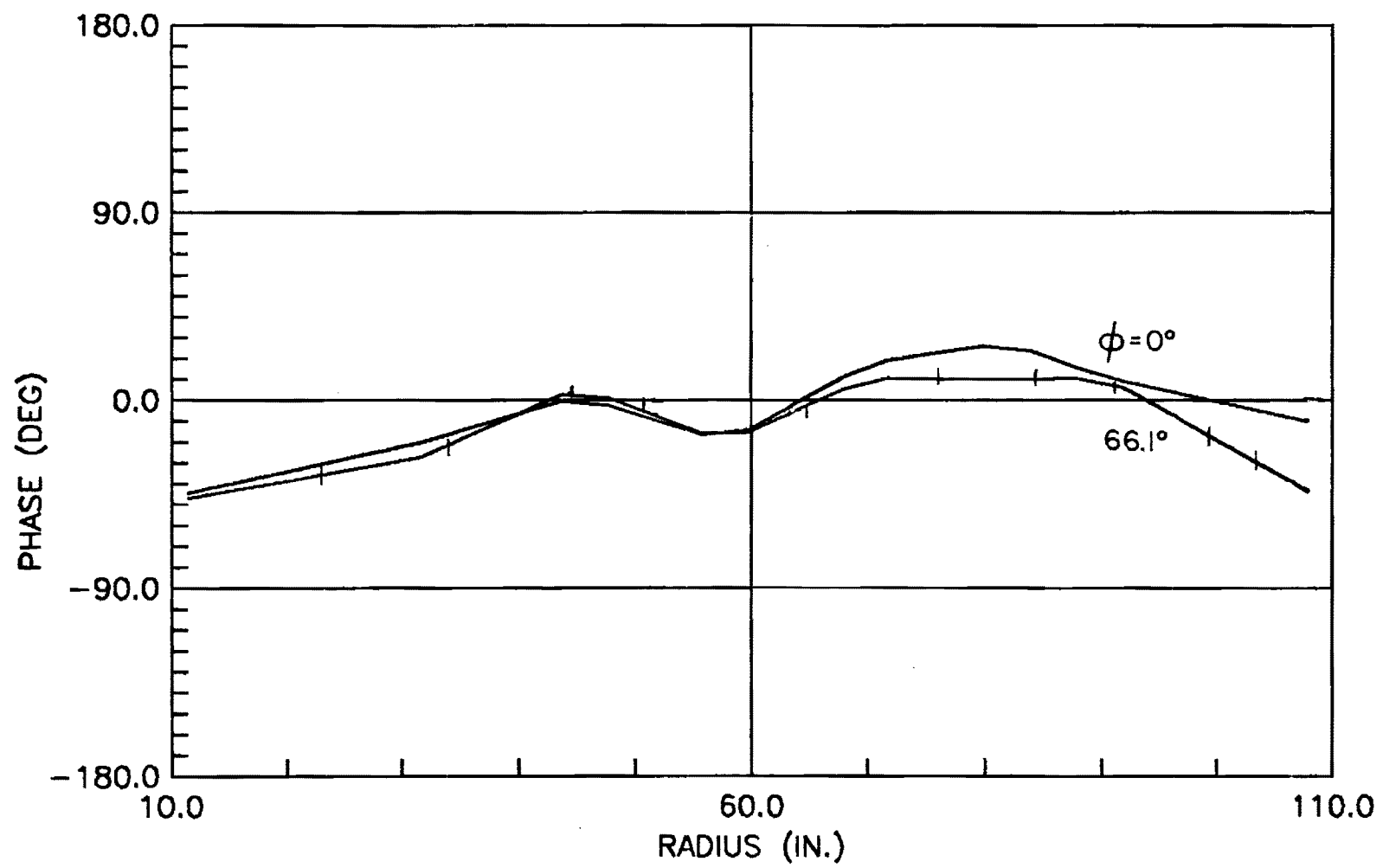


Figure C-30. Radial aperture phase for measured errors in Antenna III at 14.5 GHz.

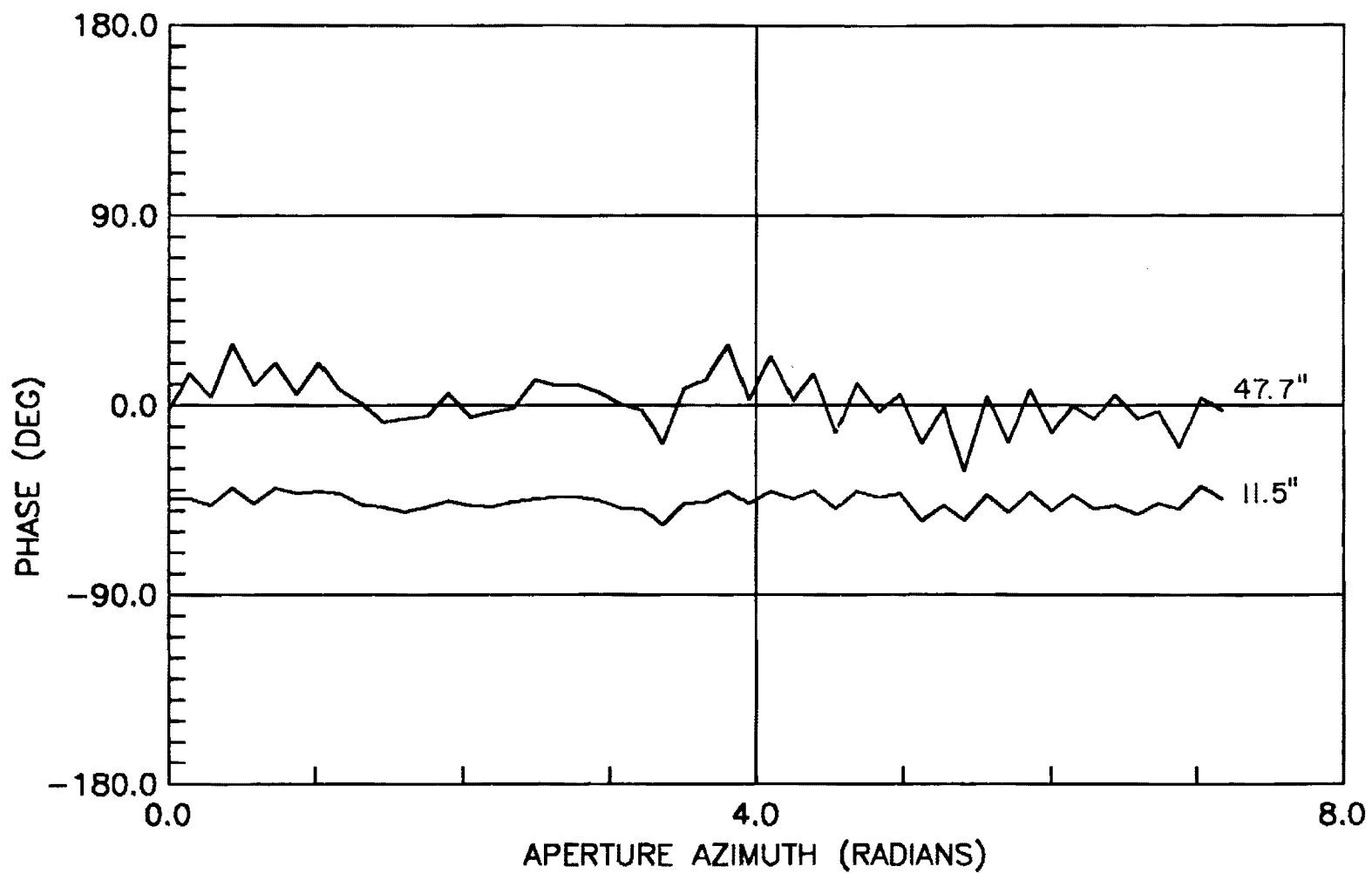


Figure C-31. Azimuthal aperture phase for measured errors in Antenna III at 14.5 GHz.

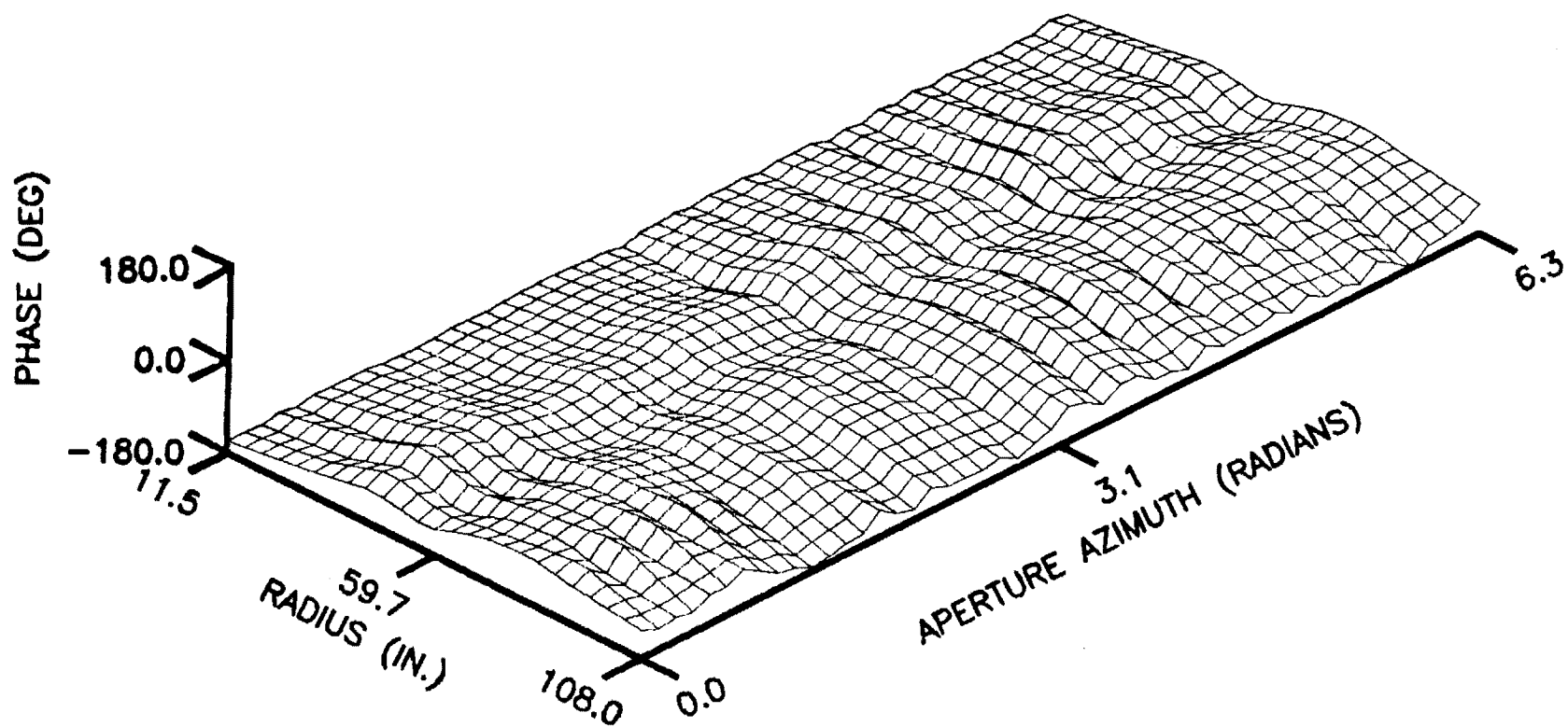


Figure C-32. Total-aperture phase for measured errors in Antenna III at 14.5 GHz.

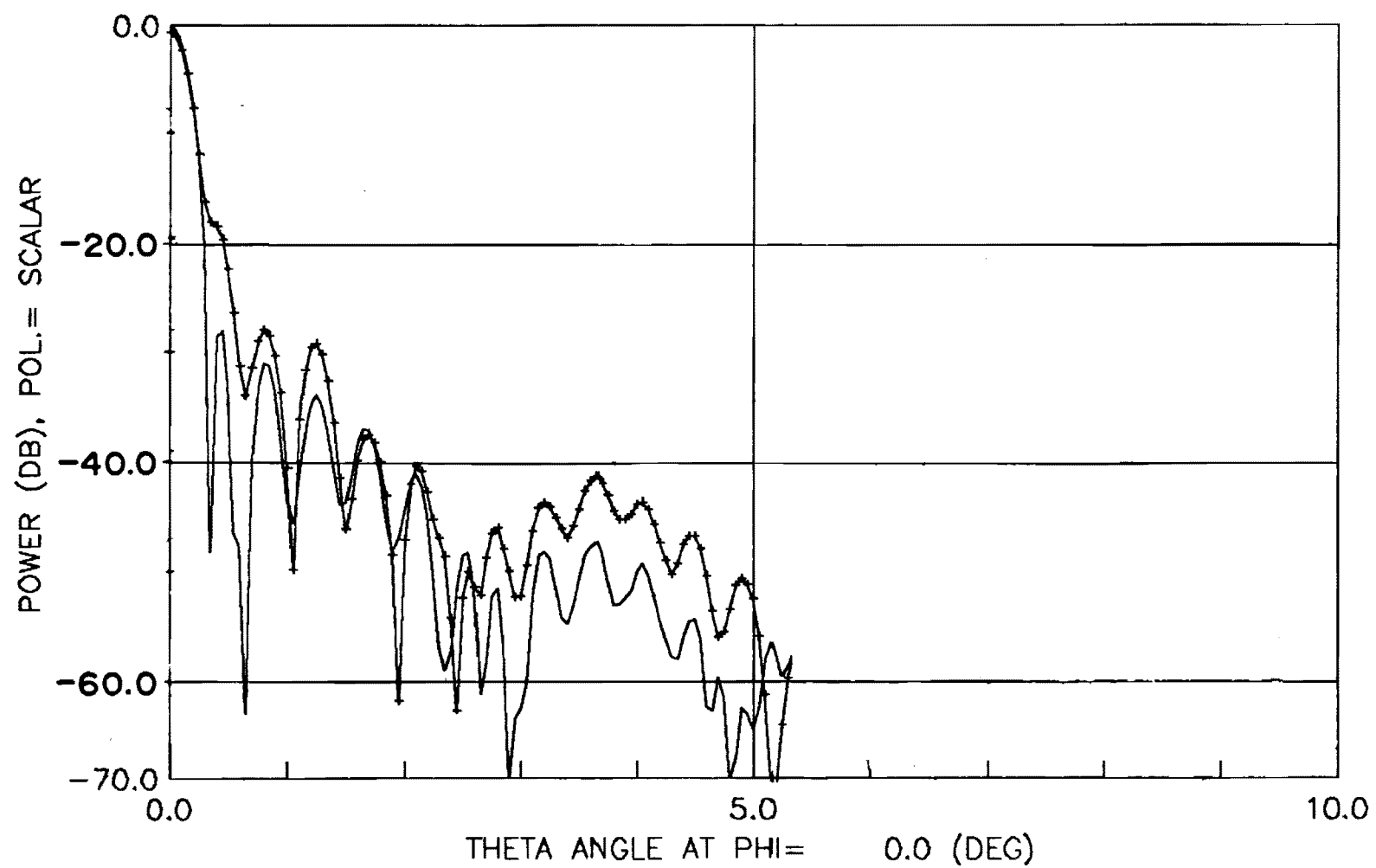


Figure C-33. Horizontal radiation pattern for measured errors in Antenna III at 11.95 GHz.

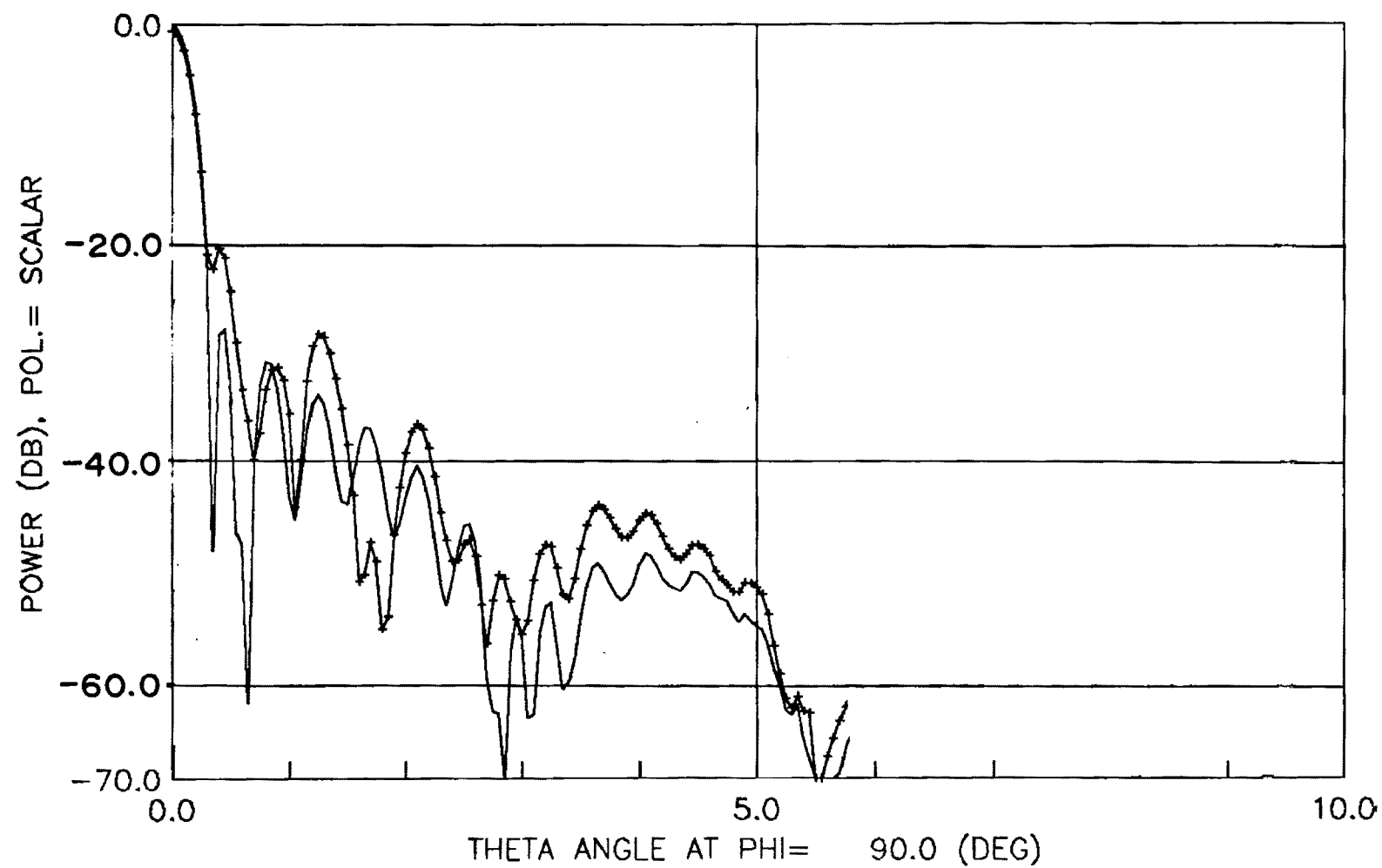


Figure C-34. Vertical radiation patterns for measured errors in Antenna III at 11.95 GHz.

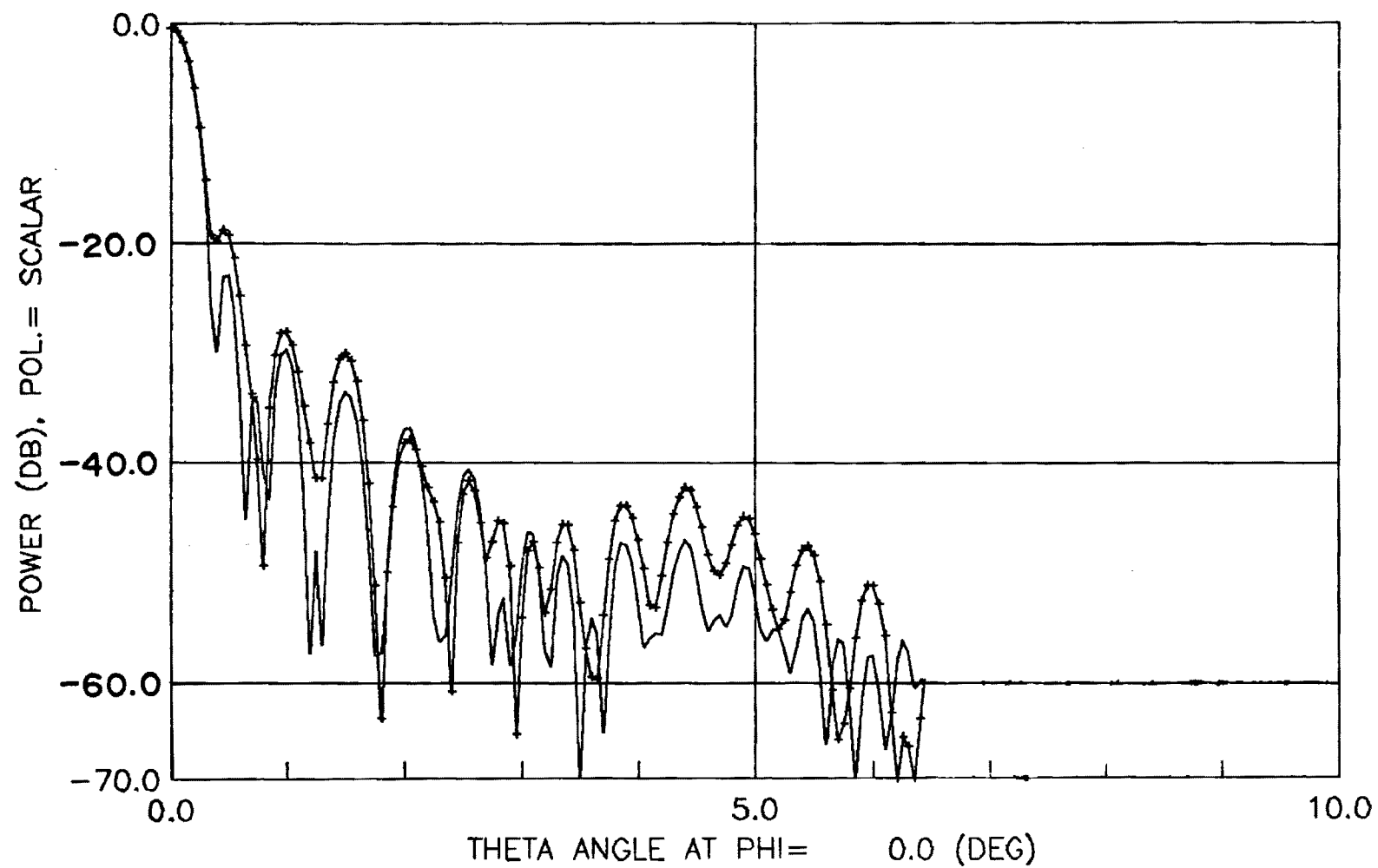


Figure C-35. Horizontal radiation pattern for measured error in Antenna III at 14.5 GHz.



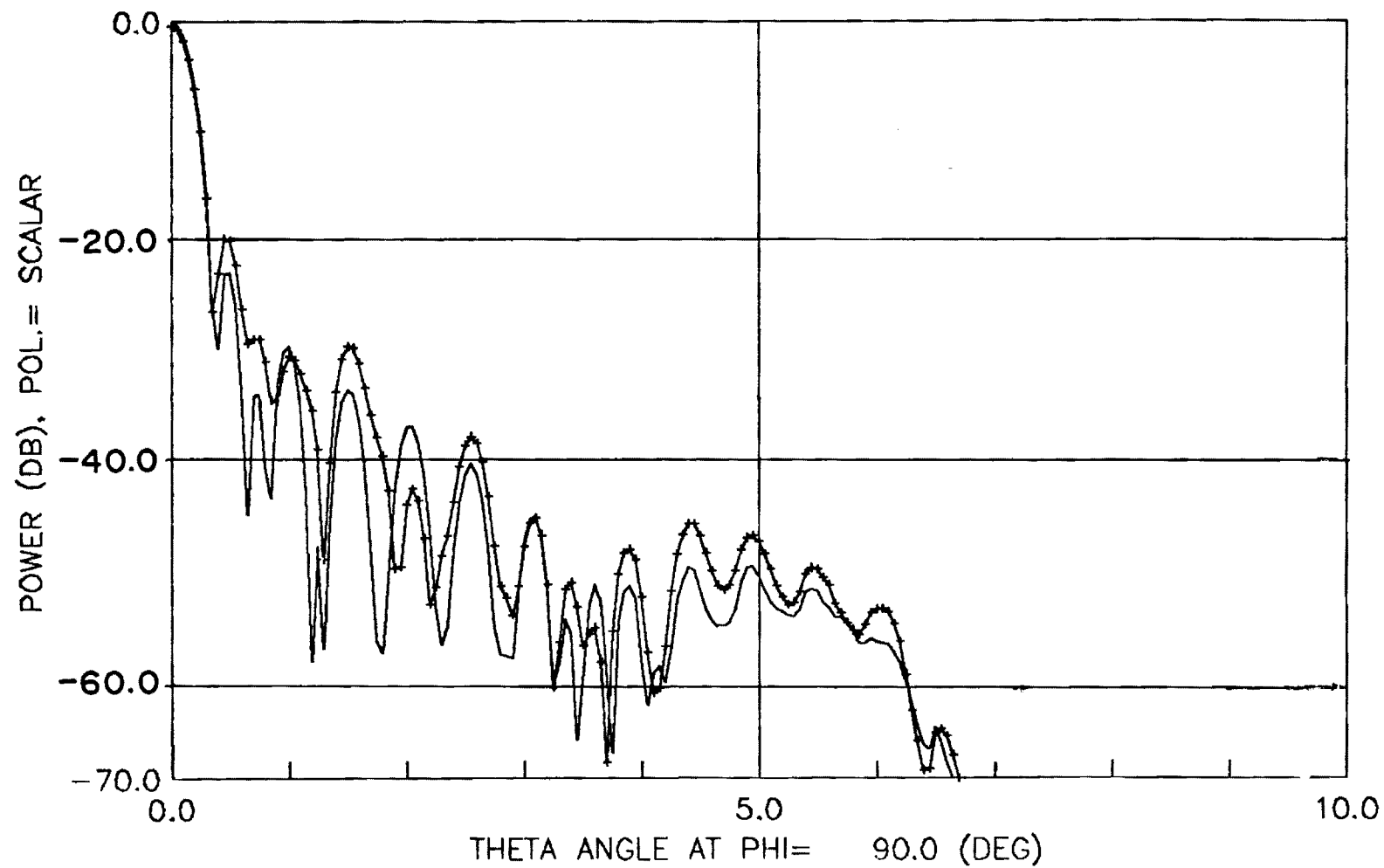


Figure C-36. Vertical radiation pattern for measured error in Antenna III at 14.5 GHz.

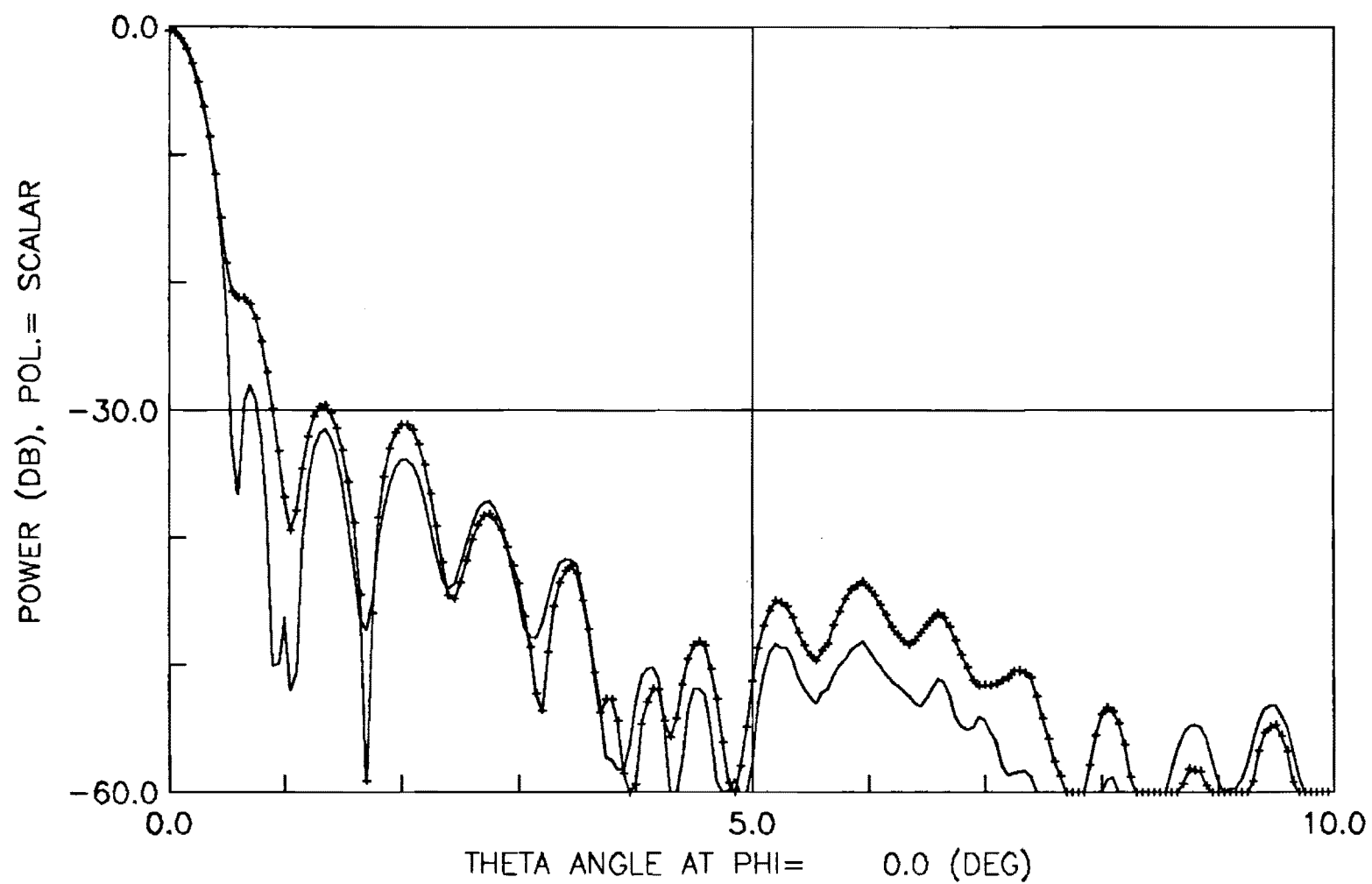


Figure C-37. Horizontal radiation pattern for .012 RMS measured error in Antenna IV at 20 GHz.

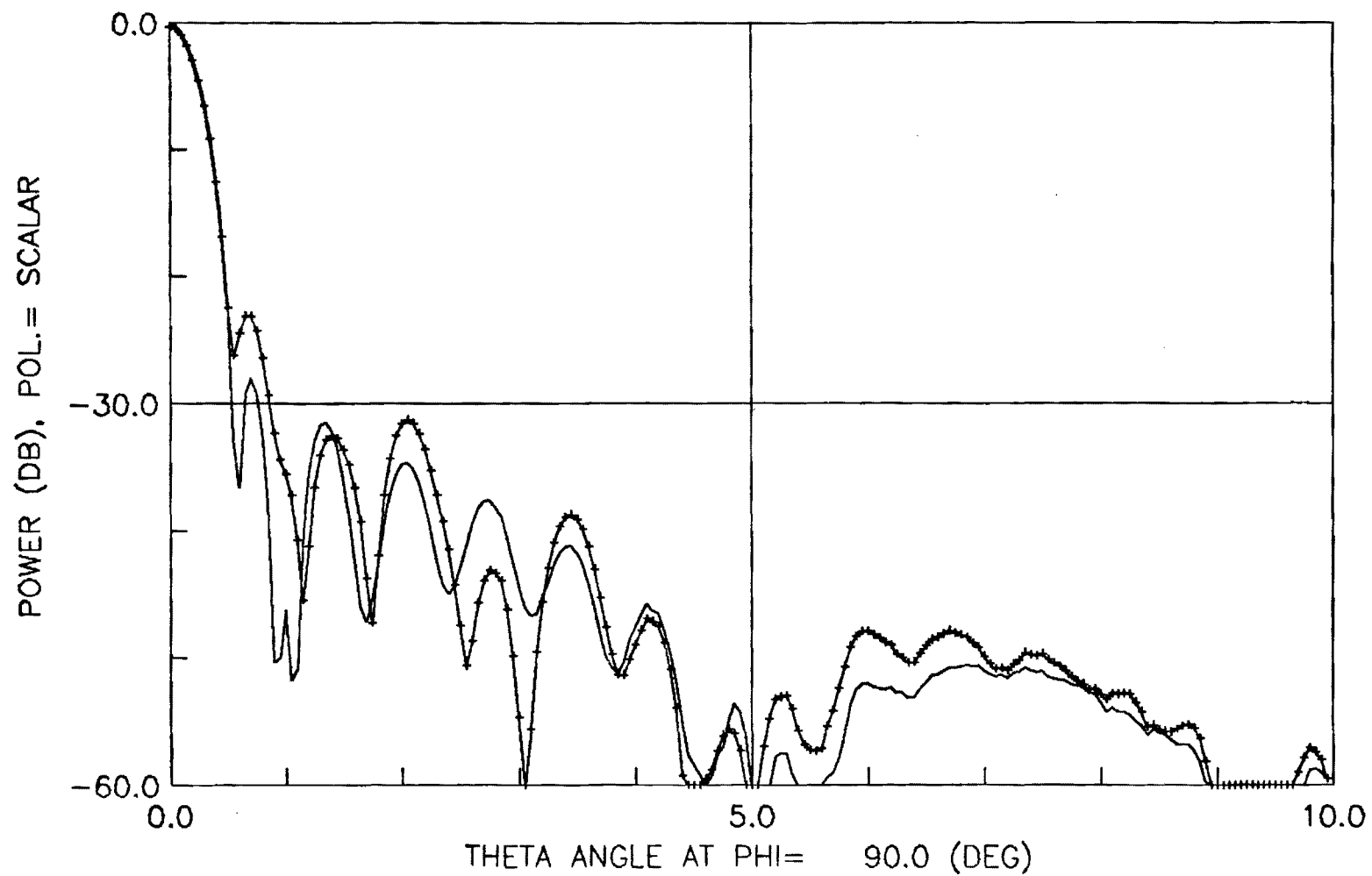


Figure C-38. Vertical radiation pattern for .012 RMS measured error in Antenna IV at 20 GHz.

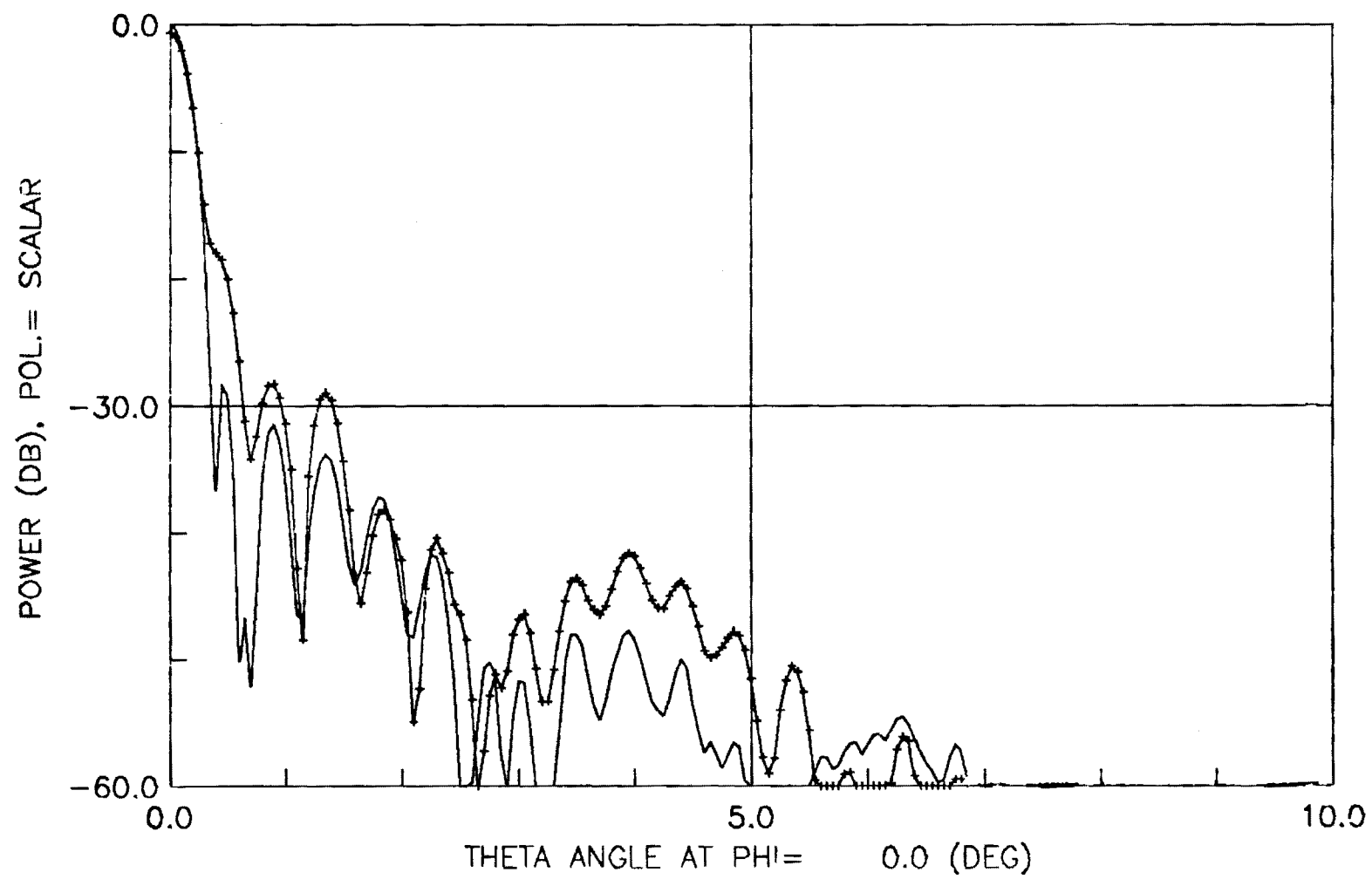


Figure C-39. Horizontal radiation pattern for .012 RMS measured error in Antenna IV at 30 GHz.

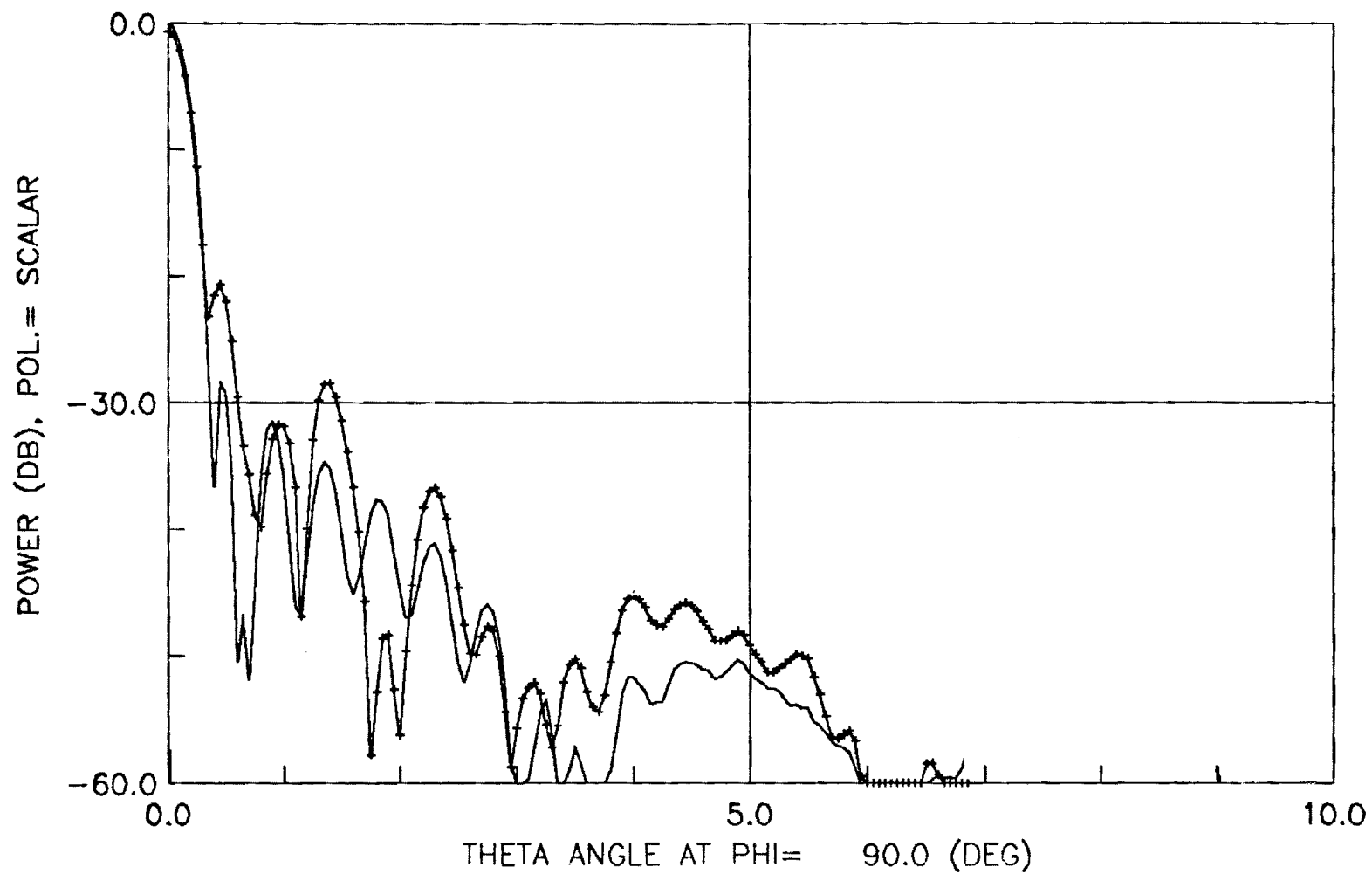


Figure C-40. Vertical radiation pattern for .012 RMS measured error in Antenna IV at 30 GHz.

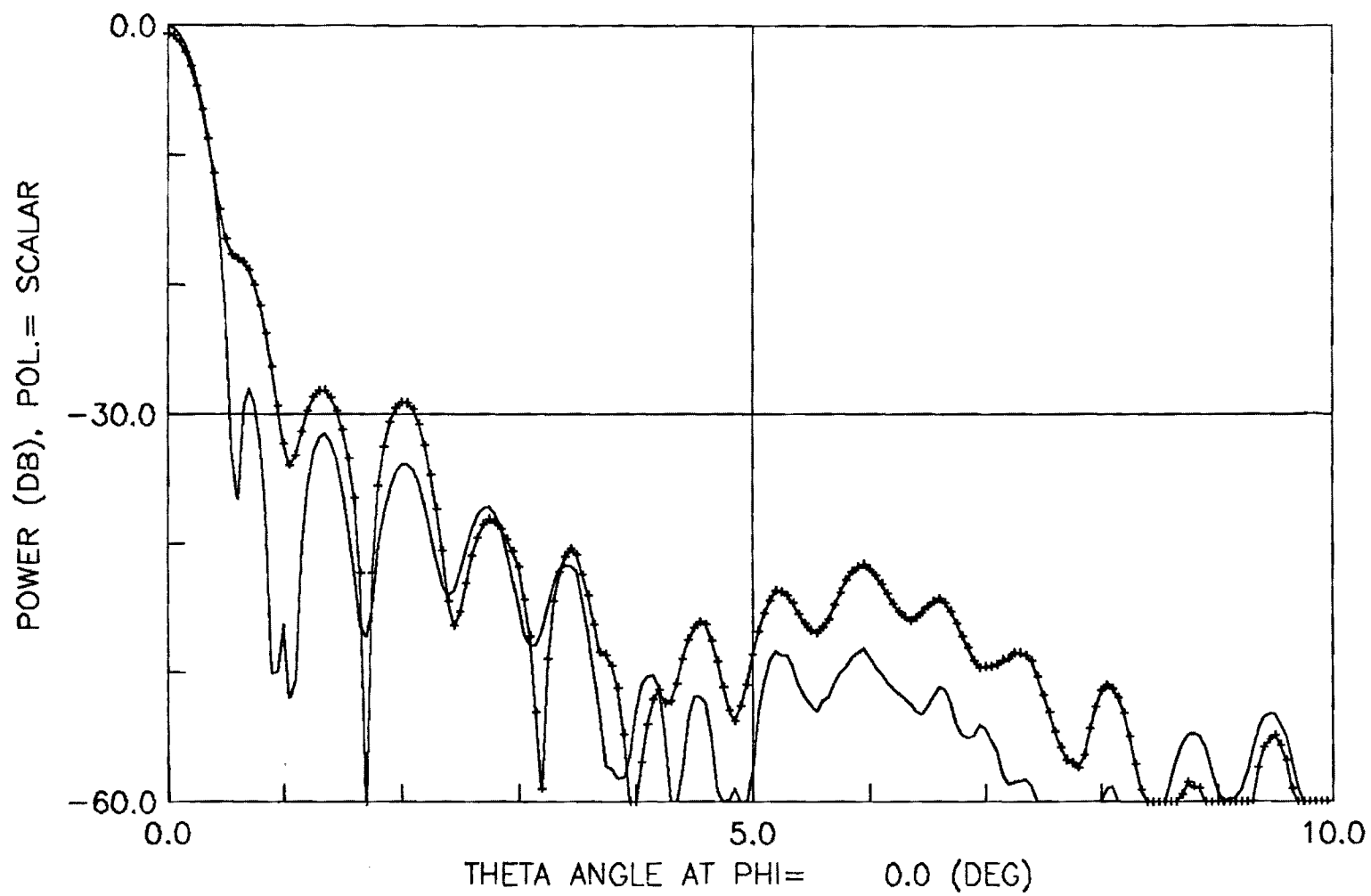


Figure C-41. Horizontal radiation pattern for .018 RMS measured error in Antenna IV at 20 GHz.

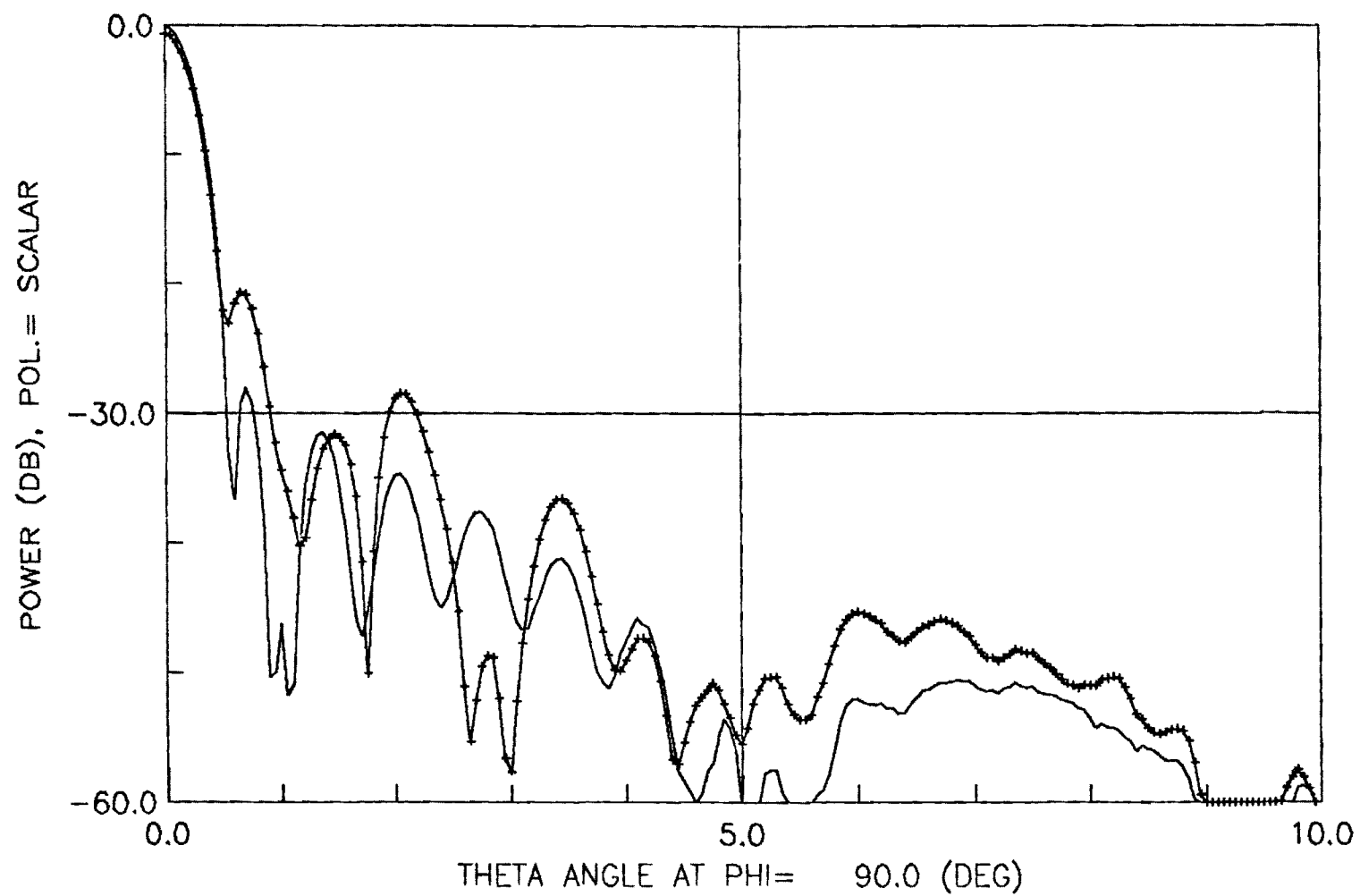


Figure C-42. Vertical radiation pattern for .018 RMS measured error in Antenna IV at 20 GHz.

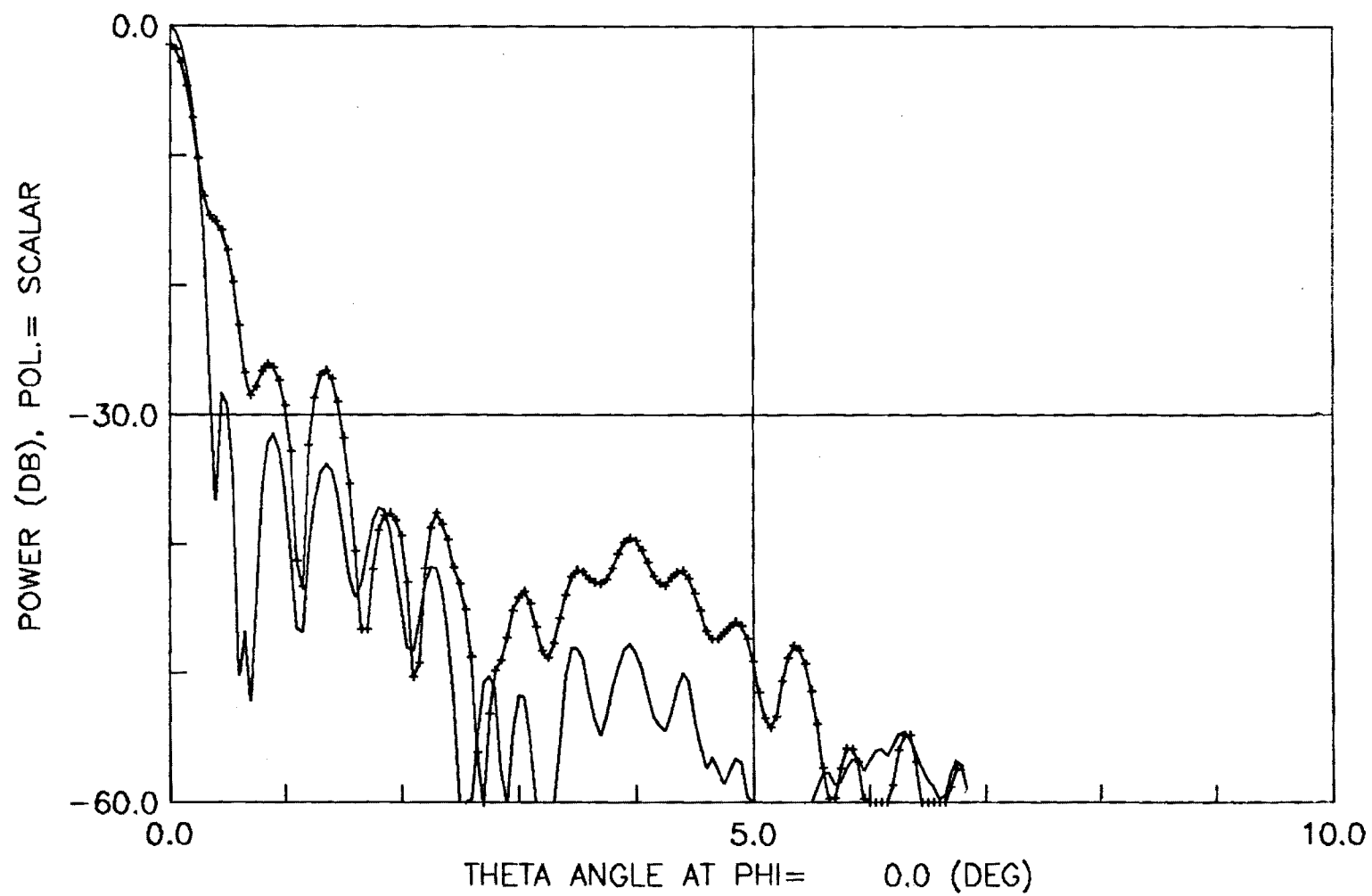


Figure C-43. Horizontal radiation pattern for .018 RMS measured error in Antenna IV at 30 GHz.



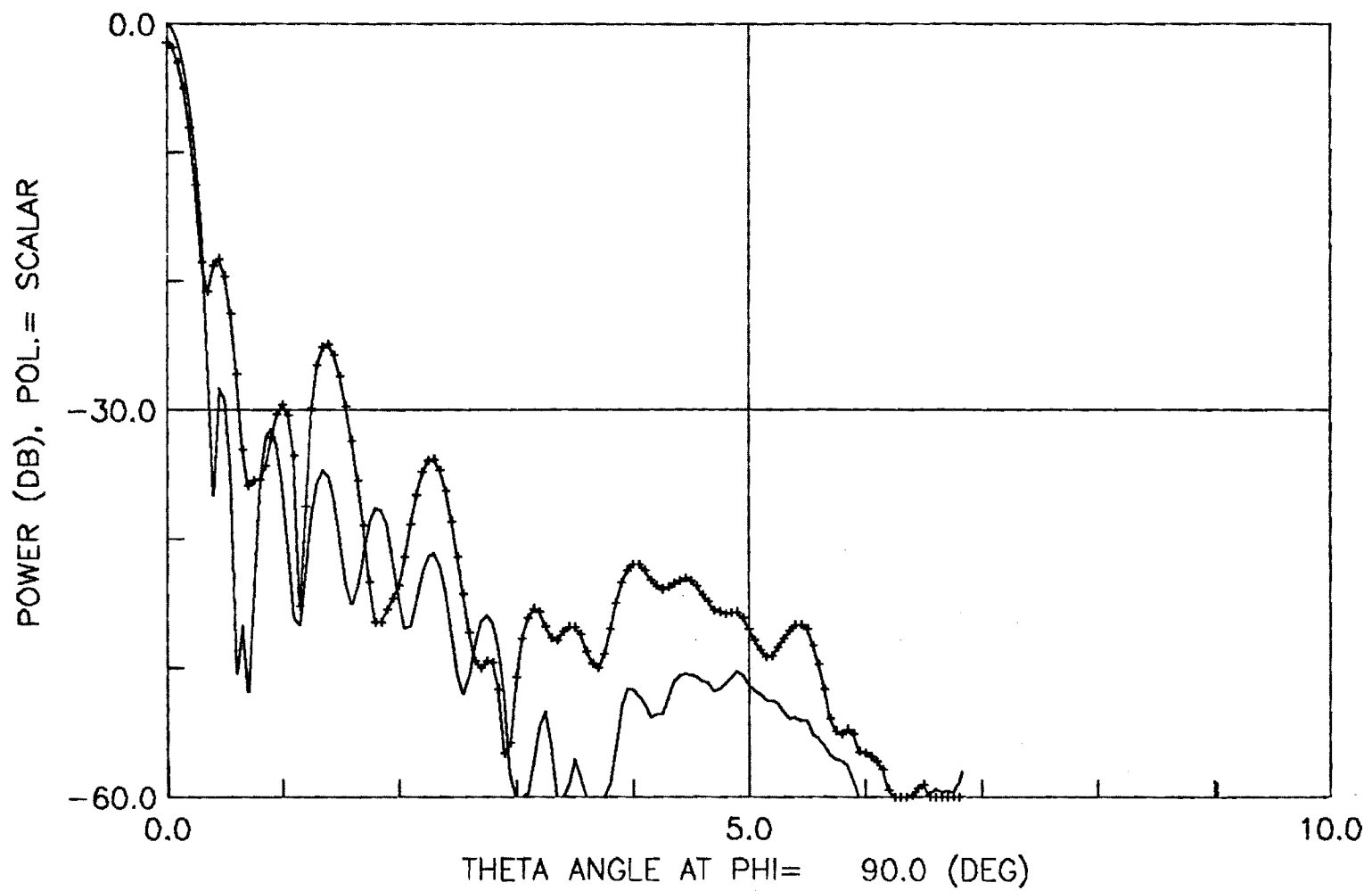


Figure C-44. Vertical radiation pattern for .018 RMS measured error in Antenna IV at 30 GHz.

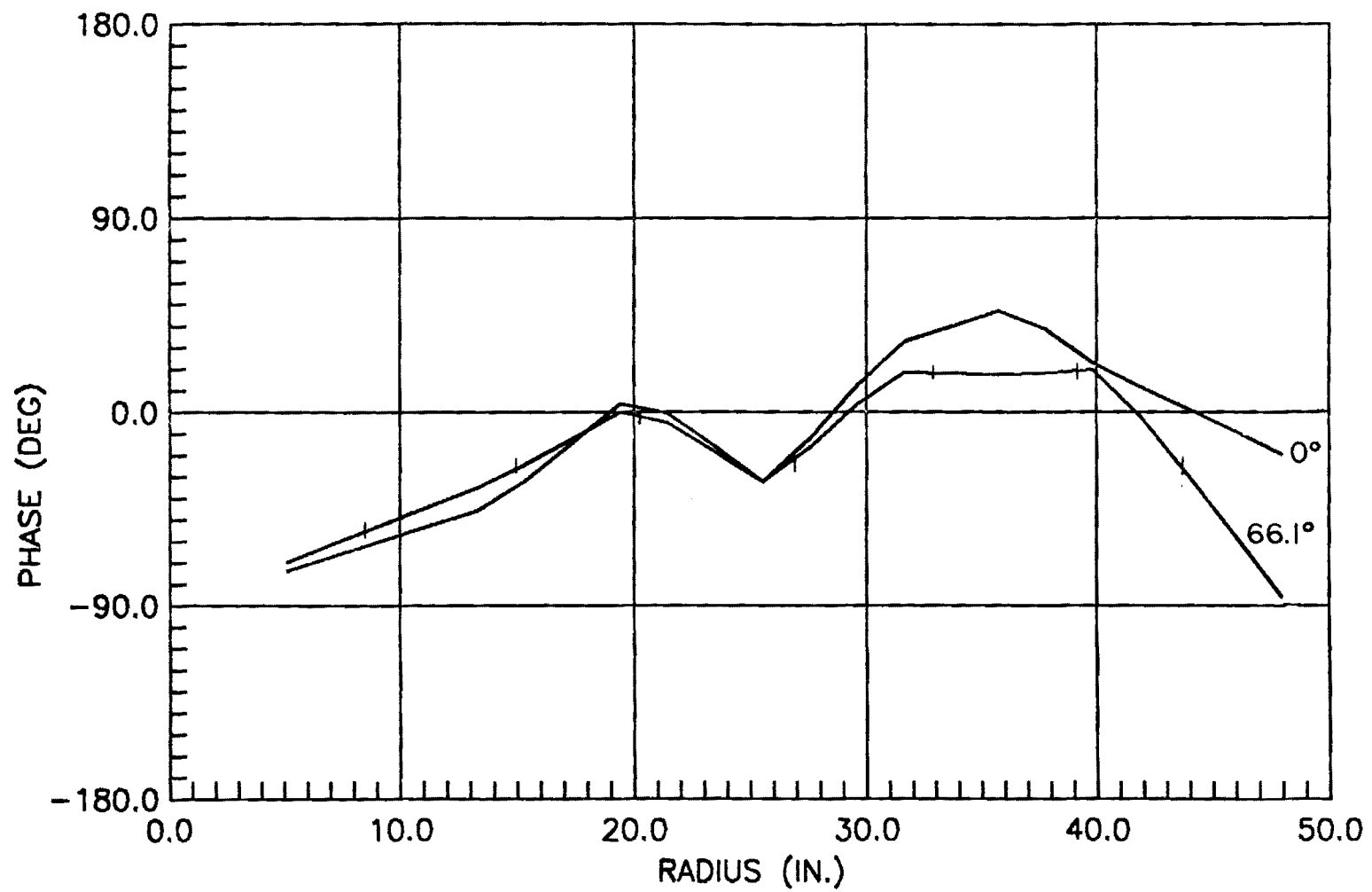


Figure C-45. Radial aperture phase for normal .018 RMS measured error in Antenna IV at 30 GHz.

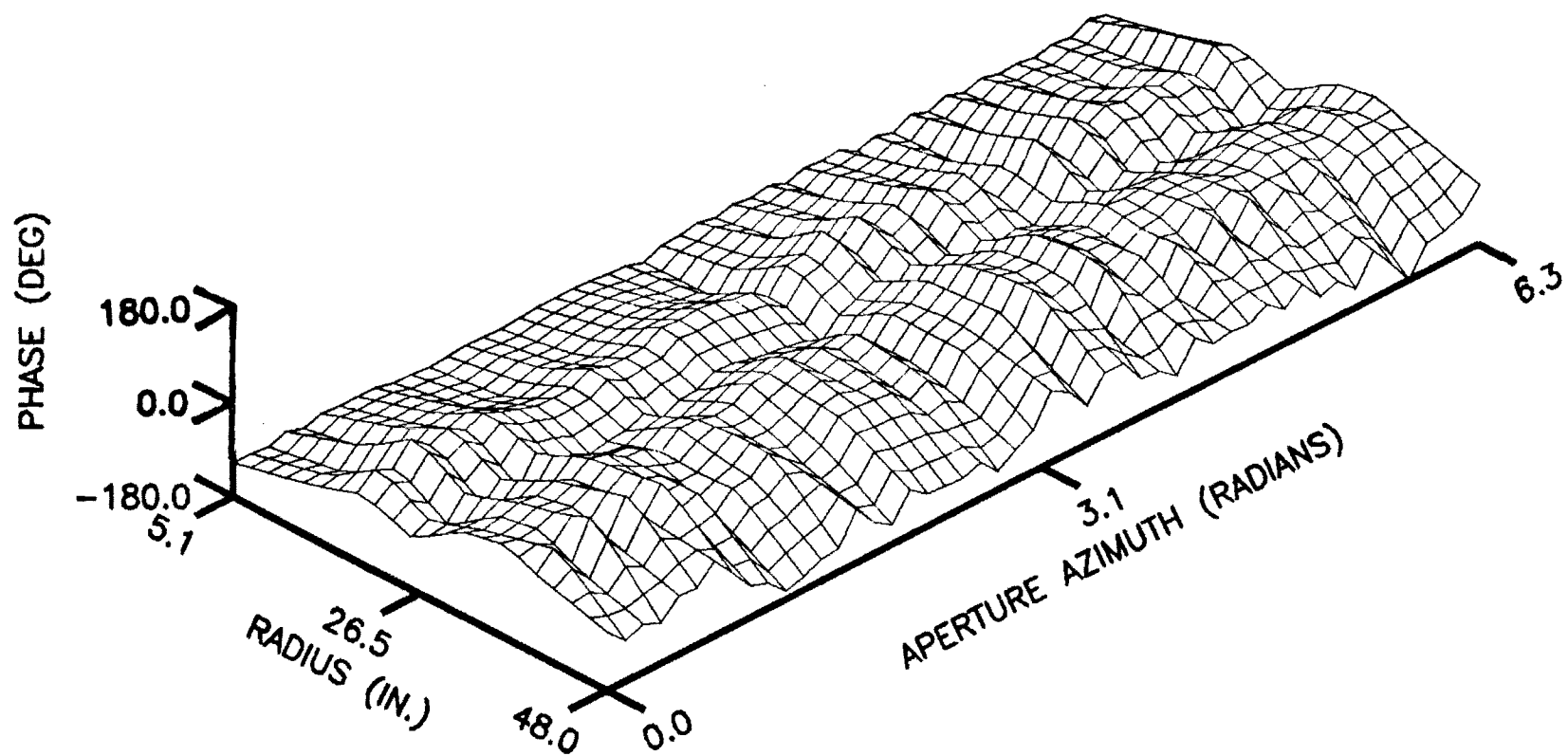


Figure C-46. Total aperture phase for normal .018 RMS measured error in Antenna IV at 30 GHz.

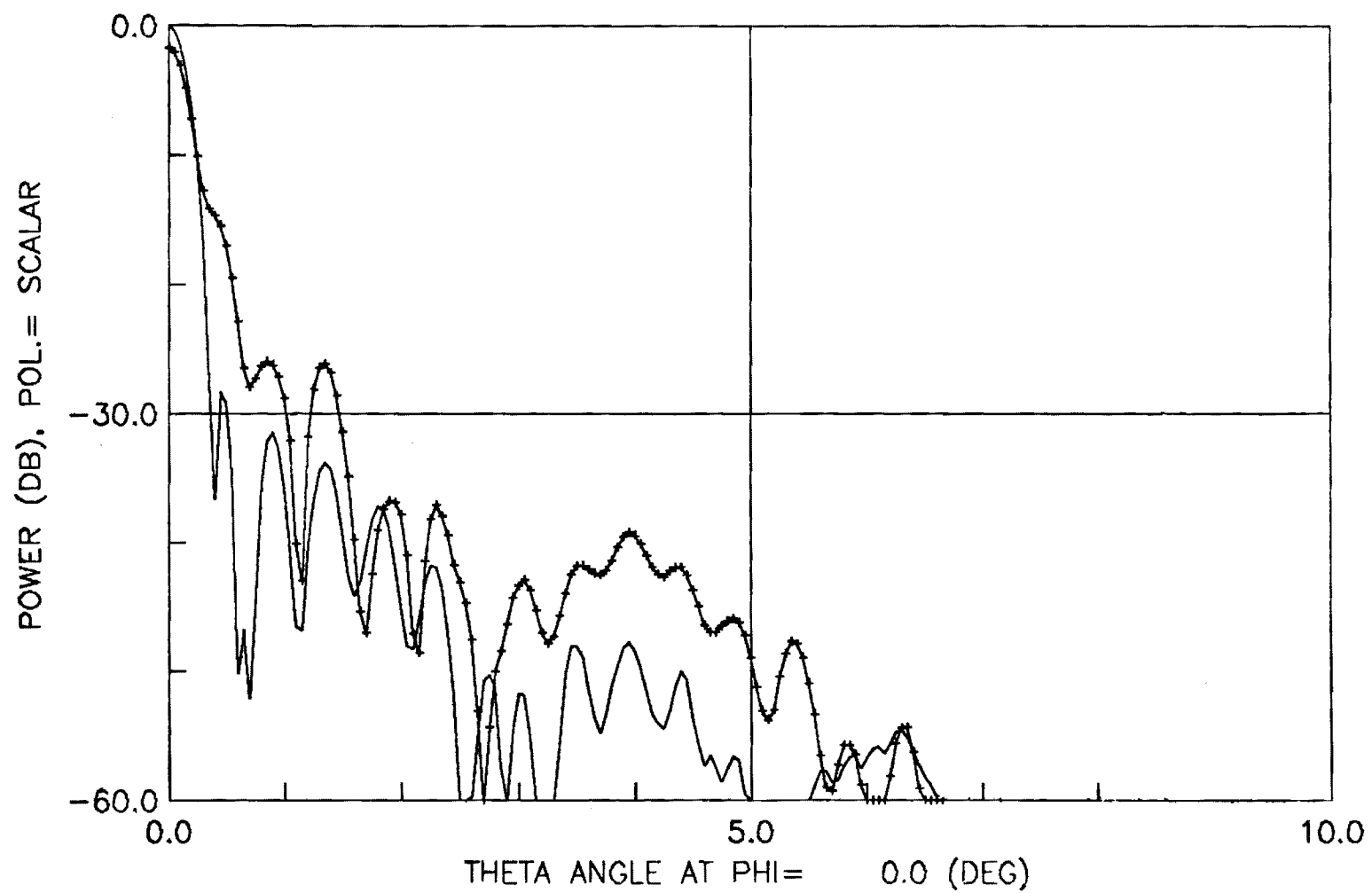


Figure C-47. Horizontal radiation pattern for normal .018 RMS measured error in Antenna IV at 30 GHz.

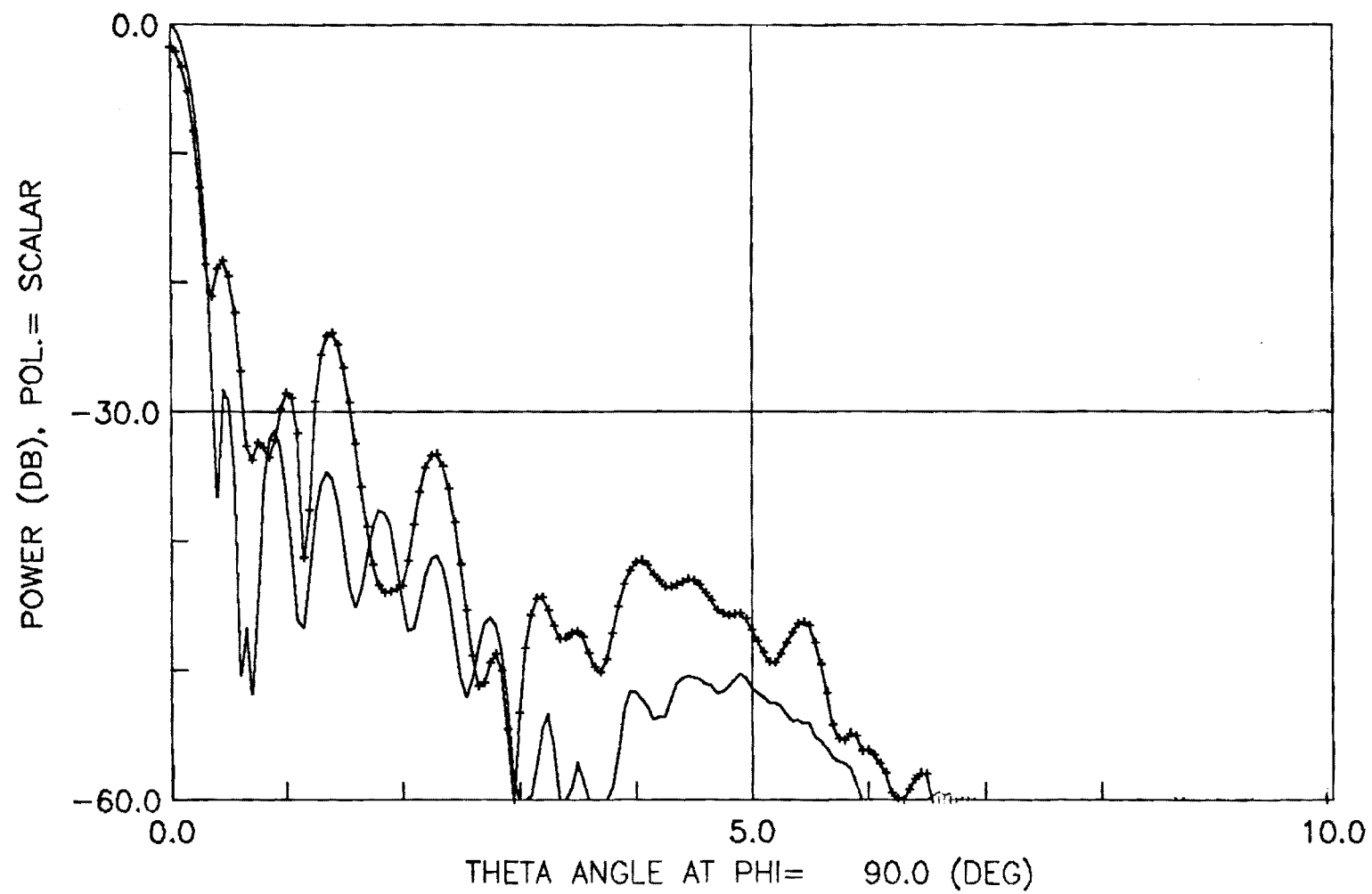


Figure C-48. Vertical radiation pattern for normal .018 RMS measured error in Antenna IV at 30 GHz.

COMPUTER PROGRAM DOCUMENTATION  
GIT/EES PROJECT A-3449

## PROGRAM FOR THE ANALYSIS OF SURFACE ERRORS IN CIRCULAR REFLECTOR ANTENNAS

By  
V. K. Tripp

July 1983

Prepared for  
SCIENTIFIC-ATLANTA, INC.  
ELECTRO PRODUCTS DIVISION  
ATLANTA, GEORGIA 30340

Under  
Purchase Order No. 580173

### **GEORGIA INSTITUTE OF TECHNOLOGY**

**A Unit of the University System of Georgia  
Engineering Experiment Station  
Atlanta, Georgia 30332**



COMPUTER PROGRAM DOCUMENTATION  
GIT/EES PROJECT A-3449

**PROGRAM FOR THE ANALYSIS OF SURFACE  
ERROR IN CIRCULAR REFLECTOR ANTENNAS**

By

V. K. Tripp

July 1983

Prepared for

Scientific-Atlanta, Inc.  
Electro Products Division  
Atlanta, Georgia 30340

Under

Purchase Order No. 580173

By

Electromagnetic Effectiveness Division  
Electronics and Computer Systems Laboratory  
Engineering Experiment Station  
Georgia Institute of Technology  
Atlanta, Georgia 30332

THIS PAGE INTENTIONALLY LEFT BLANK



## PREFACE

The computer program documented herein was developed at the Engineering Experiment Station (EES) of the Georgia Institute of Technology for the Electro Products Division of Scientific-Atlanta, Inc. in partial fulfillment of Purchase Order No. 580173. Technical direction was exercised through Mr. Jim Cook of Scientific-Atlanta, and Mr. Victor K. Tripp was the Project Director at Georgia Tech. The work was performed by the personnel of the Electronics and Computer Systems Laboratory of EES. The work was primarily performed by personnel of the Electromagnetic Effectiveness Division (EED), but a contribution was made by personnel of the Electromagnetic Compatibility Division. The work reported herein was performed between 1 January 1983 and 30 June 1983. Some of the work involved in the development of this computer program is documented in the final report for this project entitled Surface Tolerance Analysis of Symmetrical Dual-Reflector Antennas. In particular, the mathematical models and some examples of program execution are contained in that report.

The author would like to acknowledge the support provided by Mr. Jim Cook of Scientific-Atlanta and Barry J. Cown and Darrell W. Acree of Georgia Tech. Thanks are also extended to Dr. Charles E. Ryan, Jr. for administrative support and Ms. Beatriz Gonzalez for typing this report.

Respectfully submitted,

Victor K. Tripp  
Project Director

Approved:

Charles E. Ryan, Jr. ✓  
Chief,  
EM Effectiveness Division

THIS PAGE INTENTIONALLY LEFT BLANK

## TABLE OF CONTENTS

<u>Section</u>		<u>Page</u>
I.	INTRODUCTION. . . . .	1
II.	DESCRIPTION OF SUBPROGRAMS. . . . .	3
III.	FORTRAN CODE. . . . .	9
IV.	DEFINITION OF MAJOR VARIABLES . . . . .	21
V.	APDERS USER'S GUIDE . . . . .	75

THIS PAGE INTENTIONALLY LEFT BLANK

## LIST OF FIGURES

<u>Figure</u>	<u>Page</u>
1. Block diagram of entire program. . . . .	4
2. Flow chart of main program . . . . .	5
3. Definition of coordinate system and variables. . . .	72
4. File OUTPUT generated by the test case . . . . .	77
5. Pages 1 and 2 of file RESULT . . . . .	78
6. Page 3 of file RESULT. . . . .	79
7. Page 4 of file RESULT. . . . .	80
8. Page 5 of file RESULT. . . . .	81
9. Page 6 of file RESULT. . . . .	82
10. Page 7 of file RESULT. . . . .	83
11. Page 8 of file RESULT. . . . .	84
12. Aperture plot contained in files TAPE11 and TAPE21 .	87
13. Aperture plot contained in file TAPE12 . . . . .	88
14. Aperture plot contained in file TAPE22 . . . . .	89
15. Aperture plot contained in file TAPE23 . . . . .	90
16. Far-field plot contained in file TAPE40. . . . .	91
17. Far-field plot contained in file TAPE41. . . . .	92

## SECTION I

### INTRODUCTION

The purpose of this computer program is to analyze the effects of surface errors in large circularly symmetric reflector antennas. The program, as presently written, will handle dual reflector antennas, but with very minor modification could be made to handle prime focus antennas and even other symmetrical aperture antennas such as lenses. The program allows a circular reflector to be divided into any number of equal sectors for the purpose of defining errors; and therefore, the program could also be used, with some modification, to analyze sector antennas. The program assumes the primary reflector to be paraboloidal and the subreflector to be hyperboloidal. However, significant deviations of the no-error main reflector from a paraboloid are allowed in the same way that surface errors are allowed.

The program will handle either scalar or polarized fields. It uses a physical-optics integration technique over the primary reflector surface and does not include diffraction calculations. Except for random error, pattern magnitudes are consistent with each other, but they are not related to absolute gain or directivity.

There are two basic kinds of error, both of which are handled by the program: random and deterministic. The random errors are handled in a probabilistic manner as opposed to a Monte Carlo manner as discussed in the final report.<sup>1</sup> The random errors are point defects that all scatter with the same arbitrary pattern. An arbitrary number of defects is randomly positioned on one sector with an arbitrary density function, and this exact distribution is repeated on each of the other sectors. The defect position statistics are all independent and equal within one sector. The scattering function of a defect and the probability density function are changed by exchanging subroutines in this program. These random errors were designed to represent die defects in the tool used to stamp the reflector sector panels.

---

[1] "Surface Tolerance Analysis of Symmetrical Dual-Reflector Antennas," Final Technical Report, Georgia Tech Project A-3449, Purchase Order No. 580173, Scientific-Atlanta, June 1983.

The deterministic error is defined as a perturbation from the paraboloidal surface of the main reflector. This perturbation is assumed to affect only the phase of the reflected field. Thus, while the perturbations may be arbitrary, they should not be so large or abrupt that they significantly disturb the magnitude or polarization of the reflected field. Deterministic errors are defined in Subroutine PERTRB, of which there are three versions documented herein. One version calculates chordal errors to simulate the faceted construction of large reflectors. Another version applies a perturbation to one sector that is separable in the azimuthal and radial coordinates. The perturbation is then repeated for each sector. The program user can input an arbitrary azimuthal function and an arbitrary radial function to this subroutine. The third version allows the user to input an arbitrary radial function on each radial line of reflector sample points. The perturbations may be different for each radial and they are interpolated along each radial. This perturbation is also repeated for each sector, but it may also be applied to an antenna of one sector.

The program calculates the far-field patterns for the unperturbed antenna, for the antenna with deterministic errors only, and for the antenna with both random and deterministic errors. When random errors are included, the error pattern is the mean power pattern. In addition, the 3 dB point of the pattern and the first sidelobe level and location are calculated for the unperturbed and the total error patterns. A plotting package is included that provides three-dimensional plots of the aperture amplitude and phase and two-dimensional plots of aperture cuts and far-field patterns. The program can be verified by calculating the test case described in this documentation without knowing anything about the program. This is done simply by providing a double slash for every program input.

## SECTION II

### DESCRIPTION OF SUBPROGRAMS

The program is structured in a modular way to provide ease of understanding, to facilitate debugging, and to allow for future modifications. The main program calls subroutines in which many tasks are performed. The subroutines can be verified or modified separately or in small groups without changing and recompiling the whole program. Likewise, different models can be introduced without disrupting the whole program. For instance, the defect model can be completely changed simply by replacing the subroutine GPRT. A flow chart of all significant subprograms is presented in Figure 1. The number of calls and the approximate statement number of the first call are recorded for the main program. In addition, a flow chart of the main program is presented in Figure 2. It includes the more important loops, branches, and calculations.

A detailed description of the subprograms follows. All are constructed as subroutines unless otherwise indicated.

APDERS	Is the main program which reads the data from file INPUT and performs most of the unrepeated calculations ( <u>A</u> nalysis of <u>P</u> robabilistic and <u>D</u> eterministic <u>E</u> rrors in <u>R</u> eflector <u>A</u> ntennas).
APER	Calculates the complex incident electric field for the unperturbed case. Two versions have been implemented: a) a $\cos^n$ feed pattern and b) a Gaussian feed pattern.
BLOCK DATA	Is a non-executable program unit that defines many of the parameters for plotting.
CINTRP	Is a 4-point bivariate interpolation of a complex vector function.
DECIBEL	Is a function that converts complex volts to dB.
DISPLAY	Interfaces between the APDERS far-field patterns and the plot package and also tabulates patterns.
FT	Integrates over a parabolic reflector surface to obtain the Fourier transform of the aperture field E. The integrand and the exponent are interpolated at sufficient points in each cell to define the exponential factor at least once every radian.



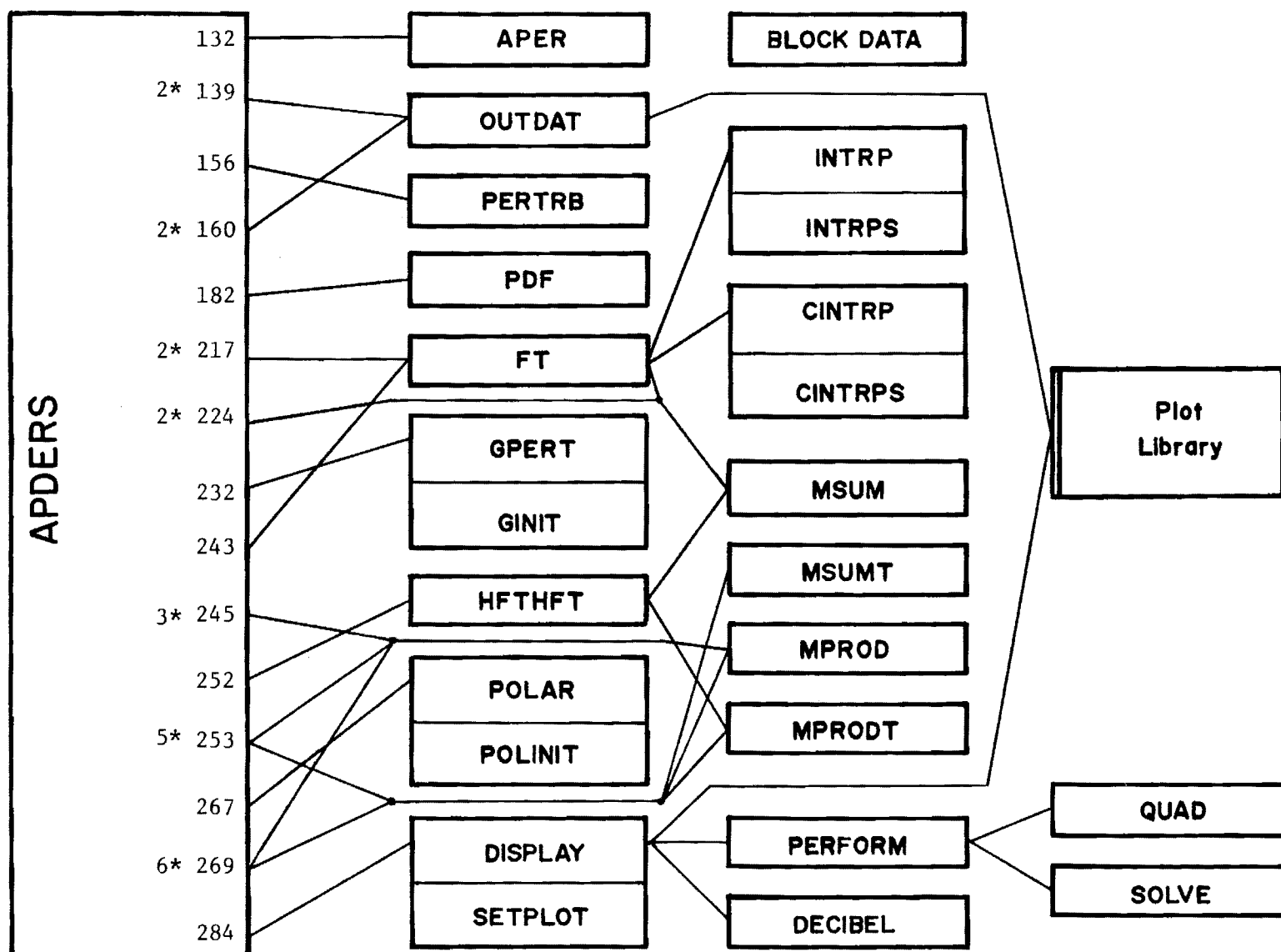


Figure 1. Block diagram of entire program.

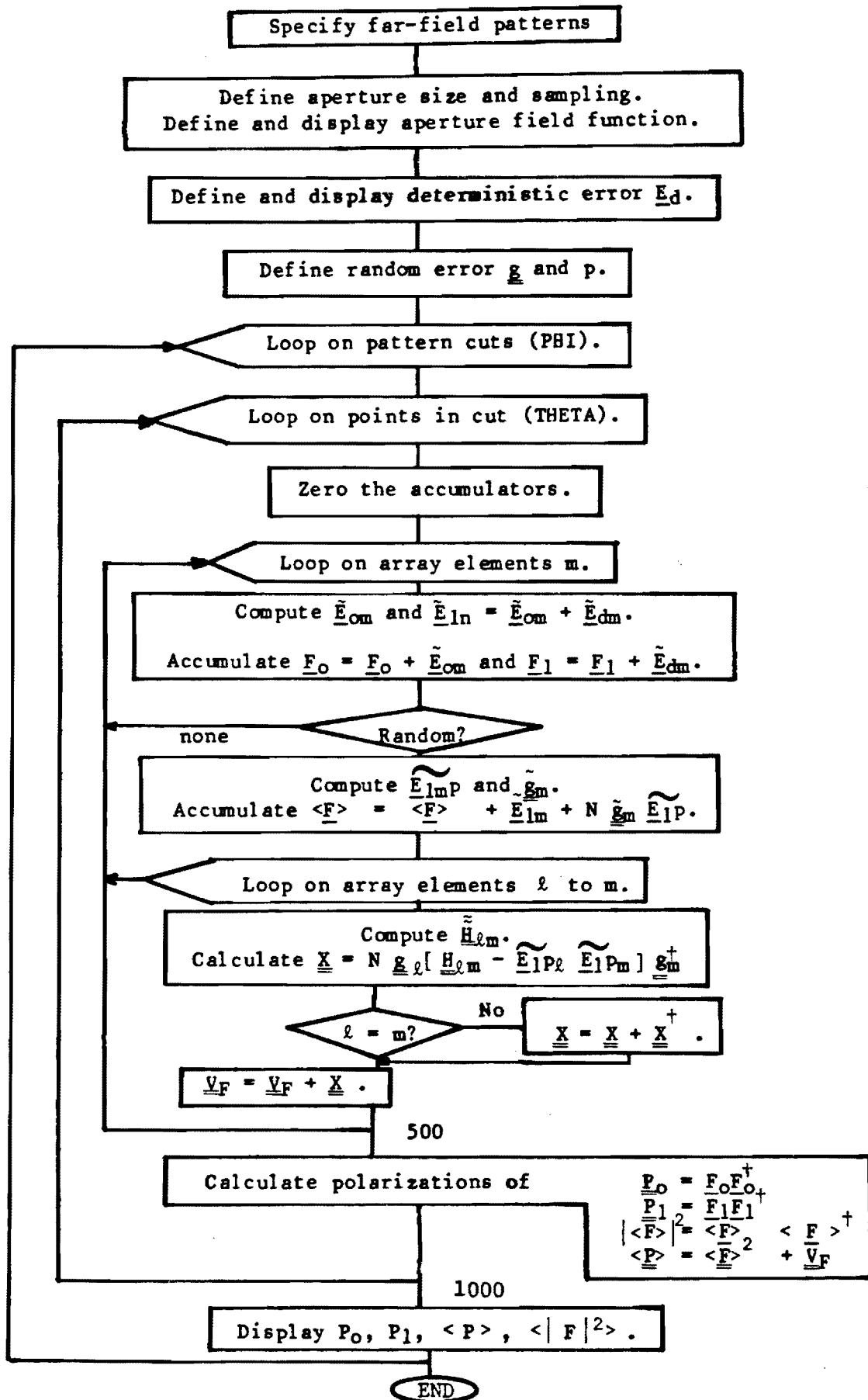


Figure 2. Flow chart of main program.

GPRT	Calculates the transform of the perturbation dyadic of a randomly positioned defect. Two functions have been implemented, a point source and a Gaussian phase bump.
HFTHFT	Calculates the double Fourier Transform of the aperture field correlation dyadic. (See Appendix B of the final report. <sup>1</sup> )
INTRP	Is a 4-point bivariate interpolation of a real vector function.
MPROD	Performs Cayley multiplication of any two compatible complex matrices.
MPRODT	Performs Cayley multiplication of any two compatible complex matrices after tranjugating the second.
MSUM	Adds any two compatible complex matrices after multiplying the second by a complex constant.
MSUMT	Adds any two compatible complex matrices after multiplying the second by a complex constant and tranjugating it.
OUTDAT	Plots the desired 3-D figures and cuts for the aperture and also tabulates the cuts.
PDF	Calculates the probability density function for a defect positioned in the aperture of one sector.
PERFORM	Calculates performance parameters for a pattern.
PERTRB	Introduces deterministic errors into the reflector surface. Three versions have been programmed: a) a function separable in azimuth and radius, b) a function defined separately on each radial, and c) chordal errors.
POLAR	Calculates the coefficients of far-fields to obtain the radiated power in the two desired orthogonal polarizations.
QUAD	Calculates the coefficients of a quadratic that fits three points.
SOLVE	Finds the roots of a quadratic.

The plot library actually includes two libraries: one that interfaces with Calcomp-compatible plotting hardware, and another, written at Georgia Tech, that interfaces between that library and the APDERS programs.

Neither of these libraries is documented in this report since experience has shown that users often prefer to use their own plotting software. Furthermore, changes may be dictated by each particular hardware installation. However, those routines that are called by the routines described above are briefly described below.

#### The Georgia Tech Library

AXIS3D	Draws axes for the three-dimensional plots.
FRAME	Draws marks for trimming the plotter paper.
GLINE	Plots an array of points.
HAXIS, VAXIS	Plots horizontal and vertical axes, respectively.
NUMCHR	Determines the number of characters in a string.
SYMBOL	Plots a string of characters.
RPLOT, PPLOT	Makes rectangular or polar plots, respectively.

#### The Calcomp Library

PLOT	Plots a point.
PLOTMX	Sets a plotting limit.
PLOTS	Initializes the plotter.
PLOT3D	Makes a three-dimensional plot.

THIS PAGE INTENTIONALLY LEFT BLANK

### SECTION III

#### FORTRAN CODE

The program was coded with the intention of making it user oriented. That is, it was developed with the philosophy that it is a dynamic tool which will be studied or modified by a variety of users. To this end, it is liberally interspersed with comments and spaces and other coding practices which make it very "readable". Sections of code are headed by a comment beginning with a string of dashes. Suggested modifications for certain applications are indicated by a string of asterisks. The first line of every subroutine is indicated by a string of slashes. Common blocks are used to group some related variables, but most communication between program units is in argument form. The argument approach makes it easier to determine which variables are used by a subroutine and, hence, what its action is. Furthermore, arguments for most subroutines are sequenced in an input/redefined/output order in the argument list, allowing one to immediately determine the function of an argument.

All reading is done from file INPUT in the main program except where noted with comment statements. Some PERTRB routines read from file TAPE5. Instructions for each input are written to file OUTPUT to provide interactive capability to the user. However, the echoing input and the output results are all written to file RESULT so that normal output is not contained in these instructions. The interactive user may wish to combine file OUTPUT and file RESULT. All parameters read from file INPUT are predefined with data statements so that the user can obtain a nominal, reasonable value by declining to input a value. Thus, he can make the program run as a learning technique before he becomes intimately familiar with its input requirements and capabilities.

The code list that follows is a FORTRAN compiler listing which has numbered lines and extensive cross-reference maps. The statement-label map indicates which references are "DO loops, reads, writes, or the actual labels. The variable map indicates which references are reads, writes, arguments, definitions, dimensions, initializations, or "IF statements". This kind of map is nearly indispensable to the serious student of the large program.

```

1      C/////APDERS  CALCULATES THE MEAN VECTOR POWER RADIATED FOR
C/      DETERMINISTIC ERRORS DEFINED OVER ONE SECTOR OF A ROTATIONALLY
C/      SYMETRICAL ANTENNA.  RANDOMLY POSITIONED DEFECTS ARE ALSO MODELED.
C/      THEY ARE EXACTLY REPEATED ON EACH ELEMENT.  THE MATHEMATICAL
5      C/      MODEL FOR ONE APERTURE IS IN "A NEW APPROACH TO THE ANALYSIS
C/      OF RANDOM ERRORS IN APERTURE ANTENNAS", TO BE PUBLISHED IN
C/      IEEE-TAP BY VICTOR K. TRIPP.
C/
10     PROGRAM APDERS( INPUT,RESULT,OUTPUT,TAPE5,TAPE6=RESULT )
C-----
C      FOR EACH ARRAY ELEMENT:
C      THE DEFECT POSITION STATISTICS ARE INDEPENDENT, IDENTICAL, AND
C      OTHERWISE ARBITRARY.  THE PERTURBATIONS CAUSED BY DEFECTS ARE
C      IDENTICAL AND OTHERWISE ARBITRARY.
C-----
15     COMPLEX  GMAX,C1,CM,CHITS,CON
COMPLEX  F0(2),F1(2),FBAR(2),VECT(2)
COMPLEX  POL3(8),DYAD(4),VF(4),HTT(4)
COMPLEX  E0T(2,32),E1T(2,32),E1PT(2,32),GT(2,2,32)
20     COMPLEX  P0(2,301),P1(2,301),F2PBAR(2,301),PBAR(2,301)
COMPLEX  E1(10000),E0(10000),E1P(1024)
DIMENSION POL(2),P(1024),AR(64),AA(256),THETA(301)
COMMON /CUT/  IPIC,ICUT,JCUT,INC,JNC,M0,N0,IBORDER,IGRID
COMMON /OUTSCR/ SCRATCH(3536)
25     COMMON /HEAD/  HEAD(8)
COMMON /CONST/  PI,PIBY2,PI3BY2,PI2,RAD,DEG,EPS,AK
DATA PI,PIBY2,PI3BY2,PI2,RAD,DEG,EPS/3.14159265,1.57079633,4.7123
*8698,6.28318531,0.01745329,57.29577951,1.E-4/
DATA HEAD(3) / " TEST CASE" /
30     DATA  R1, R2,NARR, DR, DAZ,  FREQ, IOBUG /
+ 0., 5., 6, .25, 5., 11.80285, 1 /
DATA DEFECT, GMAX, PERRAD / 1.7, (1.,0.), 1. /
DATA ZERO, C1, CM / 0., (1.,0.), (-1.,0.) /
DATA THE1,THE2,THED, PHI1,PHI2,PHID
35     * / 0., 30., 1.8, 0., 45., 45. /
DATA C, IPERT, ISYM / 11.80285, 1, 3 /

C
POW(A) = REAL(A)**2 + AIMAG(A)**2

C
40     CALL SECOND (TIME0)
C
C-----READ HEADER
C
PRINT*, " ENTER THE TITLE FOR THIS RUN"
45     READ 916, (HEAD(I), I=3,8)
CALL DATE(HEAD(1))
CALL TIME(HEAD(2))
IF (HEAD(3) .EQ. "//") HEAD(3) = " TEST CASE"
WRITE(6,920) (HEAD(I), I=1,8)
50     WRITE(6,*) " *** PROGRAM APDERS *** "
WRITE(6,*) " ANALYSIS OF DETERMINISTIC AND PROBABILISTIC ERRORS IN
* REFLECTOR ANTENNAS"
WRITE(6,*) " LATEST REVISION: 83/07/28 "
WRITE(6,920) (HEAD(I), I=1,8)

55     C
C-----DEFINE DESIRED PATTERNS
C
PRINT*, " "
PRINT*, " ENTER DEFINITION OF THETA PATTERNS"
60     PRINT*, " THETA START, STOP, AND INCREMENT; PHI LIKEWISE"
READ *, THE1,THE2,THED, PHI1,PHI2,PHID
TH1 = THE1*RAD
PH1 = PHI1*RAD
THE2 = THE2 * RAD
65     PH2 = PHI2 * RAD
THD = THED * RAD
PHD = PHID * RAD
NT = NP = 1
IF (THD .GT. 0.) NT = (TH2-TH1) / THD + 1.
70     IF (PHD .GT. 0.) NP = (PH2-PH1) / PHD + 1.5
WRITE(6,930) THE1,THE2,THED,NT, PHI1,PHI2,PHID,NP
CALL POLINIT( POL(1),POL(2),IOBUG,POL3 )
DO 60 I=1,NT

```

```

75      THETA(I) = THE1 + THED*(I-1)
      60 CONTINUE
C      READ *, IN SETPLOT
      CALL SETPLOT( THETA,P0,PBAR,P1,F2PBAR,NT,PH,POL,IOBUG )
C
C-----DEFINE APERTURE
80      C
      PRINT*, " ENTER REFLECTOR RADII: MIN, MAX, SPACING, POINTS"
      PRINT*, "          (NUMBER OF POINTS IS USED IF SPACING = 0.)"
      READ *, R1,R2,DR, NR
      PRINT*, " ENTER AZIMUTH SECTOR: (MIN=0), SECTORS, SPACING, POINTS"
85      READ *, NARR,DAZ, NA
      A2 = PI2 / NARR
      IF (DAZ .GT. 0.) GO TO 62
      PRINT*, " ENTER AZIMUTH SAMPLE POINTS (DEG)"
      READ *, (AA(I), I=1,NA)
90      DO 64 I=1,NA
      AA(I) = AA(I) * RAD
      64 CONTINUE
      DA = AA(1) - AA(2)
      IF (AA(1).EQ.0. .AND. AA(NA).EQ.A2) GO TO 61
95      PRINT*, " *** STOP *** "
      PRINT*, " SAMPLE POINTS DON'T START WITH 0. AND END WITH A2"
      STOP
      62 NA = A2 / (DAZ*RAD) + 1.5
      DA = A2 / (NA-1)
100     DO 30 J = 1, NA
      AA(J) = (J - 1)*DA
      30 CONTINUE
      61 IF (NARR .LE. 1) GO TO 63
      DO 34 J=1,NA
105     DO 34 K=2,NARR
      JK = (K-1)*NA + J
      AA(JK) = AA(J) + (K-1)*A2
      34 CONTINUE
C*****NOTE: SUBROUTINE FT ASSUMES EVEN SPACING IN AR.
110     63 IF (DR .CT. 0.) GO TO 68
      PRINT*, "ENTER RADIUS SAMPLE POINTS (IN.)"
      READ *, (AR(I), I=1,NR)
      R1 = AR(1)
      R2 = AR(NR)
115     DR = AR(1) - AR(2)
      GO TO 69
      68 NR = (R2-R1) /DR + 1.5
      DR = (R2-R1) / (NR-1)
      DO 20 I = 1, NR
120     AR(I) = (I - 1)*DR + R1
      20 CONTINUE
C
      69 NARR = NA*NR
      AREA = PI * (R2**2 - R1**2) / NARR
125     NTOTL = 2. * NR * NA
      NTOTL2 = NARR* NTOTL
C
      PRINT*, " ENTER THE FREQUENCY, DEBUG LEVEL, AND SYMETRY CODE"
      READ *, FREQ,IOBUG,ISYM
130     WAVE = C/FREQ
      AK = PI2 / WAVE
      WRITE(6,*) " APERTURE PARAMETERS "
      WRITE(6,*) " ----- "
      WRITE(6,909) IOBUG, ISYM,FREQ,WAVE
135     WRITE(6,910) R1,R2, DR,DR/WAVE, NR,
      * ZERO,A2*DEG,DA*DEG,DA*R2*WAVE,NA, NARR
      WRITE(6,920) (HEAD(I), I=1,8)
      WRITE(6,*) " UNPERTURBED APERTURE "
      WRITE(6,*) " ----- "
140     C
      READ *, IN APER
      CALL APER( AR,AA,NR,NA,NARR,IOBUG, FOCL,IPOL,E0 )
      IF (IPOL .EQ. 0) GO TO 32
      IF (ISYM .GE. 3) IPOL = 0
      IF (ISYM .GE. 3) WRITE(6,1720)
145     32 PRINT*, " ENTER THE APERTURE DISPLAY PARAMETERS"
      READ *, IPIC,ICUT,JCUT,INC,JNC,M0,N0,IBORDER,IGRID

```



```

      WRITE(6,1600) IPIC,ICUT,JCUT,INC,JNC,M0,N0,IBORDER,IGRID
      CALL OUTDAT( E0,IPOL,NR,NA,NARR,AR,AA,5 )
      IF (IPOL.NE. 0) CALL OUTDAT( E0,IPOL,NR,NA,NARR,AR,AA,5 )
150  C
      C-----DEFINE DETERMINISTIC ERROR
      C
      PRINT*, " "
      40 PRINT*, " ENTER 0 IF NO DETERMINISTIC ERRORS"
155  READ *, IPERT
      DO 70 I=1,NTOTL2
          E1(I) = E0(I)
      70 CONTINUE
      IF (IPERT.EQ. 0) GO TO 80
160  WRITE(6,920) (HEAD(I), I=1,8)
      WRITE(6,*) " PERTURBED APERTURE "
      WRITE(6,*) " ----- "
      C
      READ *, IN PERTRB
      CALL PERTRB( E0,AR,AA,NR,NA,NARR,FOCL,IOBUG, E1 )
165  PRINT*, " ENTER THE PERTURBATION DISPLAY PARAMETERS"
      READ *, IPIC,ICUT,JCUT,INC,JNC,M0,N0,IBORDER,IGRID
      WRITE(6,1600) IPIC,ICUT,JCUT,INC,JNC,M0,N0,IBORDER,IGRID
      CALL OUTDAT( E1,IPOL,NR,NA,NARR,AR,AA,5 )
      IF (IPOL.NE. 0) CALL OUTDAT( E1,IPOL,NR,NA,NARR,AR,AA,5 )
170  C
      C-----DEFINE RANDOM ERROR
      C
      80 PRINT*, "ENTER NUMBER, COMPLEX HEIGHT, AND CORRELATION OF DEFECTS"
      WRITE(6,920) (HEAD(I), I=1,8)
175  WRITE(6,*) " RANDOM DEFECTS "
      WRITE(6,*) " ----- "
      READ *, DEFECT,GMAX,PERRAD
      WRITE(6,960) DEFECT
      HITS = DEFECT
180  CHITS = CMPLX( HITS, 0. )
      IF (DEFECT.EQ. 0.) GO TO 28
      IF (DEFECT.GT. 0.) GO TO 25
      HITS = -DEFECT
      WRITE(6,965) HITS
185  25 GT(1) = GMAX
      CALL GINIT( WAVE,PERRAD, GT )
      CAREA = PI * PERRAD**2
      IF (CAREA.GT. AREA/5.) WRITE(6,995) CAREA, AREA
      UNIF = 0.
190  CALL PDF( AR,AA,NR,NA,AREA, P,UNIF )
      28 CALL SECOND( TIME1 )
      TIME2 = 0.
      TIME3 = 0.
      TIME4 = 0.
195  C
      C-----LOOP ON FAR-FIELD PATTERN POINTS
      C
      DO 2000 IP = 1,NP
          PH = PH1 + (IP-1)*PHD
200  DO 1000 IT = 1,NT
          IT2 = 2*IT - 1
          TH = TH1 + (IT-1)*THD
          STH = SIN(TH)
          CTH = COS(TH)
205  DO 50 I=1,2
          VF(I) = (0.,0.)
          VF(I+2) = (0.,0.)
          F0(I) = (0.,0.)
          F1(I) = (0.,0.)
210  FBAR(I) = (0.,0.)
      50 CONTINUE
      C
      C-----LOOP ON ARRAY ELEMENTS
      C
215  DO 600 M=1,NARR
          M1 = NTOTL * (M-1)
          M2 = 2*M - 1
          M4 = 4*M - 3
          PHM = PH - A2*(M-1)

```

```

220      AKR = AK * STH
      AKP = PHM
      C      COMPUTE TRANSFORMS OF E0, E1, AND E1P
      CALL SECOND( T1 )
      IF ( IOBUG .GE. 3 ) WRITE(6,1900) IP,IT,TH*DEG, PH*DEG
225      CALL FT( E0(M1+1),AR,AA,NR,NA,FOCL,AKR,AKP,IOBUG,IPOL
      *      , E0T(M2) )
      E1T(M2) = E0T(M2)
      E1T(M2+1) = E0T(M2+1)
      IF ( IPERT .NE. 0 )
230      *      CALL FT( E1(M1+1),AR,AA,NR,NA,FOCL,AKR,AKP,IOBUG,IPOL
      *      , E1T(M2) )
      CALL MSUM( F0,E0T(M2),C1,2,1, F0 )
      CALL MSUM( F1,E1T(M2),C1,2,1, F1 )
      IF ( IOBUG.GE.3 ) WRITE(6,1850) E0T(M2),E0T(M2+1),E1T(M2)
235      *      ,E1T(M2+1), F0(1),F0(2),F1(1),F1(2)
      CALL SECOND( T2 )
      TIME2 = TIME2 + T2 - T1
      C
      IF ( DEFECT .LE. 0 ) GO TO 600
240      CALL GPERT( AKR,AKP, GT(M4) )
      IF ( IOBUG.GE.3 ) WRITE(6,1700) AKR,AKP,M,GT(M4),GT(M4+2),
      *      GT(M4+1),GT(M4+3)
      IF ( IOBUG.GE.4 ) WRITE(6,1750)
245      DO 400 I=1,NANR
      E1P(I) = E1(I+M1) * P(I)
      E1P(I+1) = E1(I+1+M1) * P(I)
      400      CONTINUE
      E1PT(M2) = E1T(M2) * P(1)
      E1PT(M2+1) = E1T(M2+1) * P(1)
250      IF ( UNIF .EQ. 1 ) GO TO 420
      CALL FT( E1P,AR,AA,NR,NA,FOCL,AKR,AKP,IOBUG,IPOL, E1PT(M2))
      420      CALL MPROD( GT(M4),E1PT(M2),2,2,1, VECT )
      CALL MSUM( E1T(M2),VECT,CHITS,2,1, VECT )
      CALL MSUM( FBAR,VECT,C1,2,1, FBAR )
255      MP = M
      IF ( ISYM .GE. 3 ) MP = 1
      DO 500 L=1,MP
      L2 = 2*L - 1
      L4 = 4*L - 3
260      CALL HFTHFT( E1,P,L,M,AR,AA,NR,NA,AKR,AKP,IOBUG,IPOL, HTT)
      CALL MPRODT( E1PT(L2),E1PT(M2),2,1,2, DYAD )
      CALL MSUM( HTT,DYAD,CM,2,2, DYAD )
      CALL MPRODT( DYAD,GT(M4),2,2,2, DYAD )
      CALL MPROD( GT(L4),DYAD,2,2,2, DYAD )
265      IF ( L .NE. MD ) CALL MSUMT( DYAD,DYAD,C1,2,2, DYAD )
      CON = C1
      IF ( ISYM .GE. 3 ) CON = CMPLX( FLOAT(NARR-M+1), 0. )
      CALL MSUM( VF,DYAD,CON,2,2, VF )
      IF ( IOBUG.GE.4 ) WRITE(6,1800) L,HTT(1),HTT(3),DYAD(1),
270      *      DYAD(3),VF(1),VF(3),HTT(2),HTT(4),DYAD(2),DYAD(4),VF(2),VF(4)
      500      CONTINUE
      CALL SECOND( T3 )
      TIME3 = TIME3 + T3 - T2
      600      CONTINUE
275      CALL POLAR( AKR,PH,IOBUG, POL3 )
      CALL MPRODT( F0,F0,2,1,2, DYAD )
      CALL MPROD( DYAD,POL3,1,4,2, P0(IT2) )
      CALL MPRODT( F1,F1,2,1,2, DYAD )
      CALL MPROD( DYAD,POL3,1,4,2, P1(IT2) )
280      PBAR(IT2) = P1(IT2)
      PBAR(IT2+1) = P1(IT2+1)
      IF ( DEFECT .LE. 0 ) GO TO 1000
      CALL MPRODT( FBAR,FBAR,2,1,2, DYAD )
      CALL MPROD( DYAD,POL3,1,4,2, F2PBAR(IT2) )
285      CALL MSUM( DYAD,VF,CHITS,2,2, DYAD )
      CALL MPROD( DYAD,POL3,1,4,2, PBAR(IT2) )
      1000      CONTINUE
      C
      C-----DISPLAY THIS PATTERN CUT
290      C
      CALL SECOND( T3 )
      CALL DISPLAY( THETA,P0,PBAR,P1,F2PBAR,NT,PH*DEG,POL,IOBUG )

```

```

                CALL SECOND( T4 )
                TIME4 = TIME4 + T4 - T3
295      2000    CONTINUE
C
                WRITE(6,940)  TIME1-TIME0,TIME2,TIME3,TIME4,T4-TIME0
C
                STOP
300      909    FORMAT(/" THE DEBUG OUTPUT LEVEL IS",I3,
                *      " THE SYMETRY LEVEL IS", I3//
                *      " THE FREQUENCY AND WAVELENGTH (IN.) ARE:",2F10.5//)
305      910    FORMAT(/" THE APERTURE IS DEFINED BY:"//
                *      "          MINIMUM    MAXIMUM    INCREMENT(IN., WAVE)    POINTS"/
                *      "          -----
                *      "      RHO  ", 2F10.5,4X, 2F10.6, 18/
                *      "      PHI  ", 2F10.5,4X, 2F10.6, 18////////
                *      " THE NUMBER OF SECTORS IS", I5////////)
310      916    FORMAT( 6A10 )
                920    FORMAT(///"1          ", 8A10 // )
                930    FORMAT(///" PATTERN CUTS TO BE CALCULATED (THETA CUTS, DEG) "///
                *      "          BEGIN      END      STEP      POINTS"/
                *      "          -----
                *      "      THETA",3F8.2,17 / " PHI  ",3F8.2,17 //////////)
315      940    FORMAT(///"          WORK          TIME"/
                +      "          -----
                +      "      SET UP PROBLEM          ", F8.3/
                +      "      INTEGRATE E0, E1          ", F8.3/
                +      "      RANDOM ERROR CALC.        ", F8.3/
320      +      "      DISPLAY DATA          ", F8.3/
                +      "          -----
                +      "          TOTAL          ", F8.3/)
                960    FORMAT( ///" THE NUMBER OF RANDOM DEFECTS PER SECTOR IS", F8.3 )
                965    FORMAT( " THE AVERAGE NUMBER OF HITS IS", F8.3 )
325      995    FORMAT( ///" *** WARNING ***"/
                +      "      PERTURBATION AREA", F8.2, " IS NOT SMALL COMPARED TO"/
                +      "      APERTURE AREA          ", F8.2//)
                1600   FORMAT(////" THE APERTURE PLOTTING PARAMETERS ARE:"/3(3I3,1X))
                1700   FORMAT(///" FOR AKR, AKP = ",2F8.4, ", THE DEFECT SCATTERING DYADIC",
330      *      " TRANSFORM AT ELEMENT",I3," IS",// (12X,2(2F10.5)) )
                1720   FORMAT(///" THE SYMETRY SPECIFICATION OVERRIDES POLARIZATION"//)
                1750   FORMAT(/"      ELEMENT",20X,"CORRELATION TRANSFORM",20X,"TOTAL "
                *      "CONTRIBUTION",20X,"ACCUMULATION"/)
                1800   FORMAT( 110,2X, 3(2(2F9.5,1X),2X)/ 12X,3(2(2F9.5,1X),2X)/)
335      1850   FORMAT(/" EOT=",2(2F9.4,2X),"      E1T=",2(2F9.4,2X)/
                *      " F0  =",2(2F9.4,2X),"      F1  =",2(2F9.4,2X) /)
                1900   FORMAT(////" PATTERN CUT",I3," , POINT",I3," ; THETA, PHI = ",2F8.2)
                END

```

PROGRAM APDERS 74/74 TS

--COMMON BLOCKS--

10B /CONST/ 11B /CUT/ 10B /HEAD/ 6720B /OUTSCR/

--ENTRY POINTS--

262B APDERS 3B INPUT\* 125B OUTPUT\* 54B RESULT\*  
176B TAPE5\* 54B TAPE6\*

--EXTERNALS--

APER	COS.	DATE	DISPLAY	FT	FTNRP2.	GINIT	GPRT
HFTHFT	INPCI.	INPCR.	INPFI.	INPFR.	MPROD	MPRODT	MSUM
MSUMT	OUTCI.	OUTCR.	OUTDAT	OUTFI.	PDF	PERTRB	POLAR
POLINIT	SECOND	SETPLOT	SIN.	STOP.	TIME		

--STATEMENT LABELS--

.20	ID	0B	119 D	121 L				
.25		1076B	182	135 L				
.28		1120B	181	191 L				
.30	ID	0B	100 D	102 L				
.32		737B	142	145 L				
.34	ID	0B	104 D	105 D	108 L			
.40		756B	154 L					
.50	ID	0B	203 D	211 L				
.60	ID	0B	73 D	75 L				
.61		534B	94	103 L				
.62		513B	87	98 L				
.63		560B	103	110 L				
.64	ID	0B	90 D	92 L				
.68		611B	110	117 L				
.69		633B	116	123 L				
.70	ID	0B	156 D	158 L				
.80		1034B	159	173 L				
.400	ID	0B	244 D	247 L				
.420		1447B	250	252 L				
.500	ID	0B	257 D	271 L				
.600	D	1573B	215 D	239	274 L			
.909	F	2122B	134 W	300 L				
.910	F	2137B	135 W	303 L				
.916	F	2174B	45 R	309 L				
.920	F	2176B	49 W	54 W	137 W	160 W	174 W	310 L
.930	F	2202B	71 W	311 L				
.940	F	2227B	297 W	315 L				
.960	F	2262B	178 W	323 L				
.965	F	2271B	184 W	324 L				
.995	F	2276B	188 W	325 L				
.1000	D	1650B	200 D	232	287 L			
.1600	F	2312B	147 W	167 W	328 L			
.1700	F	2321B	241 W	329 L				
.1720	F	2336B	144 W	331 L				
.1750	F	2345B	243 W	332 L				
.1800	F	2360B	269 W	334 L				
.1850	F	2366B	234 W	335 L				
.1900	F	2401B	224 W	337 L				
.2000	D	1667B	198 D	295 L				

--VARIABLE MAP--

AA	R	52536B		256		22 D	89 R	91
	91 =	93	93	94 F		94 F	101 =	107
	107 =	141 A	148 A	149 A		164 A	168 A	169 A
	190 A	225 A	229 A	251 A		260 A		
AK	R	7B /CONST/				26 D	131 =	220
AKP	R	143637B				221 =	225 A	229 A
	240 A	241 W	251 A	260 A				
AKR	R	143636B				220 =	225 A	229 A

## PROGRAM APDERS 74/74 TS

APDERS	240 A	241 W	251 A	260 A	275 A		
APER	-	262B ENTRY			9 E		
AR	R	SUBROUTINE			141 X		
	R	55442B	64		22 D	112 R	113
	114	115	115	120 =	141 A	148 A	149 A
	164 A	168 A	169 A	190 A	225 A	229 A	251 A
AREA	260 A						
	R	55546B			124 =	188 F	188 W
A2	190 A						
	R	143604B			86 =	94 F	98
	99	107	135 W	219			
C	R	143566B			36 I	130	
CAREA	R	143615B			187 =	188 F	188 W
CHITS	Z	55440B			16 D	180 =	253 A
	285 A						
CM	Z	53147B			16 D	33 I	262 A
CMPLX	Z		INTRINSIC		180	267	
CON	Z	55755B			16 D	266 =	267 =
	268 A						
COS.	R		B.E.F.		204		
CTH	R	143630B			204 =		
C1	Z	3440B			16 D	33 I	232 A
	233 A	254 A	265 A	266			
DA	R	143605B			93 =	99 =	101
	135 W	135 W					
DATE	R		SUBROUTINE		46 X		
DAZ	R	53153B			30 I	85 R	87 F
	98						
DEFECT	R	143561B			32 I	177 R	178 W
	179	181 F	182 F	183	239 F	282 F	
DEG	R	5B /CONST/			26 D	27 I	135 W
	135 W	224 W	224 W	292 A			
DISPLAY	R		SUBROUTINE		292 X		
DR	R	143557B			30 I	83 R	110 F
	115 =	117	118 =	120	135 W	135 W	
DYAD	Z	125223B		4	18 D	261 A	262 A
	262 A	263 A	263 A	264 A	264 A	265 A	265 A
	265 A	268 A	269 W	269 W	269 W	269 W	276 A
	277 A	278 A	279 A	283 A	284 A	285 A	285 A
	286 A						
EPS	R	6B /CONST/			26 D	27 I	
E0	Z	55757B	10000		21 D	141 A	148 A
	149 A	157	164 A	225 A			
E0T	Z U	125023B	64		19 D	225 A	227
	228	232 A	234 W	234 W			
E1	Z	3442B	10000		21 D	157 =	164 A
	168 A	169 A	229 A	245	246	260 A	
E1P	Z	135077B	1024		21 D	245 =	246 =
	251 A						
E1PT	Z	55554B	64		19 D	248 =	249 =
	251 A	252 A	261 A	261 A			
E1T	Z	125243B	64		19 D	227 =	228 =
	229 A	233 A	234 W	234 W	248	249	253 A
FBAR	Z	52532B	2		17 D	210 =	254 A
	254 A	283 A	283 A				
FLOAT	R		INTRINSIC		267 A		
FOCL	R	143613B			141 A	164 A	225 A
	229 A	251 A					
FREQ	R	143560B			30 I	129 R	130
	134 W						
FT	R		SUBROUTINE		225 X	229 X	251 X
FTNRP2.	-		EXTERNAL.		9		
F0	Z	125017B	2		17 D	208 =	232 A
	232 A	234 W	234 W	276 A	276 A		
F1	Z	52503B	2		17 D	209 =	233 A
	233 A	234 W	234 W	278 A	278 A		
F2PBAR	Z	130327B	602		20 D	77 A	284 A
	292 A						
GINIT	R		SUBROUTINE		186 X		
GMAX	Z	52510B			16 D	32 I	177 R
	185						
GPERT	R		SUBROUTINE		240 X		
GT	Z	125443B	128		19 D	185 =	186 A

PROGRAM APDERS 74/74 TS

	240 A	241 W	241 W	241 W	241 W	252 A	263 A
	264 A						
HEAD	R	0B /HEAD/	8		25 D	29 I	45 R
	46 A	47 A	48 F	48 =	49 W	54 W	137 W
HFTHFT	160 W	174 W					
HITS	R	SUBROUTINE			260 X		
	R	52502B			179 =	180 A	183 =
HTT	184 W						
	Z	53137B	4		18 D	260 A	262 A
	269 W	269 W	269 W	269 W			
I	I	143571B			45 C	45 S	49 C
	49 S	54 C	54 S	73 C	74	74 S	89 C
	89 S	90 C	91 S	91 S	112 C	112 S	119 C
	120	120 S	137 C	137 S	156 C	157 S	157 S
	160 C	160 S	174 C	174 S	205 C	206 S	207 S
	208 S	209 S	210 S	244 C	245 S	245 S	245 S
	246 S	246 S	246 S				
IBORDER	I	7B /CUT/			23 D	146 R	147 W
	166 R	167 W					
ICUT	I	1B /CUT/			23 D	146 R	147 W
	166 R	167 W					
IGRID	I	10B /CUT/			23 D	146 R	147 W
	166 R	167 W					
INC	I	3B /CUT/			23 D	146 R	147 W
	166 R	167 W					
INPCI.	-	EXTERNAL.			45 R		
INPCR.	-	EXTERNAL.			45 R	45 R	
INPFI.	-	EXTERNAL.			61 R	83 R	85 R
	89 R	112 R	129 R	146 R	155 R	166 R	177 R
INPFR.	-	EXTERNAL.			89 R	89 R	112 R
	112 R						
INPUT#	-	3B ENTRY			45 R	61 R	83 R
	85 R	89 R	112 R	129 R	146 R	155 R	166 R
	177 R						
IOBUG	I	53152B			30 I	72 A	77 A
	129 R	134 W	141 A	164 A	224 F	225 A	229 A
	234 F	241 F	243 F	251 A	260 A	269 F	275 A
	292 A						
IP	I	143623B			198 C	199	224 W
IPERT	I	55754B			36 I	155 R	159 F
	229 F						
IPIC	I	0B /CUT/			23 D	146 R	147 W
	166 R	167 W					
IPOL	I	143614B			141 A	142 F	143 =
	148 A	149 F	149 A	168 A	169 F	169 A	225 A
	229 A	251 A	260 A				
ISYM	I	143567B			36 I	129 R	134 W
	143 F	144 F	256 F	267 F			
IT	I	143624B			200 C	201	202
	224 W						
IT2	I	143625B			201 =	277 S	279 S
	280 S	280 S	281 S	281 S	284 S	286 S	
J	I	143606B			100 C	101	101 S
	104 C	106	107 S				
JCUT	I	2B /CUT/			23 D	146 R	147 W
	166 R	167 W					
JK	I	3437B			106 =	107 S	
JNC	I	4B /CUT/			23 D	146 R	147 W
	166 R	167 W					
K	I	143607B			105 C	106	107
L	I	143643B			257 C	258	259
	260 A	265 F	269 W				
L2	I	143644B			258 =	261 S	
L4	I	143645B			259 =	264 S	
M	I	143631B			215 C	216	217
	218	219	241 W	255	260 A	265 F	267 A
MP	I	143642B			255 =	256 =	257 C
MPROD	I	SUBROUTINE			252 X	264 X	277 X
	279 X	284 X	286 X				
MPRODT	I	SUBROUTINE			261 X	263 X	276 X
	278 X	283 X					
MSUM	I	SUBROUTINE			232 X	233 X	253 X
	254 X	262 X	268 X	285 X			

PROGRAM APDERS 74/74 TS

MSUMT	I	SUBROUTINE			265 X		
M0	I	5B /CUT/			23 D	146 R	147 W
	166 R	167 W					
M1	I	143632B			216 =	225 S	229 S
	245 S	246 S					
M2	I	143633B			217 =	225 S	227 S
	227 S	228 S	228 S	229 S	232 S	233 S	234 S
	234 S	234 S	234 S	248 S	248 S	249 S	249 S
	251 S	252 S	253 S	261 S			
M4	I	143634B			218 =	240 S	241 S
	241 S	241 S	241 S	252 S	263 S		
NA	I	55552B			95 R	89 C	90 C
	94 S	98 =	99	100 C	104 C	106	123
	125	135 W	141 A	148 A	149 A	164 A	168 A
	169 A	190 A	225 A	229 A	251 A	260 A	
NANR	I	143610B			123 =	244 C	
NARR	I	53136B			30 I	35 R	86
	103 F	105 C	124	126	135 W	141 A	148 A
	149 A	164 A	168 A	169 A	215 C	267 A	
NP	I	143600B			68 =	70 =	71 W
	198 C						
NR	I	143603B			83 R	112 C	114 S
	117 =	118	119 C	123	125	135 W	141 A
	148 A	149 A	164 A	168 A	169 A	190 A	225 A
	229 A	251 A	260 A				
NT	I	143601B			68 =	69 =	71 W
	73 C	77 A	200 C	292 A			
NTOTL	I	143611B			125 =	126	216
NTOTL2	I	143612B			126 =	156 C	
N0	I	6B /CUT/			23 D	146 R	147 W
	166 R	167 W					
OUTCI.	-	EXTERNAL.			49 W	54 W	71 W
	134 W	135 W	137 W	144 W	147 W	160 W	167 W
	174 W	178 W	184 W	188 W	224 W	234 W	241 W
	243 W	269 W	297 W				
OUTCR.	-	EXTERNAL.			49 W	49 W	54 W
	54 W	137 W	137 W	160 W	160 W	174 W	174 W
OUTDAT	R	SUBROUTINE			148 X	149 X	168 X
	169 X						
OUTFI.	-	EXTERNAL.			44 W	50 W	51 W
	53 W	58 W	59 W	60 W	81 W	82 W	84 W
	88 W	95 W	96 W	111 W	128 W	132 W	133 W
	138 W	139 W	145 W	153 W	154 W	161 W	162 W
	165 W	173 W	175 W	176 W			
OUTPUT*	-	125B ENTRY			44 W	58 W	59 W
	60 W	81 W	82 W	84 W	88 W	95 W	96 W
	111 W	128 W	145 W	153 W	154 W	165 W	173 W
P	R	141101B		1024	22 D	190 A	245
	246	248	249	260 A			
PBAR	Z	132613B		602	20 D	77 A	280 =
	281 =	286 A	292 A				
PDF	R	SUBROUTINE			190 X		
PERRAD	R	55550B			32 I	177 R	186 A
	187						
PERTRB	R	SUBROUTINE			164 X		
PH	R	143602B			77 A	199 =	219
	224 W	275 A	292 A				
PHD	R	143577B			67 =	70 F	70
	199						
PHID	R	55551B			34 I	61 R	67
	71 W						
PHI1	R	143565B			34 I	61 R	63
	71 W						
PHI2	R	53151B			34 I	61 R	65
	71 W						
PHM	R	143635B			219 =	221	
PH1	R	143573B			63 =	70	199
PH2	R	143575B			65 =	70	
PI	R	0B /CONST/			26 D	27 I	124
	187						
PIBY2	R	1B /CONST/			26 D	27 I	
PI2	R	3B /CONST/			26 D	27 I	86
	131						

## PROGRAM APDERS 74/74 TS

PI3BY2	R	2B /CONST/			26 D	27 I	
POL	R	141077B	2		22 D	72 A	72 A
	77 A	292 A					
POLAR	R	SUBROUTINE			275 X		
POLINIT	R	SUBROUTINE			72 X		
POL3	Z	52512B	8		18 D	72 A	275 A
	277 A	279 A	284 A	286 A			
POW	R	STAT-FUNC			38 D		
P0	Z	126043B	602		20 D	77 A	277 A
	292 A						
P1	Z	53154B	602		20 D	77 A	279 A
	280	281	292 A				
RAD	R	4B /CONST/			26 D	27 I	62
	63	64	65	66	67	91	98
RESULT*	-	54B ENTRY					
R1	R	143556B			30 I	83 R	113 =
	117	118	120	124	135 W		
R2	R	55553B			30 I	83 R	114 =
	117	118	124	135 W	135 W		
SCRATCH	R	0B /OUTSCR/	3536		24 D		
SECOND	R	SUBROUTINE			40 X	191 X	223 X
	236 X	272 X	291 X	293 X			
SETPLOT	R	SUBROUTINE			77 X		
SIN.	R	B.E.F.			203		
STH	R	143627B			203 =	220	
STOP.	-	EXTERNAL.			97	299	
TAPE5*	-	176B ENTRY					
TAPE6*	-	54B ENTRY			49 W	50 W	51 W
	53 W	54 W	71 W	132 W	133 W	134 W	135 W
	137 W	138 W	139 W	144 W	147 W	160 W	161 W
	162 W	167 W	174 W	175 W	176 W	178 W	184 W
	188 W	224 W	234 W	241 W	243 W	269 W	297 W
TH	R	143626B			202 =	203 A	204 A
	224 W						
THD	R	143576B			66 =	69 F	69
	202						
THED	R	143564B			34 I	61 R	66
	71 W	74					
THETA	R	143101B	301		22 D	74 =	77 A
	292 A						
THE1	R	143562B			34 I	61 R	62
	71 W	74					
THE2	R	143563B			34 I	61 R	64
	71 W						
TH1	R	143572B			62 =	69	202
TH2	R	143574B			64 =	69	
TIME	R	SUBROUTINE			47 X		
TIME0	R	143570B			40 A	297 W	297 W
TIME1	R	143617B			191 A	297 W	
TIME2	R	143620B			192 =	237	237 =
	297 W						
TIME3	R	143621B			193 =	273	273 =
	297 W						
TIME4	R	143622B			194 =	294	294 =
	297 W						
T1	R	143640B			223 A	237	
T2	R	143641B			236 A	237	273
T3	R	143646B			272 A	273	291 A
	294						
T4	R	143647B			293 A	294	297 W
UNIF	R	143616B			189 =	190 A	250 F
VECT	Z	55542B	2		17 D	252 A	253 A
	253 A	254 A					
VF	Z	125233B	4		18 D	206 =	207 =
	268 A	268 A	269 W	269 W	269 W	269 W	285 A
WAVE	R	52507B			130 =	131	134 W
	135 W	135 W	186 A				
ZERO	R	55547B			33 I	135 W	

157331B PROGRAM-UNIT LENGTH 198 SYMBOLS  
1029 REFERENCES

45000B CM STORAGE USED

13.497 SECONDS



```

1      C/////APER CALCULATES THE COMPLEX APERTURE ELECTRIC FIELD.
C/     THIS MODEL IS A SCALAR DUAL REFLECTOR WITH A COS**N FEED
C/     OR A GAUSSIAN ON A PEDESTAL.
C/
5      SUBROUTINE APER( AR,AA,NR,NA,NARR,IO, FO,IP,E0 )
C
      COMPLEX E0(2,NR,NA)
      DIMENSION AA(NA),AR(NR),TYPE(2)
      DATA IPOL, FOCL, ECC, COSN, PED,ABYTHS,TYPE(1),TYPE(2)
10     * / 0, 4., 2., 16., -50.,3.8436,"COS**N","GAUSSIAN" /
      DATA IFEEED / 1 /
C
      PRINT*, " ENTER FOCAL LENGTH, ECCENTRICITY, AND FEED TYPE"
      READ *, FOCL,ECC,IFEEED
13     WRITE(6,900) TYPE(IFEEED),FOCL,ECC
      FO = FOCL
      IP = IPOL
      FAC = (ECC-1.) / ( (ECC+1.)*2.*FOCL )
      NRR = NA * NARR
20     IF (IFEEED.NE. 1) GO TO 500
      PRINT*, " ENTER COSINE EXPONANT"
      READ *, COSN
      WRITE(6,930) COSN
      IF (IO.GE. 1) WRITE(6,920)
25     DO 200 I=1,NR
          ARH02 = (FAC * AR(I))**2
          F = ( (1.-ARH02) / (1.+ARH02) )**COSN
          DIVERG = 1. + ARH02
          F = F / DIVERG
30     IF (IO.GE.1) WRITE(6,910) I,AR(I),ARH02,F
          DO 100 J=1,NRR
              E0(1,I,J) = CMPLX( F, 0.)
              E0(2,I,J) = (0.,0.)
          100 CONTINUE
35     200 CONTINUE
      RETURN
C
500 PRINT*, " ENTER GAUSSIAN PEDESTAL AND ANGLE COEFFICIENT"
      READ *, PED, ABYTHS
40     B = 10.** (PED*.05)
      WRITE(6,940) PED, ABYTHS
      IF (IO.GE. 1) WRITE(6,920)
      DO 700 I=1,NR
          ARH0 = FAC * AR(I)
45     PHI = 2.* ATAN( ARH0 )
          F = (EXP( -(ABYTHS*PHI)**2 ) + B) / (1.+B)
          DIVERG = 1. + ARH0**2
          F = F / DIVERG
50     IF (IO.GE.1) WRITE(6,910) I,AR(I),ARH0**2,F
          DO 600 J=1,NRR
              E0(1,I,J) = CMPLX( F, 0.)
              E0(2,I,J) = (0.,0.)
          600 CONTINUE
55     700 CONTINUE
      RETURN
C
900 FORMAT( //" ANTENNA MODEL IS A (SCALAR) ",A10," FEED IN AN"/
+         " AXIALLY SYMETRIC CASSEGRAIN REFLECTOR SYSTEM."//
+         " PARABOLOID FOCAL LENGTH ",F10.3/
+         " HYPERFOLOID ECCENTRICITY ",F10.3//)
60     910 FORMAT( I7,3F9.4 )
      920 FORMAT("// POINT RADIUS TAN(PHI/2)**2 FIELD"/)
      930 FORMAT("/ THE EXPONANT OF COS(THETA) IS",F8.3//)
      940 FORMAT("/ THE PEDESTAL. B (DB) IS",F9.3/
65     * " THE GAUSSIAN EXPONANT COEFFICIENT, A/THN IS",F10.4//)
      END

```

## --EXTERNALS--

ATAN. XTOY.	EXP.	INPFI.	INPUT#	OUTCI.	OUTFI.	OUTPUT#	TAPE6#
----------------	------	--------	--------	--------	--------	---------	--------

## --STATEMENT LABELS--

.100	ID	0B	31 D	34 L			
.200	ID	0B	25 D	35 L			
.500		134B	20	38 L			
.600	ID	0B	50 D	53 L			
.700	ID	0B	43 D	54 L			
.900	F	300B	15 W	57 L			
.910	F	325B	30 W	49 W	61 L		
.920	F	327B	24 W	42 W	62 L		
.930	F	335B	23 W	63 L			
.940	F	343B	41 W	64 L			

## --VARIABLE MAP--

AA	R A	0B	VAR-DIM	5 A	8 D	
ABYTHS	R	466B		9 I	39 R	41 W
	46					
APER	-	247B ENTRY		5 E		
AR	R A	0B	VAR-DIM	5 A	8 D	26
	30 W	44	49 W			
ARHO	R	471B		44 =	45 A	47
	49 W					
ARHO2	R	456B		26 =	27	27
	28	30 W				
ATAN.	R	B.E.F.		45		
B	R	451B		40 =	46	46
CMPLX	Z	INTRINSIC		32	51	
COSN	R	460B		9 I	22 R	23 W
	27					
DIVERG	R	454B		28 =	29	47 =
	48					
ECC	R	465B		9 I	14 R	15 W
	18	18				
EXP.	R	B.E.F.		46		
E0	Z A	0B	VAR-DIM	5 A	7 D	32 =
	33 =	51 =	52 =			
F	R	455B		27 =	29	29 =
	30 W	32 A	46 =	48 =	49 W	51 A
FAC	R	461B		18 =	26	44
FO	R A	0B		5 A	16 =	
FOCL	R	457B		9 I	14 R	15 W
	16	18				
I	I	467B		25 C	26 S	30 W
	30 S	32 S	33 S	44 S	49 W	49 S
	51 S	52 S				
IFEED	I	464B		11 I	14 R	15 S
	20 F					
INPFI.	-	EXTERNAL.		14 R	22 R	39 R
INPUT#	-	EXTERNAL.		14 R	22 R	39 R
IO	I A	0B		5 A	24 F	30 F
	42 F	49 F				
IP	I A	0B		5 A	17 =	
IPOL	I	462B		9 I	17	
J	I	470B		31 C	32 S	33 S
	50 C	51 S	52 S			
NA	I A	0B		5 A	7 D	8 D
	19					
NARR	I A	0B		5 A	19	
NR	I A	0B		5 A	7 D	8 D
	25 C	43 C				
NRR	I	450B		19 =	31 C	50 C
OUTCI.	-	EXTERNAL.		15 W	23 W	24 W
	30 W	41 W	42 W	49 W		
OUTFI.	-	EXTERNAL.		13 W	21 W	38 W

SUBROUTINE APER 74/74 TS

OUTPUT#	-		EXTERNAL.	13 W	21 W	38 W
PED	R	463B		9 I	39 R	40
	41 W					
PHI	R	472B		45 =	46	
TAPE6#	-		EXTERNAL.	15 W	23 W	24 W
	30 W	41 W	42 W			
TYPE	R	452B	2	8 D	9 I	9 I
	15 W					
XTOY.	-		EXTERNAL.	27	40	

473B PROGRAM-UNIT LENGTH 48 SYMBOLS  
173 REFERENCES

41000B CM STORAGE USED 1.995 SECONDS

BLOCK DATA BLKDAT. 74/74 OPT=1

FTN 4.8+577

```

1      C/////BLOCK DATA SETS MANY PLOTTING PARAMETERS
      C/
      BLOCK DATA
5      C
      COMMON /LABELS/  SIZEHM,SIZELB,SIZEHD, IDEC, ICLAB, IPLT,
+      XLABEL(4), YLABEL(4), ZLABEL(4), NXCHAR, NYCHAR, NZCHAR
      COMMON /PLTPAR/  IBOX, IGRID, XMIN, XMAX, XINC, WIDTH, YMIN, YMAX, YINC,
+      HEIGHT, TIC, STIC
10     DATA          IBOX, IGRID, XMIN, XMAX, XINC, WIDTH, YMIN, YMAX, YINC
+      / "R", 4, 0., 30., 10., 7., -50., 0., 10. /
      DATA          HEIGHT, TIC, STIC / 4.5, 0.1, 0.05 /
      DATA          SIZEHM, SIZELB, SIZEHD, IDEC, ICLAB, IPLT
+      / 0.12, 0.12, 0.1, 1, 3, 10 /
      C
15     END

```

BLOCKDATA BLKDAT. 74/74 TS

--COMMON BLOCKS--

25B /LABELS/ 14B /PLTPAR/

--VARIABLE MAP--

BLKDAT.	-	0B ENTRY	3 E	
HEIGHT	R	11B /PLTPAR/	7 D	11 I
IBOX	I	0B /PLTPAR/	7 D	9 I
ICLAB	I	4B /LABELS/	5 D	12 I
IDEC	I	3B /LABELS/	5 D	12 I
IGRID	I	1B /PLTPAR/	7 D	9 I
IPLT	I	5B /LABELS/	5 D	12 I
NXCHAR	I	22B /LABELS/	5 D	
NYCHAR	I	23B /LABELS/	5 D	
NZCHAR	I	24B /LABELS/	5 D	
SIZEHD	R	2B /LABELS/	5 D	12 I
SIZELB	R	1B /LABELS/	5 D	12 I
SIZEHM	R	0B /LABELS/	5 D	12 I
STIC	R	13B /PLTPAR/	7 D	11 I
TIC	R	12B /PLTPAR/	7 D	11 I
WIDTH	R	5B /PLTPAR/	7 D	9 I
XINC	R	4B /PLTPAR/	7 D	9 I
XLABEL	R	6B /LABELS/ 4	5 D	
XMAX	R	3B /PLTPAR/	7 D	9 I
XMIN	R	2B /PLTPAR/	7 D	9 I
YINC	R	10B /PLTPAR/	7 D	9 I
YLABEL	R	12B /LABELS/ 4	5 D	
YMAX	R	7B /PLTPAR/	7 D	9 I
YMIN	R	6B /PLTPAR/	7 D	9 I
ZLABEL	R	16B /LABELS/ 4	5 D	

511B PROGRAM-UNIT LENGTH 25 SYMBOLS  
43 REFERENCES

41000B CM STORAGE USED .160 SECONDS

SUBROUTINE CINTRP 74/74 OPT=1

FTN 4.8+577

```

1      C/////CINTRP  IS A FOUR POINT BIVARIATE INTERPOLATION OF A COMPLEX
      C/    VECTOR.
      C/
5      C      SUBROUTINE CINTRP( N,P,Q,  V )
      C      COMPLEX  V(N,1),APQ(9),AP(9),AQ(9),A(9)
      C      DO 100  I=1,N
          V(I) = APQ(I)*P*Q + AP(I)*P + AQ(I)*Q + A(I)
10     100  CONTINUE
      C      RETURN
      C      ENTRY CINTRPS
      C
15     DO 200  I=1,N
          APQ(I) = V(I,1) + V(I,4) - V(I,2) - V(I,3)
          AP(I)  = V(I,2) - V(I,1)
          AQ(I)  = V(I,3) - V(I,1)
          A(I)   = V(I,1)
20     200  CONTINUE
      C      RETURN
      C      END

```

SUBROUTINE CINTRP 74/74 TS

--ENTRY POINTS--

163B CINTRP 61B CINTRPS

--STATEMENT LABELS--

.100	ID	0B	8 D	10 L
.200	ID	0B	15 D	20 L

--VARIABLE MAP--

A	Z	267B	9	6 D	9	19 =
AP	Z	201B	9	6 D	9	17 =
APQ	Z	223B	9	6 D	9	16 =
AQ	Z	245B	9	6 D	9	18 =
CINTRP	-	163B ENTRY		4 E		
CINTRPS	-	61B ENTRY		13 E		
I	I	311B		8 C	9 S	9 S
	9 S	9 S	9 S	15 C	16 S	16 S
	16 S	16 S	17 S	17 S	16 S	16 S
	18 S	19 S	19 S		18 S	18 S
N	I A	0B		4 A	6 D	8 C
	15 C					
P	R A	0B		4 A	9	9
Q	R A	0B		4 A	9	9
V	Z A	0B		4 A	6 D	9 =
	16	16	16	17	17	18
	18	19				

312B	PROGRAM-UNIT LENGTH	13 SYMBOLS
60	REFERENCES	

41000B	CM STORAGE USED	.580 SECONDS
--------	-----------------	--------------

FUNCTION DECIBEL 74/74 OPT=1

FTN 4.8+577

```

1      C/////DECIBEL CONVERTS COMPLEX VOLTS TO DB
      C
      C      FUNCTION DECIBEL( FIELD  )
5      C      COMPLEX FIELD
      C
      DECIBEL = -200.
      FMAG = ABS( REAL(FIELD) )
      IF (FMAG .LE. 1.E-20) RETURN
10     DECIBEL = 10. * ALOG10( FMAG )
      RETURN
      END

```

FUNCTION DECIBEL 74/74 TS

--EXTERNALS--

ALOG10.

--VARIABLE MAP--

ABS	R	INTRINSIC	8		
ALOG10.	R	B.E.F.	10		
DECIBEL	-	ENTRY	3	E	
FIELD	Z A	0B	3	A	5 D
FMAG	R	30B	8	=	9 F
REAL	R	INTRINSIC	8	A	10 A
VALUE.	R	27B	3		7 =
	12				10 =

31B PROGRAM-UNIT LENGTH  
14 REFERENCES

7 SYMBOLS

41000B CM STORAGE USED

.103 SECONDS

```

1      C/////DISPLAY  INTERFACES BETWEEN THE APERS FAR FIELDS AND THE PLOTTER.
C/
      SUBROUTINE DISPLAY( TH,P1,P2,P3,P4,NT,ANG,POL,IO )
C
5      COMPLEX P1(2,128),P2(2,128),P3(2,128),P4(2,128)
      COMMON /HEAD/ HEAD(8)
      COMMON /LABELS/ SIZENM,SIZELB,SIZEHD,IDEC,ICLAB,IPLT,
+      XLABEL(4),YLABEL(4),ZLABEL(4),NXCHAR,NYCHAR,NZCHAR
10     COMMON /PLTPAR/ IBOX,IGRID,XMIN,XMAX,XINC,WIDTH,YMIN,YMAX,YINC,
+      HEIGHT,TIC,STIC
      DIMENSION TH(NT),POL(2)
      COMMON / OUTSCR / IBUF(512),PTABLE(361,5)
      DATA IUNIT,NPHEAD,ICLAB,IPCOL,CLAMP,INTERP / 40,1, 1 ,3,"Y",0 /
C
15     C-----INITIALIZE PLOTTING
C
      CALL PLOTS( IBUF,512,IUNIT,40)
      IUNIT = IUNIT + 1
      CALL PLOT( 0., -10., -3 )
20     CALL PLOT( 0.5, 0.3, -3 )
      PAGE = AMAX1( 11., WIDTH+3. )
      XMAX2 = 0.
      ENCODE( 40,1006,XLABEL ) ANG
25     1006 FORMAT( "THETA ANGLE AT PHI=",F7.1," (DEG)" )
C
C-----FILL PLOTTER ARRAY WITH DATA IN DB
C
      K = 1
      100 ENCODE( 40,1100,YLABEL ) POL(K)
30     1100 FORMAT( " POWER (DB), POL.= ",A10)
      PNORM = DECIBEL( P1(1,1) )
      40 DO 50 I=1,NT
          PTABLE(I,1) = TH(I)
          PTABLE(I,2) = DECIBEL(P1(K,I)) - PNORM
35         PTABLE(I,3) = DECIBEL(P2(K,I)) - PNORM
          PTABLE(I,4) = DECIBEL(P3(K,I)) - PNORM
          PTABLE(I,5) = DECIBEL(P4(K,I)) - PNORM
      50 CONTINUE
C
40     C-----ANALYZE AND LIST PATTERNS
C
      WRITE(6,920) (HEAD(I), I=1,8)
      WRITE(6,930) ANG, PNORM
      IF (IO.GE.0) CALL PERFORM( PTABLE,NT,IPCOL )
45     WRITE(6,1900) POL(K),ANG,(I,(PTABLE(I,J),J=1,5),I=1,NT)
C
C-----PLOT THE ARRAYS
C
      900 XMAX2 = XMAX2 + PAGE + 2.
50     CALL PLOTMX( XMAX2 )
      NXCHAR = NUMCHR(XLABEL)
      NYCHAR = NUMCHR(YLABEL)
C
      IF (IBOX.EQ. "R")
55     +CALL RPLOT( PTABLE,NT,IPCOL+1,CLAMP,INTERP,HEAD,NPHEAD )
      IF (IBOX.NE. "R")
      +CALL PPLOT( PTABLE,NT,IPCOL+1,CLAMP,INTERP,HEAD,NPHEAD )
C
      IF (K.EQ. 2) GO TO 999
60     IF(POL(2).EQ. "0") GO TO 999
      K = 2
      GO TO 100
C
65     999 CALL PLOT( 0.,0.,999 )
      RETURN
      920 FORMAT(///"1 ", 8A10 // )
      930 FORMAT( " PERFORMANCE PARAMETERS OF PATTERNS AT PHI = ",F9.3,
*      " NORMALIZED TO", F9.4/)
C
70     C
C      ENTRY SETPLOT
C
      BOTH = "Y"

```

```

75      PRINT*, " DO YOU WANT BOTH ORTHOGONAL COMPONENTS (Y,N) "
      READ 1000, BOTH
      PRINT*, "      COMPONENTS TO PLOT:  UNPERTURBED CASE (1) "
      PRINT*, "                                MEAN FOR TOTAL ERROR (2) "
      PRINT*, "                                DETERMINISTIC ERROR (3) "
      PRINT*, "                                UNCORRELATED ERRORS (4) "
80      READ*, IPCOL
      C
      2000 PRINT*, " DO YOU WANT TO SPECIFY THE CALCOMP GRID (Y,N) "
      READ 1000, ANS
      IF (ANS .EQ. "Y") GO TO 2240
85      IF (IUNIT .NE. 40) RETURN
      XMIN = TH(1)
      XMAX = TH(NT)
      XINC = 0.
      RETURN
90      2240 PRINT*, " DO YOU WANT A POLAR(P) OR RECTANGULAR(R) PLOT"
      READ 1000, IBOX
      PRINT*, " GRID MIN X VALUE, MAX X VALUE, X INCREMENT, WIDTH (IN) "
      READ*, XMIN, XMAX, XINC, WIDTH
      2250 PRINT*, " GRID MIN Y VALUE, MAX Y VALUE, Y INCREMENT, HEIGHT (IN) "
95      READ*, YMIN, YMAX, YINC, HEIGHT
      IF(HEIGHT.LT.8.5) RETURN
      PRINT*, "HEIGHT IS TOO BIG FOR 11" PAPER. DO YOU WISH TO CHANGE"
      READ 1000, IRE
      IF (IRE .EQ. "Y") GO TO 2250
100      C
      RETURN
      1900 FORMAT( // A10, " POLARIZATION PATTERNS AT PHI = ", F10.3//7X,
      * "THETA UNPERTURBED ALL ERRORS DETERMINISTIC UNCORRELATED"/7
      *X, "-----" )
105      */ (I4,F8.2,4F13.3) )
      1000 FORMAT(A1)
      END

```



SUBROUTINE DISPLAY 74/74 TS

--COMMON BLOCKS--

10B /HEAD/ 25B /LABELS/ 4415B /OUTSCR/ 14B /PLTPAR/

--ENTRY POINTS--

360B DISPLAY 252B SETPLOT

--EXTERNALS--

DECIBEL ENCODI. INPCI. INPFI. INPUT# NUMCHR OUTCI. OUTCR.  
OUTFI. OUTPUT# PERFORM PLOT PLOTMX PLOTS PLOT RPLT  
TAPE6#

--STATEMENT LABELS--

.40		44B	32 L				
.50	ID	0B	32 D	38 L			
.100		31B	29 L	62			
.900		175B	49 L				
.920	F	512B	42 W	66 L			
.930	F	516B	43 W	67 L			
.999		246B	59	60	64 L		
.1000	F	555B	75 R	83 R	91 R	98 R	106 L
.1006	F	501B	23 W	24 L			
.1100	F	506B	29 W	30 L			
.1900	F	527B	45 W	102 L			
.2000		300B	82 L				
.2240		326B	84	90 L			
.2250		336B	94 L	99			

--VARIABLE MAP--

AMAX1	R		INTRINSIC		21		
ANG	R A	0B			3 A	23 W	43 W
	45 W						
ANS	R	1004B			83 R	84 F	
BOTH	R	1003B			73 =	75 R	
CLAMP	R	772B			13 I	54 A	56 A
DECIBEL	R		FUNCTION		31	34	35
	36	37					
DISPLAY	-	360B	ENTRY		3 E		
ENCODI.	-		EXTERNAL.		23 W	29 W	
HEAD	R	0B	/HEAD/	8	6 D	42 W	54 A
	56 A						
HEIGHT	R	11B	/PLTPAR/		9 D	95 R	96 F
I	I	1002B			32 C	33 S	33 S
	34 S	34 S	35 S	35 S	36 S	36 S	37 S
	37 S	42 C	42 S	45 C	45 W	45 S	
IBOX	I	0B	/PLTPAR/		9 D	54 F	56 F
	91 R						
IBUF	I	0B	/OUTSCR/	512	12 D	17 A	
ICLAB	I	4B	/LABELS/		7 D	13 I	
IDEC	I	3B	/LABELS/		7 D		
ICRID	I	1B	/PLTPAR/		9 D		
INPCI.	-		EXTERNAL.		75 R	83 R	91 R
	98 R						
INPFI.	-		EXTERNAL.		80 R	93 R	95 R
INPUT#	-		EXTERNAL.		75 R	80 R	83 R
	91 R	93 R	95 R	98 R			
INTERP	I	1000B			13 I	54 A	56 A
IO	I A	0B			3 A	44 F	
IPCOL	I	773B			13 I	44 A	54 A
	56 A	80 R					
IPLT	I	5B	/LABELS/		7 D		
IRE	I	774B			98 R	99 F	
IUNIT	I	775B			13 I	17 A	18
	18 =	85 F					

## SUBROUTINE DISPLAY 74/74 TS

J	I	770B			45 C	45 S	
K	I	771B			28 =	29 S	34 S
	35 S	36 S	37 S	45 S	59 F	61 =	
NPHEAD	I	777B			13 I	54 A	56 A
NT	I A	0B			3 A	11 D	32 C
	44 A	45 C	54 A	56 A	87 S		
NUMCHR	I	FUNCTION			51	52	
NXCHAR	I	22B /LABELS/			7 D	51 =	
NYCHAR	I	23B /LABELS/			7 D	52 =	
NZCHAR	I	24B /LABELS/			7 D		
OUTCI.	-	EXTERNAL.			42 W	43 W	45 W
OUTCR.	-	EXTERNAL.			42 W	42 W	45 W
	45 W	45 W					
OUTFI.	-	EXTERNAL.			74 W	76 W	77 W
	78 W	79 W	82 W	90 W	92 W	94 W	97 W
OUTPUT#	-	EXTERNAL.			74 W	76 W	77 W
	78 W	79 W	82 W	90 W	92 W	94 W	97 W
PAGE	R	776B			21 =	49	
PERFORM	R	SUBROUTINE			44 X		
PLOT	R	SUBROUTINE			19 X	20 X	64 X
PLOTMX	R	SUBROUTINE			50 X		
PLOTS	R	SUBROUTINE			17 X		
PNORM	R	1001B			31 =	34	35
	36	37	43 W				
POL	R A	0B	2		3 A	11 D	29 W
	45 W	60 F					
PLOT	R	SUBROUTINE			56 X		
PTABLE	R	1000B /OUTSCR/	1805		12 D	33 =	34 =
	35 =	36 =	37 =	44 A	45 W	54 A	56 A
P1	Z A	0B	256		3 A	5 D	31 A
	34 A						
P2	Z A	0B	256		3 A	5 D	35 A
P3	Z A	0B	256		3 A	5 D	36 A
P4	Z A	0B	256		3 A	5 D	37 A
RLOT	R	SUBROUTINE			54 X		
SETPLOT	-	252B ENTRY			71 E		
SIZEHD	R	2B /LABELS/			7 D		
SIZELB	R	1B /LABELS/			7 D		
SIZENM	R	0B /LABELS/			7 D		
STIC	R	13B /PLTPAR/			9 D		
TAPE6#	-	EXTERNAL.			42 W	43 W	45 W
TH	R A	0B	VAR-DIM		3 A	11 D	33
	86	87					
TIC	R	12B /PLTPAR/			9 D		
WIDTH	R	5B /PLTPAR/			9 D	21 A	93 R
XINC	R	4B /PLTPAR/			9 D	88 =	93 R
XLABEL	R	6B /LABELS/	4		7 D	23 ;	51 A
XMAX	R	3B /PLTPAR/			9 D	87 =	93 R
XMAX2	R	767B			22 =	49	49 =
	50 A						
XMIN	R	2B /PLTPAR/			9 D	86 =	93 R
YINC	R	10B /PLTPAR/			9 D	95 R	
YLABEL	R	12B /LABELS/	4		7 D	29 ;	52 A
YMAX	R	7B /PLTPAR/			9 D	95 R	
YMIN	R	6B /PLTPAR/			9 D	95 R	
ZLABEL	R	16B /LABELS/	4		7 D		

5473B PROGRAM-UNIT LENGTH  
258 REFERENCES

84 SYMBOLS

43000B CM STORAGE USED

2.827 SECONDS

```

1      C/////FT INTEGRATES OVER A PARABOLIC REFLECTOR SURFACE TO OBTAIN THE
C/      FOURIER TRANSFORM OF THE APERTURE FIELD, E. THE INTEGRAND AND
C/      EXPONANT ARE INTERPOLATED IN EACH CELL SUFFICIENT TO DEFINE THE
C/      EXPONENTIAL FACTOR AT LEAST ONCE EVERY RADIAN.
5      C/
C      SUBROUTINE FT( E,AR,AA,NR,NA,F,AKR,AKP,IO,IPOL, ET )
C
C      COMPLEX E(2,NR,NA),ET(2),SUMR(3),SUMP(3),EINT(3),CIN(2,4),CC
10     DIMENSION AA(NA),AR(NR),INCR(32),EXP1(32),DELR(32),RIN(4)
COMMON /CONST/ P1, P1BY2, P13BY2, P12, RAD, DEG, EPS, AK
DATA ACC / 1.0 /
C
AKZ2 = AK**2 - AKR**2
AKZ = 0.
15     IF (AKZ2 .GT. 0.) AKZ = SQRT( AKZ2 )
NMID = (NA+1) / 2
RFAC = .25 / F
C
C-----DETERMINE FINENESS OF INTEGRATION IN EACH RHO INTERVAL
C      AND CALCULATE THE EXPONANTS FOR THE FIRST RAY
C
FAC1 = AKR * COS( AKP-AA(1) )
FACM = AKR * COS( AKP-AA(NMID) )
FACMA = AKR * COS( AKP-AA(NMID/2) )
25     IF (ABS(FACMA) .GT. ABS(FACM)) FACM = FACMA
EXP01 = 0.
DO 50 I=1,NR
EXP0 = AR(I)*FACM + (AKZ-AK) * ( RFAC*AR(I)**2 - F )
INCR(I) = ACC * ABS(EXP0-EXP01) + 1.1
30     EXP01 = EXP0
DELR(I) = 1. / INCR(I)
EXP1(I) = AR(I) * FAC1 + (AKZ-AK) * ( RFAC*AR(I)**2 - F )
C      ZIG(I) = ( COS(AA(1))*E(1,I,1) + SIN(AA(1))*E(2,I,1) )
C      *      * AR(I) * 2. * RFAC
35     *      *
50     CONTINUE
DELR(1) = DELR(2)
C
C-----LOOP ON CELLS DEFINED BY AA AND AR
C
40     IF (IO .GE. 5) WRITE(6,1000)
ET(1) = ET(2) = (0.,0.)
C      THE INDICES I,J ARE THE UPPER CORNER OF THE CELL IN PROCESS
DO 500 J=2,NA
FACEX = AKR * COS( AKP-AA(J) )
45     EXP21 = AR(1) * FACEX + (AKZ-AK) * ( RFAC*AR(1)**2 - F )
DO 400 I=2,NR
EXP22 = AR(I) * FACEX + (AKZ-AK) * ( RFAC*AR(I)**2 - F )
C-----CALCULATE THE COEFFICIENTS OF THE BILINEAR SURFACE
DO 110 K=1,2
50     CIN(K,1) = E(K,I-1,J-1)
CIN(K,2) = E(K,I,J-1)
CIN(K,3) = E(K,I-1,J)
CIN(K,4) = E(K,I,J)
110    CONTINUE
55     CALL CINTRPS( 2,Z,Z,CIN )
RIN(1) = EXP1(I-1)
RIN(2) = EXP1(I)
RIN(3) = EXP21
RIN(4) = EXP22
60     CALL INTRPS( 1,Z,Z,RIN )
C-----INTEGRATE ONE CELL
IR = INCR(I)
IF (I .EQ. NR) IR = IR + 1
C      DR, DP ARE NOT IN INCHES OR RAD, BUT RATHER INTERVALS.
65     C      E.G. FRACTIONS OF AR(I)-AR(I-1)
DR = DELR(I)
IP = ACC * ABS( EXP1(I) - EXP22 ) + 2.1
C      " INTERP" ASSUMES BOTH INTERVALS = 1.
DP = 1. / (IP-1)
70     SUMR(1) = SUMR(2) = ( 0.,0. )
RHO1 = AR(I-1)
DO 300 II=1,IR
R = (II-1) * DR

```

```

75      RHO = RHO1 + R * (AR(I)-RHO1)
      W1 = DR
      IF (II.EQ.1) W1 = .5 * (DR+DELR(I-1))
C***** THIS ONLY WORKS CORRECTLY IF UNIFORM RADIAL SPACING
      IF (II.EQ.IR .AND. I.EQ.NR) W1 = .5 * DR
      SUMP(1) = SUMP(2) = (0.,0.)
80      DO 200 JJ=1,IP
          P = (JJ-1) * DP
          CALL CINTRP( 2,R,P, EINT )
          CALL INTRP( 1,R,P, EXPO )
          WT = W1
85      IF (JJ.EQ.1 .OR. JJ.EQ.IP) WT = .5 * W1
          CC = CMPLX( COS(EXPO)*WT, SIN(EXPO)*WT )
          CALL MSUM( SUMP,EINT,CC,2,1, SUMP )
          200 CONTINUE
          CC = RHO
90      CALL MSUM( SUMR,SUMP,CC,2,1, SUMR )
          300 CONTINUE
C      CC = DP * (AR(I)-AR(I-1)) * (AA(J)-AA(J-1))
      THIS COULD BE SIMPLIFIED IF INTERP UPGRADED TO INC.NE.1.
      CALL MSUM( ET,SUMR,CC,2,1, ET )
95      IF (IO.GE.5) WRITE(6,2000) I,J,AR(I),AA(J),IR,IP,SUMR(1),ET(1)
C      IF (IO.GE.5 .AND. IPOL.NE.0) WRITE(6,3000) SUMR(2),ET(2)
      EXP1(I-1) = EXP21
      EXP21 = EXP22
      400 CONTINUE
100     EXP1(NR) = EXP22
      500 CONTINUE
C
      RETURN
105     1000 FORMAT(// " POINT NOS. COORDINATES DIVISIONS CONTRIBUTION",
      * " ACCUMULATION (CROSS POL.) ")
      2000 FORMAT( 2I5,2X,2F7.3,2X,2I4,2(2F9.4,2X) )
      3000 FORMAT( "+",80X, 2(2F9.4,2X) )
      END

```

SUBROUTINE FT 74/74 TS

--COMMON BLOCKS--

10B /CONST/

--EXTERNALS--

CINTRP	CINTRPS	COS.	INTRP	INTRPS	MSUM	OUTCI.	SIN.
SQRT.	TAPE6#						

--STATEMENT LABELS--

.50	ID	0B	27 D	35 L
.110	ID	0B	49 D	54 L
.200	ID	0B	80 D	88 L
.300	ID	0B	72 D	91 L
.400	ID	0B	46 D	99 L
.500	ID	0B	43 D	101 L
.1000	F	531B	40 W	104 L
.2000	F	545B	95 W	106 L
.3000	F	552B	107 L	

--VARIABLE MAP--

AA	R A	0B	VAR-DIM	6 A	9 D	22 A
ABS	23 A	24 A	44 A 92	92	95 W	
	R	INTRINSIC		25 F	25 F	29
ACC	67					
AK	R	1073B		11 I	29	67
AKP	R	7B /CONST/		10 D	13	28
AKR	32	45	47			
AKZ	R A	0B		6 A	22 A	23 A
AKZ2	24 A	44 A				
AR	R A	0B		6 A	13	22
	23	24	44			
CC	R	1010B		14 =	15 =	28
	32	45	47			
AKZ2	R	1074B		13 =	15 F	15 A
AR	R A	0B	VAR-DIM	6 A	9 D	28
	28	32	45	45	47	47
	71	74	92	95 W		
CC	Z	1071B		8 D	86 =	87 A
	89 =	90 A	92 = 94 A			
CIN	Z	1051B	8	8 D	50 =	51 =
	52 =	53 = 55 A				
CINTRP	R	SUBROUTINE		82 X		
CINTRPS	R	SUBROUTINE		55 X		
CMPLX	Z	INTRINSIC		86		
COS.	R	B.E.F.		22	23	24
	44	86 A				
DEC	R	5B /CONST/		10 D		
DELR	R	1011B	32	9 D	31 =	36
	36 =	66	76			
DP	R	717B		69 =	81	92
DR	R	1001B		66 =	73	75
	76	78				
E	Z A	0B	VAR-DIM	6 A	8 D	50
	51	52	53			
EINT	Z	651B	3	8 D	82 A	87 A
EPS	R	6B /CONST/		10 D		
ET	Z A	0B	2	6 A	8 D	41 =
	41 =	94 A	94 A 95 W			
EXP0	R	1102B		28 =	29 A	30
	83 A	86 A	86 A			
EXP01	R	1002B		26 =	29 A	30 =
EXP1	R	657B	32	9 D	32 =	56
	57	67 A	97 = 100 =			
EXP21	R	720B		45 =	58	97
	98 =					
EXP22	R	1104B		47 =	59	67 A

## SUBROUTINE FI

69/64 15

F	98	100				6 A	17	28
	R A	0B						
FACEX	32	45	47			44 =	45	47
FACM	R	1000B				23 =	25 A	25 =
	28							
FACMA	R	1100B				24 =	25 A	25
FAC1	R	721B				22 =	32	
FT	-	513B ENTRY				6 E		
I	I	1101B				27 C	28 S	28 S
	29 S	31 S	31 S	32 S		32 S	32 S	46 C
	47 S	47 S	50 S	51 S		52 S	53 S	56 S
	57 S	62 S	63 F	66 S		67 S	71 S	74 S
	76 S	78 F	92 S	92 S		95 W	93 S	97 S
II	I	1110B				72 C	73	76 F
INCR	78 F							
	I	723B	32			9 D	29 =	31
	62							
INTRP	I		SUBROUTINE			83 X		
INTRPS	I		SUBROUTINE			60 X		
IO	I A	0B				6 A	40 F	95 F
IP	I	1106B				67 =	69	80 C
	85 F	95 W						
IPOL	I A	0B				6 A		
IR	I	1105B				62 =	63	63 =
	72 C	78 F	95 W					
J	I	1103B				43 C	44 S	50 S
	51 S	52 S	53 S	92 S		92 S	95 W	95 S
JJ	I	1113B				80 C	81	85 F
	85 F							
K	I	722B				49 C	50 S	50 S
	51 S	51 S	52 S	52 S		53 S	53 S	
MSUM	I		SUBROUTINE			87 X	90 X	94 X
NA	I A	0B				6 A	8 D	9 D
	16	43 C						
NMID	I	1075B				16 =	23 S	24 S
NR	I A	0B				6 A	8 D	9 D
	27 C	46 C	63 F	78 F		100 S		
OUTCI.	-		EXTERNAL.			40 W	95 W	
P	R	1114B				81 =	82 A	83 A
PI	R	0B /CONST/				10 D		
PIBY2	R	1B /CONST/				10 D		
PI2	R	3B /CONST/				10 D		
PI3BY2	R	2B /CONST/				10 D		
R	R	777B				73 =	74	82 A
	83 A							
RAD	R	4B /CONST/				10 D		
RFAC	R	1076B				17 =	28	32
	45	47						
RHO	R	1111B				74 =	89	
RHO1	R	1107B				71 =	74	74
RIN	R	1004B				9 D	56 =	57 =
	58 =	59 =	60 A	4				
SIN.	R		B.E.F.			86 A		
SQRT.	R		B.E.F.			15		
SUMP	Z	763B		3		8 D	79 =	79 =
	87 A	87 A	90 A					
SUMR	Z	771B		3		8 D	70 =	70 =
	90 A	90 A	94 A	95 W				
TAPE6*	-		EXTERNAL.			40 W	95 W	
WT	R	1115B				84 =	85 =	86 A
	86 A							
W1	R	1112B				75 =	76 =	78 =
	84	85						
Z	R	1003B				55 A	55 A	60 A
	60 A							

1126B PROGRAM-UNIT LENGTH  
329 REFERENCES

79 SYMBOLS

41000B CM STORAGE USED

3.998. SECONDS

SUBROUTINE GPERT

74/74 OPT=1

FTN 4.8+577

```

1      C/////GPERT CALCULATES THE TRANSFORM OF THE PETURBATION DYADIC OF A
      C/      RANDOMLY POSITIONED DEFECT.
      C/      G IS THE FOURIER TRANSFORM OF A POINT SOURCE.
      C*****CHECK ITS RELATION TO THE PHYSICAL OPTICS FIELD.
5      C/
      SUBROUTINE GPERT( AKR,AKP,  GT )
      C
      COMPLEX GT(2,2),GMAX
      COMMON /GPERTC/  C1,C2
10     COMMON /CONST/ PI, PIBY2, PI3BY2, PI2, RAD, DEG, EPS, AK
      C
      GT(1,2) = GT(2,1) = (0.,0.)
      GT(1,1) = C1 * GMAX
      GT(2,2) = GT(1,1)
15     C      TO COMPARE WITH FFTMC, NEEDS FACTOR OF LAMDA
      C*****PUT IN COS**N FEATURE
      RETURN
      C
      ENTRY GINIT
20     GMAX = GT(1,1)
      WAVE = AKR
      C1 = WAVE
      EXPON = AKP
      EXPON = 0.
25     WRITE(6,900) GMAX,EXPON
      RETURN
      C
900    FORMAT (// " POINT SOURCE DEFECTS WITH RADIATION PEAK", 2F8.4,
30      +      " AND SHAPE, COS**", F3.1 / )
      END

```

SUBROUTINE GPERT 74/74 TS

--COMMON BLOCKS--

10B /CONST/ 2B /GPERTC/

--ENTRY POINTS--

27B GINIT 56B GPERT

--EXTERNALS--

OUTCI. TAPE6\*

--STATEMENT LABELS--

.900 F 64B 25 W 28 L

--VARIABLE MAP--

AK	R	7B /CONST/	10 D		
AKP	R A	0B	6 A	23	
AKR	R A	0B	6 A	21	
C1	R	0B /GPERTC/	9 D	13	22 =
C2	R	1B /GPERTC/	9 D		
DEG	R	5B /CONST/	10 D		
EPS	R	6B /CONST/	10 D		
EXPON	R	106B	23 =	24 =	25 W
GINIT	-	27B ENTRY	19 E		
GMAX	Z	104B	8 D	13	20 =
	25 W				
GPERT	-	56B ENTRY	6 E		
GT	Z A	0B	6 A	8 D	12 =
	12 =	13 =	14	4	14 =
OUTCI.	-	EXTERNAL.	20		
PI	R	0B /CONST/	25 W		
PIBY2	R	1B /CONST/	10 D		
PI2	R	3B /CONST/	10 D		
PI3BY2	R	2B /CONST/	10 D		
RAD	R	4B /CONST/	10 D		
TAPE6*	-	EXTERNAL.	25 W		
WAVE	R	103B	21 =	22	

121B PROGRAM-UNIT LENGTH 21 SYMBOLS  
39 REFERENCES

41000B CM STORAGE USED .254 SECONDS



```

1      C/////GPERT CALCULATES THE TRANSFORM OF THE PETURBATION DYADIC OF A
C/      RANDOMLY POSITIONED DEFECT.
C/      G IS THE FOURIER TRANSFORM OF  $\exp(j \cdot P(R)) - 1$ 
C*****CHECK ITS RELATION TO THE PHYSICAL OPTICS FIELDS.
5      C/      WHERE  $P(R) = GMAX * \exp(-(ABS(R)/PERRAD)**2)$ 
C/      ( GAUSSIAN PHASE BUMPS )
C/
C      SUBROUTINE GPERT( AKR,AKP,  GT )
C
10     COMPLEX GT(2,2),GMAX,SUM,CFAC,TERM
COMMON /GPERTC/  C1,C2
COMMON /CONST/  PI, PIBY2, PI3BY2, PI2, RAD, DEG, EPS, AK
C
GT(1,2) = GT(2,1) = (0.,0.)
15     ARG = C2 * AKR**2
SUM = GMAX * EXP( ARG )
CFAC = GMAX
DO 20  N=2,100
ENI = 1. / N
20     CFAC = CFAC * GMAX * ENI
TERM = CFAC * ENI * EXP( ARG*ENI )
SUM = SUM + TERM
IF (ABS(REAL(TERM)/REAL(SUM)) + ABS(AIMAG(TERM)/AIMAG(SUM))
+
.LT. .001) GO TO 30
25     20 CONTINUE
WRITE(6,920) ARG
920  FORMAT( " WARNING---GT DID NOT CONVERGE FOR (CK/2)**2 =",F8.3 )
C
30     GT(1,1) = C1 * SUM
GT(2,2) = GT(1,1)
RETURN
C
ENTRY GINIT
GMAX = GT(1)
35     WAVE = AKR
PERRAD = AKP
WRITE(6,900) GMAX,PERRAD
IF (REAL(GMAX) .NE. 0.) GO TO 40
C2 = -( PERRAD*PI/WAVE )**2
40     C THIS FACTOR INCLUDES A K0 SCALE FOR X AND Y
C1 = PI * PERRAD**2
RETURN
C
45     40 PRINT*, " *** STOP ***          GMAX MUST BE IMAGINARY"
STOP
900  FORMAT (// " GAUSSIAN PHASE BUMPS OF HEIGHT ",2F8.4," AND RADIUS ",
+
F8.4//)
END

```

SUBROUTINE GPERT 74/74 TS

--COMMON BLOCKS--

10B /CONST/ 2B /GPERTC/

--ENTRY POINTS--

115B GINIT 160B GPERT

--EXTERNALS--

EXP. OUTCI. OUTFI. OUTPUT\* STOP. TAPE6\*

--STATEMENT LABELS--

.20	D	74B	18 D	25 L
.30		101B	23	29 L
.40		152B	38	44 L
.900	F	204B	37 W	46 L
.920	F	175B	26 W	27 L

--VARIABLE MAP--

ABS	R	INTRINSIC	23 F	23 F	
AIMAG	R	INTRINSIC	23 A	23 A	
AK	R	7B /CONST/	12 D		
AKP	R A	0B	8 A	36	
AKR	R A	0B	8 A	15	35
ARG	R	237B	15 =	16 A	21 A
	26 W				
CFAC	Z	241B	10 D	17 =	20
	20 =	21			
C1	R	0B /GPERTC/	11 D	29	41 =
C2	R	1B /GPERTC/	11 D	15	39 =
DEC	R	5B /CONST/	12 D		
ENI	R	247B	19 =	20	21
	21 A				
EPS	R	6B /CONST/	12 D		
EXP.	R	B. E. F.	16	21	
GINIT	-	115B ENTRY	33 E		
GMAX	Z	245B	10 D	16	17
	20	34 =			
GPERT	-	160B ENTRY	8 E		
GT	Z A	0B	8 A	10 D	14 =
	14 =	29 =	30	30 =	
N	I	236B	34		
OUTCI.	-	EXTERNAL.	18 C	19	
OUTFI.	-	EXTERNAL.	26 W	37 W	
OUTPUT*	-	EXTERNAL.	44 W		
PERRAD	R	240B	44 W		
	41		36 =	37 W	39
PI	R	0B /CONST/	12 D	39	41
PIBY2	R	1B /CONST/	12 D		
PI2	R	3B /CONST/	12 D		
PI3BY2	R	2B /CONST/	12 D		
RAD	R	4B /CONST/	12 D		
REAL	R	INTRINSIC	23 A	23 A	38 F
STOP.	-	EXTERNAL.	45		
SUM	Z	243B	10 D	16 =	22
	22 =	23 A			
TAPE6*	-	EXTERNAL.	26 W	37 W	
TERM	Z	234B	10 D	21 =	22
	23 A	23 A			
WAVE	R	233B	35 =	39	

262B PROGRAM-UNIT LENGTH 38 SYMBOLS  
97 REFERENCES

41000B CM STORAGE USED .655 SECONDS

```

1      C/////HFTHFT CALCULATES THE DOUBLE FOURIER TRANSFORM OF THE APERTURE
C/      FIELD CORRELATION DYADIC. SEE T.M. OF 27 JAN. BY VIC TRIPP
C/      ON PROJ. A-3449
C/
5      SUBROUTINE HFTHFT( E,P,L,M,AR,AA,NR,NA,AKR,AKP,IO,IPOL, HTT )
C
C*****THE PRESENT ALGORITHM DOES NOT SUBDIVIDE TO LIMIT THE
C      CHANGE OF THE EXPONANT.
10     COMPLEX E(2,NR,NA),HTT(2,2),DYAD(2,2),SUMR(2,2),PDREX,DAC
      DIMENSION AR(NR),AA(NA),P(NR,NA)
      COMMON /CONST/ PI,PIBY2,PI3BY2,PI2,RAD,DEG,EPS,AK
C
C*****CALCULATIONS CAN BE REDUCED BY USING HERMITIAN PROPERTY OF HTT
      DANG = AA(NA) * .5 * (L-M)
15     CANG = DANG + PIBY2 - AKP
      DMAG = 2. * AKR * SIN( DANG )
      TEST1 = AR(NR) * DMAG * COS( CANG )
      HTT(1) = HTT(2) = HTT(3) = HTT(4) = (0.,0.)
      DO 200 J=1,NA
20     RUDOTK = DMAG * COS( AA(J)+CANG )
      TEST = AR(NR) * RUDOTK
      DEL = ABS( TEST-TEST1 )
      IF (DEL .GT. PIBY2 .AND. IO.GE.1) WRITE(6,1100) DEL,M,L,J
      TEST1 = TEST
25     JL = (L-1) * NA + J
      JM = (M-1) * NA + J
      ARG1 = -AR(1) * RUDOTK
      SUMR(1) = SUMR(2) = SUMR(3) = SUMR(4) = (0.,0.)
      DO 100 I=2,NR
30     ARG = -AR(I) * RUDOTK
      DEL = ABS( ARG-ARG1 )
      IF (DEL .GT. PIBY2 .AND. IO.GE.1) WRITE(6,1200) DEL,M,L,J,I
      ARG1 = ARG
      CALL MPRODT( E(1,1,JL),E(1,1,JM),2,1,2, DYAD )
35     PDR = P(1,J) * (AR(MIN0(NR,I+1))- AR(I-1)) * .5 * AR(I)
      PDREX = PDR * CMPLX( COS(ARG), SIN(ARG) )
      CALL MSUM( SUMR,DYAD,PDREX,2,2, SUMR )
      IF (IO .GE. 6) WRITE(6,1000) I,J,ARG,SUMR(1)
40     100 CONTINUE
      DA = (AA(MIN0(NA,J+1)) - AA(MAX0(1,J-1))) * .5
      DAC = CMPLX(DA,0.)
      CALL MSUM( HTT,SUMR,DAC,2,2, HTT )
      IF (IO .GE. 5) WRITE(6,1000) L,M,AKR,HTT
45     200 CONTINUE
C
      RETURN
1000 FORMAT( 2I5,2X,F10.4,2X,4(2F9.4,2X) )
1100 FORMAT( " EXPONANT CHANGE (AZ) =",F8.4," FOR M,L,J =",3I5 )
1200 FORMAT( " EXPONANT CHANGE(RAD) =",F8.4," FOR M,L,J,I =",4I5 )
50     END

```

## SUBROUTINE HFTHFT 74/74 TS

--COMMON BLOCKS--

10B /CONST/

--EXTERNALS--

COS. MPRODT MSUM OUTCI. SIN. TAPE6\*

--STATEMENT LABELS--

.100	ID	0B	29 D	39 L	
.200	ID	0B	19 D	44 L	
.1000	F	302B	38 W	43 W	47 L
.1100	F	306B	23 W	48 L	
.1200	F	315B	32 W	49 L	

--VARIABLE MAP--

AA	R A	0B	VAR-DIM	5 A	10 D	14
ABS	20 A	40				
AK	R	40	INTRINSIC	22	31	
AKP	R A	7B	/CONST/	11 D		
AKR	R A	0B		5 A	15	
AR	R A	0B		5 A	16	43 W
		0B	VAR-DIM	5 A	10 D	17
ARC	21	27	30	35	35	
	R	453B	35	30 =	31 A	33
ARG1	36 A	36 A	38 W			
ARG1	R	416B		27 =	31 A	33 =
CANG	R	442B		15 =	17 A	20 A
CMPLX	Z		INTRINSIC	36	41	
COS.	R		B.E.F.	17	20	36 A
DA	R	455B		40 =	41 A	
DAC	Z	446B		9 D	41 =	42 A
DANG	R	443B		14 =	15	16 A
DEC	R	5B	/CONST/	11 D		
DEL	R	415B		22 =	23 F	23 W
	31 =	32 F	32 W			
DMAC	R	441B		16 =	17	20
DYAD	Z	427B	4	9 D	34 A	37 A
E	Z A	0B	VAR-DIM	5 A	9 D	34 A
	34 A					
EPS	R	6B	/CONST/	11 D		
HFTHFT	-	270B	ENTRY	5 E		
HTT	Z A	0B	4	5 A	9 D	18 =
	18 =	18 =	18 =	42 A	43 W	
I	I	452B		29 C	30 S	32 W
	34 S	34 S	35 S	35 A	35 S	38 W
IO	I A	0B		5 A	23 F	32 F
	38 F	43 F				
IPOL	I A	0B		5 A		
J	I	413B		19 C	20 S	23 W
	25	26	32 W	38 W	40 A	40 A
JL	I	450B		25 =	34 S	
JM	I	451B		26 =	34 S	
L	I A	0B		5 A	14	23 W
	25	32 W	43 W			
M	I A	0B		5 A	14	23 W
	26	32 W	43 W			
MAX0	I		INTRINSIC	40 S		
MIN0	I		INTRINSIC	35 S	40 S	
MPRODT	I		SUBROUTINE	34 X		
MSUM	I		SUBROUTINE	37 X	42 X	
NA	I A	0B		5 A	9 D	10 D
	10 D	14 S	19 C	25	40 A	
NR	I A	0B		5 A	9 D	10 D
	10 D	17 S	21 S	35 A		
OUTCI.	-		EXTERNAL.	23 W	32 W	38 W
	43 W					

SUBROUTINE HFTHFT 74/74 TS

P	R A	0B	VAR-DIM	5 A	10 D	35
PDR	R	454B		35 =	36	
PDREX	Z	444B		9 D	36 =	37 A
PI	R	0B /CONST/		11 D		
PIBY2	R	1B /CONST/		11 D	15	23 F
	32 F					
PI2	R	3B /CONST/		11 D		
PI3BY2	R	2B /CONST/		11 D		
RAD	R	4B /CONST/		11 D		
RUDOTK	R	414B		20 =	21	27
	30					
SIN.	R	B.E.F.		16	36 A	
SUMR	Z	417B	4	9 D	28 =	28 =
	28 =	28 =	37 A	37 A	42 A	
TAPE6#	-	EXTERNAL.		38 W	32 W	38 W
	43 W					
TEST	R	437B		21 =	22 A	24
TEST1	R	440B		17 =	22 A	24 =

466B PROGRAM-UNIT LENGTH 56 SYMBOLS  
197 REFERENCES

41000B CM STORAGE USED 1.977 SECONDS

SUBROUTINE INTRP

74/74 OPT=1

FTN 4.8+577

```

1      C/////INTRP  IS A FOUR POINT BIVARIATE INTERPOLATION OF A VECTOR
      C/
      SUBROUTINE INTRP( N,P,Q, V )
      C
      DIMENSION V(N,1),APQ(9),AP(9),AQ(9),A(9)
      C
      DO 100 I=1,N
      V(I) = APQ(I)*P*Q + AP(I)*P + AQ(I)*Q + A(I)
      C
      100 CONTINUE
      RETURN
      C
      ENTRY INTRPS
      C
      DO 200 I=1,N
      APQ(I) = V(I,1) + V(I,4) - V(I,2) - V(I,3)
      AP(I) = V(I,2) - V(I,1)
      AQ(I) = V(I,3) - V(I,1)
      A(I) = V(I,1)
      C
      200 CONTINUE
      RETURN
      END

```

SUBROUTINE INTRP 74/74 TS

--ENTRY POINTS--

102B INTRP 25B INTRPS

--STATEMENT LABELS--

```

.100 ID      0B      7 D      9 L
.200 ID      0B     14 D     19 L

```

--VARIABLE MAP--

A	R	143B	9	5 D	8	18 =
AP	R	110B	9	5 D	8	16 =
APQ	R	121B	9	5 D	8	15 =
AQ	R	132B	9	5 D	8	17 =
I	I	154B		7 C	8 S	8 S
	8 S	8 S	8 S	14 C	15 S	15 S
	15 S	15 S	16 S	16 S	16 S	17 S
	17 S	18 S	18 S			
INTRP	-	102B ENTRY		3 E		
INTRPS	-	25B ENTRY		12 E		
N	I A	0B		3 A	5 D	7 C
	14 C					
P	R A	0B		3 A	8	8
Q	R A	0B		3 A	8	8
V	R A	0B		3 A	5 D	8 =
	15	15	15	16	16	17
	17	18				

135B PROGRAM-UNIT LENGTH  
60 REFERENCES

13 SYMBOLS

41000B CM STORAGE USED

.394 SECONDS

SUBROUTINE MPROD

74/74 OPT=1

FTN 4.8+577

```

1      C/////MPROD PERFORMS CAYLEY MULTIPLICATION OF ANY TWO COMPATABLE
      C/    COMPLEX MATRICES
      C/
5      SUBROUTINE MPROD( A,B,LL,MM,NN, R )
      COMPLEX A(LL,MM),B(MM,NN),R(LL,NN),V(9,9)
      C
      DO 10 L=1,LL
        DO 10 N=1,NN
          V(L,N) = (0.,0.)
10      DO 10 M=1,MM
          V(L,N) = V(L,N) + A(L,M)*B(M,N)
        10 CONTINUE
      DO 20 L=1,LL
        DO 20 N=1,NN
15      R(L,N) = V(L,N)
        20 CONTINUE
      C
      RETURN
      END

```

SUBROUTINE MPROD 74/74 TS

--STATEMENT LABELS--

.10	ID	0B	7 D	8 D	10 D	12 L
.20	ID	0B	13 D	14 D	16 L	

--VARIABLE MAP--

A	Z A	0B	VAR-DIM	4 A	3 D	11
B	Z A	0B	VAR-DIM	4 A	3 D	11
L	I	372B		7 C	9 S	11 S
	11 S	11 S	13 C	15 S		
LL	I A	0B		4 A	5 D	5 D
	7 C	13 C				
M	I	126B		10 C	11 S	11 S
MM	I A	0B		4 A	5 D	5 D
	10 C					
MPROD	-	110B ENTRY		4 E		
N	I	127B		8 C	9 S	11 S
	11 S	11 S	14 C	15 S	15 S	
NN	I A	0B		4 A	5 D	5 D
	8 C	14 C				
R	Z A	0B	VAR-DIM	4 A	5 D	15 =
V	Z	130B	B1	5 D	9 =	11
	11 =	15				

373B PROGRAM-UNIT LENGTH  
55 REFERENCES

13 SYMBOLS

41000B CM STORAGE USED

.366 SECONDS

SUBROUTINE MPRODT

74/74 OPT=1

FTN 4.8+577

```

1      C/////MPRODT PERFORMS CAYLEY MULTIPLICATION OF ANY TWO COMPATABLE
      C/ COMPLEX MATRICES AFTER TRANJUGATING THE SECOND.
      C/
5      SUBROUTINE MPRODT( A,B,LL,MM,NN, R )
      COMPLEX A(LL,MM),B(NN,MM),R(LL,NN),V(9,9)
      C
      DO 10 L=1,LL
        DO 10 N=1,NN
          V(L,N) = (0.,0.)
10     DO 10 M=1,MM
          V(L,N) = V(L,N) + A(L,M)*CONJG(B(N,M))
      10 CONTINUE
      DO 20 L=1,LL
        DO 20 N=1,NN
15     R(L,N) = V(L,N)
      20 CONTINUE
      C
      RETURN
      END

```

SUBROUTINE MPRODT 74/74 TS

--STATEMENT LABELS--

.10	ID	0B	7 D	8 D	10 D	12 L
.20	ID	0B	13 D	14 D	16 L	

--VARIABLE MAP--

A	Z A	0B	VAR-DIM	4 A	5 D	11
B	Z A	0B	VAR-DIM	4 A	5 D	11 A
CONJG	Z		INTRINSIC	11		
L	I	367B		7 C	9 S	11 S
LL	11 S	11 S	13 C	15 S		
LL	I A	0B		4 A	5 D	5 D
	7 C	13 C				
M	I	123B		10 C	11 S	11 S
MM	I A	0B		4 A	5 D	5 D
	10 C					
MPRODT	-	105B ENTRY		4 E		
N	I	124B		8 C	9 S	11 S
	11 S	11 S	14 C	15 S		
NN	I A	0B		4 A	5 D	5 D
	8 C	14 C				
R	Z A	0B	VAR-DIM	4 A	5 D	15 =
V	Z	125B	81	5 D	9 =	11
	11 =	15				

370B PROGRAM-UNIT LENGTH  
56 REFERENCES

14 SYMBOLS

41000B CM STORAGE USED

.373 SECONDS



SUBROUTINE MSUM

74/74 OPT=1

FTN 4.8+577

```

1      C/////MSUM  ADDS ANY TWO COMPATABLE COMPLEX MATRICES AFTER
      C/      MULTIPLYING THE SECOND BY A COMPLEX CONSTANT.
      C/
5      SUBROUTINE MSUM( A,B,CON,MM,NN,  R )
      C      COMPLEX  A(MM,NN),B(MM,NN),R(MM,NN),CON
      C
      DO 10  M=1,MM
        DO 10  N=1,NN
          R(M,N) = A(M,N) + CON*B(M,N)
10     10    CONTINUE
      C
      RETURN
      END

```

SUBROUTINE MSUM

74/74 TS

--STATEMENT LABELS--

.10	ID	0B	7 D	8 D	10 L
-----	----	----	-----	-----	------

--VARIABLE MAP--

A	Z A	0B	VAR-DIM	4 A	5 D	9
B	Z A	0B	VAR-DIM	4 A	5 D	9
CON	Z A	0B		4 A	5 D	9
M	I	66B		7 C	9 S	9 S
	9 S					
MM	I A	0B		4 A	5 D	5 D
	5 D	7 C				
MSUM	-	56B ENTRY		4 E		
N	I	67B		8 C	9 S	9 S
	9 S					
NN	I A	0B		4 A	5 D	5 D
	5 D	8 C				
R	Z A	0B	VAR-DIM	4 A	5 D	9 =

70B PROGRAM-UNIT LENGTH  
34 REFERENCES

10 SYMBOLS

41000B CM STORAGE USED

.204 SECONDS

SUBROUTINE MSUMT

74/74 OPT=1

FTN 4.8+577

```

1      C/////MSUMT ADDS ANY TWO COMPATABLE COMPLEX MATRICES AFTER
      C/ MULTIPLYING THE SECOND BY A COMPLEX CONSTANT AND
      C/ TRANJUGATING IT.
5      SUBROUTINE MSUMT( A,B,CON,MM,NN, R )
      C/ COMPLEX A(MM,NN),B(NN,MM),R(MM,NN),CON,V(9,9)
      C
      DO 10 M=1,MM
        DO 10 N=1,NN
          V(M,N) = A(M,N) + CON*CONJG(B(N,M))
10      CONTINUE
        DO 20 M=1,MM
          DO 20 N=1,NN
            R(M,N) = V(M,N)
15      CONTINUE
      C
      RETURN
      END

```

SUBROUTINE MSUMT 74/74 TS

--STATEMENT LABELS--

.10	ID	0B	8 D	9 D	11 L
.20	ID	0B	12 D	13 D	15 L

--VARIABLE MAP--

A	Z A	0B	VAR-DIM	5 A	6 D	10
B	Z A	0B	VAR-DIM	5 A	6 D	10 A
CON	Z A	0B		5 A	6 D	10
CONJG	Z		INTRINSIC	10		
M	I	102B		8 C	10 S	10 S
	10 S	12 C	14 S	14 S		
MM	I A	0B		5 A	6 D	6 D
	6 D	8 C	12 C			
MSUMT	-	70B ENTRY		5 E		
N	I	103B		9 C	10 S	10 S
	10 S	13 C	14 S	14 S		
NN	I A	0B		5 A	6 D	6 D
	6 D	9 C	13 C			
R	Z A	0B	VAR-DIM	5 A	6 D	14 =
V	Z	104B	81	6 D	10 =	14

346B PROGRAM-UNIT LENGTH  
49 REFERENCES

13 SYMBOLS

41000B CM STORAGE USED

.308 SECONDS

```

1      C/////OUTDAT PLOTS DESIRED 3-D FIGURES AND CUTS FOR THE APERTURE
C/      AND ALSO LISTS THE FIELDS FOR THE CUTS.
C/
5      C      SUBROUTINE OUTDAT( DATA, IPOL, NX, NY1, NARR, X, Y, IOBUG )
C
      COMPLEX DATA(2, NX, NY1)
      DIMENSION X(NX), Y(NY1), POL(3), PLABEL(4)
      COMMON /CUT/ IPIC, ICUT, JCUT, INC, JNC, M0, N0, IBORDER, IGRID
10     COMMON /OUTSCR/ PHOTO(2000), BUFF(512), AMP(128), PHS(128), HID(512)
      + EL(128), AZ(128)
      COMMON /HEAD/ HEAD(8)
      COMMON /PLT3D/ ANGLE, JX, JY, HFACTOR, VFACTOR,
C      * XMIN, XMAX, YMIN, YMAX, WIDTH, HEIGHT
C      THESE LIMITS ARE APERTURE RHO AND PHI, NOT THETA AND POWER
15     COMMON /LABELS/ SIZENM, SIZELB, SIZEHD, IDEC, ICLAB, IPLT,
      + XLABEL(4), YLABEL(4), ZLABEL(4), NXCHAR, NYCHAR, NZCHAR
      COMMON /CONST/ PI, PIBY2, PI3BY2, PI2, RAD, DEG, EPS, AK
      DATA NF, M0, N0, IPIC, ICUT, JCUT, INC, JNC, IBORDER, IGRID
20     * / 1, 1, 1, 2, 1, 0, 1, 5, 0, 4 /
      DATA DBMIN, DBMAX, DBINC, PHMIN, PHMAX, PHINC, SLOPE, WIDTH, HEIGHT
      * / -40., 0., 10., -180., 180., 90., 30., 7., 4.5 /
      DATA POL(1), POL(2), POL(3) / ", POL.=X", " ", POL.=Y", " " /
C
      PHASE(IP, I, J) = DEG*ATAN2(AIMAG(DATA(IP, I, J)), REAL(DATA(IP, I, J)))
25     POWER(IP, I, J) = REAL(DATA(IP, I, J))**2+AIMAG(DATA(IP, I, J))**2
C
      IP = MAX0(1, IPOL)
      IQ = IPOL
      IF (IQ .EQ. 0) IQ = 3
30     ENCODE( 40, 1100, XLABEL )
1100    FORMAT( "RADIUS (IN.)" )
      NXCHAR = NUMCHR( XLABEL )
      ENCODE( 40, 1200, YLABEL )
35     1200    FORMAT( "APERTURE AZIMUTH (RADIAN)" )
      NYCHAR = NUMCHR( YLABEL )
      ENCODE( 40, 1300, PLABEL ) POL(IQ)
40     1300    FORMAT( "POWER (DB) ", A10 )
      NPCHAR = NUMCHR( PLABEL )
45     1400    FORMAT( "PHASE (DEG) ", A10 )
      XMIN = X(1)
      XMAX = X(NX)
      YMIN = Y(1)
      NY = MIN0( NY1*NARR, 2000/NX )
      YMAX = Y(NY)
      PNORM = 10. * ALOG10( POWER(IP, 1, 1) )
C
C-----MAKE 3-D PLOTS OF AMPLITUDE AND PHASE
C
50     LT = 1 + NF
      JX = NX + IBORDER
      JY = MIN0( NY+IBORDER, 2000/JX )
      IF (IBORDER.LE.0) GO TO 80
      DO 70 I=1, 2000
          PHOTO(I) = 0.
55     70     CONTINUE
      80     HFACTOR = WIDTH / FLOAT( JX+JY-2 )
          HSCALE=FLOAT( JX+JY-2 )*.706138/WIDTH
C
60     100    IF ( IPIC .LE. 0 ) GO TO 300
      CALL PLOTS(BUFF, 512, IPLT+1, 0)
      CALL PLOTMX( 4.0*WIDTH )
      CALL AMPCAL( DATA, IP, NX, NY, JX, JY, DBMIN+PNORM, IBORDER, PHOTO )
      CALL PLOT( 1.0, 0.0, -3 )
      CALL SYMBOL( 2.0, 9.5, 0.105, HEAD, 0.0, 80 )
65     CALL PLOT( 11., 0., -3 )
      CALL FRAME
      CALL PLOT(-8.75, 1.80, -3)
      ANGLE = SLOPE*RAD
      VFACTOR = HFACTOR * SIN(ANGLE)
70     VSCALE = (DBMAX-DBMIN)/(HEIGHT-(FLOAT( JX+JY-2 )*VFACTOR/2.0))
      VSCALE = VSCALE * 0.884885
      ENCODE( 40, 1300, ZLABEL ) POL(IQ)
      NZCHAR = NUMCHR( ZLABEL )

```

```

      CALL AXIS3D( DBMIN,DBMAX,IBORDER )
75      CALL PLOT(0.0,0.0,3)
      CALL PLOT3D(HSCALE,VSCALE,SLOPE,PHOTO,JX,JY,HID)
      CALL PLOT(0.0,0.0,999)
C
200 IF (IPIC .LE. 1) GO TO 300
80      CALL PLOTS(BUFF,512,IPLT+2,0)
      CALL PLOTMX(4.0*WIDTH)
      CALL PHSCAL( DATA,IP,NX,NY,JX,JY,PHMIN,IBORDER, PHOTO )
      CALL PLOT( 1.0, 0.0, -3 )
      CALL SYMBOL( 2.0, 9.5, 0.105, HEAD, 0.0, 80 )
85      CALL PLOT( 11., 0., -3 )
      CALL FRAME
      CALL PLOT(-8.75,1.80,-3)
      VSCALE = (PHMAX-PHMIN)/(HEIGHT-(FLOAT(JX+JY-2)*VFACTOR/2.))
      VSCALE = VSCALE * 0.884885
90      ENCODE( 40,1400, ZLABEL ) POL(IQ)
      NZCHAR = NUMCHR( ZLABEL )
      CALL AXIS3D( PHMIN,PHMAX,IBORDER )
      CALL PLOT(0.0,0.0,3)
      CALL PLOT3D(HSCALE,VSCALE,SLOPE,PHOTO,JX,JY,HID)
95      CALL PLOT(0.0,0.0,999)
C
C-----ANALYZE X-CUTS BEGINNING WITH THE PEAK
C
300 IF (ICUT .LE. 0) GO TO 400
100      XI = 0.
      CALL PLOTS(BUFF,512,IPLT+3,50)
      CALL PLOTMX(4.0*WIDTH)
      CALL PLOT( 1.0, 0.0, -3 )
      CALL SYMBOL( 2.0, 9.5, 0.105, HEAD, 0.0, 80 )
105      CALL SYMBOL(14.0, 9.5, 0.105, HEAD, 0.0, 80 )
      CALL PLOT( 11., 0., -3 )
      CALL FRAME
      CALL PLOT(12.0,0.0,-3)
      CALL FRAME
110      CALL PLOT(-20.5,1.8,-3)
      CALL HAXIS( XMIN,XMAX,XI,WIDTH,HEIGHT,XLABEL,NXCHAR,SIZENM,SIZELB,
* IGRID )
      CALL VAXIS( DBMIN,DBMAX,DBINC,WIDTH,HEIGHT,PLABEL,NPCHAR,SIZENM,
* SIZELB,IGRID )
115      CALL PLOT(12.0,0.0,-3)
      CALL HAXIS( XMIN,XMAX,XI,WIDTH,HEIGHT,XLABEL,NXCHAR,SIZENM,SIZELB,
* IGRID )
      CALL VAXIS( PHMIN,PHMAX,PHINC,WIDTH,HEIGHT,ZLABEL,NZCHAR,SIZENM,
* SIZELB,IGRID )
120      CALL PLOT(-12.0,0.0,-3)
      WRITE(6,940) HEAD
      DO 320 JS=1,ICUT
      J=N0+((JS-1)*INC)
      ANG = 0.
125      IF (ABS(Y(J)).GE.1. .OR. LT.NE.1) GO TO 305
      ANG = ASIN(Y(J)) * DEG
      DEN = SQRT( 1. - Y(J)**2 )
305 IF (1.GT.J.OR.J.GT.NY) GO TO 320
      DO 310 I=1,NX
130      AMP(I) = -99.
      PHS(I) = 0.
      A = POWER(IP,I,J)
      IF (A .LE. 0.) GO TO 310
      AMP(I) = 10.*ALOG10(A) - PNORM
135      PHS(I)=PHASE(IP,I,J)
      EL(I)=ANG
      AZ(I)=0.0
      IF (LT.NE. 1) GO TO 310
      ARG = X(I) / DEN
140      IF (ABS(ARG) .LE. 1.) AZ(I) = DEG * ASIN(ARG)
310 IF (AMP(I).LT.DBMIN) AMP(I)=DBMIN
      IF (LT.EQ.1) WRITE(6,950) "X",Y(J),POL(IQ),(I,J,X(I),EL(I),AZ(I),
+ AMP(I),PHS(I),I=1,NX)
      IF(LT.EQ.2) WRITE(6,960) "X",Y(J),POL(IQ),(I,J,X(I),AMP(I),PHS(I),
+ I=1,NX)
145      CALL GLINE(0.0,0.0,XMIN,DBMIN,WIDTH,HEIGHT,XMAX,DBMAX,X,AMP,NX)

```

```

      CALL PLOT(12.0,0.0,-3)
      CALL GLINE(0.0,0.0,XMIN,PHMIN,WIDTH,HEIGHT,XMAX,PHMAX,X,PHS,NX)
      CALL PLOT(-12.0,0.0,-3)
150      320 CONTINUE
      CALL PLOT(0.0,0.0,999)
C
C-----ANALYZE Y-CUTS BEGINNING WITH PEAK
C
155      400 IF (JCUT .LE. 0) GO TO 500
      YI = 0.
      CALL PLOTS(BUFF,512,IPLT+4,50)
      CALL PLOTMX(4.0*WIDTH)
      CALL PLOT( 1.0, 0.0, -3 )
160      CALL SYMBOL( 2.0, 9.5, 0.105, HEAD, 0.0, 80 )
      CALL SYMBOL(14.0, 9.5, 0.105, HEAD, 0.0, 80 )
      CALL PLOT( 11., 0., -3 )
      CALL FRAME
      CALL PLOT(12.0,0.0,-3)
165      CALL FRAME
      CALL PLOT(-20.5,1.8,-3)
      CALL HAXIS( YMIN,YMAX,YI,WIDTH,HEIGHT,YLABEL,NYCHAR,SIZENM,SIZELB,
      *IGRID )
      CALL VAXIS( DBMIN,DBMAX,DBINC,WIDTH,HEIGHT,PLABEL,NPCHAR,SIZENM,
170      * SIZELB,IGRID )
      CALL PLOT(12.0,0.0,-3)
      CALL HAXIS( YMIN,YMAX,YI,WIDTH,HEIGHT,YLABEL,NYCHAR,SIZENM,SIZELB,
      *IGRID )
      CALL VAXIS( PHMIN,PHMAX,PHINC,WIDTH,HEIGHT,ZLABEL,NZCHAR,SIZENM,
175      * SIZELB,IGRID )
      CALL PLOT(-12.0,0.0,-3)
      WRITE(6,940) HEAD
      DO 420 IS=1,JCUT
      I=M0+((IS-1)*JNC)
180      IF (1.GT.I.OR.I.GT.NX) GO TO 420
      DO 410 J=1,NY
      AMP(J) = -99.
      PHS(J) = 0.
      A = POWER(IP,I,J)
      IF (A .LE. 0.) GO TO 410
      AMP(J) = 10.*ALOG10(A) - PNORM
      PHS(J)=PHASE(IP,I,J)
      EL(J)=0.0
      AZ(J)=0.0
190      IF (LT .NE. 1) GO TO 410
      IF (ABS(Y(J)) .GE. 1.) GO TO 410
      EL(J) = ASIN(Y(J)) * DEG
      ARG = X(I) / SQRT( 1.-Y(J)**2 )
      IF (ABS(ARG) .LE. 1.) AZ(J) = ASIN(ARG) * DEG
195      410 IF (AMP(J).LT.DBMIN) AMP(J)=DBMIN
      IF (LT.EQ.1) WRITE(6,950) "Y",X(I),POL(IQ),(I,J,Y(J),EL(J),AZ(J),
      + AMP(J),PHS(J),J=1,NY1)
      IF (LT.EQ.2) WRITE(6,960) "Y",X(I),POL(IQ),(I,J,Y(J),AMP(J),PHS(J),
      * J = 1,NY1)
200      CALL GLINE(0.0,0.0,YMIN,DBMIN,WIDTH,HEIGHT,YMAX,DBMAX,Y,AMP,NY)
      CALL PLOT(12.0,0.0,-3)
      CALL GLINE(0.0,0.0,YMIN,PHMIN,WIDTH,HEIGHT,YMAX,PHMAX,Y,PHS,NY)
      CALL PLOT(-12.0,0.0,-3)
205      420 CONTINUE
      CALL PLOT(0.0,0.0,999)
C
      500 IPLT=IPLT+10
C
      RETURN
210 C
      940 FORMAT ("1",8A10)
      950 FORMAT(//5X,A1,"-CUT IN SPECTRUM AT",F9.4,". POLARIZATION",A10//
      + " ARRAY DIRECTION ELEVATION AZIMUTH ",
      + " AMPLITUDE PHASE "/
      + " POINT COSINE (DEGREES) (DEGREES) ",
      + " (DB) (DEGREES) "/
      + " ----- "
      + " ----- "/
      + 1000(/" ",2I4,F10.5,4F11.3))

```

SUBROUTINE OUTDAT      74/74    OPT=1

FTN 4.8+577

```
220      960 FORMAT(//5X,A1,"-CUT IN APERTURE AT",F9.4,". POLARIZATION",A10//
      +      "      ARRAY      POSITION  AMPLITUDE  PHASE  "/
      +      "      "      POINT  (IN./RAD)      (DB)      (DEGREES)"/
      +      "      "      -----
      +      1000(/" ",2I4,F9.3,2F11.3))
225      1000 FORMAT (A1)
      C
      END
```

SUBROUTINE OUTDAT 74/74 TS

--COMMON BLOCKS--

10B /CONST/  
6720B /OUTSCR/

11B /CUT/  
13B /PLT3D/

10B /HEAD/

25B /LABELS/

--EXTERNALS--

ALOG10.	AMPCAL	ASIN.	ATAN2.	AXIS3D	ENCODI.	FRAME	GLINE
HAXIS	NUMCHR	OUTCI.	OUTCR.	PHSCAL	PLOT	PLOTMX	PLOTS
PLOT3D	SIN.	SQRT.	SYMBOL	TAPE6*	VAXIS		

--STATEMENT LABELS--

.70	ID	0B	53 D	55 L			
.80		122B	52	56 L			
.100		132B	59 L				
.200		227B	79 L				
.300		315B	59	79	99 L		
.305		426B	125	128 L			
.310	D	526B	129 D	133	138	141 L	
.320	D	641B	122 D	128	150 L		
.400		646B	99	155 L			
.410	D	1046B	181 D	185	190	191	195 L
.420	D	1157B	178 D	180	204 L		
.500		1164B	155	207 L			
.940	F	1251B	121 W	177 W	211 L		
.950	F	1254B	142 W	196 W	212 L		
.960	F	1314B	144 W	198 W	220 L		
.1000	F	1344B	225 L				
.1100	F	1232B	30 W	31 L			
.1200	F	1235B	33 W	34 L			
.1300	F	1242B	36 W	37 L	72 W		
.1400	F	1245B	39 L	90 W			

--VARIABLE MAP--

A	R	2104B		132 =	133 F	134 A
ABS	R	184 =	185 F 186 A			
AIMAG	R	194 F	INTRINSIC	125 F	140 F	191 F
AK	R	184 A	INTRINSIC	45 A	132 A	135 A
ALOG10.	R	7B /CONST/		17 D		
AMP	R	B.E.F.		45	134	186
	R	4720B /OUTSCR/	128	9 D	130 =	134 =
	141 F	141 =	142 W	144 W	146 A	182 =
	195 F	195 =	196 W	198 W	200 A	186 =
AMPCAL	R		SUBROUTINE	62 X		
ANG	R	2102B		124 =	126 =	136
ANGLE	R	0B /PLT3D/		12 D	68 =	69 A
ARG	R	2105B		139 =	140 A	140 A
	193 =	194 A	194 A			
ASIN.	R	B.E.F.		126	140	192
	194					
ATAN2.	R	B.E.F.		135 A	187 A	
AXIS3D	R	SUBROUTINE		74 X	92 X	
AZ	R	6520B /OUTSCR/	128	9 D	137 =	140 =
	142 W	189 =	194 =	196 W		
BUFF	R	3720B /OUTSCR/	512	9 D	60 A	80 A
	101 A	157 A				
DATA	Z A	0B	VAR-DIM	4 A	6 D	45 A
	45 A	62 A	82 A	132 A	135 A	135 A
	184 A	184 A	187 A	187 A		
DBINC	R	2056B		20 I	113 A	169 A
DBMAX	R	2066B		20 I	70	74 A
	113 A	146 A	169 A	200 A		
DBMIN	R	2065B		20 I	62 A	70
	74 A	113 A	141 F	141	146 A	169 A
	195	200 A				195 F

## SUBROUTINE OUTDAT 74/74 TS

DEG	R	5B /CONST/	17 D	126	133 A
	140	187 A 192	194		
DEN	R	2103B	127 =	139	
EL	R	6320B /OUTSCR/	9 D	136 =	142 W
	138 =	192 = 196 W			
ENCODI.	-	EXTERNAL.	30 W	33 W	36 W
	72 W	90 W			
EPS	R	6B /CONST/	17 D		
FLOAT	R	INTRINSIC	56	57	70
	88				
FRAME	R	SUBROUTINE	66 X	86 X	107 X
	109 X	163 X 165 X			
GLINE	R	SUBROUTINE	146 X	148 X	200 X
	202 X				
HAXIS	R	SUBROUTINE	111 X	116 X	167 X
	172 X				
HEAD	R	0B /HEAD/	11 D	64 A	84 A
	104 A	105 A 121 W	161 A	177 W	
HEIGHT	R	12B /PLT3D/	12 D	20 I	70
	88	111 A 113 A	118 A	146 A	148 A
	167 A	169 A 172 A	200 A	202 A	
HFACTOR	R	3B /PLT3D/	12 D	56 =	69
HID	R	5320B /OUTSCR/	9 D	76 A	94 A
HSCALE	R	2047B	57 =	76 A	94 A
I	I	2075B	53 C	54 S	129 C
	130 S	131 S 132 S	134 S	135 S	135 S
	135 S	136 S 137 S	140 S	141 S	141 S
	142 C	142 W 142 S	142 S	142 S	142 S
	144 C	144 W 144 S	144 S	179 =	180 F
	180 F	184 S 184 S	187 S	193 S	196 S
	196 W	198 S 198 W			
IBORDER	I	7B /CUT/	8 D	18 I	50
	51 A	52 F 62 A	82 A	92 A	
ICLAB	I	4B /LABELS/	15 D		
ICUT	I	1B /CUT/	8 D	18 I	99 F
	122 C				
IDEC	I	3B /LABELS/	15 D		
IGRID	I	10B /CUT/	8 D	18 I	111 A
	113 A	116 A 118 A	169 A	172 A	174 A
INC	I	3B /CUT/	8 D	18 I	123
IOBUG	I A	0B	4 A		
IP	I	2071B	27 =	45 S	45 S
	62 A	82 A 132 S	132 S	135 S	135 S
	184 S	187 S 137 S			184 S
IPIC	I	0B /CUT/	8 D	18 I	59 F
	79 F				
IPLT	I	5B /LABELS/	15 D	60 A	80 A
	101 A	137 A 207	207 =		
IPOL	I A	0B	4 A	27 A	28
IQ	I	2072B	28 =	29 F	29 =
	36 S	72 S 90 S	144 S	196 S	198 S
IS	I	2107B	178 C	179	
J	I	2101B	123 =	125 S	126 S
	127 S	128 F 128 F	132 S	132 S	135 S
	142 S	142 W 144 S	144 W	181 C	182 S
	184 S	184 S 186 S	187 S	187 S	188 S
	189 S	191 S 192 S	192 S	193 S	194 S
	195 S	196 C 196 W	196 S	196 S	196 S
	196 S	198 C 198 W	198 S	198 S	
JCUT	I	2B /CUT/	8 D	18 I	153 F
	178 C				
JNC	I	4B /CUT/	8 D	18 I	179
JS	I	2100B	122 C	123	
JX	I	1B /PLT3D/	12 D	50 =	51 A
	56 A	57 A 62 A	76 A	82 A	88 A
	94 A				
JY	I	2B /PLT3D/	12 D	51 =	56 A
	57 A	62 A 70 A	82 A	88 A	94 A
LT	I	2074B	49 =	125 F	138 F
	142 F	144 F 190 F	198 F		
MAX0	I	INTRINSIC	27		
MIN0	I	INTRINSIC	43	51	
M0	I	5B /CUT/	8 D	18 I	179



## SUBROUTINE OUTDAT 74/74 TS

NARR	I A	0B		4 A	43 A	
NF	I	2064B		18 I	49	
NPCHAR	I	2073B		38 =	113 A	169 A
NUMCHR	I	FUNCTION		32	35	38
	73	91				
NX	I A	0B		4 A	6 D	7 D
	41 S	43 A	50	82 A	129 C	142 C
	144 C	146 A	148 A	180 F		
NXCHAR	I	22B /LABELS/		15 D	32 =	111 A
	116 A					
NY	I	2055B		43 =	44 S	51 A
	62 A	82 A	128 F	181 C	200 A	202 A
NYCHAR	I	23B /LABELS/		15 D	35 =	167 A
	172 A					
NY1	I A	0B		4 A	6 D	7 D
	43 A	196 C	198 C			
NZCHAR	I	24B /LABELS/		15 D	73 =	91 =
	118 A	174 A				
N0	I	6B /CUT/		8 D	18 I	123
OUTCI.	-	EXTERNAL.		121 W	142 W	144 W
	177 W	196 W	198 W			
OUTCR.	-	EXTERNAL.		142 W	142 W	144 W
	144 W	196 W	196 W	198 W		
OUTDAT	-	1171B ENTRY		4 E		
PHASE	R	STAT-FUNC		24 D	135	187
PHINC	R	2067B		20 I	118 A	174 A
PHMAX	R	2054B		20 I	88	92 A
	118 A	148 A	174 A	202 A		
PHMIN	R	2053B		20 I	82 A	88
	92 A	118 A	148 A	174 A	202 A	
PHOTO	R	0B /OUTSCR/	2000	9 D	54 =	62 A
	76 A	82 A	94 A			
PHS	R	5120B /OUTSCR/	128	9 D	131 =	135 =
	142 W	144 W	148 A	183 =	187 =	196 W
	202 A					
PHSCAL	R	SUBROUTINE		82 X		
PI	R	0B /CONST/		17 D		
PIBY2	R	1B /CONST/		17 D		
PI2	R	3B /CONST/		17 D		
PI3BY2	R	2B /CONST/		17 D		
PLABEL	R	2057B	4	7 D	36 ,	38 A
	113 A	169 A				
PLOT	R	SUBROUTINE		63 X	65 X	67 X
	75 X	77 X	83 X	85 X	93 X	95 X
	103 X	106 X	108 X	110 X	115 X	120 X
	149 X	151 X	159 X	162 X	164 X	166 X
	176 X	201 X	203 X	205 X		
PLOTMX	R	SUBROUTINE		61 X	81 X	102 X
	158 X					
PLOTS	R	SUBROUTINE		60 X	80 X	101 X
	157 X					
PLOT3D	R	SUBROUTINE		76 X	94 X	
PNORM	R	2063B		45 =	62 A	134
	186					
POL	R	2050B	3	7 D	22 I	22 I
	22 I	36 W	72 W	90 W	142 W	144 W
	198 W					196 W
POWER	R	STAT-FUNC		25 D	45 A	132
	184					
RAD	R	4B /CONST/		17 D	68	
REAL	R	INTRINSIC		45 A	132 A	135 A
	184 A	187 A				
SIN.	R	B.E.F.		69		
SIZEHD	R	2B /LABELS/		15 D		
SIZELB	R	1B /LABELS/		15 D	111 A	113 A
	116 A	118 A	167 A	169 A	172 A	174 A
SIZEZM	R	0B /LABELS/		15 D	111 A	113 A
	116 A	118 A	167 A	169 A	172 A	174 A
SLOPE	R	2070B		20 I	68	76 A
	94 A					
SQRT.	R	B.E.F.		127	193	
SYMBOL	R	SUBROUTINE		64 X	84 X	104 X
	105 X	160 X	161 X			

SUBROUTINE OUTDAT 74/74 1S

TAPE6#	-	EXTERNAL.	121 W	142 W	144 W
VAXIS	177 W	196 W 198 W			
	R	SUBROUTINE	113 X	118 X	169 X
VFACTOR	174 X				
	R	4B /PLT3D/	12 D	69 =	70
	88				
VSCALE	R	2076B	70 =	71	71 =
	76 A	88 = 89 89 =	94 A		
WIDTH	R	11B /PLT3D/	12 D	20 I	56
	57	61 A 81 A 102 A	111 A	113 A	116 A
	118 A	146 A 148 A 158 A	167 A	169 A	172 A
	174 A	200 A 202 A			
X	R A	0B VAR-DIM	4 A	7 D	40
	41	139 142 W 144 W	146 A	148 A	193
	196 W	198 W			
XI	R	2077B	100 =	111 A	116 A
XLABEL	R	6B /LABELS/ 4	15 D	30 ;	32 A
	111 A	116 A			
XMAX	R	6B /PLT3D/	12 D	41 =	111 A
	116 A	146 A 148 A			
XMIN	R	5B /PLT3D/	12 D	40 =	111 A
	116 A	146 A 148 A			
Y	R A	0B VAR-DIM	4 A	7 D	42
	44	125 A 126 A 127 A	142 W	144 W	191 A
	192 A	193 A 196 W 198 W	200 A	202 A	
YI	R	2106B	156 =	167 A	172 A
YLABEL	R	12B /LABELS/ 4	15 D	33 ;	35 A
	167 A	172 A			
YMAX	R	10B /PLT3D/	12 D	44 =	167 A
	172 A	200 A 202 A			
YMIN	R	7B /PLT3D/	12 D	42 =	167 A
	172 A	200 A 202 A			
ZLABEL	R	16B /LABELS/ 4	15 D	72 ;	73 A
	90 ;	91 A 118 A 174 A			

11121B PROGRAM-UNIT LENGTH  
755 REFERENCES

135 SYMBOLS

43000B CM STORAGE USED

5.896 SECONDS

SUBROUTINE PDF

74/74 OPT=1

FTN 4.8+577

```

1      C/////PDF CALCULATES THE PROBABILITY DENSITY FUNCTION FOR
C/      A DEFECT POSITION IN THE APERTURE OF ONE SECTOR.
C/
5      SUBROUTINE PDF( AR,AA,NR,NA,AREA, P,UNIF )
C
C      DIMENSION AR(NR),AA(NA),P(NR,NA)
C
C      UNIF = 1.
C      PROB = 1./AREA
10     DO 100 J=1,NA
C      DO 100 I=1,NR
C      P(I,J) = PROB
100    CONTINUE
15     WRITE(6,900) PROB
C      RETURN
900    FORMAT(" PROBABILITY DENSITY IS UNIFORM OVER A SECTOR"/
+           " WITH A VALUE OF",F10.6//)
C      END

```

SUBROUTINE PDF

74/74 TS

--EXTERNALS--

OUTCI. TAPE6\*

--STATEMENT LABELS--

.100	ID	0B	10 D	11 D	13 L
.900	F	44B	14 W	16 L	

--VARIABLE MAP--

AA	R A	0B	VAR-DIM	4 A	6 D	
AR	R A	0B	VAR-DIM	4 A	6 D	
AREA	R A	0B		4 A	9	
I	I	65B		11 C	12 S	
J	I	64B		10 C	12 S	
NA	I A	0B		4 A	6 D	6 D
NR	10 C			4 A	6 D	6 D
	11 C	0B				
OUTCI.	-	EXTERNAL.		14 W		
P	R A	0B	VAR-DIM	4 A	6 D	12 =
PDF	-	37B ENTRY		4 E		
PROB	R	63B		9 =	12	14 W
TAPE6*	-	EXTERNAL.		14 W		
UNIF	R A	0B		4 A	8 =	

66B PROGRAM-UNIT LENGTH  
34 REFERENCES

15 SYMBOLS

41000B CM STORAGE USED

.207 SECONDS

SUBROUTINE PDF

74/74 OPT=1

FTN 4.8+577

```

1      C/////PDF CALCULATES THE PROBABILITY DENSITY FUNCTION FOR
C/      A DEFECT POSITION IN THE APERTURE OF ONE SECTOR.
C/
5      C      SUBROUTINE PDF( AR,AA,NR,NA,AREA, P,UNIF )
C
C      DIMENSION AR(NR),AA(NA),P(NR,NA)
C
C      UNIF = 0.
C      AREA1 = AREA * (AA(2)-AA(1)) / (AA(NA)-AA(1))
10     C      PROB = 2./AREA1
C      THE 2 IS BECAUSE P IS NOT LEVEL OVER AREA1, BUT SLOPES TO 0.
C      DO 100 J=1,NA
C      DO 100 I=1,NR
C      P(I,J) = 0.
15     C      IF (J.EQ. 1) P(I,J) = PROB
C      CONTINUE
C      WRITE(6,900) PROB
C      RETURN
20     C      900 FORMAT(// " PROBABILITY DENSITY IS ZERO EXCEPT AT PHI = 0." /
+      " WITH A VALUR OF",F10.6//)
C      END

```

SUBROUTINE PDF

74/74 1S

--EXTERNALS--

OUTCI. TAPE6#

--STATEMENT LABELS--

.100	ID	0B	12 D	13 D	16 L
.900	F	63B	17 W	19 L	

--VARIABLE MAP--

AA	R A	0B	VAR-DIM	4 A	6 D	9
AR	9	9	9			
AREA	R A	0B	VAR-DIM	4 A	6 D	
AREA1	R A	0B		4 A	9	
I	R	106B		9 =	10	
J	I	107B		13 C	14 S	15 S
	I	105B		12 C	14 S	15 F
NA	15 S					
	I A	0B		4 A	6 D	6 D
NR	9 S	12 C				
	I A	0B		4 A	6 D	6 D
	13 C					
OUTCI.			EXTERNAL.			
P	R A	0B	VAR-DIM	17 W		
	15 =			4 A	6 D	14 =
PDF		56B	ENTRY	4 E		
PROB	R	104B		10 =	15	17 W
TAPE6#			EXTERNAL.	17 W		
UNIF	R A	0B		4 A	8 =	

110B PROGRAM-UNIT LENGTH  
45 REFERENCES

16 SYMBOLS

41000B CM STORAGE USED

.258 SECONDS

```

1      C/////PERFORM CALCULATES PERFORMANCE PARAMETERS OF A PATTERN.
      C/
      SUBROUTINE PERFORM(P,NP,N)
      C
5      C*****
      C
      C      THE FOLLOWING PARAMETERS ARE PASSED BY THE CALLER:
      C      P, A 361 X N ARRAY CONTAINING THE DATA TO BE
      C      ANALYZED;
10     C      NP, THE NUMBER OF POINTS IN EACH PATTERN;
      C      N, THE NUMBER OF PATTERNS.
      C
      C      THE ABSCISSA VARIABLE IS ASSUMED TO BE IN DEGREES;
      C      THE ORDINATE VARIABLE IS ASSUMED TO BE IN DB.
15     C
      C      WRITTEN BY D.W.ACREE, APRIL, 1983
      C*****
      C
      REAL P(361,N)
20     C
      IF (NP .LE. 1) RETURN
      WRITE(6,44)
44     FORMAT(5X,"PEAK",8X,"BEAMWIDTH",8X,"3DB POINT",8X,"1ST SIDELobe"
      #,2X,"1ST SIDELobe")
25     WRITE(6,45)
45     FORMAT(5X,"(DB)",10X,"(DEG)",12X,"(DEG)",14X,"LEVEL",
      #5X," LOC (DEG) ")
      WRITE(6,46)
46     FORMAT(5X,"____",8X,"____",8X,"____",8X,"____",
30     #2X,"____"/)
      NP1=N+1
      C
      DO 1000 I=2,NP1
      PK=P(1,I)
35     C
      C***** COMPUTE 3DB POINT *****
      C
      Y1 = P(2,I)
      Y2 = P(1,I)
40     Y3 = P(2,I)
      X1 = -P(2,I)
      X2 = P(1,I)
      X3 = P(2,I)
      SW2=1.
45     NM = 1
      IF (NP .LE. 2) GO TO 700
      TDBP=P(1,I)-3.01
      DO 10 J=1,NP
      IF(P(J,I).GE.TDBP) GO TO 10
50     IF (J.LT.3) GO TO 20
      Y1=P(J-2,I)
      Y2=P(J-1,I)
      Y3=P(J,I)
      X1=P(J-2,I)
55     X2=P(J-1,I)
      X3=P(J,I)
      NM=J
      GO TO 20
10     CONTINUE
      SW2=0.
      NM=1
      GO TO 700
20     CONTINUE
      C
65     CALL QUAD(X1,X2,X3,Y1,Y2,Y3, A,B,C)
      CALL SOLVE(A,B,C,TDBP, X3DB)
      C
      X3DB=X3DB
      BWD=2.*X3DB
70     C
      C
      C***** COMPUTE SIDELobe LOC AND LEVEL *****
      C

```

```

75      700  SW1=0.
          NPM1=NP-1
          DO 50 J=NM,NPM1
            IF(P(J+1,I).LE.P(J,I)) GO TO 50
            SW1=1.
            NB=J
80      50    GO TO 300
          300  CONTINUE
            IF(SW1.EQ.0.) GO TO 350
            NPM1=NP-1
            DO 60 J=NB,NPM1
85      60    IF(P(J+1,I).GE.P(J,I)) GO TO 60
            Y1=P(J-1,I)
            Y2=P(J,I)
            Y3=P(J+1,I)
            X1=P(J-1,1)
90      90    X2=P(J,1)
            X3=P(J+1,1)
            GO TO 500
          60    CONTINUE
          C
95      500  CALL QUAD(X1,X2,X3,Y1,Y2,Y3,  A,B,C)
          C
            XPT=-B/(2.*A)
            SLL=PK-(A*XPT**2 + B*XPT +C)
            XPT=XPT
100     350  IF(SW1.EQ.1..AND.SW2.EQ.1.) WRITE(6,77) PK,
          *BWD,X3DB,SLL,XPT
            IF(SW1.EQ.1..AND.SW2.EQ.0.) WRITE(6,78) PK,
          *SLL,XPT
            IF(SW1.EQ.0..AND.SW2.EQ.1.) WRITE(6,79) PK,
105     105  *BWD,X3DB
            IF(SW1.EQ.0..AND.SW2.EQ.0.) WRITE(6,80) PK
77      77    FORMAT(1X,F9.3,5X,F9.3,8X,F9.3,10X,F9.3,5X,F9.3
          *)
78      78    FORMAT(1X,F9.3,9X,"NONE",13X,"NONE",11X,F9.3,5X,F9.3)
110     79    FORMAT(1X,F9.3,5X,F9.3,8X,F9.3,14X,"NONE",10X,"NONE")
80      80    FORMAT(1X,F9.3,9X,"NONE",13X,"NONE",15X,"NONE",10X,"NONE")
          C
1000    1000  CONTINUE
          RETURN
115     END

```

SUBROUTINE PERFORM 74/74 TS

--EXTERNALS--

OUTC1. QUAD SOLVE TAPE6#

--STATEMENT LABELS--

.10	D	122B	48 D	49	59 L
.20		133B	50	58	63 L
.44	F	322B	22 W	23 L	
.45	F	333B	25 W	26 L	
.46	F	343B	28 W	29 L	
.50	D	166B	76 D	77	81 L
.60	D	234B	84 D	85	93 L
.77	F	354B	100 W	107 L	
.78	F	361B	102 W	109 L	
.79	F	367B	104 W	110 L	
.80	F	375B	106 W	111 L	
.300		171B	80	82 L	
.350		252B	82	100 L	
.500		237B	92	93 L	
.700		144B	46	62	74 L
.1000	D	310B	33 D	113 L	

--VARIABLE MAP--

A	R	507B			65 A	66 A	95 A
	97	98					
B	R	467B			65 A	66 A	95 A
	97	98					
BWD	R	502B			69 =	100 W	104 W
C	R	470B			65 A	66 A	95 A
	98						
I	I	473B			33 C	34 S	38 S
	39 S	40 S	47 S	49 S	51 S	52 S	53 S
	77 S	77 S	85 S	85 S	86 S	87 S	88 S
J	I	474B			48 C	49 S	50 F
	51 S	52 S	53 S	54 S	55 S	56 S	57
	76 C	77 S	77 S	79	84 C	85 S	85 S
	86 S	87 S	38 S	89 S	90 S	91 S	
N	I A	0B			3 A	19 D	31
NB	I	503B			79 =	84 C	
NM	I	477B			45 =	57 =	61 =
	76 C						
NP	I A	0B			3 A	21 F	46 F
	48 C	75	83				
NPM1	I	512B			75 =	76 C	83 =
	84 C						
NP1	I	504B			31 =	33 C	
OUTC1.	-	EXTERNAL.			22 W	25 W	28 W
	100 W	102 W	104 W	106 W			
P	R A	0B	VAR-DIM		3 A	19 D	34
	38	39	40	41	42	43	47
	49 F	51	52	53	54	55	56
	77 F	77 F	85 F	85 F	86	87	88
	89	90	91				
PERFORM	-	316B ENTRY			3 E		
PK	R	472B			34 =	98	100 W
	102 W	104 W	106 W				
QUAD	R	SUBROUTINE			65 X	95 X	
SLL	R	476B			98 =	100 W	102 W
SOLVE	R	SUBROUTINE			66 X		
SW1	R	511B			74 =	78 =	82 F
	100 F	102 F	104 F	106 F			
SW2	R	475B			44 =	60 =	100 F
	102 F	104 F	106 F				
TAPE6#	-	EXTERNAL.			22 W	25 W	28 W
	100 W	102 W	104 W	106 W			
TDBP	R	471B			47 =	49 F	66 A
XPT	R	513B			97 =	98	98
	99	99 =	100 W	102 W			

SUBROUTINE PERFORM 74/74 TS

X1	R	500B		41 =	54 =	65 A
	89 =	95 A		42 =	55 =	65 A
X2	R	465B		43 =	56 =	65 A
	90 =	95 A		66 A	68	68 =
X3	R	506B		38 =	51 =	65 A
	91 =	95 A		39 =	52 =	65 A
X3DB	R	510B	104 W	40 =	53 =	65 A
	69	100 W				
Y1	R	501B				
	86 =	95 A				
Y2	R	466B				
	87 =	95 A				
Y3	R	505B				
	88 =	95 A				

514B PROGRAM-UNIT LENGTH  
228 REFERENCES

47 SYMBOLS

41000B CM STORAGE USED

2.308 SECONDS



```

1      C/////PERTRB INTRODUCES DETERMINISTIC ERRORS INTO THE REFLECTOR SURFACE.
C/      THIS VERSION IS FOR CHORDAL ERRORS. (2 SAMPLE POINTS PER
C/      CHORD IN AZIMUTH.)
C/
5      SUBROUTINE PERTRB( E0,AR,AA,NR,NA,NARR,FOCL,IO, E1 )
C
      COMPLEX E0(2,NR,NA),E1(2,NR,NA),PERT
      DIMENSION AR(NR),AA(NA)
      COMMON /CONST/ PI,PIBY2,PI3BY2,PI2,RAD,DEG,EPS,AK
10     C
      NCH = (NA-1) / 2
      IF (2*NCH+1 .NE. NA) WRITE(6,900)
      WRITE(6,910) NCH
      NCHR = NCH * NARR
15     C
      IF (IO .GE. 2) WRITE(6,920)
      FAC = 2.*AK * (COS(PI/NCHR)**2 - 1) / (4.*FOCL)
      DO 200 I=1,NR
        PHS = FAC * AR(I)**2
20     PERT = CMPLX( COS(PHS), SIN(PHS) )
        IF (IO .GE. 2) WRITE(6,930) I,AR(I),PHS
        DO 200 K=1,NARR
          J1 = (K-1) * NA + 1
          J2 = J1 + NA - 1
25     DO 200 JK=J1,J2,2
          E1(1,I,JK) = E0(1,I,JK) * PERT
          E1(2,I,JK) = E0(2,I,JK) * PERT
          E1(1,I,JK+1) = E0(1,I,JK+1)
          E1(2,I,JK+1) = E0(2,I,JK+1)
30     200 CONTINUE
      RETURN
900 FORMAT(// " *** WARNING ***" //
+         " NA SHOULD BE ODD FOR ANALYSIS OF CHORDAL ERRORS" //)
910 FORMAT( " CHORDAL ERROR IS MODELED FOR",I3," CHORDS PER SECTOR")
35 920 FORMAT(// " CHORDAL PERTURBATION" / " POINT RADIUS PHASE")
930 FORMAT( I7, 2F9.2 )
      END

```

## SUBROUTINE PERTRB 74/74 TS

--COMMON BLOCKS--

10B /CONST/

--EXTERNALS--

COS.	INPFI.	INPFR.	INPUT*	OUTCI.	OUTCR.	OUTPUT*	SIN.
SQRT.	TAPE6*						

--STATEMENT LABELS--

.100	ID	0B	23 D	27 L		
.200	ID	0B	18 D	20 D	28 L	
.900	F	227B	12 W	33 L		
.910	F	241B	14 W	35 L		
.1000	F	252B	29 W	37 L		
.2000	F	277B	30 W	41 L		

--VARIABLE MAP--

AA	R A	0B	VAR-DIM	5 A	8 D	30 W
AAP	R	361B	64	8 D	10 I	15 R
	21	30 W				
AK	R	7B /CONST/		9 D	19	
AR	R A	0B	VAR-DIM	5 A	8 D	19 A
	29 W					
ARP	R	465B	64	8 D	10 I	13 R
	19	29 W				
CMPLX	Z	INTRINSIC		22		
COS.	R	B.E.F.		22 A		
DEG	R	5B /CONST/		9 D		
EPS	R	6B /CONST/		9 D		
E0	Z A	0B	VAR-DIM	5 A	7 D	25
	26					
E1	Z A	0B	VAR-DIM	5 A	7 D	25 =
	26 =					
FOCL	R A	0B		5 A	17	
F2I	R	463B		17 =	19 A	
I	I	565B		13 C	13 S	15 C
	15 S	18 C	19 S	25 S	25 S	26 S
	26 S	29 C	29 W	29 S		
INPFI.	-	EXTERNAL.		13 R	15 R	
INPFR.	-	EXTERNAL.		13 R	13 R	15 R
	15 R					
INPUT*	-	EXTERNAL.		13 R	15 R	
IO	I A	0B		5 A		
J	I	566B		20 C	21 S	24
	30 C	30 W	30 S			
JK	I	360B		24 =	25 S	25 S
	26 S	26 S				
K	I	567B		23 C	24	
NA	I A	0B		5 A	7 D	7 D
	8 D	14 W	15 C	24	30 C	
NARR	I A	0B		5 A	23 C	
NR	I A	0B		5 A	7 D	7 D
	8 D	12 W	13 C	29 C		
OUTCI.	-	EXTERNAL.		12 W	14 W	29 W
	30 W					
OUTCR.	-	EXTERNAL.		29 W	29 W	30 W
	30 W					
OUTPUT*	-	EXTERNAL.		12 W	14 W	
PERT	Z	461B		7 D	22 =	25
	26					
PERTRB	-	221B ENTRY		5 E		
PHS	R	464B		21 =	22 A	22 A
PHSFAC	R	357B		19 =	21	
PI	R	0B /CONST/		9 D		
PIBY2	R	1B /CONST/		9 D		
PI2	R	3B /CONST/		9 D		

SUBROUTINE PERTRB 74/74 TS

PI3BY2	R	2B /CONST/	9 D	
RAD	R	4B /CONST/	9 D	
SIN.	R	B.E.F.	22 A	
SQRT.	R	B.E.F.	19	
TAPE6*	-	EXTERNAL.	29 W	30 W

600B PROGRAM-UNIT LENGTH 45 SYMBOLS  
134 REFERENCES

41000B CM STORAGE USED 1.297 SECONDS

```

1      C/////PERTRB INTRODUCES DETERMINISTIC ERRORS INTO THE REFLECTOR SURFACE.
      C/   THIS VERSION ALLOWS A PERTURBATION OF THE REFLECTOR SECTOR,
      C/   NORMAL TO IT, TO BE READ IN. (SEPERABLE IN RHO AND PHI)
      C/
5      SUBROUTINE PERTRB( E0,AR,AA,NR,NA,NARR,FOCL,IO, E1 )
      C
      COMPLEX E0(2,NR,NA),E1(2,NR,NA),PERT
      DIMENSION AR(NR),AA(NA),ARP(64),AAP(64)
      COMMON /CONST/ PI,PIBY2,PI3BY2,PI2,RAD,DEG,EPS,AK
10     DATA ARP,AAP / 128*1. /
      C
      PRINT 900, NR
      READ *, (ARP(I),I=1,NR)
      PRINT 910, NA
15     READ *, (AAP(I),I=1,NA)
      C
      F2I = (.5/FOCL)**2
      DO 200 I=1,NR
      PHSFAC = 2.*AK*ARP(I) * SQRT( AR(I)**2*F2I + 1. )
20     DO 200 J=1,NA
      PHS = PHSFAC * AAP(J)
      PERT = CMPLX( COS(PHS), SIN(PHS) )
      DO 100 K=1,NARR
      JK = J + (K-1)*NA
25     E1(1,I,JK) = E0(1,I,JK) * PERT
      E1(2,I,JK) = E0(2,I,JK) * PERT
100    CONTINUE
200    CONTINUE
      WRITE(6,1000) (I,AR(I),ARP(I), I=1,NR)
30     WRITE(6,2000) (J,AA(J),AAP(J), J=1,NA)
      RETURN
      C
      900 FORMAT( " INPUT DEFORMATION (IN.) NORMAL TO THE REFLECTOR FOR",I3/
      + " POINTS ALONG THE RADIUS")
35     910 FORMAT( " INPUT NORMALIZED PERTURBATION FOR",I3/
      + " AZIMUTHAL POINTS FOR ONE SECTOR." )
      1000 FORMAT(// " THE REFLECTOR PERTURBATION IS SEPARABLE IN RHO AND PHI"
      * " THE DISPLACEMENT (IN.) NORMAL TO THE SURFACE AS A",
      * " FUNCTION OF RADIUS IS:"//
40     * " POINT RADIUS DISPLACEMENT"// (I5,F10.3,F14.4) )
      2000 FORMAT(// " THE NORMALIZED PERTURBATION AS A FUNCTION OF AZIMUTH:"
      * " POINT AZIMUTH DISPLACEMENT"// (I5,F10.3,F14.4) )
      C
      END

```

SUBROUTINE PERTRB 74/74 TS

--COMMON BLOCKS--

10B /CONST/

--EXTERNALS--

COS. OUTCI. SIN. TAPE6#

--STATEMENT LABELS--

.200	ID	0B	18 D	22 D	25 D	30 L
.900	F	216B	12 W	32 L		
.910	F	227B	13 W	34 L		
.920	F	236B	16 W	35 L		
.930	F	245B	21 W	36 L		

--VARIABLE MAP--

AA	R A	0B	VAR-DIM	5 A	8 D	
AK	R	7B /CONST/		9 D	17	
AR	R A	0B	VAR-DIM	5 A	8 D	19
	21 W					
CMPLX	Z	INTRINSIC		20		
COS.	R	B.E.F.		17	20 A	
DEG	R	5B /CONST/		9 D		
EPS	R	6B /CONST/		9 D		
E0	Z A	0B	VAR-DIM	5 A	7 D	26
	27	28	29			
E1	Z A	0B	VAR-DIM	5 A	7 D	26 =
	27 =	28 =	29 =			
FAC	R	305B		17 =	19	
FOCL	R A	0B		5 A	17	
I	I	306B		18 C	19 S	21 W
	21 S	26 S	26 S	27 S	28 S	28 S
	29 S	29 S				
IO	I A	0B		5 A	16 F	21 F
JK	I	275B		25 C	26 S	26 S
	27 S	27 S	28 S	29 S	29 S	
J1	I	307B		23 =	24	25 C
J2	I	302B		24 =	25 C	
K	I	277B		22 C	23	
NA	I A	0B		5 A	7 D	7 D
	8 D	11	12 F	24		
NARR	I A	0B		5 A	14	22 C
NCH	I	276B		11 =	12 F	13 W
	14					
NCHR	I	304B		14 =	17 A	
NR	I A	0B		5 A	7 D	7 D
	8 D	18 C				
OUTCI.	-	EXTERNAL.		12 W	13 W	16 W
	21 W					
PERT	Z	300B		7 D	20 =	26
	27					
PERTRB	-	210B ENTRY		5 E		
PHS	R	303B		19 =	20 A	20 A
	21 W					
PI	R	0B /CONST/		9 D	17 A	
PIBY2	R	1B /CONST/		9 D		
PI2	R	3B /CONST/		9 D		
PI3BY2	R	2B /CONST/		9 D		
RAD	R	4B /CONST/		9 D		
SIN.	R	B.E.F.		20 A		
TAPE6#	-	EXTERNAL.		12 W	13 W	16 W
	21 W					

```

1      C/////PERTRB INTRODUCES DETERMINISTIC ERRORS INTO THE REFLECTOR SURFACE.
      C/ THIS VERSION ALLOWS A PERTURBATION OF THE REFLECTOR,
      C/ NORMAL TO IT, TO BE READ IN. (INTERPOLATED IN RHO DIMENSION)
      C/
5      SUBROUTINE PERTRB( E0,AR,AA,NR,NA,NARR,FOCL,IO, E1 )
      C
      COMPLEX E0(2,NR,NA),E1(2,NR,NA),PERT
      DIMENSION AR(NR),AA(NA),ARP(64),RP(64)
      COMMON /CONST/ PI, P1BY2, P13BY2, PI2, RAD, DEG, EPS, AK
10     DATA ARP / 64*1. /
      C
      PRINT*, " THE REFL. SURFACE ERROR DATA ARE BEING READ FROM TAPES "
      READ (5,*) NRP, (RP(K), K=1,NRP)
      WRITE(6,930) (RP(K), K=1,NRP)
15     WRITE(6,935)
      F2I = (.5/FOCL)**2
      NAM = NA - 1
      DO 200 J=1,NAM
        READ (5,*) (ARP(K), K=1,NRP)
        IF (IO .GE. 1) WRITE(6,940) J, (ARP(K), K=1,NRP)
20     K1 = 2
      C-----INTERPOLATE ERRORS
      DO 100 I=1,NR
        R = AR(I)
25     DO 40 K=K1,NRP
          IF (RP(K) .LT. R) GO TO 40
          GO TO 50
        40    CONTINUE
        K = NRP
30     50    ERR = (R-RP(K-1))*(ARP(K)-ARP(K-1))/(RP(K)-RP(K-1)) +ARP(K-1)
        K1 = K
      C-----CALCULATE PERTURBATION (WITH CORRECTION FROM NORMAL)
      PHS = 2.*AK*ERR * SQRT( R**2*F2I + 1. )
      PERT = CMPLX( COS(PHS), SIN(PHS) )
35     E1(1,I,J) = E0(1,I,J) * PERT
      E1(2,I,J) = E0(2,I,J) * PERT
      100    CONTINUE
      200    CONTINUE
      DO 300 I=1,NR
        E1(1,I,NA) = E1(1,I,1)
        E1(2,I,NA) = E1(2,I,1)
40     300    CONTINUE
      RETURN
      C
45     930 FORMAT(" THE RADII AT WHICH ERROR IS DEFINED ARE: "//(5X,18F7.3) )
      935 FORMAT(" THE ERRORS (INCHES NORMAL TO THE REFLECTOR) ARE: "//)
      940 FORMAT( 15,(18F7.3) )
      END

```

SUBROUTINE PERTRB 74/74 TS

--COMMON BLOCKS--

10B /CONST/

--EXTERNALS--

COS. INPFI. INPFR. OUTCI. OUTCR. OUTFI. OUTPUT\* SIN.  
SQRT. TAPE5# TAPE6#

--STATEMENT LABELS--

.40	D	114B	25 D	26	28 L
.50		120B	27	30 L	
.100	D	215B	23 D	37 L	
.200	D	221B	18 D	38 L	
.300	ID	0B	39 D	42 L	
.930	F	300B	14 W	45 L	
.935	F	307B	15 W	46 L	
.940	F	316B	20 W	47 L	

--VARIABLE MAP--

AA	R A	0B	VAR-DIM	5 A	8 D	
AK	R	7B /CONST/		9 D	33	
AR	R A	0B	VAR-DIM	5 A	8 D	24
ARP	R	460B	64	8 D	10 I	19 R
	20 W	30	30	30		
CMPLX	Z	INTRINSIC		34		
COS.	R	B.E.F.		34 A		
DEG	R	5B /CONST/		9 D		
EPS	R	6B /CONST/		9 D		
ERR	R	565B		30 =	33	
E0	Z A	0B	VAR-DIM	5 A	7 D	35
	36					
E1	Z A	0B	VAR-DIM	5 A	7 D	35 =
	36 =	40	40 =	41	41 =	
FOCL	R A	0B		5 A	16	
F2I	R	356B		16 =	33 A	
I	I	563B		23 C	24 S	35 S
	35 S	36 S	36 S	40 S	40 S	41 S
	41 S					
INPFI.	-	EXTERNAL.		13 R	19 R	
INPFR.	-	EXTERNAL.		13 R	13 R	19 R
IO	19 R					
J	I A	0B		5 A	20 F	
	I	561B		18 C	20 W	35 S
	35 S	36 S	36 S			
K	I	353B		13 C	13 S	14 C
	14 S	19 C	19 S	20 S	25 C	26 S
	29 =	30 S	30 S	30 S	30 S	30 S
	31					
K1	I	562B		21 =	25 C	31 =
NA	I A	0B		5 A	7 D	7 D
	8 D	17	40 S	41 S		
NAM	I	560B		17 =	18 C	
NARR	I A	0B		5 A		
NR	I A	0B		5 A	7 D	7 D
	8 D	23 C	39 C			
NRP	I	352B		13 R	13 C	14 C
	19 C	20 C	25 C	29		
OUTCI.	-	EXTERNAL.		14 W	15 W	20 W
OUTCR.	-	EXTERNAL.		14 W	14 W	20 W
	20 W					
OUTFI.	-	EXTERNAL.		12 W		
OUTPUT*	-	EXTERNAL.		12 W		
PERT	Z	354B		7 D	34 =	35
	36					
PERTRB	-	263B ENTRY		5 E		
PHS	R	457B		33 =	34 A	34 A

SUBROUTINE PERTRB 74/74 TS

PI	R	0B /CONST/			9 D		
PIBY2	R	1B /CONST/			9 D		
PI2	R	3B /CONST/			9 D		
PI3BY2	R	2B /CONST/			9 D		
R	R	564B			24 =	26 F	30
	33 A						
RAD	R	4B /CONST/			9 D		
RP	R U	357B	64		8 D	13 R	14 W
	26 F	30	30	30			
SIN.	R	B.E.F.			34 A		
SQRT.	R	B.E.F.			33		
TAPE5*	-	EXTERNAL.			13 R	19 R	
TAPE6*	-	EXTERNAL.			14 W	15 W	20 W

576B PROGRAM-UNIT LENGTH 51 SYMBOLS  
162 REFERENCES

41000B CM STORAGE USED 1.654 SECONDS



SUBROUTINE POLAR

74/74 OPT=1

FTN 4.8+577

```

1      C/////POLAR  CALCULATES THE COEFFICIENTS OF *CONJG(F(I))*F(J)
      C/      TO OBTAIN THE RADIATED POWER IN TWO ORTHOGONAL POLS (K)
      C/
      C/      THIS VERSION IS FOR THE SCALAR CASE
5      C/
      SUBROUTINE POLAR( AKR,AKP,IO,  P )
      COMPLEX P(2,2,2)
      COEFFICIENTS (I,J,K) ARE COMPLEX TO WORK SITH MSUM ROUTINE.
10     C
      DO 10  I=1,8
          P(I) = (0.,0.)
10     CONTINUE
          P(1) = (1.,0.)
          P(8) = (1.,0.)
15     C      IF (IO .GE. 1) WRITE(6,910)  P
      RETURN
      C
      ENTRY POLINIT
      C
20     AKR = " SCALAR "
      AKP = "0"
      WRITE(6,900)
      C
      RETURN
25     900 FORMAT("/" THE SCALAR APPROXIMATION WILL BE DISPLAYED"////)
      910 FORMAT(" COEFFICIENTS OF CONJG(F(I))*F(J) FOR POLARIZATION"//
      *      (4(2F10.4,2X))  )
      END

```

SUBROUTINE POLAR

74/74

TS

--ENTRY POINTS--

51B POLAR

31B POLINIT

--EXTERNALS--

OUTCI. TAPE6\*

--STATEMENT LABELS--

.10	ID	0B	10 D	12 L
.900	F	65B	22 W	25 L
.910	F	74B	26 L	

--VARIABLE MAP--

AKP	R A	0B	6 A	21 =
AKR	R A	0B	6 A	20 =
I	I	110B	10 C	11 S
IO	I A	0B	6 A	
OUTCI.	-	EXTERNAL.	22 W	
P	Z A	0B	6 A	7 D
	13 =	14 =	8	11 =
POLAR	-	51B ENTRY	6 E	
POLINIT	-	31B ENTRY	18 E	
TAPE6*	-	EXTERNAL.	22 W	

111B PROGRAM-UNIT LENGTH  
21 REFERENCES

12 SYMBOLS

41000B CM STORAGE USED

.214 SECONDS

SUBROUTINE QUAD

74/74 OPT=1

FTN 4.8+577

```

1      C/////QUAD  CALCULATED THE COEFFICIENTS OF A QUADRATIC THAT FITS
      C/    THREE POINTS.
      C/
5      C      SUBROUTINE QUAD(X1,X2,X3,Y1,Y2,Y3,    A,B,C)
      DET=1./(X1*X1*(X2-X3) - X1*(X2*X2-X3*X3) + X2**2*X3-X2*X3**2)
      A=(X2-X3)*Y1+(X3-X1)*Y2+(X1-X2)*Y3
      A=A*DET
      B=(X3**2-X2**2)*Y1+(X1**2-X3**2)*Y2+(X2**2-X1**2)*Y3
10     B=B*DET
      C=(X2**2*X3-X2*X3**2)*Y1+(X1*X3**2-X1**2*X3)*Y2
      C= C*DET
      RETURN
15     END

```

SUBROUTINE QUAD

74/74 TS

--VARIABLE MAP--

A	R A	0B	4 A	7 =	8
	8 =				
B	R A	0B	4 A	9 =	10
	10 =				
C	R A	0B	4 A	11 =	13
	13 =				
DET	R	70B	6 =	8	10
	13				
QUAD	-	65B ENTRY	4 E		
X1	R A	0B	4 A	6	6
	6	7	9	11	11
	11	11			
X2	R A	0B	4 A	6	6
	6	6	7	9	9
	11	11	11		
X3	R A	0B	4 A	6	6
	6	6	7	9	9
	11	11	11		
Y1	R A	0B	4 A	7	9
	11				
Y2	R A	0B	4 A	7	9
	11				
Y3	R A	0B	4 A	7	9
	11				

71B PROGRAM-UNIT LENGTH  
69 REFERENCES

11 SYMBOLS

41000B CM STORAGE USED

.384 SECONDS

FTN 4.8+577 83/08/11. 15.54.36 PAGE 93  
SUBROUTINE SOLVE 74/74 TS

```

C/////SOLVE FINDS THE ROOTS OF A QUADRATIC.
C/
SUBROUTINE SOLVE(A,B,C,TDBP, X3DB)
C
5 RAD=B*B-4.*A*(C-TDBP)
IF(A.NE.0.) X3DB1=(-B-SQRT(RAD))/(2.*A)
IF(A.NE.0.) X3DB2=(-B+SQRT(RAD))/(2.*A)
XX1=2.*A*X3DB1+B
XX2=2.*A*X3DB2+B
10 IF(XX1.LE.0.) X3DB=X3DB1
IF(XX2.LE.0.) X3DB=X3DB2
IF(A.EQ.0..AND.B.NE.0.) X3DB=(TDBP-C)/B
C
RETURN
15 END

```

SUBROUTINE SOLVE 74/74 TS

--EXTERNALS--

SQRT.

--VARIABLE MAP--

A	R A	0B			3 A	5	6 F
	6	7 F	7	8	9	12 F	
B	R A	0B			3 A	5	5
	6	7	8	9	12 F	12	
C	R A	0B			3 A	5	12
RAD	R	104B			5 =	6 A	7 A
SOLVE	-	76B	ENTRY		3 E		
SQRT.	R		B.E.F.		6	7	
TDBP	R A	0B			3 A	5	12
XX1	R	105B			8 =	10 F	
XX2	R	106B			9 =	11 F	
X3DB	R A	0B			3 A	10 =	11 =
	12 =						
X3DB1	R	102B			6 =	8	10
X3DB2	R	103B			7 =	9	11

107B PROGRAM-UNIT LENGTH 12 SYMBOLS  
44 REFERENCES

41000B CM STORAGE USED .239 SECONDS

# SECTION IV

## DEFINITION OF MAJOR VARIABLES

The purpose of this section is to provide a convenient reference to one who has occasion to study the program in more depth than normal usage would require. It is intended that all variables except those that are either very temporary or those with obvious definitions are listed here. Coordinates are best described by a diagram. The reflector coordinate system and the far-field coordinates are presented in Figure 3. The following list does not include those variables that are described in the input section of the user's guide.

<u>Variable</u>	<u>Type</u>	<u>Definition</u>
AK	R	Free-space propagation constant $ \underline{k}  = 2\pi/\lambda$
AKP, AKR	R	Two of the three cylindrical components of $k_\rho$ and $k_\phi$ .
AREA	R	Area of the projection of the reflector in the z direction.
A2	R	Angular width of a sector.
C	R	Speed of light (Giga-inches per second).
CAREA	R	Area of a randomly positioned defect.
DA	R	Azimuthal reflector sample spacing in radians.
EO (10,000)	C	Unperturbed aperture fields.
EOT (2,32)	C	Physical-optics integral of EO.
E1 (10,000)	C	Aperture fields with deterministic error.
E1PT (2,32)	C	Physical optics integral of E1 x P.



<u>Variable</u>	<u>Type</u>	<u>Definition</u>
EIT (2,32)	C	Physical-optics integral of El.
FBAR (2)	C	Mean radiated field accumulation.
FO (2)	C	Unperturbed radiated field accumulation.
F1 (2)	C	Accumulation of radiated field with deterministic errors.
F2PBAR (2,301)	C	Pattern of mean uncorrelated error.
GT (2,2,32)	C	Dyadic scattering pattern of one random defect.
HTT (4)	C	Dyadic arising from correlation of random errors between sectors.
IPOL	I	Polarization flag passed from subroutine APER.
NANR	R	Number of sample points in a sector.
NTOTL	I	Total number of sample points in the reflector.
NTOTL2	I	Number of aperture field samples for both polarizations
P (1024)	R	Probability density as a function of position on a sector.
PBAR (2,301)	C	Mean total radiated power pattern.
POL (2)	R	Alpha-numeric polarization labels defined by subroutine POLAR.
POL3 (8)	C	Matrix required to calculate polarization components defined by routine POLAR.
PO (2,301)	C	Unperturbed radiated pattern.
P1 (2,301)	C	Radiated pattern with deterministic errors.
THETA (301)	R	Angles at which radiated pattern is calculated.

<u>Variable</u>	<u>Type</u>	<u>Definition</u>
UNIF	R	Flag indicating that variable P is constant.
WAVE	R	Wavelength. $\lambda = c/\text{frequency}$ .

SECTION V  
APDERS USER'S GUIDE

A. Installation and Execution

The program package includes all the component routines required for execution except those which are intrinsic in standard FORTRAN and a few other general purpose routines. The latter group of routines is believed to be widely available with the computers of most users, but they may require slight modification of calling format. The unfurnished, undocumented routines are as follows:

- a) Computer Intrinsic
  - DATE        accesses computer calendar
  - TIME        accesses computer clock
  - SECOND      reads computer clock as a variable
- b) Calcomp Library
  - PLOT        moves plotter pen
  - PLOTS       initializes plotter
  - PLOTMX      sets plotter security limit
  - NUMBER      draws a number
  - SYMBOL      draws a symbol or a letter
  - CIRCLE      plots an arc of a circle

The program was developed on a CDC CYBER 760 computer and requires 241,000 words of core. This requirement is for a dimension of 10,000 for the complex aperture arrays. The dimension specifications may be changed by changing only statements 21 and 22 in the main program. The aperture sector dimensions can be varied arbitrarily by the input parameters NA and NR. It is only required that  $(NA+1) + NR + NARR$  be less than the half this specified dimension.

The computer time required for the calculation of patterns for a 250 wavelength reflector with no random error is about 16 seconds per pattern point on the CYBER 730 computer. This time was observed for the scalar case with one sector and for 400 pattern points.

Communication with the program is accomplished through three data files declared in the program statement and by a variable number of undeclared plot files. The details of these files are specified in the following subsections. Output is discussed first so that the very last subsection of this document is the most used one, the input guide.



## B. APDERS Output

A good way to describe computer output is by example. Therefore, a sample program has been analyzed, and the actual results are shown in this section. This approach, perhaps more importantly, provides the user with a convenient means of verifying a new installation.

1. File OUTPUT     This file contains the instructions for program input. When the program is used interactively, an instruction appears at the user's terminal before each set of input parameters. When the program is run in batch mode, the instructions appear all together as shown in Figure 4. Even in batch mode, this output is useful in identifying and debugging the various parameters in the input file. These instructions, of course, are not fixed but depend on previous input parameters and on the version of the subroutine chosen for PDF, GERT and PERTRB.
  
2. File RESULT (Unit 6)     The sample output for the test case, as produced by a line printer, is presented in Figures 5 through 11. It is generally self explanatory, but there are some features to note. All pages begin with a header containing the date, time, and run title that uniquely define each execution. This header is also repeated on every plot file, saving time and risk of error in cataloging results. All input variables are echoed in this file in very nearly the order of occurrence in file INPUT. Where more than one version of a subroutine exists, the one used will be identified in this file. For instance, in Figure 8 the surface error perturbation is identified as the separable type. All values are dimensioned in inches, degrees, and dB unless otherwise noted. The word "field" indicates the dimension of volts.

Figure 9 shows a special "warning" printed by the program when the random defect scattering is not very localized. Figures 9 and 10 contain a series of warnings that subroutine HFTHFT writes to indicate that integration may not be accurate enough. A warning is printed whenever the change of exponents across in integration cell in either the azimuth or radial direction is larger than  $\pi/2$ .

```

ENTER THE TITLE FOR THIS RUN
ENTER DEFINITION OF THETA PATTERNS
  THETA START, STOP, AND INCREMENT; PHI LIKEWISE
DO YOU WANT BOTH ORTHOGONAL COMPONENTS (Y,N)-
  COMPONENTS TO PLOT: UNPETERBED CASE (1)
                     MEAN FOR TOTAL ERROR (2)
                     DETERMINISTIC ERROR (3)
                     UNCORRELATED ERRORS (4)
DO YOU WANT TO SPECIFY THE CALCOMP GRID (Y,N)
ENTER REFLECTOR RADII: MIN, MAX, SPACING, POINTS
  (NUMBER OF POINTS IS USED IF SPACING = 0.)
ENTER AZIMUTH SECTOR: (MIN=0), SECTORS, SPACING, POINTS
ENTER THE FREQUENCY, DEBUG LEVEL, AND SYMETRY CODE
ENTER FOCAL LENGTH, ECCENTRICITY, AND FEED TYPE
ENTER COSINE EXPONANT
ENTER THE APERTURE DISPLAY PARAMETERS
ENTER 0 IF NO DETERMINISTIC ERRORS
INPUT DEFORMATION (IN.) NORMAL TO THE REFLECTOR FOR 21
POINTS ALONG THE RADII
INPUT NORMALIZED PERTURBATION FOR 13
AZIMUTHAL POINTS FOR ONE SECTOR.
ENTER THE PERTURBATION DISPLAY PARAMETERS
ENTER NUMBER, COMPLEX HEIGHT, AND CORRELATION OF DEFECTS

```

Figure 4. File OUTPUT generated by the test case.

83/08/15. 15.45.15. TEST CASE

" \*\*\* PROGRAM APDERS \*\*\* "  
" ANALYSIS OF DETERMINISTIC AND PROBABILISTIC ERRORS IN REFLECTOR ANTENNAS"  
" LATEST REVISION: 83/07/28 "

83/08/15. 15.45.15. TEST CASE

PATTERN CUTS TO BE CALCULATED (THETA CUTS, DEG)

	BEGIN	END	STEP	POINTS
THETA	0.00	30.00	1.80	17
PHI	0.00	45.00	45.00	2

THE SCALAR APPROXIMATION WILL BE DISPLAYED

" APERTURE PARAMETERS "  
" ----- "

THE DEBUG OUTPUT LEVEL IS 1 THE SYMETRY LEVEL IS 3

THE FREQUENCY AND WAVELENGTH (IN.) ARE: 11.80285 1.00000

THE APERTURE IS DEFINED BY:

	MINIMUM	MAXIMUM	INCREMENT(IN., WAVE)		POINTS
RHD	0.00000	5.00000	.250000	.250000	21
PHI	0.00000	60.00000	5.000000	.436332	13

THE NUMBER OF SECTORS IS 6

Figure 5. Pages 1 and 2 of file RESULT.

03/08/15. 15.45.15. TEST CASE

" UNPERTURBED APERTURE "  
" ----- "

ANTENNA MODEL IS A (SCALAR) COS\*\*N FEED IN AN  
AXIALLY SYMETRIC CASSEGRAIN REFLECTOR SYSTEM.

PARABOLOID FOCAL LENGTH 4.000  
HYPERPOLOID ECCENTRICITY 2.000

THE EXPONANT OF COS(THETA) IS 16.000

POINT	RADIUS	TAN(PHI/2)**2	FIELD
1	0.0000	0.0000	1.0000
2	.2500	.0001	.9964
3	.5000	.0004	.9858
4	.7500	.0010	.9683
5	1.0000	.0017	.9443
6	1.2500	.0027	.9144
7	1.5000	.0039	.8791
8	1.7500	.0053	.8391
9	2.0000	.0069	.7952
10	2.2500	.0088	.7483
11	2.5000	.0109	.6991
12	2.7500	.0131	.6484
13	3.0000	.0156	.5972
14	3.2500	.0183	.5461
15	3.5000	.0213	.4957
16	3.7500	.0244	.4469
17	4.0000	.0278	.3999
18	4.2500	.0314	.3553
19	4.5000	.0352	.3135
20	4.7500	.0392	.2746
21	5.0000	.0434	.2388

THE APERTURE PLOTTING PARAMETERS ARE:  
2 1 0 1 5 1 1 0 4

Figure 6. Page 3 of file RESULT.

83/08/15. 15.45.15. TEST CASE

X-CUT IN APERTURE AT 0.0000. POLARIZATION

ARRAY POINT		POSITION (IN./RAD)	AMPLITUDE (DB)	PHASE (DEGREES)
1	1	0.000	0.000	0.000
2	1	.250	-.031	0.000
3	1	.500	-.124	0.000
4	1	.750	-.280	0.000
5	1	1.000	-.498	0.000
6	1	1.250	-.778	0.000
7	1	1.500	-1.120	0.000
8	1	1.750	-1.524	0.000
9	1	2.000	-1.990	0.000
10	1	2.250	-2.519	0.000
11	1	2.500	-3.110	0.000
12	1	2.750	-3.763	0.000
13	1	3.000	-4.478	0.000
14	1	3.250	-5.255	0.000
15	1	3.500	-6.095	0.000
16	1	3.750	-6.997	0.000
17	1	4.000	-7.961	0.000
18	1	4.250	-8.987	0.000
19	1	4.500	-10.076	0.000
20	1	4.750	-11.227	0.000
21	1	5.000	-12.440	0.000

Figure 7. Page 4 of file RESULT.

83/08/15. 15.45.15. TEST CASE

" PERTURBED APERTURE "  
" ----- "

THE REFLECTOR PERTURBATION IS SEPARABLE IN RHO AND PHI  
THE DISPLACEMENT (IN.) NORMAL TO THE SURFACE AS A FUNCTION OF RADI

POINT	RADIUS	DISPLACEMENT
1	0.000	1.0000
2	.250	1.0000
3	.500	1.0000
4	.750	1.0000
5	1.000	1.0000
6	1.250	1.0000
7	1.500	1.0000
8	1.750	1.0000
9	2.000	1.0000
10	2.250	1.0000
11	2.500	1.0000
12	2.750	1.0000
13	3.000	1.0000
14	3.250	1.0000
15	3.500	1.0000
16	3.750	1.0000
17	4.000	1.0000
18	4.250	1.0000
19	4.500	1.0000
20	4.750	1.0000
21	5.000	1.0000

THE NORMALIZED PERTURBATION AS A FUNCTION OF AZIMUTH:

POINT	AZIMUTH	DISPLACEMENT
1	0.000	1.0000
2	.087	1.0000
3	.175	1.0000
4	.262	1.0000
5	.349	1.0000
6	.436	1.0000
7	.524	1.0000
8	.611	1.0000
9	.698	1.0000
10	.785	1.0000
11	.873	1.0000
12	.960	1.0000
13	1.047	1.0000

THE APERTURE PLOTTING PARAMETERS ARE:  
2 1 0 1 5 1 1 0 4

Figure 8. Page 5 of file RESULT.

03/08/15. 15.45.15. TEST CASE

" RANDOM DEFECTS "  
" ----- "

THE NUMBER OF RANDOM DEFECTS PER SECTOR IS 1.700

POINT SOURCE DEFECTS WITH RADIATION PEAK 1.0000 0.0000 AND SHAPE, COS\*\*

\*\*\* WARNING \*\*\*  
PERTURBATION AREA 3.14 IS NOT SMALL COMPARED TO  
APERTURE AREA 13.09

PROBABILITY DENSITY IS UNIFORM OVER A SECTOR  
WITH A VALUE OF .076394

EXPONANT CHANGE (AZ) =	1.5942	FOR M,L,J =	5	1	12
EXPONANT CHANGE (AZ) =	1.6065	FOR M,L,J =	5	1	13
EXPONANT CHANGE (AZ) =	1.6009	FOR M,L,J =	4	1	12
EXPONANT CHANGE (AZ) =	1.7018	FOR M,L,J =	4	1	13
EXPONANT CHANGE (AZ) =	1.6145	FOR M,L,J =	5	1	9
EXPONANT CHANGE (AZ) =	1.6666	FOR M,L,J =	5	1	10
EXPONANT CHANGE (AZ) =	1.7061	FOR M,L,J =	5	1	11
EXPONANT CHANGE (AZ) =	1.7325	FOR M,L,J =	5	1	12
EXPONANT CHANGE (AZ) =	1.7458	FOR M,L,J =	5	1	13
EXPONANT CHANGE (AZ) =	1.6050	FOR M,L,J =	4	1	11
EXPONANT CHANGE (AZ) =	1.7271	FOR M,L,J =	4	1	12
EXPONANT CHANGE (AZ) =	1.8360	FOR M,L,J =	4	1	13
EXPONANT CHANGE (AZ) =	1.5900	FOR M,L,J =	5	1	7
EXPONANT CHANGE (AZ) =	1.6722	FOR M,L,J =	5	1	8
EXPONANT CHANGE (AZ) =	1.7418	FOR M,L,J =	5	1	9
EXPONANT CHANGE (AZ) =	1.7980	FOR M,L,J =	5	1	10
EXPONANT CHANGE (AZ) =	1.8406	FOR M,L,J =	5	1	11
EXPONANT CHANGE (AZ) =	1.8691	FOR M,L,J =	5	1	12
EXPONANT CHANGE (AZ) =	1.8835	FOR M,L,J =	5	1	13
EXPONANT CHANGE (AZ) =	1.5767	FOR M,L,J =	4	1	10
EXPONANT CHANGE (AZ) =	1.7207	FOR M,L,J =	4	1	11
EXPONANT CHANGE (AZ) =	1.8516	FOR M,L,J =	4	1	12
EXPONANT CHANGE (AZ) =	1.9684	FOR M,L,J =	4	1	13
EXPONANT CHANGE (AZ) =	1.6035	FOR M,L,J =	5	1	6
EXPONANT CHANGE (AZ) =	1.7046	FOR M,L,J =	5	1	7
EXPONANT CHANGE (AZ) =	1.7928	FOR M,L,J =	5	1	8
EXPONANT CHANGE (AZ) =	1.8673	FOR M,L,J =	5	1	9
EXPONANT CHANGE (AZ) =	1.9276	FOR M,L,J =	5	1	10
EXPONANT CHANGE (AZ) =	1.9733	FOR M,L,J =	5	1	11
EXPONANT CHANGE (AZ) =	2.0039	FOR M,L,J =	5	1	12
EXPONANT CHANGE (AZ) =	2.0193	FOR M,L,J =	5	1	13
EXPONANT CHANGE (AZ) =	1.6812	FOR M,L,J =	4	1	10
EXPONANT CHANGE (AZ) =	1.8347	FOR M,L,J =	4	1	11
EXPONANT CHANGE (AZ) =	1.9743	FOR M,L,J =	4	1	12
EXPONANT CHANGE (AZ) =	2.0988	FOR M,L,J =	4	1	13
EXPONANT CHANGE (AZ) =	1.5889	FOR M,L,J =	5	1	5
EXPONANT CHANGE (AZ) =	1.7098	FOR M,L,J =	5	1	6
EXPONANT CHANGE (AZ) =	1.8176	FOR M,L,J =	5	1	7
EXPONANT CHANGE (AZ) =	1.9116	FOR M,L,J =	5	1	8
EXPONANT CHANGE (AZ) =	1.9910	FOR M,L,J =	5	1	9
EXPONANT CHANGE (AZ) =	2.0554	FOR M,L,J =	5	1	10

Figure 9. Page 6 of file RESULT.

83/08/15. 15.45.15. TEST CASE

PERFORMANCE PARAMETERS OF PATTERNS AT PHI = 0.000 NORMALIZED TO 32.4024

PEAK (DB)	BEAMWIDTH (DEG)	3DB POINT (DEG)	1ST SIDELOBE LEVEL	1ST SIDELOBE LOC (DEG)
0.000	6.764	3.382	26.324	11.091
-0.656	7.278	3.639	24.305	15.634
-1.742	7.256	3.628	26.673	15.407

SCALAR POLARIZATION PATTERNS AT PHI = 0.000

THETA	UNPERTURBED	ALL ERRORS	DETERMINISTIC	UNCORRELATED
1 0.00	0.000	-0.656	-1.742	-0.681
2 1.80	-0.824	-1.396	-2.487	-1.426
3 3.60	-3.418	-3.605	-4.708	-3.647
4 5.40	-8.280	-7.050	-8.184	-7.124
5 7.20	-17.120	-10.692	-11.884	-10.824
6 9.00	-38.083	-13.486	-14.722	-13.661
7 10.80	-26.552	-16.872	-18.201	-17.140
8 12.60	-32.449	-22.293	-24.284	-23.224
9 14.40	-38.443	-25.448	-29.170	-28.110
10 16.20	-31.597	-25.063	-28.884	-27.824
11 18.00	-35.904	-26.749	-33.428	-32.368
12 19.80	-46.783	-27.872	-43.100	-42.039
13 21.60	-35.387	-26.988	-35.269	-34.209
14 23.40	-36.470	-27.053	-36.401	-35.341
15 25.20	-47.676	-27.587	-46.994	-45.933
16 27.00	-41.301	-27.346	-41.285	-40.225
17 28.80	-38.679	-27.096	-38.914	-37.853
EXPONANT CHANGE (AZ) = 1.6666 FOR M,L,J = 3 1 2				
EXPONANT CHANGE (AZ) = 1.6145 FOR M,L,J = 3 1 3				
EXPONANT CHANGE (AZ) = 1.7980 FOR M,L,J = 3 1 2				
EXPONANT CHANGE (AZ) = 1.7418 FOR M,L,J = 3 1 3				
EXPONANT CHANGE (AZ) = 1.6722 FOR M,L,J = 3 1 4				
EXPONANT CHANGE (AZ) = 1.5900 FOR M,L,J = 3 1 5				
EXPONANT CHANGE (AZ) = 1.9276 FOR M,L,J = 3 1 2				
EXPONANT CHANGE (AZ) = 1.8673 FOR M,L,J = 3 1 3				
EXPONANT CHANGE (AZ) = 1.7928 FOR M,L,J = 3 1 4				
EXPONANT CHANGE (AZ) = 1.7046 FOR M,L,J = 3 1 5				
EXPONANT CHANGE (AZ) = 1.6035 FOR M,L,J = 3 1 6				
EXPONANT CHANGE (AZ) = 1.5767 FOR M,L,J = 4 1 2				
EXPONANT CHANGE (AZ) = 2.0554 FOR M,L,J = 3 1 2				
EXPONANT CHANGE (AZ) = 1.9910 FOR M,L,J = 3 1 3				
EXPONANT CHANGE (AZ) = 1.9116 FOR M,L,J = 3 1 4				
EXPONANT CHANGE (AZ) = 1.8176 FOR M,L,J = 3 1 5				
EXPONANT CHANGE (AZ) = 1.7098 FOR M,L,J = 3 1 6				
EXPONANT CHANGE (AZ) = 1.5889 FOR M,L,J = 3 1 7				
EXPONANT CHANGE (AZ) = 1.6812 FOR M,L,J = 4 1 2				
EXPONANT CHANGE (AZ) = 2.1810 FOR M,L,J = 3 1 2				
EXPONANT CHANGE (AZ) = 2.1128 FOR M,L,J = 3 1 3				
EXPONANT CHANGE (AZ) = 2.0285 FOR M,L,J = 3 1 4				
EXPONANT CHANGE (AZ) = 1.9287 FOR M,L,J = 3 1 5				
EXPONANT CHANGE (AZ) = 1.8143 FOR M,L,J = 3 1 6				
EXPONANT CHANGE (AZ) = 1.6861 FOR M,L,J = 3 1 7				
EXPONANT CHANGE (AZ) = 1.7840 FOR M,L,J = 4 1 2				
EXPONANT CHANGE (AZ) = 1.6075 FOR M,L,J = 4 1 3				

Figure 10. Page 7 of file RESULT.



83/08/15. 15.45.15. TEST CASE

PERFORMANCE PARAMETERS OF PATTERNS AT PHI = 45.000 NORMALIZED TO 32.4024

PEAK (DB)	BEAMWIDTH (DEG)	3DB POINT (DEG)	1ST SIDELOBE LEVEL	1ST SIDELOBE LOC (DEG)
-----	-----	-----	-----	-----
0.000	6.764	3.382	26.324	11.091
-.656	7.287	3.643	25.109	22.052
-1.742	7.256	3.628	26.673	15.407

SCALAR POLARIZATION PATTERNS AT PHI = 45.000

	THETA	UNPERTURBED	ALL ERRORS	DETERMINISTIC	UNCORRELATED
	-----	-----	-----	-----	-----
1	0.00	0.000	-.656	-1.742	-.681
2	1.80	-.824	-1.394	-2.487	-1.426
3	3.60	-3.418	-3.598	-4.708	-3.647
4	5.40	-8.280	-7.027	-8.184	-7.124
5	7.20	-17.120	-10.625	-11.884	-10.824
6	9.00	-38.083	-13.336	-14.722	-13.661
7	10.80	-26.552	-16.528	-18.201	-17.140
8	12.60	-32.449	-21.282	-24.284	-23.224
9	14.40	-38.443	-23.920	-29.170	-28.110
10	16.20	-31.597	-23.937	-28.884	-27.824
11	18.00	-35.904	-25.350	-33.428	-32.368
12	19.80	-46.783	-26.267	-43.100	-42.039
13	21.60	-35.387	-25.786	-35.269	-34.209
14	23.40	-36.470	-25.945	-36.401	-35.341
15	25.20	-47.676	-26.434	-46.994	-45.933
16	27.00	-41.301	-26.363	-41.285	-40.225
17	28.80	-38.679	-26.289	-38.914	-37.853

WORK	TIME
-----	-----
SET UP PROBLEM	10.219
INTEGRATE EO, E1	267.501
RANDOM ERROR CALC.	60.204
DISPLAY DATA	1.091
-----	-----
TOTAL	339.250

Figure 11. Page 8 of file RESULT.

The user can decide, based on the size of these changes and his accuracy requirements whether the accuracy of the calculations is adequate. This accuracy only affects the analysis of random errors. The integration involved for deterministic errors has an automatic reduction of cell size to maintain accuracy.

The last column of the pattern tables in Figures 10 and 11 requires some explanation. The correlation of the random errors is defined by the subroutine GPRT. This last column shows what the total error pattern would be in the absence of any correlation. Most users will probably use this column only for debugging. As mentioned in Section I, this column and the column labeled "all errors" are mean power patterns. That is, each number is the average power level at the given direction in space that would be produced by a large ensemble of antennas with the described random errors in the presence of the specified deterministic errors.

The pattern of total error appears to have a higher gain than that for deterministic error only. That is because the scattering from defects is not properly normalized to the same units as the integration in subroutine FT. Thus, relative gain is not meaningful when random errors are included.

Additional output can be obtained in this file by increasing the appropriate input parameter, but it is considered debugging output and is usually not desired. It was not included in the sample for that reason, and because it is generally self explanatory unless the most extreme levels of output are called for.

3. File TAPEn (Unit n) Many plot files can be generated as desired by the user. They appear as local files with names of the type TAPEnij where i and j are numerical digits. Digit i is 1 for plots of the unperturbed aperture, 2 for plots of the aperture with perturbations, and 4 or more for far-field plots. When i is less than 4, digit j is between 1 and 4 and indicates the type of plot:

j = 1 three-dimensional amplitude  
2 three-dimensional phase  
3 radial cut amplitude and phase  
4 azimuthal cut amplitude and phase

Examples for the test run are shown in Figures 12 through 17. When polarization is used the vertical axis of these plots will indicate the polarization being plotted. These figures have been reduced to show the guide marks for cutting a standard 8½ x 11 size perimeter around each plot. The original plots are properly proportioned for this standard paper size.

Figures 16 and 17 show the far field plots produced on files beginning with unit 40. The unit number n is then incremented for as many times as there are patterns to be plotted. Here the solid line is the unperturbed far-field pattern and the hashed line is the mean total error pattern.

### C. APDERS Input

There are two input files declared in the program statement. INPUT and TAPE5. TAPE5 is used to provide perturbation data for the reflector surface and is read by subroutine PERTRB. INPUT provides all other input data.

#### 1. File TAPE5 (Unit 5)

This file contains data read by the version of PERTRB that specifies the error along each radial sample line. It was designed to correspond very closely with surface measurement data. It may contain any number of columns because the aperture points are interpolated along each radial. The first line contains NRP, the number of radii at which to read data. Following this, it must contain NA rows, where NA is read from file INPUT. The first row is the set of radius points at which the following surface errors are defined, then NA-1 rows of error are read (the last is the same as the first). All values are dimensioned in inches.

#### 2. File INPUT

This is the only data file that is always required for the execution of APDERS, and it is completely underwritten by default values. Thus the program can be executed without any knowledge of the requirements of this file. Indeed, the test case for which output is presented in the

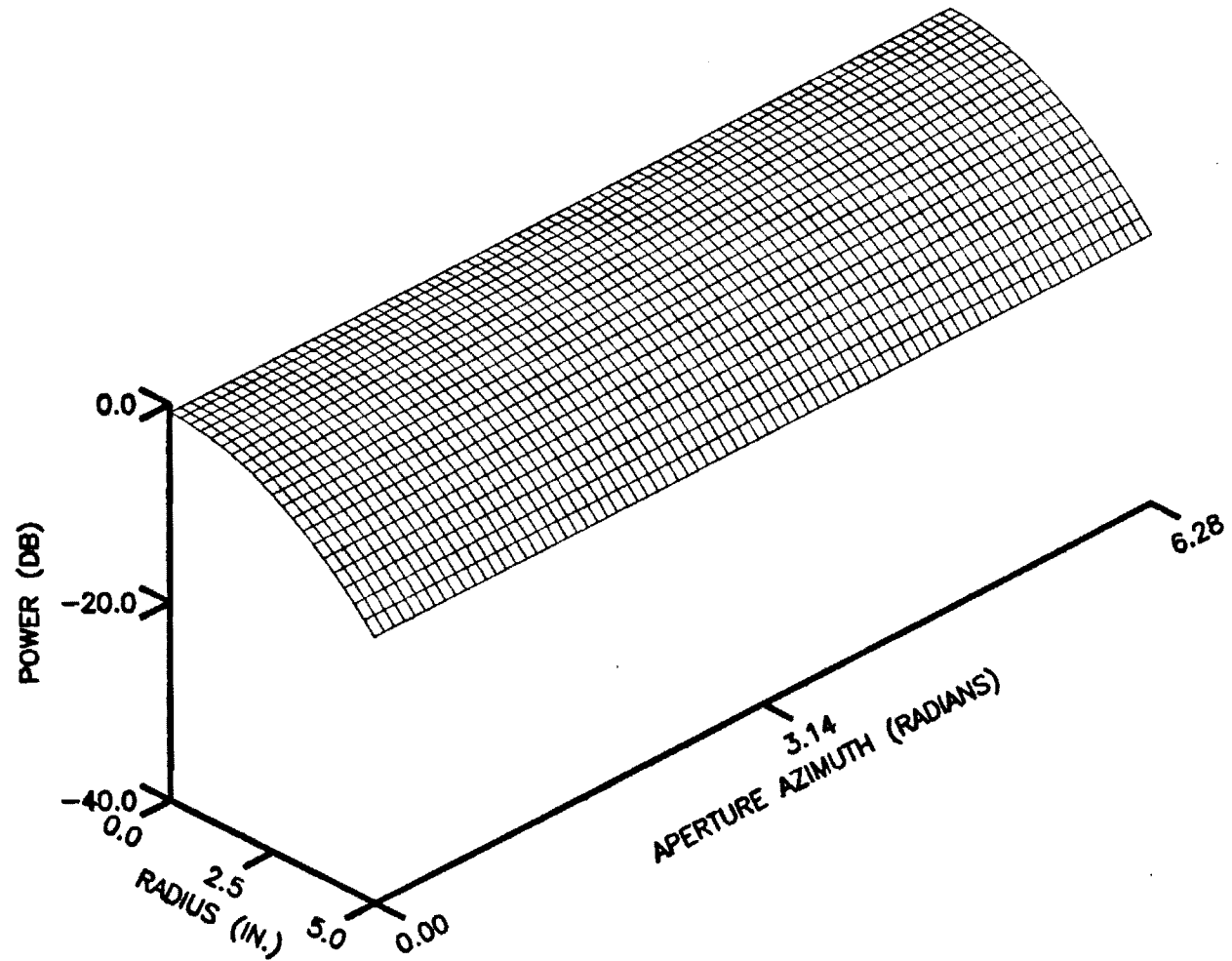


Figure 12. Aperture plot contained in files TAPE11 and TAPE21.

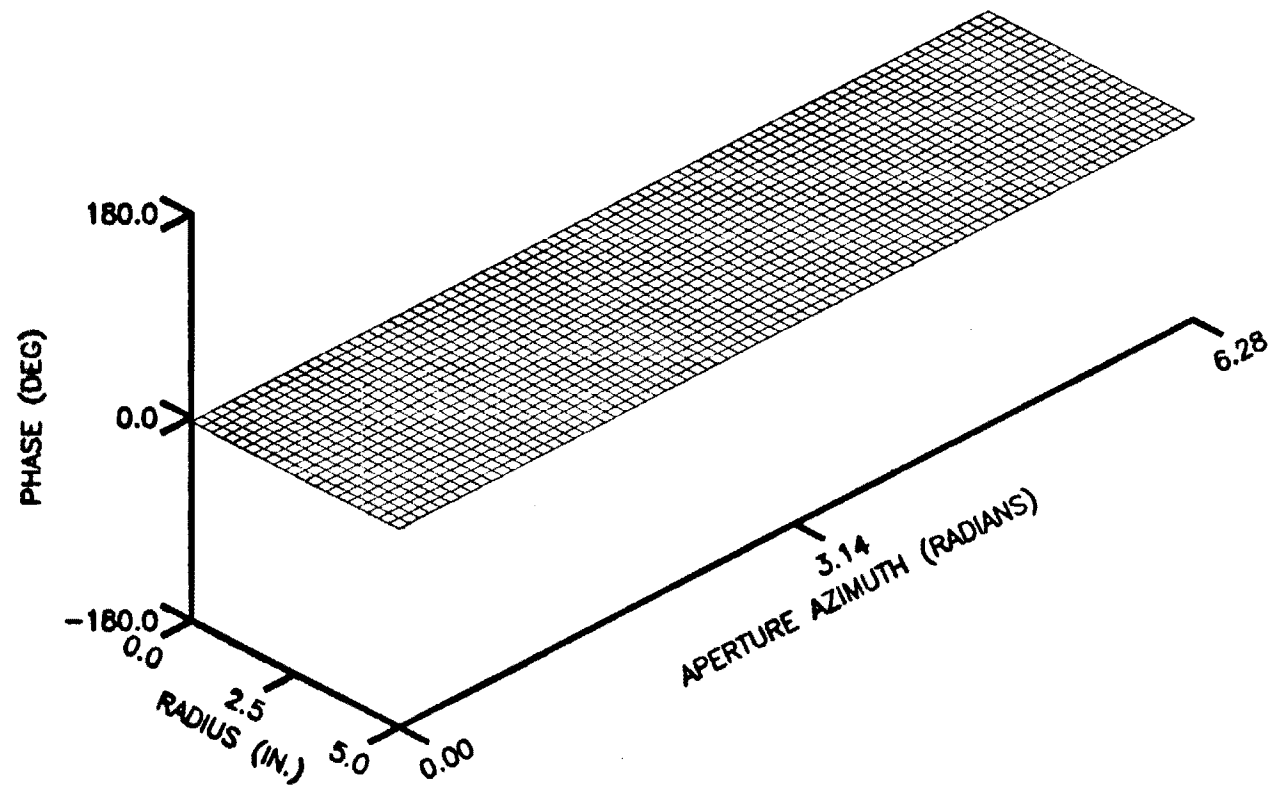


Figure 13. Aperture plot contained in file TAPE12.

83/08/15. 15.45.15. TEST CASE

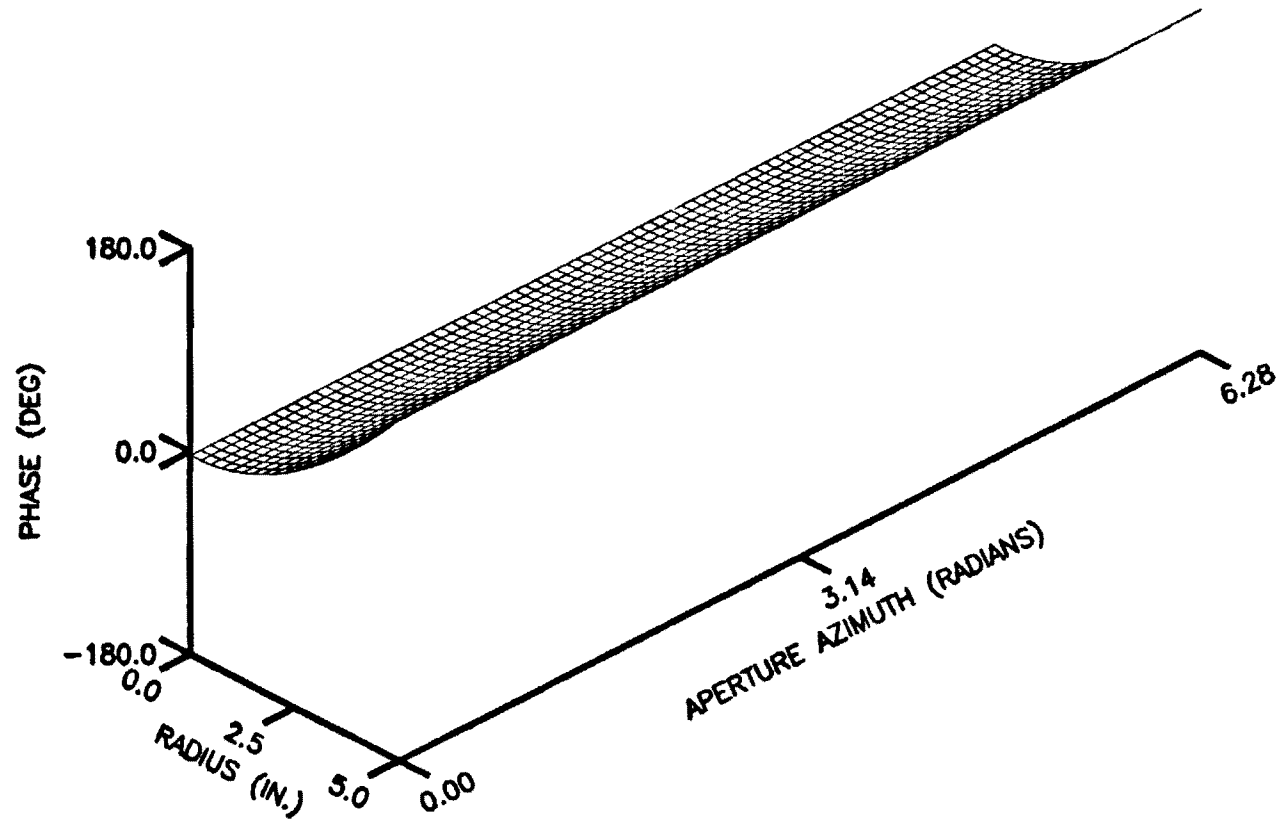
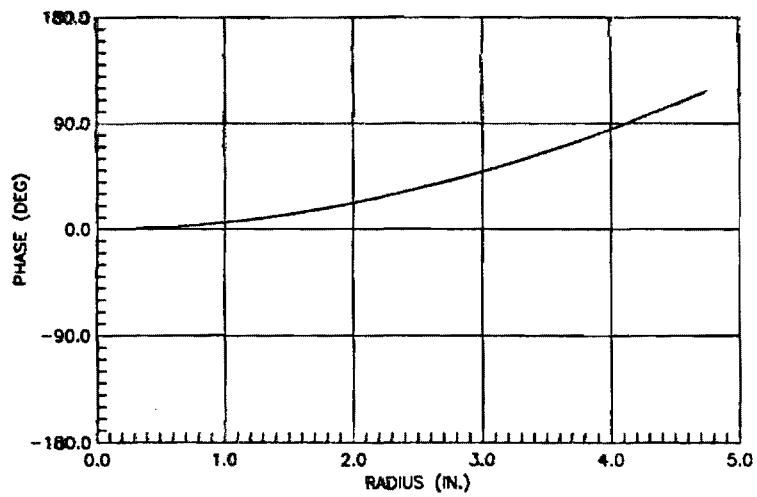


Figure 14. Aperture plot contained in file TAPE22.

83/08/15. 15.45.15. TEST CASE



83/08/15. 15.45.15. TEST CASE

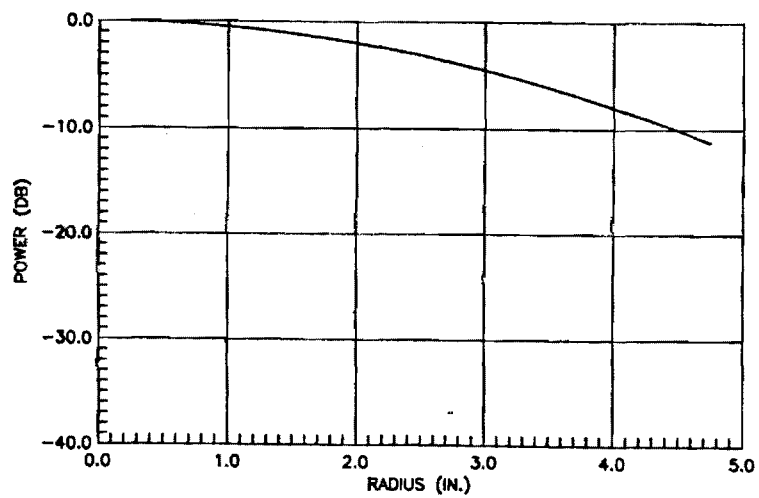


Figure 15. Aperture plot contained in file TAPE23.

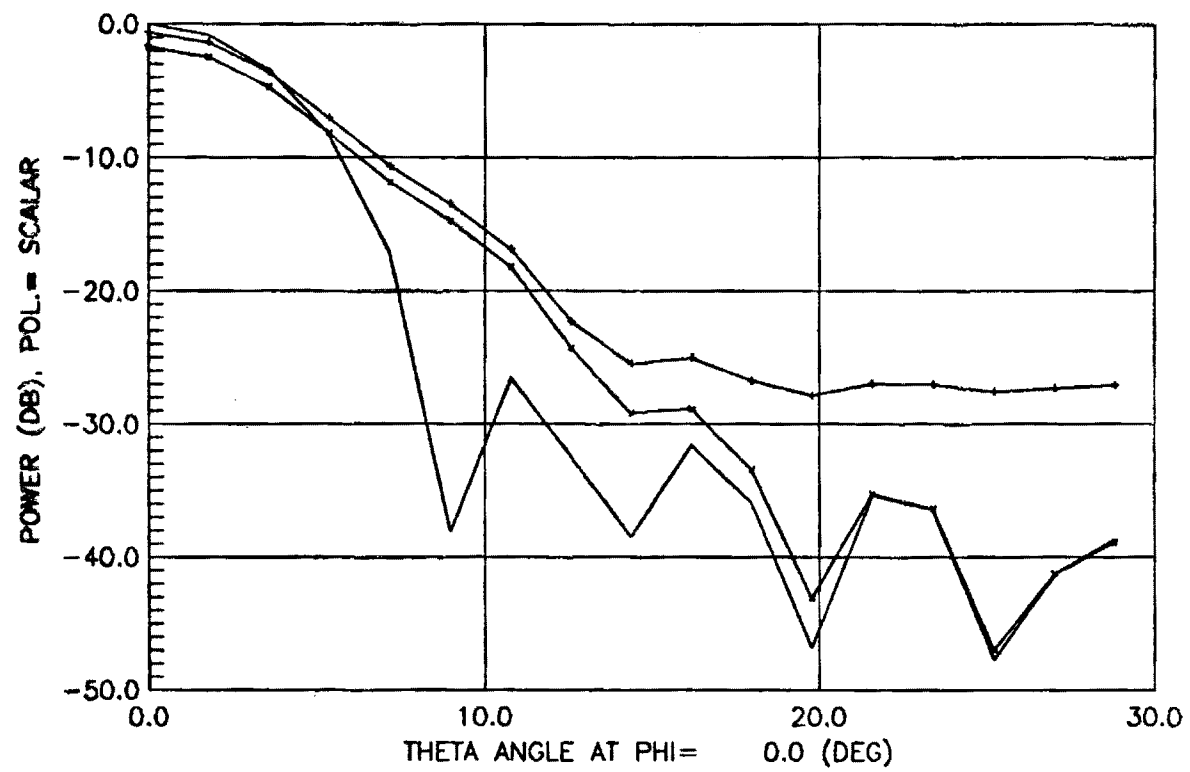


Figure 16. Far-field plot contained in file TAPE40.



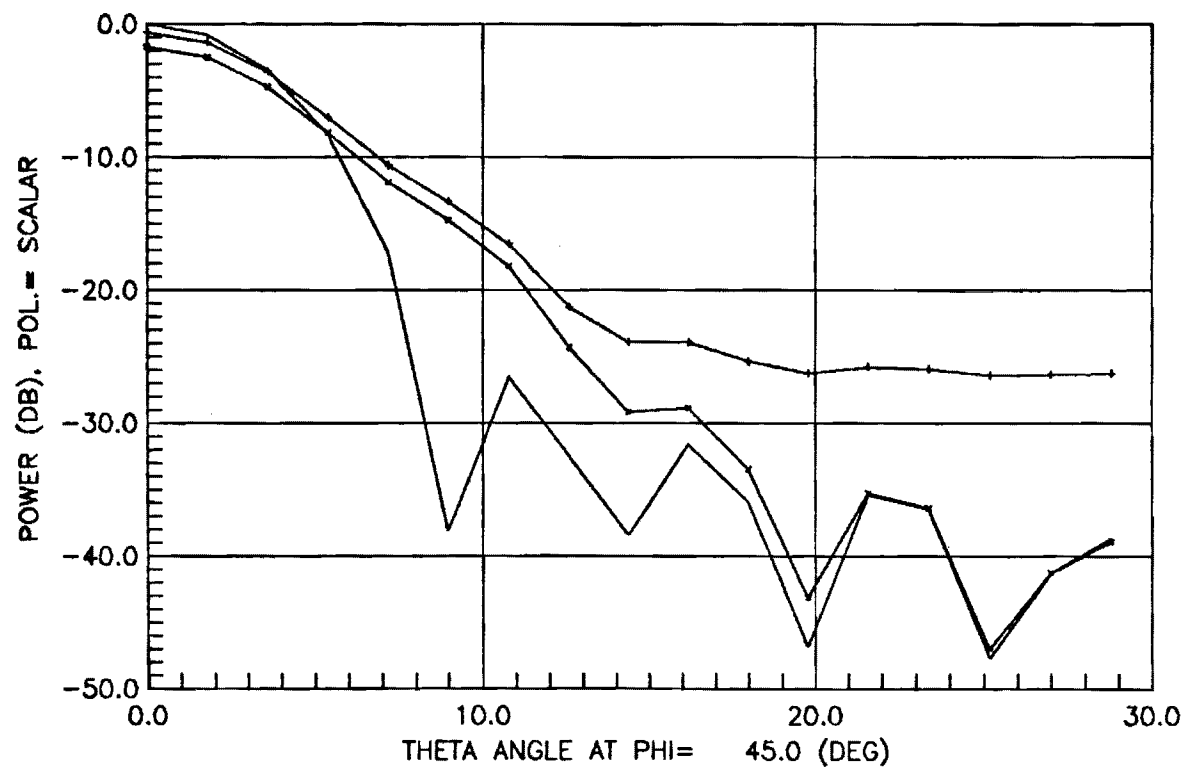


Figure 17. Far-field plot contained in file TAPE41.

previous subsection was obtained by using all the default values of this file. In the free format this file uses, the defaults are triggered by a slash in the first column of each line (except that two slashes are needed in the first line to obtain the default header). If the default values are not desired for a whole line, the end of that line can be defaulted by placing a slash after the partial input line. To default a whole line following a line that does not end in a slash requires two slashes in the first two columns of that line.

In the detailed description of file INPUT that follows, values are in dimensions of inches, degrees, and decibels unless otherwise specified. It is presented only on right-hand pages for convenient use in preparing the file at a computer terminal.

THIS PAGE INTENTIONALLY LEFT BLANK

DESCRIPTION OF FILE "INPUT"

<u>Line</u>	<u>Variable</u>	<u>Default</u>	<u>Value</u>	<u>Description</u>
1.	HEAD (8)	TEST CASE	(alpha)	Heading string desired on output.
2.	THE1, THE2, THED	0. 30. 1.8	$\left. \begin{array}{l} < \text{THE2} \\ < \cot^{-1} R2/FOCL \\ > 0. \\ \leq 0. \end{array} \right\}$	$\left. \begin{array}{l} \text{Polar angles at which pattern} \\ \text{points will start, stop and} \\ \text{increment. (Should start at 0.)} \\ \text{Only first pattern point will be} \\ \text{calculated.} \end{array} \right\}$
	PHE1, PHE2, PHED	0. 45. 45.	$\left. \begin{array}{l} \text{PHE1} < \text{PHE2} \\ > 0. \\ \leq 0. \end{array} \right\}$	$\left. \begin{array}{l} \text{Azimuthal angles at which pattern} \\ \text{cuts will start, stop and incre-} \\ \text{ment.} \\ \text{Only first cut will be calculated.} \end{array} \right\}$
3.	BOTH	Y	N Y	Plot only the primary polarization. Plot also the orthogonal polar- ization.
4.	IPCOL	3	1 2 3 4	Plot unperturbed pattern only. Also plot total mean error pattern. Also plot deterministic error pattern. Also plot mean uncorrelated error.
5.	ANS	N	N Y	Use the default plotting grid. Read the following plot specifi- cations.
5a.	IBOX	R	R,P	Rectangular or polar grid.
5b.	XMIN, XMAX,  XINC  WIDTH	0. 30.  10.  7.0	$\left. \begin{array}{l} \text{XMIN} \neq \text{XMAX} \\ \\ \neq 0. \\ 0. \\ > 0. \end{array} \right\}$	$\left. \begin{array}{l} \text{Minimum and maximum grid data} \\ \text{values for the horizontal (or} \\ \text{azimuthal axis.} \\ \text{Increment for grid lines and axis} \\ \text{numbers.} \\ \text{Program will select an appropriate} \\ \text{increment.} \\ \text{Length of horizontal axis (or} \\ \text{diameter of polar plot).} \end{array} \right\}$

THIS PAGE INTENTIONALLY LEFT BLANK

DESCRIPTION OF FILE "INPUT" - (continued)

<u>Line</u>	<u>Variable</u>	<u>Default</u>	<u>Value</u>	<u>Description</u>
5c.	YMIN,	-50.	} YMIN ≠ YMAX	Minimum and maximum grid data values for vertical (or radial) axis.
	YMAX	0.		
	YINC	10.	≠ 0.	Increment for grid lines and axis numbers.
			= 0.	Program will select appropriate increment.
	HEIGHT	4.5	< 8.5	Length of vertical axis.
6.	R1,	0.	} R1 > R2	Inner radius, outer radius of reflector sample grid.
	R2	5.		
	DR	.25	> 0.	The radial increment.
			≤ 0.	The sample points will be read (6a).
	NR	-	> 1	The number of radial points to read (calculated when AR not read).
7.	NARR	6	> 0	Number of equal reflector sectors.
	DAZ	5.	> 0.	The azimuthal increment.
			≤ 0.	The sample points will be read (7a)
	NA	-	> 1	The number of azimuthal sample points (per sector) to be read in. (calculated when AA not read)
7a.	AA (256)	-	0. ≤ ' < A2 (ascending)	Azimuthal grid points at which reflector and aperture fields are defined.
6a.	AR (64)	-	(ascending)	Radial grid points at which reflector and aperture fields are defined.

THIS PAGE INTENTIONALLY LEFT BLANK

DESCRIPTION OF FILE "INPUT" - (continued)

<u>Line</u>	<u>Variable</u>	<u>Default</u>	<u>Value</u>	<u>Description</u>
8.	FREQ	11.80285	>0.	Frequency (GHz).
			<0	Minimum output.
	IOBUG	1	0	Also pattern analysis.
			1	Also aperture function and warnings of integration inaccuracy.
			2	Also debugging output within the pattern point loops.
			3	Also debugging output within the sector loop.
			>3	Etc.
	ISYM	3	<3	No symmetry (not fully implemented)
			>3	Rotational symmetry by sector.
9.	FOCL	4.	>0.	Main reflector focal length.
	ECC	2.	>1.	Subreflector eccentricity.
	IFEED	1	1	Select cos <sup>n</sup> feed pattern.
			≠1	Select Gaussian-on-a-pedestal feed pattern.
10.	COSN	16.	>0.	Cos exponent read if IFEED =1.
10a.	PED	-50.	<0.	Pedestal read if IFEED (dB).
	ABYTHS	3.8436	-	Coefficient of $-\theta_f^2$ in Gaussian exponent ( $\theta_f$ is angle of feed radiation).
11.	IPIC	2	0,1,2	Three-dimensional plots: none, amplitude, amplitude and phase.
	ICUT, JCUT	1	0<' < NR	Number of radial and azimuthal cuts
		0	0<' < NA	
	INC, JNC	1	1<' < NR	Increment between radial and azimuthal cuts.
		5	1<' < NA	
	MO, NO	1	1<' < NR	Point at which to make first cuts.
		1	1<' < NA	
	IBORDER	0	>0	Number of increments with zero value to add around 3-D plots.



THIS PAGE INTENTIONALLY LEFT BLANK

DESCRIPTION OF FILE "INPUT" - (continued)

<u>Line</u>	<u>Variable</u>	<u>Default</u>	<u>Value</u>	<u>Description</u>
	IGRID	4	0 1 ≥2	Plot axes only. Also plot grid outline. Also plot lines at major intervals (30° for polar plots).
12.	IPERT	1	0 1	No deterministic errors are specified. Define deterministic errors.
12a.	The separable version of PERTRB reads:			
	ARP (64)	1.	*	Normal reflector displacement as a function of radius.
	AAP (64)	1.	*	Reflector displacement coefficient as a function of azimuth over one sector.
13.	DEFECT	1.7	-	Number of randomly positioned defects.
	GMAX	(1.0,0.0)	-	Coefficient of the field scattered from each defect.
	PERRAD	1.0	>0.	Radius of aperture perturbation (not used with point source version).

\*These perturbations must not be so large or abrupt that they affect reflected amplitude or polarization.